Charles University in Prague, Faculty of Science
Department of Parasitology

Ph.D. study program: Parasitology

Proteomic Analysis of *Trichomonas vaginalis* hydrogenosome

Mgr. Neritza Campo Beltrán

Ph.D. Thesis

Thesis supervisor: Prof. RNDr. Jan Tachezy, PhD.

Prague 2016

Data presented in this thesis resulted from team collaboration at the Laboratory of Molecular and Biochemical Parasitology of Charles University in Prague and from collaboration with our partners. I declare that the involvement of Mgr. Neritza Campo Beltrán in this work was substantial and that she contributed significantly to the presented results.

.....

Prof. RNDr. Jan Tachezy, PhD.

Thesis supervisor

Declaration of the author: I declare that I elaborated the PhD thesis independently. I also proclaim that the literary sources were cited properly and neither this work nor the substantial part of it has been used to reach the same or any other academic degree.

Prohlášení: Prohlašuji, že jsem závěrečnou práci zpracovala samostatně a že jsem uvedla všechny použité informační zdroje a literaturu. Tato práce ani její podstatná část nebyla předložena k získání jiného nebo stejného akademického titulu.

V Praze, 30.06.2016

.....

Mgr. Neritza Campo Beltrán

DEDICATION

I dedicate my dissertation work to God for being with me and guide me always, my wonderful parents, Argemiro Campo and Sara Beltrán for believing in me, supporting me in all my dreams and prompted me with their words and example to finish my Ph.D. My sisters, Sandra Havith and Sara Zulay for being my complices, my friends, for their support and patience. A special feeling of gratitude to my lovely daughter Daniela for being the engine of my life, the origin of my strength and source of motivation. I also dedicate this dissertation to other members of my family and friends who have supported me throughout the process.

Neritza Campo Beltrán

ACKNOWLEDGEMENTS

I wish to thank Professor Jan Tachezy for giving me the opportunity to participate in this research, for his support, for his patience, for his expertise and dedication. I am also grateful with all members of the laboratory, especially Eva Nývltová, Ivan Hrdý and Michaela Marcincikova for their unconditional support. Special thanks to Professor Jaroslav Kulda for sharing with me his knowledge about metronidazole resistance and always be willing to provide assistance when necessary.

Neritza Campo Beltrán

CONTENTS:

ABSTRACT

Trichomonas vaginalis is a human pathogen that affects annually approximately 258 million people worldwide. This parasite possesses organelles of mitochondrial origin called hydrogenosomes, which generate ATP under anaerobic conditions. The identification of the protein content at the subcellular level may provide new targets for antiparasitic drugs developments as well as it contributes for our understanding of the organelles function and evolution. The availability of protocols for organelles purification and the complete genome sequence allow the study of the organellar proteomes using mass spectrometry and bioinformatics, providing a powerful strategy that combine cell biology and proteomics. In our research, we used several approaches to identify the protein composition in hydrogenosomes and mitosomes. We performed transcriptomic and proteomic analysis to investigate the molecular responses of *Trichomonas vaginalis* upon iron availability. Furthermore, the changes in the proteome during the development of metronidazole resistance were also studied. The organelles separated by differential and Optiprep-sucrose gradient centrifugation were analyzed with nano-RP-HPLC/MALDI-TOF/TOF. We also used Triton X-114 phase partitioning to separate membrane proteins and iTRAQ technique to label the peptides of the samples used for comparative proteomic analyses. In order to confirm the mitochondrial localization of the proteins, the data was analyzed using 5 different bioinformatic tools such as PSORT II, TargetP, Euk-mPLoc 2.0, Yloc and Hunter. The present study makes a significant contribution to understanding the overall organelles network.

1. Introduction

Mitochondria play a key role in iron metabolism. Iron is a component of catalytic and redox cofactors such as heme and iron-sulfur (Fe-S) clusters, prosthetic groups that are utilized by proteins in various critical processes. In addition to their well-established role in providing the cell with ATP, mitochondria are important for formation of iron-sulfur clusters as well as heme synthesis. The synthesis and insertion of Fe-S clusters to the apoproteins is mediated by iron sulfur cluster (ISC) assembly machinery (Smid et al., 2006; Lill and Kispal, 2000; Lill et al., 1999; Lill et al, 2005; Rouault and Tong, 2005). On the other hand, the steps leading to heme synthesis are distributed between the cytosol and mitochondria. While many of the intermediate steps are cytoplasmic, the first and last step of the synthesis takes place in the organelle. The process ends with the insertion of the ferrous iron into the porphyrin ring by the aid of the ferrochelatase enzyme (Camadro et al., 1988).

The human parasite *T. vaginalis* lacks the classical aerobic mitochondria. Instead, trichomonads possess an organelle of mitochondrial origin called hydrogenosome (Martin and Müller, 1998). Similarly to mitochondria, hydrogenosomes possess the multiprotein machinery responsible for iron-sulfur cluster biosynthesis (Šutak et al., 2004). Initial experiments in trichomonads have revealed the iron-dependent changes in enzyme activities and host cell interactions associated with pathogenicity (Vanácová et al., 2001; Lehker et al., 1992; Arroyo et al., 1992; Alderete et al., 1995; Arroyo and Alderete, 1995; Garcia et al., 2003; Moreno-Brito et al., 2005). The most significant changes upon iron availability were observed in the expression of hydrogenosomal proteins, including the Fe-S and non-FeS proteins involved in energy metabolism (Vanácová et al., 2001).

Trichomoniasis is a sexual transmitted disease (STD) caused by *T. vaginalis*. The infection has been efficiently treated with derivatives of the 5-nitroimidazoles although presence of resistant strains has been reported (Dunne et al., 2003; Kirkcaldy et al., 2012; Upcroft et al., 2009). The proteins involved in the activation of the drug to its toxic form localize to the hydrogenosome and it is in the organelle where metabolic changes leading to development of drug resistance take place (Kulda et al., 1984; Kulda et al., 1993; Brown et al., 1999), although alternative cytosolic flavin-based mechanism has been proposed (Leitsch et al., 2010).

T. vaginalis is the most extensively studied member of the Parabasala group. The genome sequence was published in 2007 (Carlton et al., 2007). Approximately 60 000 protein-coding genes were predicted, which opened new perspectives to study the metabolism of the parasite. This information has to be corroborated with research at the proteome level which will provide a more direct knowledge about biological processes.

In the present study we perform comparative proteomic analyses of highly purified hydrogenosomes from *T. vaginalis* grown under iron rich and iron depleted conditions. Protein levels were rigorously analyzed and the proteins were classified into groups according to their biological functions. The observed changes in protein levels were supported by a transcriptomic analysis. We identified 179 proteins, of which 58 were differentially expressed. Iron deficiency led to the upregulation of proteins involved in Fe-S cluster assembly and the downregulation of enzymes involved in carbohydrate metabolism.

In addition, a proteomic analysis of highly purified hydrogenosomes isolated from metronidazole-susceptible parent strain TV10-02 and from the *in vitro* developed resistant derivatives growing with 3, 5 and 100 μg/ml metronidazole (MR3, MR5, and MR100) was compared, to observe the changes in the expression during the development of metronidazole resistance in the parasite. From a total of 700 proteins identified, approximately 140 were hydrogenosomal proteins found in all cell lines. Changes in protein expression were rather low in MR3 and MR5 strains while the highly resistant strain MR100 displayed marked downregulation of the enzymes involved in energy and amino acid metabolism. In contrast, increased protein levels were observed for key components of ISC assembly machinery and for hydrogenase maturases. Interestingly, the highest increase was observed for hybrid cluster protein (HCP) which might be involved in scavenging of toxic products of nitrate metabolism including hydroxylamine. These data has not been published yet.

2. *Trichomonas vaginalis*

T. vaginalis is a parasite from the Excavata group and the class Parabasala (Cavalier-Smith T, 2002). It infects the genitourinary tract of humans with approximately 258 million

cases occurring annually worldwide (Schmid et al., 2011). The parasite is exposed to adverse conditions in its natural environment: acidic pH, presence of lactobacillus, hormonal changes, low nutrients, menstrual flow and fluctuations in iron concentrations during the menstrual cycle. However, the parasite is well adapted to cross the vaginal mucus, adhere to the epithelium, multiply and colonize the urogenital tract and survive for long periods of time causing a chronic infection in humans called trichomoniasis (Harp et al., 2011), the most common non-viral sexually transmitted infection (Petrin et al., 1998; Schwebke and Burgess, 2004).

Trichomoniasis has been associated with adverse pregnancy outcomes (Cotch, 1990; Hardy et al., 1984), cervix and prostate cancer (Stark et al., 2009) and increased risk to human immunodeficiency virus infection, HIV (Laga et al., 1993; Chesson et al., 2004; Van der Pol et al., 2008; Serwin et al., 2013). The infection is efficiently treated with derivatives of the 5-nitroimidazole however, presence of strains that are resistant to the drug have been reported (Dombrowski et al., 1987; Grossman et al., 1990; Heyworth et al., 1980; Kulda et al., 1982; Coelho, 1997; Kellock et al., 1996; Kirkcaldy et al., 2012; Upcroft et al., 2009). The medical implications, the unique biology, and the interesting evolution of trichomonads have raised a special interest to study these parasites.

A remarkable feature of trichomonads is the presence of hydrogenosomes, which were discovered in *Tritrichomonas foetus* in 1973 (Lindmark and Müller M., 1973; Müller, 1993) and extensively studied in *T. vaginalis* (Müller, 1988; Müller, 1993; Tachezy, 2008; Müller, 2003; Müller, 2007).

T. vaginalis has a repetitive genome of ~160Mb with approximately 60 000 protein-coding genes encoded on six chromosomes. The genome is surprisingly large in comparison to other parasites such as *Giardia intestinalis* (~11.7 Mb) or *Entamoeba histolytica* (~24 Mb) and it has one of the highest coding capacities in eukaryotes reported to date. The genome reflects a recent genetic expansion such as amplification of specific gene families implicated in pathogenesis and phagocytosis of host proteins, which is considered as a result of the parasite adaptation to the genital environment. In addition, the genome contains many genes of bacterial origin acquired by lateral gene transfer. Interestingly, the genome sequence provided

evidences to support the common origin of hydrogenosomes and mitochondria. Additionally, the identification of genes which have been implicated in metronidazole resistance in bacteria could give clues to the potential mechanisms that clinically resistant parasites may use (Carlton et al., 2007).

3. Mitochondria and organelles of mitochondrial origin

Mitochondria are eukaryotic organelles mainly known for their role as "powerhouses" of the cell. These organelles evolved most likely from α-proteobacteria through endosymbiosis (Margulis et al., 1970). The strongest bases for this theory provided physiological and biochemical similarities between these organelles and prokaryotic cells, such as the presence of a double membrane with a typical bacterial lipid in the inner membrane called cardiolipin surrounding the organelle, and the presence of an organellar genome in mitochondria that shares similarity with bacterial DNA (Yang et al., 1985; Margulis, 1970; Esser et al., 2004; Embley and Martin, 2006; Dyall and Johnson, 2000).

Important evidence in support of the endosymbiotic theory comes from analysis of the organellar genomes (Zimorski et al., 2014). Phylogenetic analyses of small subunit rRNA encoded by mitochondrial genomes supported a view that the origin of mitochondria is the result of an endosymbiotic process where an ancient eukaryotic host, probably an archae methanogen, engulfed and retain a bacteria most likely of α-proteobacterial origin (Yang et al., 1985; Margulis et al., 1970; Anderson et al., 1998; Esser et al.,2004; Embley and Martin, 2006; Horner et al., 1996).

According to the last classification of the organelles of mitochondrial origin, mitochondria are membrane bounded organelles, oxygen respiring which generate the bulk of ATP by oxidative phosphorylation (Müller et al., 2012). It has the complex I to V of the electron transport chain and key subunits of these complexes are encoded by genes found in the mitochondrial genome (Allen, 2003). The organelle has been named aerobic mitochondria and it uses O_2 as a terminal electron acceptor (Müller et al., 2012).

Not all eukaryotes harbour the classical aerobic mitochondria. The absence of organelles with classical mitochondrial structure in some species led to the assumption that

these organisms represent ancient or early-branching eukaryotes without mitochondria (Martin and Müller, 1998; Cavalier – Smith, 1987; Hjort et al., 2010). Later on, the discovery of highly modified mitochondria such as hydrogenosomes and mitosomes in the so-called "amitochondriate organisms" changed this view. It is believed that during the evolution, the original mitochondria diverged into several different forms, which we called now organelles of mitochondrial origin. Most of these organelles lost their genomes and the genes of the original endosymbiont were lost or transferred to the host nucleus (Rivera and Lake, 2004; Hackstein et al., 2006; Hjort et al., 2010).

In the latest years, different organelles have been described in a number of protists (Lindmark and Müller, 1973; Millet et al., 2013; Putignani et al., 2004; Stechmann et al., 2003, Hashimoto et al., 1998; Hackstein et al., 2006). The information provided by these studies has helped to demonstrate that all eukaryotic groups possess an organelle of mitochondrial origin. However, recently was reported that the oxymonad *Monocercomonoides spp.* is the first eukaryote lacking even the most reduced form of mitochondrion which has important implications for cellular processes and our understanding of reductive mitochondrial evolution across the eukaryotic tree of life (Karnkowska et al., 2016).

Based on the character of energy metabolism and the contribution of bacterial anaerobic enzymes, particularly hydrogenase, five types of mitochondrial organelles were distinguished (Müller et al., 2012). Aerobic mitochondria are the classical organelles described above that produce ATP and use O_2 as a terminal electron acceptor. The yeast *Sacharomyces cerevisiae* represents a major eukaryotic model organism for the identification and characterization of protein functions and cellular pathways in aerobic mitochondria (Kai et al., 2002; Sickmann et al., 2013).

Anaerobic mitochondria have been found in protist and also in multicellular organisms like parasitic nematodes. The organelle has typical mitochondrial features but it uses an endogenous product such as fumarate as a final electron acceptor, although environmental acceptors like nitrate are also used. Anaerobic mitochondria produce ATP with the help of a proton-pumping electron transport, but they do not need O_2. The end product of electron

transport is not H_2O, but could be nitrite (NO_2), nitric oxide (NO) and succinate among others (Tielens et al., 2002; Risgaard -Petersen et al., 2006).

The hydrogen-producing mitochondria have been studied in the ciliate *Nyctotherus ovalis* (Akhmanova et al., 1998; Hackstein et al., 1999; Hackstein and Yarlett, 2006). The organelle possesses an electron transport chain but additionally it expresses the protein Fe-hydrogenase, therefore it can use protons as a terminal electron acceptor. The organelle harbour enzymes of the tricarboxylic acid cycle (TCA), some homologues of mitochondrial import and processing machinery, and various mitochondrial-type metabolite transporters (de Graaf et al., 2011). Hydrogen-producing mitochondria represent a very recent adaptation to hypoxic environments. It is considered to represent the link between aerobic mitochondria and hydrogenosomes since they harbour an electron transport chain and DNA like the aerobic mitochondria and they produce hydrogen like hydrogenosomes (Martin, 2005; Akhmanova et al., 1998; Boxma et al., 2005; Hackstein et al., 1999; Hackstein and Yarlett, 2006).

Hydrogenosomes are double-membrane-bounded and H_2-producing organelles. The organelle lacks a genome, cytochromes and the electron transport chain. Moreover, the synthesis of ATP is strictly mediated by substrate-level phosphorylation. The organelles have been mostly studied in the human parasite *T. vaginalis* although they have been found in anaerobic protists of various eukaryotic lineages (Müller, 2003; van der Giezen, 2009). The organelle will be described in more detail in the next chapter.

Mitosomes are the most reduced forms of mitochondria identified to date. The organelle has been found in multiple eukaryotic lineages mainly in anaerobic protist or intracellular parasites. It has been characterized in the human parasites *Giardia intestinalis* (Tovar et al., 2003) and *Entamoeba histolytica* (Tovar et al., 1999). These organelles do not synthesize ATP and they are unique among the organelles of mitochondrial origin that lack this function. Mitosomes of some lineages have retained components of ISC assembly machinery (Goldberg et al., 2008; Tovar et al., 2003) and others have retained components of sulfate activation (Mi-ichi et al., 2009; Clark and Roger, 1995).

Despite the diversification and metabolic differences between these organelles, all of them with exception of the mitosome in *Entamoeba hystolytica* play a role in iron-sulfur (Fe-S) cluster assembly (Tachezy et al., 2001; Goldberg et al., 2008; Tovar et al., 2003; Rada et al., 2009; Smíd et al., 2006; Maralikova et al., 2010). In mitochondria, the assembly of Fe-S

clusters mediated by ISC assembly machinery is the only essential function identified thus far and the disruption of the Fe-S cluster assembly machinery leads to cell death by iron accumulation (Lill et al., 1999; Lill and Kispal, 2000; Mühlenhoff and Lill, 2000).

3.1 Hydrogenosomes

Hydrogenosomes were discovered in 1973 in the cattle parasite *T. foetus* (Lindmark and Müller, 1973) but the biochemistry and structure of the organelle has been studied in detail in the human parasite *T. vaginalis* (Hrdý et al., 2007; Müller, 2003; Müller et al., 2012; Benchimol, 2009; Benchimol, 2000). Information about hydrogenosomes in other organisms is rather limited (Müller, 2003; Dyall, 2000; Hackstein et al, 1999).

Hydrogenosomes measure from 300 nm to 1 μm, however larger organelles and abnormal shapes have been observed under stress conditions. In most hydrogenosomes-bearing organisms, the organelles have been observed as granules with rounded or elongated appearance that are usually associated with cytoskeletal structures like the axostyle and costa (Benchimol, 2009; Benchimol, 2000).

The organelles has been described in different phylogenetic lineages like parabasalids (Lindmark and Müller, 1973) amoeboflagellates (Barbera et al., 2010; Brul et al., 1994; Broers,1992), chytrid fungi (O'Fallon et al., 1991; Marvin-Sikkema et al.,1994; Yarlett et al.,1986), free living ciliates (Fenchel and Finlay, 1991; van Bruggen et al., 1984; Dyer, 1989; Broers et al., 1991), and symbiotic ciliates (Yarlett et al., 1981; Lloyd et al., 1989; Paul et al., 1990) and archamoebae (Nyvltova et al., 2013). These findings indicate a multiple independent origin of hydrogenosomes as an adaptation to anaerobic conditions (Embley, 2006).

The study of the hydrogenosomal metabolism has been conducted at level of individual pathways. Hydrogenosomal localization has been experimentally confirmed only for limited number of proteins involved in known pathways. The possibility to perform proteomic analyses is limited by the need of an axenic culture with an appropriate amount of cells. *Trichomonas spp.* and *Neocallimastix spp.* are the only hydrogenosome-bearing organisms that could meet these requirements (Müller and Lindmark, 1978; van der Giezen et al., 1997) . However, the genome sequence is essential for a large scale proteomic approach which renders *T. vaginalis*

hydrogenosomes as the only possibility for the proteomic characterization (Carlton et al., 2007; Henze, 2008).

4. Hydrogenosomal metabolism in *T. vaginalis*

4.1 Energy metabolism

The energy metabolism was the first function discovered in hydrogenosomes (Čerkasov et al., 1978; Lindmark and Muller, 1974). It was demonstrated that isolated organelles generate equivalent amounts of ATP, acetate, CO2 and hydrogen per mol of pyruvate under anaerobic conditions (Steinbüchel and Müller, 1986). Presence of this metabolic pathway was confirmed by determination of enzymatic activities found in the isolated organelles and it was later supported by molecular data and finally by the analysis of the *T. vaginalis* genome sequence (Hrdý and Müller, 1995a; Hrdý and Müller, 1995b; Doležal, 2004; Hrdý et al., 2004; Thong and Coombs, 1987; Steinbüchel and Müller, 1986; Müller, 1998, Carlton et al., 2007).

In *T. vaginalis*, pyruvate and malate are produced from glucose in the cytosol during anaerobic glycolysis. Both substrates enter the hydrogenosome and serve as sources for energy metabolism. Malate is oxidatively decarboxylated by the hydrogenosomal NAD-dependent malic enzyme, the most abundant hydrogenosomal protein in *T. vaginalis,* to produce pyruvate, CO_2 and NADH (Drmota et al., 1996; Hrdý and Müller, 1995a). To maintain the redox balance, NADH is reoxidized by the NADH: ferredoxin oxidoreductase. The enzyme is composed of two subunits with homology to the 24- and 51-kDa subunits of the Complex I (NADH dehydrogenase, NDH) of the mitochondrial respiratory chain (Hrdý et al. 2004; Thong and Coombs, 1987; Steinbüchel and Müller, 1986).

Pyruvate is oxidatively decarboxylated by pyruvate: ferredoxin oxidoreductase (PFOR), a Fe-S protein possessing several [4Fe4S] clusters (Müller, 1993; Hrdý and Müller, 1995b; Hrdý et al., 2004; Müller, 1993; Docampo et al., 1987; Ragsdale, 2003). PFOR is associated with the hydrogenosomal membrane and shows high sensitivity to oxygen (Williams et al., 1987). The genome annotation revealed seven different genes coding for PFOR (Carlton et al., 2007). PFOR from *T. vaginalis* was biochemically studied and purified to homogeneity by Williams in 1987. The enzymatic reaction catalyzed by PFOR generates acetyl-CoA, CO2 and two electrons that are transferred to ferredoxin (Fdx) (Bui et al., 1996; Payne et al., 1993), an

iron sulfur protein of low molecular weight with [2Fe-2S] cluster (Hrdý et al, 2004). Fdx acquires the electrons from PFOR and/or NDH and transfer these electrons to [FeFe] hydrogenase (Bui et al., 1996; Payne et al., 1993; Zwart et al., 1988), which uses them to generate molecular hydrogen (end product) (Hrdý et al., 2004; Müller, 1993).

The CoA moeity of acetyl-CoA is transferred by the acetate: succinate CoA- transferase (ASCT) to succinate yielding succinyl-CoA and acetate as a metabolic end product (Steinbüchel and Müller, 1986; Lahti et al., 1992; Lahti et al., 1994; Lindmark, 1976). ASCT enzyme was described for the first time in trichomonads. The enzyme was characterized at the molecular level and it differs from the ASCT found in mitochondria of other parasites such as trypanosomes (Lindmark, 1976; van Grinsven et al., 2008). Succinyl-CoA synthetase (SCS) also known as succinate thiokinase is an energy conserving enzyme that uses succinyl-CoA as a substrate to produce ATP/GTP by substrate level phosphorylation. SCS is the only enzyme from the Krebs cycle that has been found in *T. vaginalis* hydrogenosomes. Adenylate kinase is a phosphotransferase enzyme that catalyzes the interconversion of adenine nucleotides by the transfer of a phosphate group between two molecules of ADP forming ATP and AMP. The enzyme is also present in hydrogenosomes (Declerck and Müller, 1987; Lange et al., 1994).

Whether the hydrogenosomal energy metabolism is essential or not for the parasite is not clear. The hydrogenosomes from the *T. vaginalis* strain with high level of resistance to metronidazole lack the enzymatic activities involved in the synthesis of ATP (Edwards, 1993; Kulda 1999; Upcroft and Upcroft, 2001; Dunne et al. 2003; Cudmore et al. 2004; Vanácová et al., 2001). However, it was proposed that the enzymatic activity of PFOR could be replaced by an alternative 2-keto acid oxidoreductase, which is probably present in hydrogenosomes and thus contributes to ATP synthesis (Brown et al., 1999).

4.2 Iron-sulfur clusters assembly machinery

Iron-sulfur clusters are inorganic cofactors necessary for the biological functions of proteins. The synthesis and insertion of these groups to the apoproteins is mediated by the iron sulfur cluster assembly machinery (ISC) (Lill and Kispal, 2000; Lill et al., 1999; Lill and Muhlenhoff, 2005; Rouault and Tong, 2005). The system was initially found in the mitochondria of *S. cerevisiae.* Later on, it was demonstrated that the formation of Fe-S clusters

is a fundamental function shared by mitochondria, mitosomes and hydrogenosomes, which also confirm a common origin of these organelles (Šutak et al., 2004).

The first indication that the ISC assembly machinery was present in the hydrogenosome was the finding of two gene paralogues coding for a pyridoxal-5′-phosphate-dependent cysteine desulfurase (IscS), an essential enzyme for Fe-S clusters assembly, are present in *T. vaginalis* genome and they are phylogenetically related to their mitochondrial homologs (Tachezy et al., 2001). In 2004, Šutak et al., confirmed that hydrogenosomes of *T. vaginalis* contain the key enzyme of Fe-S center biosynthesis, cysteine desulfurase (TviscS-2). Moreover, they demonstrated that isolated hydrogenosomes catalyze the assembly and insertion of Fe-S clusters to apoferredoxin (Šutak et al., 2004). Later, genes for all components of the iron-sulfur cluster assembly machinery were identified in the genome of *T. vaginalis* (Carlton et al., 2007).

Mechanism of ISC assembly machinery-dependent Fe-S cluster formation includes two main steps. In the first step, the IscS/Isd11 complex provides sulfur to the scaffold protein IscU while frataxin is the source of iron (Santos et al, 2004; Doležal et al, 2007). Isd11 is a protein that was found only in eukaryotes and it supports activity of IscS. Since there is not bacterial homologue of Isd11, the protein has been proposed to be the eukaryotic invention to the ISC assembly machinery (Richards and van der Giezen, 2006). Two genes coding for homologues of Isd11 has been found in *T. vaginalis* genome (Carlton et al., 2007). Besides IscU which is encoded by a single gene, there are alternative scaffold proteins named Nfu and IscA encoded by multiple genes. IscA is an alternative scaffold protein which is involved in the maturation of more complex Fe-S clusters ([4Fe4S]). IscA homologues in mitochondria (Isa1 and Isa2) are involved in the maturation of aconitase and the activation of SAM complex, known also as biotin synthase and lipoic-acid synthase (Gelling et al., 2008). Aconitase is not present in *T. vaginalis* hydrogenosomes but the organelle possesses the hydrogenase maturases (HydE, HydF and HydG) from which functional HydE, a homologue of biotin synthase that possess [4Fe4S] cluster, is necessary for the assembly and insertion of Fe-S clusters and ligands into the H-cluster, the active site of the trichomonad [FeFe] hydrogenases (Pütz et al, 2006). Therefore, it is possible that IscA participates in the activation of HydE maturase, among other [4Fe4S] proteins in the hydrogenosome.

In the second step, preassembled transient Fe-S clusters in IscU are transferred to the apoproteins, a process that is mediated by the chaperone system, which includes the Hsp70, co-chaperone Jac1 (DnaJ), and ADP/ATP nucleotide exchange factor. Fe-S cluster formation also requires reducing equivalents, which are provided by [2Fe2S] ferredoxin. There are seven genes coding for [2Fe2S] ferredoxin in *T. vaginalis* genome and all gene products localize in the hydrogenosome. This electron transfer protein has a key role in energy metabolism. However, it is not clear which ferredoxin paralogue is involved in energy metabolism and which participates in the synthesis of Fe-S clusters.

Surprisingly, the transcription of *T. vaginalis* IscS and frataxin is upregulated under iron deficiency, which was explained by a higher demand for the formation of new Fe-S clusters (Šutak et al, 2004). This finding contrast with the mitochondrial homologue (Yfh1), which showed upregulation under iron enriched conditions. It has been suggested that frataxin may serve as iron storage in mitochondria (Santos et al, 2004). In contrary, the hydrogenosomal frataxin most likely lacks the iron storage function; the protein possibly donates iron for the formation of Fe-S clusters in hydrogenosomes (Doležal et al, 2007).

The mitochondrial ISC assembly machinery of yeast and mammalian cells was found essential not only for the formation of mitochondrial Fe-S proteins but cytosolic and nuclear Fe-S proteins too (Kispal et al., 1999; Lange et al., 2000). Although the nature of the compound exported from mitochondria to the cytosol is unknown, a Fe-S cluster export machinery has been identified which consists of ABC half-transporter Atm1, sulfhydryloxidase Erv1 and the tripeptide glutathione (GSH) (Kispal et al., 1999; Lange et al., 2000; Balk et al., 2004; Lange et al., 1991; Sipos et al., 2002). In 2003 was identified the first component of the cytosolic Fe-S cluster assembly machinery (CIA) which, together with the Fe-S cluster export machinery are responsible of maturation of nuclear and cytosolic Fe-S proteins (Roy et al., 2003). *T. vaginalis* genome sequence has revealed the presence of putative homologues of the cytosolic Fe-S cluster assembly (CIA) including Cia1, Cia2B , Nar1 and Nbp35/Cfd1, while homologues of Dre2, Tah18 and MMS19 were not found (Carlton et al., 2007). Recently it was reported that Cia2A and Cia2B form protein complexes with Cia1 and MMS19 and they are involved in the maturation of the Fe-S cluster of the iron regulatory protein 1 (IRP1) which is critical for cellular iron homeostasis. It was also demonstrated that the complexes stabilize the iron regulatory protein 2 (IRP2) and then the protein connects the cytosolic Fe-S protein

maturation with cellular iron regulation (Stehling et al., 2013). Cia2A has not been identified in yeast and its presence in *T.vaginalis* is under study (Unpublished results). Homologues of the membrane components involved in Fe-S cluster export machinery (Erv1, Atm1 and GSH) have not been found either. Hence, it is not clear whether the hydrogenosomal ISC machinery produces essential components for the formation of extra-hydrogenosomal Fe-S proteins as it was reported in mitochondria.

4.3 Amino acid and polyamine metabolism

Before the analysis of *T. vaginalis* genome, the knowledge of the aminoacid metabolism in *T. vaginalis* was limited to the arginine decarboxylation and some transaminase activities (Zuo et al., 1995; Yarlett et al., 1994; Yarlett et al., 1996). The parasite can use aminoacids like arginine, threonine, leucine and methionine as a source of energy when carbohydrates are scarce (Zuo et al., 1995). Later on, the genome sequencing revealed the presence of two enzymes from the glycine decarboxylase complex (GDC) and a serine hydroxymethyltransferase (SHMT) with predicted N-terminal hydrogenosomal presequences suggesting presence of more hydrogenosomal pathways for amino acid metabolism (Carlton et al, 2007).

4.3.1 Arginine metabolism

Arginine is the precursor for the biosynthesis of polyamines, organic compounds that are important for oxidative stress protection and membrane stability (Tadolini, 1988; Tabor and Tabor, 1976; Pegg, 1986). Four enzymes participate in the arginine dihydrolase pathway that converts arginine to ATP (Linstead and Cranshaw, 1983). Arginine deaminase is the enzyme that catalyzes the hydrolysis of arginine to citrulline. This product is converted to ornithine and carbamoyl phosphate by ornithine carbamoyl transferase, which is the second enzyme of the pathway. In the third reaction, putrescine is formed from ornithine by ornithine decarboxylase. Finally, the pathway generates ATP by the enzyme carbamate kinase, which breaks carbamoyl phosphate, an energy storage molecule, forming bicarbonate and ammonia (Yarlett et al., 1994).

T. vaginalis uses a bacterial type of arginine dihydrolase pathway, which is probably important source of ATP for the parasite *in situ* (Petrin et al., 1988). Analyses of vaginal discharges from infected patients showed decreased levels of arginine while putrescine levels increased (Chen et al., 1982). The cells that were grown *in vitro* with an abundant supply of glucose produced ATP mainly by the carbohydrate metabolism with only 1% of the ATP produced by the arginine metabolism (Yarlett et al., 1996; Petrin et al., 1988). The inactivation of components of the arginine dihydrolase pathway decreases putrescine levels, which results in hydrogenosomal damage caused reactive oxygen species (ROS) (Reis et al., 1999).

The only enzyme of the arginine dihydrolase pathway that has been found in the hydrogenosome is the arginine deaminase (ADI) (Yarlett et al., 1994). Three different genes coding for arginine deaminase were found in the genome of *T. vaginalis* and all of them were experimentally localized in the hydrogenosome (Yarlett et al., 1994; Morada et al., 2011). However, the other three enzymes of the pathway showed cytosolic activities. The reason of the hydrogenosomal localization of arginine deaminase is unknown (Yarlett et al., 1994).

4.3.2 Glycine decarboxylase complex and serine hydroxymethyltransferase

Glycine decarboxylase complex (GDC) and serine hydroxymethyltransferase (SHMT) are present in prokaryotes and eukaryotes and they are linked together to release one carbon units from serine. Active one carbon units are essential in a number of biosynthetic processes being the most important for the synthesis of nucleotides. The system is activated when high amount of glycine is present and it is responsible for the synthesis of serine and/or glycine when the aminoacids are required.

In eukaryotes, GDC is present only in the mitochondria. The system is composed of four weakly associated enzymes forming an unstable complex. The four enzymes of the complex are: the amino methyl transferase (T protein), the glycine decarboxylase (P protein), the dihydrolipoamide dehydrogenase (L protein), and the glycine cleavage (H protein). The H protein has the essential cofactor 5[3-(1,2)-dithiolanyl] pentanoic acid (lipoic acid), which interacts consecutively with the other three components of the system to catalyze the oxidative decarboxylation and deamination of glycine.

T. vaginalis has two paralogues coding for H proteins. The products of both genes are effective substrates for the L protein, which is encoded by a single gene. H and L proteins have

an amino-terminal hydrogenosomal targeting presequences and they have been localized in hydrogenosomes by immunofluorescence microscopy (Carlton et al., 2007; Mukherjee et al., 2006a). The other two components of the complex, the T and P proteins seems to be absent in the parasite. However, it is possible that the homologues in T. *vaginalis* of the components T and P are highly divergent by comparison with the proteins that have been identified in other organisms. A recent study reported that the incomplete glycine decarboxylase complex (GDC) in *T. vaginalis* actually constitutes an NADH- and lipoate-dependent redox system for peroxide detoxification which is catalyzed by hydrogenosomal OsmC peroxidase (Nývltová et al., 2016).

SHMT is a reversible enzyme important in the catalytic conversion of serine to glycine. The enzyme depends on the pyridoxal phosphate (PLP) cofactor that is present in the active site of the enzyme identified single gene coding for SHMT was identified in *T. vaginalis* and which is targeted to the hydrogenosome. The active-site lysyl residue in *T. vaginalis* SHMT forms an internal aldimine with PPL. This feature makes *T. vaginalis* SHMT different from its prokaryotic and eukaryotic homologues and makes this protein a potential drug target (Mukherjee et al., 2006b).

4.4 Protein import machinery

Hydrogenosomes lack organellar genome and hence, the whole set of organellar proteins are nuclear encoded and after synthesis on free ribosomes they are imported to the organelle (Clemens and Johhson, 2000).

In order to assure the delivery of nuclear encoded proteins into mitochondria, eukaryotic cells has created the protein import machinery in the mitochondrial membranes (Pfanner and Geissler, 2001; Dyall et al., 2004; Wickner and Schekman, 2005; Doležal et al., 2006; Stewart, 2007; Chacinska et al., 2009). The machinery has been well characterized in the mitochondria of the yeast *Saccharomyces cerevisiae*. However, information about proteins in the hydrogenosomal membranes that facilitate protein transport and the exchange of metabolites is quite limited.

The targeting of matrix proteins is dependent on N-terminal cleavable presequences or internal targeting signals (Bradley et al., 1997; Mentel et al., 2008; Rada et al., 2015, Garg et al., 2015). Analysis of hydrogenosomal proteins revealed the presence of short N-terminal

targeting presequences that are encoded in the genes but are not present in the mature protein. Hydrogenosomal presequences are cleaved from the mature protein upon translocation by a hydrogenosomal processing peptidase which consists of two subunits similar to mitochondrial processing peptidase (MPP) (Bradley et al., 1997; Smid et al., 2008; Mentel et al., 2008).

In order to enter the mitochondria, the nuclear encoded proteins are recognized by the protein translocases inserted in the outer mitochondrial membrane called the Translocase of outer membrane (TOM) complex (Meisinger et al., 2001; Hill et al., 1998). The machinery includes protein complexes that consist of core module subunits that are common to all eukaryotes and additional subunits that have been acquired during evolution in individual eukaryotic lineages (Macasev et al., 2004; Doležal et al., 2006).

The second major import machinery in the outer membrane is the Sorting and assembly machinery (SAM50) complex, function of which is the integration and assembly of outer membrane proteins including the TOM complex (Bohnert et al., 2007; Kozjak et al., 2003). SAM50 works with the assistance of small Tim proteins which guide the substrates to the complex (Hoppins and Nargang, 2004; Koehler, 2004; Wiedemann et al., 2004).

Once the mitochondrial protein has passed through the TOM channel, it interacts with the Translocase of inner membrane (TIM) machines, two molecular systems inserted in the inner mitochondrial membrane called TIM22 and TIM23 (Rehling et al., 2003; Kovermann et al., 2002). TIM22 mediates the insertion of the proteins that have to be integrated in the inner mitochondrial membrane such as the proteins of the mitochondrial carrier family (MCF) that are guided by small Tim proteins (Rehling et al., 2003). TIM23 is the second protein channel designed for the translocation of proteins targeted to the mitochondrial matrix (Chacinska et al., 2009; Doležal et al., 2006; Neupert, 2007; Martinez-Caballero et al., 2007; Meinecke et al., 2006; Koehler, 2004; Glick et al., 1992; Stuart, 2002).

Finally, presequence translocase-associated motor (PAM), pulls the preprotein from the TIM23 channel into the matrix. In yeast the core components of the PAM complex are Ssc1 or mt-Hsp70, which is assisted by Mge1, Pam18, Pam16, Pam17 and Tim44 (van der Laan et al., 2006; Bohnert et al., 2007). PAM components except Pam17 have been found essential for cell viability (Craig et al., 1987; Maarse et al., 1992; Bolliger et al.,1994; D´Silva et al.,2003; Mokranjac et al.,2003; Truscott et al., 2003; Frazier et al., 2004; Kozany et al., 2004; Li et al., 2004; van der Laan et al., 2005). (Fig.1)

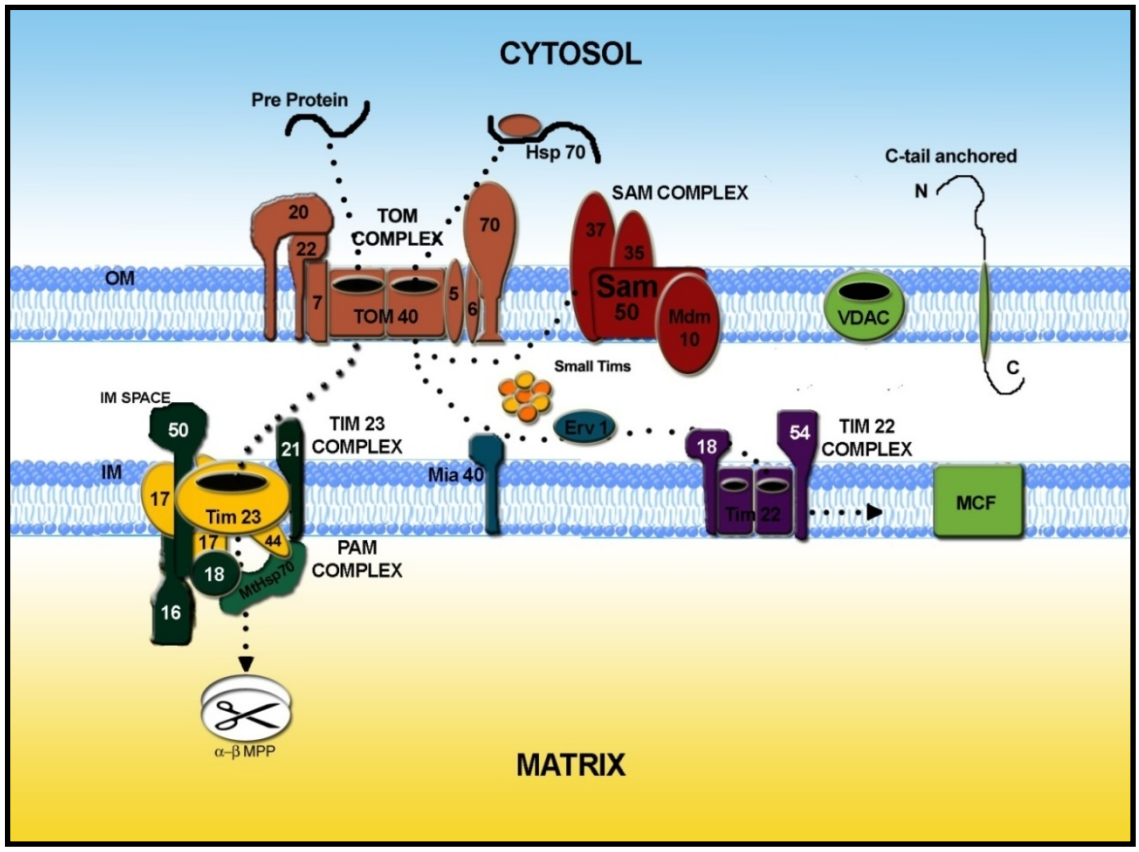

Figure1. Mitochondrial import pathways for precursor proteins (Kutik et al., 2007)

Considering that hydrogenosomes need channels for protein import and exchange of metabolites with the cytosol as mitochondria, we can expect presence of homologues of mitochondrial translocases and carriers in the membranes of the hydrogenosome. However, only two hydrogenosomal membrane proteins, i.e., Hmp31 and Hmp35, have been described in *T. vaginalis,* thus far, without homology to mitochondrial proteins (Dyall et al., 2000; Tjaden et al., 2004). Homologs to components of the SAM50, PAM and TIM23 complexes have been detected in *T. vaginalis* genome and some of them have been localized to the hydrogenosome (Carlton et al., 2007; Bui et al., 1996; Germot et al.,1996; Bozner, 1997; Dyall et al., 2003; Doležal et al., 2005; Doležal et al., 2006). Unexpectedly, initial analysis of the *T. vaginalis* genome did not reveal any TOM candidate, although some components of TOM complex have been reported in organisms with mitosomes like *Giardia intestinalis* (Dagley et al., 2009; Regoes et al., 2005; Dyall and Doležal, 2008).

4.5 Oxidative stress protection

T. vaginalis is a microaerophilic parasite with optimal growth when low oxygen concentration (less than 0.25 μM) is present (Paget and Lloyd, 1990). It is also known that the concentrations of oxygen higher than the ones found in the vaginal environment (above ≈60 μM) are lethal for the parasite (Ellis et al., 1994).

Two important hydrogenosomal proteins (PFOR and HYD) are highly sensitive to oxygen and reactive oxygen species (ROS) (Lindmark and Müller, 1973; Lloyd and Kristensen, 1985) which makes the presence of a detoxifying system in the organelle essential for the enzyme protection (Linstead and Bradley, 1988). The parasite does not need oxygen for energy metabolism. *T. vaginalis* is a fermentative organism without the ability to carry out oxidative phosphorylation. Eventhough, the hydrogenosomes displayed respiration when the gas is present in the environment.

Two cytosolic pyridine nucleotide dehydrogenases called NADH and NADPH oxidases are the main oxygen reducing enzymes in the parasite. NADH and NADPH oxidases have high activity and efficiently to reduce oxygen to water and hydrogen peroxide, respectively, which contribute to maintain the anaerobic conditions within the parasite (Linstead and Bradley, 1988; Tanabe, 1979). It is believed that *T. vaginalis* relies upon cytosolic NADH and NADPH oxidases to prevent the permeation of oxygen into the hydrogenosomes. Protons are the final electron acceptors in the hydrogenosomal metabolism of *T. vaginalis* but, when the concentration of oxygen is too high that saturates the cytosolic oxygen reductases, the gas difuses into the hydrogenosome and oxygen becomes the final electron acceptor in the organelle metabolism. At this point the hydrogen production ceased (Lloyd and Kristensen, 1985). Recently it was found that the flavin reductase enzyme, previously known as NADPH oxidase and responsible of the reduction of free flavins, is a key protein in the development of metronidazole resistance in *T. vaginalis* (Leitsch et al., 2014).

In addition to NAD(P) oxidases, trichomonads are equipped with several other detoxification mechanisms that protect the parasite from the effect of oxygen and ROS. Glutathione, a widespread antioxidant among eukaryotes, is absent in *T. vaginalis*, however cysteine is considered the major redox buffer and antioxidant in the parasite (Ellis et al., 1994). In addition, *T. vaginalis* is able to generate thiols from the action of a bacterial-like enzyme called methionine-γ-lyase that has antioxidant properties (McKie et al., 1998).

The existence of a hydrogenosomal oxygen reductase was proposed by Čerkasov in 1978 but the protein was just recently characterized as a flavodiiron protein (FDP) (Smutná et al., 2009). FDPs belong to a superfamily with a role in detoxification of oxygen and nitric oxide in anaerobic prokaryotes (Saraiva et al., 2004; Gardner et al., 2002; Gomes et al., 2002; Seedorf et al., 2004). *T. vaginalis* encodes four homologues of FDPs but only one of them carries the hydrogenosomal targeting sequence (Carlton et al., 2007; Hrdý et al., 2007). The hydrogenosomal localization of *T. vaginalis* FDP (TvFDP) was confirmed by immunofluorescence microscopy. TvFDP belongs to the Class A flavodiiron proteins. The protein reduces dioxygen to water using four electrons per cycle derived from pyruvate or NADH via ferredoxin (Smutná et al., 2009). In the same study, it was demonstrated that TvFDP is unable to utilize nitric oxide as a substrate, which was previously observed in *G. intestinalis* FDP homologue (Di Matteo et al.., 2008).

The incomplete oxygen reduction leads to the formation of reactive oxygen species (ROS) such as the superoxide radical and hydrogen peroxide. These two compounds react with iron ions through the Fenton chemistry forming the hydroxyl radicals, which are highly toxic and inactivate hydrogenosomal enzymes causing parasite dead (Hrdý et al., 2007).

The activities of catalase and other peroxide-reducing enzymes were not detectable in *T. vaginalis,* which is probably the cause for the parasite sensitivity to oxygen concentrations above physiological levels (Ellis et al., 1994). The iron-containing superoxide dismutase (FeSOD) is the superoxide-scavenging enzyme in trichomonads, which is present both in the cytosol and in the hydrogenosome of the parasite (Lindmark and Müller, 1974; Kitchener et al, 1984; Rasoloson et al., 2001; Viscogliosi et al., 1998; Ellis et al., 1994). The enzyme converts two superoxide molecules to hydrogen peroxide and oxygen (Lindmark and Müller, 1974). Seven genes encoding iron-containing superoxide dismutase (FeSODs) were identified by classical molecular methods and this finding was later confirmed by analysis of the *T. vaginalis* genome (Carlton et al., 2007).

Rubrerythrin is an enzyme with peroxidase-like activity (Jin et al., 2002) found only in anaerobic prokaryotes and *Entamoeba histolytica* (Pütz et al.,2005). Six rubrerythrin genes have been found in the genome of *T. vaginalis* and the hydrogenosomal localization of one of these gene products has been confirmed by immunofluorescence microscopy (Carlton et al., 2007; Pütz et al., 2005). In the cytosol of *T. vaginalis*, thioredoxin peroxidase together with

thioredoxin and thioredoxin reductase (TrxR) form the peroxiredoxin system (Coombs et al., 2004). Thioredoxin peroxidase belongs to a thiol peroxidase family of proteins named peroxiredoxins (McGonigle et al., 1998). The protein is a peroxide sensor that reduces toxic hydrogen peroxide, alkyl peroxides and peroxynitrites with electrons provided by thioredoxin (Rhee et al., 2005; Hofmann et al., 2002; Wood et al., 2003). TrxR is a low molecular weight protein that reduces the oxidized thioredoxin.

Components of the peroxiredoxin system have been found also in the hydrogenosome of *T. vaginalis (*Pütz et al., 2005; Henze et al., 2008). Thioredoxin and peroxiredoxin thiol peroxidase have been identified in the hydrogenosomal proteome. Thioredoxin has an N-terminal extension resembling hydrogenosomal targeting presequences (Pütz et al., 2005). Later on, two *T. vaginalis* TrxR homologues without a hydrogenosomal targeting sequence were expressed in the hydrogenosome (Henze, 2008). The study also demonstrated that N-terminal targeting sequence is not indispensable for the protein import in the hydrogenosomes and the targeting is mediated by internal signals (Coombs et al., 2004; Pütz et al., 2005; Henze, 2008).

OsmC and Ohr are proteins involved in oxygen stress protection that has been identified only in prokaryotes, so far. The proteins are involved in defense against oxidative stress caused by exposure to organic hydroperoxides (Lesniak et al., 2002; Lesniak et al., 2003). The catalytic activity of these proteins depends on highly reactive cysteine thiol groups (as in the case of peroxiredoxins) to convert hydrogen peroxides to less toxic metabolites (Lesniak et al., 2003). OsmC protein was identified in the hydrogenosome of *T. vaginalis* by a proteomic analysis and four putative homologues were identified in the *T. vaginalis* genome showing that the cysteine residues are conserved in all the sequences identified (Carlton et al., 2007). The proteins have an N-terminal sequence similar to hydrogenosomal targeting sequences and they have a role in detoxification of peroxides in hydrogenosomes (Hrdý et al., 2007; Nývltova et al., 2016).

5. A role of iron in *Trichomonas vaginalis*

T. vaginalis and other pathogens depend on its capability to acquire essential nutrients, such as iron, from the host environment to establish infection. Iron is a deleterious reductant for

living beings because it produces free radicals, so its concentrations have to be strictly regulated. Therefore, host-iron is not freely available, but tighly bound to iron-transport proteins like transferrin and lactoferrin (Dunn et al., 2007), intracellularly stored in ferritin or incorporated to functional domains of various enzymes, carriers and other proteins. Iron has numerous and diverse functions as a component of haem in haemoproteins which function as O_2 carriers, Fe-S clusters involved mainly in electron transfer and other iron containing-proteins without haem or Fe-S clusters involved in iron transport and iron storage (Crichton, 2001).

Trichomonads have high requirements for extracellular iron (50 – 100μM) and therefore have developed specific receptor-mediated mechanisms to acquire iron from lactoferrin, transferrin, haem and low-molecular-weight iron complexes (Tachezy et al., 1996; Šutak et al., 2008; Peterson and Alderete, 1984; Lehker et al., 1990; Tachezy, 1999). In *T. vaginalis* energy metabolism and oxidative stress protection are processes mainly dependent on Fe-S proteins (Vanácová et al, 2001; Gorrel, 1985). The hydrogenosome of *T. vaginalis* contains a number of Fe-S proteins that are involved in energy metabolism such as PFO, ferredoxin, NDH, ferredoxin, hydrogenase, which may explain the high requirement for iron by the parasite (Hrdý et al, 2004). Iron is indispensable also for the function of cytosolic and nuclear proteins. Rli1p is an essential protein in ribosome biogenesis and function, the protein is highly conserved among eukaryotes including *T. vaginalis* (Kispal et al, 2005; Yarunin et al., 2005; Smid et al., 2008).

In addition to housekeeping functions, iron also influences interactions between the parasite and the host cell. Previous studies have shown that the levels of cytoadherence of *T. vaginalis* cells are regulated by iron (Mundodi et al., 2006). The expression of surface adhesins (Sommer et al., 2005; Solano-Gonzalez et al., 2007; Kummer et al., 2008; Alvarez-Sánchez et al., 2007) and the increased resistance of trichomonads to complement-mediated lysis are also iron-regulated processes (Alderete et al, 1995). Importance of the ability to uptake iron by trichomonads from the host was shown to be an important virulence factor (Kulda et al, 1999; Ryu et al., 2001). Moreover, when compared with organisms grown in excess of iron, parasites cultivated under low iron concentrations showed a reduction in the rate of protein synthesis up to 80%, morphological alterations, three-fold decreased cellular densities and extended generation time up to 2.5 times (Lehker and Alderete, 1992; Melo-Braga et al., 2003; de Jesus

et al., 2007; Vanácová et al., 2001). However, the mechanisms controlling the iron-dependent regulation of these processes are unknown, so far.

The expression of the hydrogenosomal ME and PFO is positively regulated by iron at the transcriptional level (Vaňáčová et al., 2001). Transcriptional regulation has been implicated as one of the major regulatory mechanism in modulating expression of certain *T. vaginalis* virulence phenotypes in response to changing iron supply (Lehker et al., 1991). Iron dependent transcription was studied in the malic enzyme (ME) gene which encodes a 65-kDa hydrogenosomal malic enzyme. This protein was detected also as a surface adhesine AP-65-1 (Alderete et al., 1995; Hrdý and Müller M., 1995a). It was experimentally demonstrated that iron-induced transcription of the *ap-65-1* gene is regulated by the interaction of DNA regulatory elements and nuclear proteins (Tsai et al., 2002; Ong et al., 2004; Ong et al., 2006; Ong et al., 2007; Hsu et al., 2009); however, this type of iron regulatory elements have not been found in other positively iron-regulated genes that suggests the presence of another iron regulatory mechanism for gene expression. Indeed, it has been showed that expression of two cysteine proteases (TVCP4 and TVCP12) is regulated post-transcriptionally based on the interactions between cytoplasmic iron regulatory proteins (IRPs) and iron-responsive elements (IREs) located in the untranslated regions (UTRs) of messenger RNAs (mRNA) of for TVCP4 and TVCP12 (Solano-Gonzalez et al., 2007; Torres-Romero and Arroyo, 2009). This IRE/IRP system is well known for proteins involved in the storage and utilization of iron and other iron-dependent proteins (Haile et al., 1992; Hentze et al., 1996; Pantopoulos, 2004).

6. Treatment of *Trichomonas vaginalis* infection

Derivatives of 5-nitroimidazole, such as tinidazole and metronidazole, are the drug of choice for treatment of trichomoniasis and other infections caused by anaerobic or microaerophilic organisms of eukaryotic or prokaryotic origin. 5-nitroimidazoles are the only class of antimicrobial medications known to be effective against *T. vaginalis* and the drug was introduced for the treatment of trichomoniasis in 1960 (Lindmark and Müller, 1976a; Watt and Jennison., 1960; Moffett and McGill, 1960). The recommended treatment of a single dose of 2 g orally has shown a cure rate of approximately 84% - 98% (Thin et al., 1979; Spence et al., 1997; Workowski and Bolan, 2015). Although most recurrent *T. vaginalis* infections are the result of a reinfection from an untreated sex partner, 4 - 10% of treatment refractory cases

might be attributed to metronidazole resistance (Schmid et al., 2001; Schwebke and Barrientes, 2006; Kirkcaldy et al., 2012; Upcroft et al., 2009). Tinidazole is equivalent or superior to metronidazole in achieving parasitologic cure and resolution of symptoms (Wood and Monro, 1975). In addition, tinidazole resistance occurs only in 1% of the cases of trichomoniasis, but this alternative is more expensive compared with metronidazole (Schwebke and Barrientes, 2006; Workowski and Bolan, 2015). Although the prevalence of resistance is rather low, dependance on a single group of antimicrobial agents increases the possibility to develop cross-resistance in the parasite. The importance of studying the metabolic pathways involved in metronidazole activation and the biochemical mechanisms involved in drug resistance by the parasite lies in the need for new therapeutic alternatives.

6.1 Metronidazole activation

5-Nitroimidazoles are activated within the susceptible target cell by metabolic reduction producing cytotoxic radical anions that damage macromolecules. The inactive prodrug enters the cell by passive diffusion (Müller and Lindmark, 1976; Müller and Gorrell, 1983). In trichomonads, drug activation most likely takes place in the hydrogenosome where the drug enters by passive diffusion. However, recently another mechanism of the drug activation has been reported that involves cytosolic proteins (Leitsch et al., 2010).

In hydrogenosomes, the electrons generated by PFOR during pyruvate decarboxylation are transferred to hydrogenase. In the presence of metronidazole, the electrons are preferentially captured by the drug and hydrogenase production ceased (Lloyd and Kristensen, 1985). The reduction of the nitro group of the prodrug is via a single step electron transfer which results in the formation of reactive intermediates. The generation of nitro anion radicals in intact cells, cell homogenates and organelles has been demonstrated several times by EPR spectroscopy (Chapman et al., 1985; Yarlett et al., 1987; Rasoloson et al., 2002).

The alternative hydrogenosomal pathway does not involve PFOR activity (Hrdý et al., 2005). In this case, the electrons required for the reduction of the drug are generated by the NAD-dependent malic enzyme during the oxidative decarboxylation of malate. The NADH produced in this reaction is reoxidized by an enzyme with NADH: ferredoxin oxidoreductase

activity which has been identified as a homologue of the NADH dehydrogenase (NDH) module of the mitochondrial respiratory Complex I (Hrdý et al., 2004). *T. vaginalis* NDH is involved in electron transfer to metronidazole but cannot donate electrons directly to the drug. Thus, ferredoxin acts as an essential electron donor in both pyruvate- and malate-dependent pathways (Rasoloson et al., 2002; Hrdý et al., 2005).

In 2009, another model of metronidazole activation was proposed by Leitsch and colleagues. The study demonstrated that nitroimidazole drugs form covalent adducts, with proteins that have a role in maintenance of the redox balance in the parasite, like the enzymes from the thioredoxin system. Hence, it was found that the flavin enzyme thioredoxin reductase displays nitroreductase activity with nitroimidazoles, including metronidazole. It was shown that the formation of covalent adducts with protein and non-protein thiols enhance the toxicity of nitroimidazoles by the disruption of the cellular redox system (Leitsch et al., 2009). This mechanism seems to take place in the cytosol and challenged the model of hydrogenosomal activation of nitroimidazole drugs.

6.2 Metronidazole resistance

T. vaginalis can develop two types of metronidazole resistance named aerobic and anaerobic according to the conditions at which the resistance could be observed.

Aerobic resistance is typically found in clinical isolates from treatment-refractory patients (Ellis et al., 1994; Rasoloson et al., 2001; Meingassner and Thurner, 1979; Kirkcaldy et al., 2012) and it can be induced *in vitro* by exposing the metronidazole-sensitive *T. vaginalis* to low doses of metronidazole for a relatively short period of time (Tachezy et al., 1993; Rasoloson et al., 2002). This type of resistance has been attributed to the defect in oxygen scavenging system which leads to increased level of intracellular oxygen. It probably causes re-oxidation of the metronidazole radical ion, and consequently the detoxification of the drug (Lloyd and Pedersen, 1985; Yarlett et al., 1986). It is important to notice that the natural habitat of *T. vaginalis* is not anaerobic and the parasite is exposed to a variable oxygen tension at the vaginal surface (Wagner and Levin, 1978). In cells expressing the aerobic type of resistance, the hydrogenosomal pathway responsible for the activation of the drug remains active and the cells are susceptible to metronidazole under anaerobic conditions (Müller and

Gorrell 1983; Ellis et al., 1992; Tachezy et al., 1993). *T. vaginalis* strains displaying aerobic resistance showed decreased tolerance to oxygen (Ellis et al., 1994; Rasoloson et al., 2001) which affects the viability of the cell under oxygen stress. Aerobic resistance also showed up-regulation of the iron-containing superoxide dismutase (Fe-SOD) that was observed in both clinical isolates and the in-vitro induced strain probably as a response to the presence of intracellular oxygen and its reactive metabolites (Ellis et al. 1994; Rasoloson et al., 2001).

Initially it has been suggested that aerobic resistance could be mediated by an altered ferredoxin function or insufficient amount of ferredoxin based on the reduction of gene transcription in resistant strains (between 40% and 65%) which results in decreased intracellular levels of the protein in the resistant strain compared with the sensitive strain (Yarlett et al. 1986b; Quon et al. 1992). However, no significant differences in ferredoxin levels between the drug-susceptible *T. vaginalis* strain and its aerobically resistant derivative were found on protein level in later studies (Rasoloson et al., 2001; Rasoloson et al., 2002). Moreover, identical signals for functional ferredoxin iron sulfur centers were found in the aerobic resistant strain induced *in vitro*, the susceptible strain and a clinical isolate expressing aerobic resistance (Rasoloson et al., 2001).

Leitsch and colleagues (2010) demonstrated that metronidazole resistance in the parasite is associated with lost of flavins and thioredoxin reductases activities. This is supported by observation that treatment of *T. vaginalis* with DPI (diphenyleneiodonium), a flavin´s inhibitor, which inhibited thioredoxin reductase activity and reduced free flavins (Leitsch et al., 2010). The results were corroborated by the measurement of thioredoxin reductase activity in a highly metronidazole-resistant strain developed *in vitro* showing that the activity was completely absent in this cell line (Leitsch et al., 2009). Taken together, DPI-treated cells displayed a flavin metabolism similar to that found in metronidazole-resistant *T. vaginalis* strain. However, PFOR activity was upregulated in DPI-treated cells under low oxygen tension. Therefore, they proposed that the loss of hydrogenosomal pathways could be linked with the absence of flavins reducing enzymes that affect the cellular redox status in the cell and the reduced expression of hydrogenosomal enzymes could be a consequence and not the cause of the resistance to metronidazole. The study showed that thioredoxin reductase is only an essential enzyme under aerobic conditions because not even the growth was inhibited under anaerobic condition in DPI-treated *T.vaginalis* (Leitsch et al., 2010).

The anaerobic type of resistance was induced in *vitro* and it is associated with loss of the metronidazole activation pathway. The development of resistance was accomplished by exposing the drug-susceptible cells to daily passages in culture medium containing increasing concentrations of metronidazole (2-100 ug/ml) for a prolonged period of time in vitro (1-2 years) (Kulda et al., 1984; Kulda et al., 1993; Brown et al., 1999). The resistant strains developed high tolerance to the drug and were able to multiply in the presence of 100µl/ml of metronidazole. The uptake of metronidazole by these strains was undetectable and therefore the signals for nitro free radicals were absent in the EPR spectra, indicating that the drug was not activated (Kulda et al., 1989). The resistance to metronidazole was acquired in a stepwise process; the aerobic resistance was induced at the first stage (growth at 3 ug/ml metronidazole) and the gradual elimination of the hydrogenosomal enzymes responsible for the drug activation was observed during adaptation to 5-100 ug/ml (Rasoloson et al. 2002).

Absence of PFOR activity was observed in the strain cultivated at 5 µg/ml of metronidazole which represented the early stage of anaerobic resistance (Rasoloson et al., 2002) The susceptibility to the higher concentrations could be attributed to the alternative pathway of the drug activation that involves the hydrogenosomal malic enzyme, NDH and ferredoxin, which are active at this stage of resistance development (Rasoloson et al. 2002). At this stage, the hydrogenosomes generate metronidazole anion radicals as detected by EPR spectroscopy (Hrdý et al., 2005). A gradual reduction of hydrogenase activity was observed with increasing resistance; however, the decrease was slower than that found in PFOR and the activity of hydrogenase disappear later (Kabíčková et al., 1988; Rasoloson et al., 2002). The enzymatic activities of PFOR, malic enzyme, NDH, hydrogenase, and ferredoxin were lost in the hydrogenosomes of fully anaerobic resistant parasites, in which production of metronidazole anion radicals was not observed (Kulda et al., 1989; Rasoloson et al., 2002; Hrdý et al., 2005). Additionally, NAD(P)H nitroreductases and Nim proteins have been reported to have a role in metronidazole activation, and metronidazole resistance, respectively. At least five genes coding for nitroreductases have been found in *T. vaginalis* genome however, none of them have the hydrogenosomal targeting sequence, suggesting a cytosolic localization of nitroreductases in *T. vaginalis.* In the pathogenic bacteria *Helicobacter pylori* resistance to metronidazole has been associated with mutation in the chromosomal genes encoding nitroreductases. These proteins can convert metronidazole into a toxic product such as

hydroxylamine which is both bactericidal and mutagenic (Goodwin et al., 1998; Jenks et al., 1999; Jeong et al., 2000; Mendz and Mégraud, 2002). Nim proteins confer 5-nitroimidazole resistance in certain strains of *Bacteroides fragilis*. It was shown that the resistant bacteria produce nitro anion radicals; however, the radicals are rapidly converted to a non toxic amine derivative in the presence of the Nim (Carlier et al. 1997). Studies of the crystal structures of the NimA protein from *Deinococcus radiodurans* have identified a catalytically important histidine residue along with pyruvate and antibiotic binding sites. The reaction mechanism involves the 2-electron reduction of the antibiotic that prevents the accumulation of the toxic nitro radical (Leiros et al., 2004). Three Nim homologues have been found in *T. vaginalis*, two of them with predicted hydrogenosomal targeting signal (Carlton et al., 2007) and all of them possess the conserved histidine residue found in *Deinococcus radiodurans* (Leiros et al., 2004).

7. Aims of the thesis

- To develop the method for isolation of highly purified hydrogenosomes and mitosomes from *Trichomonas vaginalis* and *Giardia intestinalis* respectively.
- To compare the gene expression in *Trichomonas vaginalis* cultivated under different iron level.
- To analyze iron-dependent changes in the proteome of *Trichomonas vaginalis* hydrogenosome using mass spectrometry.
- To investigate changes in the proteome of *Trichomonas vaginalis* strains during *in vitro* induction of resistance to metronidazole.

8. List of Publications

Beltrán NC, Horváthová L, Jedelský PL, Sedinová M, Rada P, Marcinčiková M, Hrdý I, Tachezy J. (2013) Iron-induced changes in the proteome of *Trichomonas vaginalis* hydrogenosomes. PLoS One. 5:e65148. 50%

Horváthová L, Šafaríková L, Basler M, Hrdý I, **Campo NB**, Shin JW, Huang KY, Huang PJ, Lin R, Tang P, Tachezy J (2012) Transcriptomic identification of iron-regulated and iron-independent gene copies within the heavily duplicated *Trichomonas vaginalis* genome. Genome Biol Evol. 10:1017-29. 20%

Rada P, Doležal P, Jedelský PL, Bursac D, Perry AJ, Šedinová M, Smíšková K, Novotný M, **Beltrán NC**, Hrdý I, Lithgow T, Tachezy J. (2011) The core components of organelle biogenesis and membrane transport in the hydrogenosomes of *Trichomonas vaginalis*. PLoS One. 9:e24428. 20%

Jedelský PL, Doležal P, Rada P, Pyrih J, Smíd O, Hrdý I, Sedinová M, Marcinčiková M, Voleman L, Perry AJ, **Beltrán NC**, Lithgow T, Tachezy J. (2011) The minimal proteome in the reduced mitochondrion of the parasitic protist *Giardia intestinalis*. PLoS One. 2:e17285. 20%

Zedníková V, **Beltrán NC**, Tachezy J, Hrdý I. (2012) Alternative 2-keto acid oxidoreductases in *Trichomonas vaginalis*: artifact of histochemical staining. Mol Biochem Parasitol. 1:57-9. 10%

8.1 Iron-induced changes in the proteome of *Trichomonas vaginalis* hydrogenosomes.

OPEN ACCESS Freely available online

PLOS ONE

Iron-Induced Changes in the Proteome of *Trichomonas vaginalis* Hydrogenosomes

Neritza Campo Beltrán, Lenka Horváthová, Petr L. Jedelský, Miroslava Šedinová, Petr Rada, Michaela Marcinčiková, Ivan Hrdý, Jan Tachezy*

Department of Parasitology, Charles University in Prague, Faculty of Science, Prague, Czech Republic

Abstract

Iron plays a crucial role in metabolism as a key component of catalytic and redox cofactors, such as heme or iron-sulfur clusters in enzymes and electron-transporting or regulatory proteins. Limitation of iron availability by the host is also one of the mechanisms involved in immunity. Pathogens must regulate their protein expression according to the iron concentration in their environment and optimize their metabolic pathways in cases of limitation through the availability of respective cofactors. *Trichomonas vaginalis*, a sexually transmitted pathogen of humans, requires high iron levels for optimal growth. It is an anaerobe that possesses hydrogenosomes, mitochondrion-related organelles that harbor pathways of energy metabolism and iron-sulfur cluster assembly. We analyzed the proteomes of hydrogenosomes obtained from cells cultivated under iron-rich and iron-deficient conditions employing two-dimensional peptide separation combining IEF and nano-HPLC with quantitative MALDI-MS/MS. We identified 179 proteins, of which 58 were differentially expressed. Iron deficiency led to the upregulation of proteins involved in iron-sulfur cluster assembly and the downregulation of enzymes involved in carbohydrate metabolism. Interestingly, iron affected the expression of only some of multiple protein paralogues, whereas the expression of others was iron independent. This finding indicates a stringent regulation of differentially expressed multiple gene copies in response to changes in the availability of exogenous iron.

Citation: Beltrán NC, Horváthová L, Jedelský PL, Šedinová M, Rada P, et al. (2013) Iron-Induced Changes in the Proteome of *Trichomonas vaginalis* Hydrogenosomes. PLoS ONE 8(5): e65148. doi:10.1371/journal.pone.0065148

Editor: Gunnar F. Kaufmann, The Scripps Research Institute and Sorrento Therapeutics, Inc., United States of America

Received March 5, 2013; **Accepted** April 17, 2013; **Published** May 31, 2013

Funding: This work was supported by the Czech Ministry of Education (MSM 0021620858) and Charles University in Prague (UNCE 204017). The funders had no role in study design, data collection and analysis, decision to publish, or preparation of the manuscript.

Competing Interests: The authors have declared that no competing interests exist.

* E-mail: tachezy@natur.cuni.cz

Introduction

Iron is an essential element for virtually all forms of life. It plays an indispensable role as a component of metalloproteins, either bound to more or less complex prosthetic groups, such as heme or iron-sulfur (FeS) clusters, or alone, such as in the case of ribonucleotide reductase, the key enzyme of DNA metabolism. Metalloproteins are involved in many vital cellular functions, including electron transport, enzymatic catalysis, redox sensing and regulation of gene expression [1]. In addition to housekeeping functions, iron influences the virulence of pathogenic microorganisms, which is underlined by the observations that host iron withholding is markedly reinforced during microbial infection [2]. Therefore, invading pathogens have evolved effective iron-acquisition mechanisms to meet their needs for iron [3].

Trichomonas vaginalis is a sexually transmitted anaerobic parasitic protist of the Excavata group that infects humans, with an estimated worldwide annual incidence of 170 million cases [4,5]. One of the most prominent characteristics of this parasite is the lack of "classical" oxygen-respiring mitochondria. Instead, trichomonads possess hydrogenosomes, mitochondria-type organelles that produce molecular hydrogen and among other functions, synthesize ATP through substrate-level phosphorylation [6]. Trichomonads require unusually high concentrations of iron in in vitro cultures [7]. This need has been largely attributed to the dependence of trichomonads upon the activities of FeS cluster-containing proteins, which mediate vital energy-conserving reactions in the parasite's hydrogenosomes [8], but it may also be related to the fact that trichomonads apparently lack substantial levels of iron-storage proteins, such as ferritin [3]. Thus, high extracellular iron may be required to furnish the turnover of FeS proteins. Lactoferrin, heme and low-molecular-weight iron complexes can serve as an external source of iron for *T. vaginalis* [9].

The FeS proteins involved in hydrogenosomal energy metabolism are pyruvate:ferredoxin oxidoreductase (PFO), electron carrier ferredoxin, [FeFe]-hydrogenase and two-subunit remnants of respiratory complex I. PFO oxidatively decarboxylates pyruvate, which is supplied from the cytosol or through the activity of non-FeS hydrogenosomal malic enzyme, to acetyl-CoA, which is converted to acetate by the activity of acetate:succinate-CoA transferase in a succinate-dependent reaction. The resulting succinyl-CoA serves as a substrate for ATP synthesis by succinate thiokinase, while electrons released from pyruvate are transported via ferredoxin to hydrogenase, which forms molecular hydrogen (see [9] for review). NADH resulting from the malic enzyme reaction can be reoxidized by the complex I remnant [10]. In addition to the proteins involved in hydrogenosomal carbohydrate metabolism, other hydrogenosomal Fe-containing proteins include FeS flavoproteins, the flavodiiron oxygen reductase, peroxidase rubrerythrin, proteins of the FeS cluster assembly system (ISC), hybrid cluster protein, Fe superoxide dismutase and possibly others [11–14].

Iron availability markedly influences hydrogenosomal catabolism, and increased activities of FeS enzymes involved in hydrogenosomal energy metabolism have been observed upon iron supplementation [7,8,15]. Clearly, there is effective regulation linking the activity/expression of FeS proteins and iron availability. Even the expression of non-FeS proteins, such as malic enzyme, has been shown to be regulated by iron [8,15–16]. The list of iron-regulated genes has been greatly extended by our previous work, which demonstrated a marked effect of iron on the *T. vaginalis* transcriptome [18]. Among the hundreds of regulated genes identified in this study, hydrogenosomal carbohydrate metabolism and ISC assembly machinery appeared to be the most important pathways influenced by this critical nutrient. *T. vaginalis* genes are typically present in multiple copies [19], and intriguingly, in most cases expression of only certain paralogues was regulated by iron [18]. The effect of iron limitation on *T. vaginalis* morphology and overall proteome changes was studied by De Jesus et al. [20]. Cells from iron-depleted medium displayed altered morphology, including the internalization of flagella and the axostyle and transformation to a larger and rounded shape. Observed changes in protein expression included the downregulation of PFO and cysteine proteases, while actin was upregulated in iron-depleted trichomonads [21]. However, the two-dimensional gel electrophoresis (2DE) used to separate the protein samples prior to MS identifications in the previous study is known to often fail to resolve membrane proteins, low-abundance proteins, proteins with extreme pI values and very small or large proteins [22], resulting in an incomplete list of identified proteins, potentially including those affected by changes in external conditions. Therefore, to obtain a better picture of the effect of iron limitation on trichomonads, we utilized a gel-free approach based on isobaric tag labeling (iTRAQ), isoelectric focusing of tryptic peptides and nano-LC-MALDI identification. We specifically focused on hydrogenosomes because many FeS proteins reside in these organelles, along with the FeS cluster assembly machinery.

Methods

Parasite Cultivation

Trichomonas vaginalis strain T1 (J.H. Tai, Institute of Biomedical Sciences, Taipei, Taiwan) was grown in Diamond's trypticase-yeast-extract-maltose (TYM medium) supplemented with 10% heat-inactivated horse serum without agar at pH 6.2 [23]. The iron-supplemented medium was prepared by adding ammonium ferric citrate to a final iron concentration of 86 μM. Iron-restricted cells were subcultured for 10 passages in iron-deficient TYM medium prepared without ammonium ferric citrate and supplemented with 2,2′-dipyridyl (Sigma Chemical Co., St. Louis, Missouri) to a final concentration of 70 μM.

Cell Fractionation and Hydrogenosome Isolation

One-liter cultures of *T. vaginalis* cells grown under iron-enriched (+Fe) and iron-depleted (−Fe) conditions were harvested by centrifugation at 1300×g for 12 minutes at 4°C and washed twice with 50 ml of phosphate-buffered saline (PBS) and once with 50 ml of isotonic ST buffer (250 mM sucrose, 10 mM Tris, and 0.5 mM KCl, pH 7.2). Subsequent steps were performed at 4°C in ST buffer supplemented with the protease inhibitors TLCK 50 μg/ml (tosyl lysyl chloromethyl ketone) and leupeptin 10 μg/ml. Cell pellets were resuspended in 40 ml of ST buffer and sonicated on ice until approximately 90% of the cells were disrupted. The homogenate was centrifuged at 800×g for 15 minutes to remove the nuclei and unbroken cells. The supernatant was centrifuged at 17000×g for 20 minutes, resulting in an enriched large granular fraction (LGF, sediment) and crude cytosolic fraction (supernatant). The enriched LGF was further fractionated using a discontinuous Optiprep^{tm} gradient (Axis-Shield). To prepare the gradient, 0.5 ml of 50% (w/v) Optiprep working solution was applied to the bottom of the tube, and 1 ml of each lower-density solution (ranging from 36 to 18% in 2% steps) was layered successively. The Optiprep working solution was prepared by diluting the original Optiprep^{tm} to 50% using a diluent recommended for general purposes (0.25 M sucrose, 6 mM EDTA and 60 mM Tris-HCl, pH 7.4). Successive gradient solutions were prepared by diluting the 50% working solution with homogenization buffer (0.25 M sucrose, 1 mM EDTA and 10 mM Tris-HCl, pH 7.4) to the specific concentration. The LGF was resuspended in 0.5 ml of homogenization buffer and layered on top of the gradient. The gradient was centrifuged in a swinging bucket rotor at 200,000×g for 2 hours at 4°C. The separated fractions were then carefully removed using a micropipette, and each fraction was washed separately with ST buffer containing protease inhibitors at 21,000×g for 20 minutes at 4°C.

SDS-PAGE and Western Blotting

SDS-PAGE and Western blotting were used to analyze the protein composition of Optiprep-sucrose-purified hydrogenosomes. SDS-PAGE was performed with a Bio-Rad miniprotean gel apparatus using a 12% gel. Electrophoretically resolved proteins were stained with Coomassie brilliant blue or transferred to a nitrocellulose membrane to be probed with polyclonal rabbit antiserum against hydrogenosomal malic enzyme [24].

Transmission Electron Microscopy (TEM)

Pellets of each fraction obtained from the Optiprep-sucrose gradients were fixed for 24 hours in 2.5% glutaraldehyde in 0.1 M cacodylate buffer (pH 7.2) and postfixed in 2% OsO_4 in the same buffer. Fixed specimens were dehydrated with an ascending ethanol and acetone series and embedded in an Araldite - Poly/Bed® 812 resin mixture. Thin sections were cut on a Reichert-Jung Ultracut E ultramicrotome and stained using uranyl acetate and lead citrate. Sections were examined and photographed using a JEOL JEM-1011 electron microscope with a Megaview III camera and analySIS 3.2 software (Soft Imaging System®).

Determination of Enzymatic Activities

The activities of hydrogenosomal and non-hydrogenosomal enzymes were measured spectrophotometrically at 25°C in all fractions. Hydrogenosomal malic enzyme was measured aerobically at 340 nm as the rate of malate-dependent NAD^+ reduction [24], and the lysosomal marker enzyme acid phosphatase was measured according to Barret (1972). The activities were determined immediately after organelle isolation. Protein concentrations in the fractions were determined by the Lowry method.

Protein Digestion and iTRAQ Labeling

Aliquots of hydrogenosomal fractions containing 100 μg of total protein were precipitated with 300 μl of acetone overnight at −20°C. The precipitate was centrifuged, acetone was carefully removed, and the remaining traces of acetone were left to evaporate for 5 minutes. Sample dissolution, reduction, alkylation, digestion and iTRAQ 4-plex labeling were performed according to the manufacturer's instructions (AB Sciex, Foster City, CA) using sequencing-grade porcine trypsin (Promega). Combined samples were precipitated with 500 μl of acetone overnight at −20°C.

Isoelectric Focusing, Extraction and HPLC

Combined iTRAQ-labeled samples were dissolved in 250 µl of 2 M urea and poured into the 17 cm focusing tray of a Protean IEF Cell (Bio-Rad, Hercules, CA, USA). The sample was covered with 17 cm IPG strips (pH 3–10, Bio-Rad) without paper wicks or oil. Active rehydration at 50 V for 2 hours was followed by voltage steps of 100, 250, 500 and 1000 V for 15 minutes and a maximum of 10 kV until 40 kVHrs was reached. The final step was set at 500 V forever. The current was limited to 50 µA, and only one strip was focused at a time.

The strip was cut into pieces approximately 2–3 mm wide. The pieces were sonicated for 15 minutes in 20 µl of 10% acetonitrile (ACN) with 0.1% trifluoroacetic acid. The supernatants were mixed 1:1 with water and subjected to nano-reverse-phase HPLC. LC separation was performed with an Ultimate 3000 HPLC system (Dionex, Framingham, MA) coupled to a Probot micro-fraction collector (Dionex). A PepMap 100 C18 RP column (particle size 3 µm, length 15 cm, internal diameter 75 µm; Dionex) with pre-column (PepMap 300 C18, particle size 5 µm, 300 Å wide pore, length 5 mm, internal diameter 300) was used for separation with a gradient of 4% (v/v) acetonitrile and 0.1% (v/v) trifluoroacetic acid to 80% (v/v) acetonitrile and 0.1% (v/v) trifluoroacetic acid for 60 minutes. The flow rate was set to 300 nl/min. The eluate was mixed 1:3 with matrix solution (2 mg/ml α-cyano-4-hydroxycinnamic acid in 80% ACN) with the Probot micro-fraction spotter prior to spotting onto a MALDI target. The spotting frequency was 5 spots per minute; i.e., 60 nl eluate +180 nl matrix solution per MALDI spot.

Mass Spectrometry

Spectra were acquired on a 4800 Plus MALDI TOF/TOF analyzer (AB Sciex) equipped with an Nd:YAG laser (355 nm, firing rate 200 Hz). All spots were first measured in MS mode from m/z 800 to 4,000, and then, up to the 15 strongest precursors were selected for MS/MS analysis, which was performed with 1 kV collision energy and the operating pressure of the collision cell set to 10^{-6} Torr. Tandem mass spectra were processed with a 4000 Series Explorer with subtract baseline enabled (peak width 50), Gaussian smoothing applied with filter width 5, minimum signal to noise 8, local noise window width 250 m/z, minimum peak width at full width half max 2.9 bins, cluster area signal to noise optimization enabled (threshold 15) and flag monoisotopic peaks enabled (generic formula C_6H_5NO).

Proteomic Data Analysis

A database search was performed with GPS Explorer v. 3.6 (AB Sciex) with locally installed Mascot v. 2.1 (Matrix Science) against the database of annotated *T. vaginalis* protein sequences from TrichDB (http://trichdb.org, release-1.2, 21-Sep-2010, 119344 sequences) with trypsin digestion, methyl methanethiosulfonate modification of cysteines and N-terminal and an ε-amino group of lysine modified with iTRAQ 4-plex reagents as fixed modifications and methionine oxidation as the variable modification. Precursor tolerance was set to 100 ppm, and the MS/MS fragment tolerance was 0.2 Da. The maximum peptide rank was 1, and the minimum ion score confidence interval (CI) per peptide was 95%. Spectra assigned to more than one protein were not used for quantitation. Average iTRAQ ratios and standard deviations were calculated for each protein using all of the available treatment/control iTRAQ pairs.

Bioinformatic searches based on protein BLAST (http://www.ncbi.nlm.nih.gov/blast) and hidden Markov models (http://toolkit.tuebingen.mpg.de/hhpred) were used to verify and manually edit TrichDB annotations. All identified protein sequences were analyzed using programs for subcellular localization prediction, including PSORT II (http://psort.hgc.jp/form2.html), TargetP (http://www.cbs.dtu.dk/services/TargetP/), Euk-mPLoc 2.0 (http://www.csbio.sjtu.edu.cn/bioinf/euk-multi-2/) and Yloc (http://abi.inf.uni-tuebingen.de/Services/YLoc/webloc.cgi). The NetBeans Platform application (Hunter software) was used to predict hydrogenosomal N-terminal targeting sequences as described previously [25].

Results and Discussion

Identification of Hydrogenosomal Proteins by Mass Spectrometry

To investigate changes in the *T. vaginalis* hydrogenosomal proteome caused by iron limitation, trichomonads were grown in media supplemented with 70 µM of the iron chelator 2,2-dipyridyl (iron-restricted conditions, −Fe). As a control, we used trichomonads grown in media supplemented with ammonium ferric citrate to a final iron concentration of 86 µM (iron-rich conditions, +Fe). Highly purified hydrogenosomes were obtained from homogenates of both cultures through differential centrifugation followed by preparative centrifugation of the large granular fraction using a discontinuous Optiprep (iodixanol) gradient. Ten distinct bands with variable thickness and density were obtained under both iron conditions. The band appearance/distribution differed between the +Fe and -Fe conditions (Fig. 1). Western blot analyses of fractions showed that the hydrogenosomal marker malic enzyme was particularly enriched in fractions #7 and #8 under iron-rich (+Fe) conditions and fractions #6 and #7 under iron-depleted (−Fe) conditions (Fig. 1). The fraction purity was further examined with electron microscopy (Fig. 1) and the determination of enzymatic activities of the hydrogenosomal and lysosomal markers malic enzyme and acid phosphatase, respectively (Fig. S1). Based on these results, fraction #7 appeared to be the purest hydrogenosomal fraction with the least contamination and was therefore chosen for the comparative proteomic analysis.

Proteins in this fraction were digested and labeled using the iTRAQ 4-plex kit. The labeled peptides were fractionated using isoelectric focusing and analyzed using LC-MS/MS. Five independent biological replicates were included in the analysis. Two pairs of biological replicates were processed and measured in two iTRAQ -LC-MS analyses, and one pair was measured in a separate analysis. In total, we acquired over 64,000 MS/MS spectra in 200 LC runs. The Mascot 2.1 search engine identified a total of 631 proteins, which were then classified into functional categories (Table S1). Spectra assigned to more than one protein were not used for quantitation. The average ratio for each protein was calculated from all available iTRAQ pairs. Only values calculated using at least three pairs were included. Proteins with an average ratio (fold change) of at least ±2.0 were considered differentially expressed.

To distinguish hydrogenosomal proteins from non-hydrogenosomal contamination, five different bioinformatic tools for the prediction of subcellular localization (PSORT II, TargetP, Euk-mPLoc 2.0, and Yloc and Hunter) were used (Table S1). A protein was considered putatively hydrogenosomal if mitochondrial localization was predicted by at least one of the tools. These predictions yielded 287 putative hydrogenosomal proteins (Table S1). In the final list of hydrogenosomal proteins (Table S2), we excluded all proteins in categories that were not related to the hydrogenosome and were most likely externally associated with other organelles (cytoskeleton, histone/DNA, vacuolar proteins, protein synthesis and modification, signaling pathways, signal transduction and vesicle transport) [14] and proteins for which

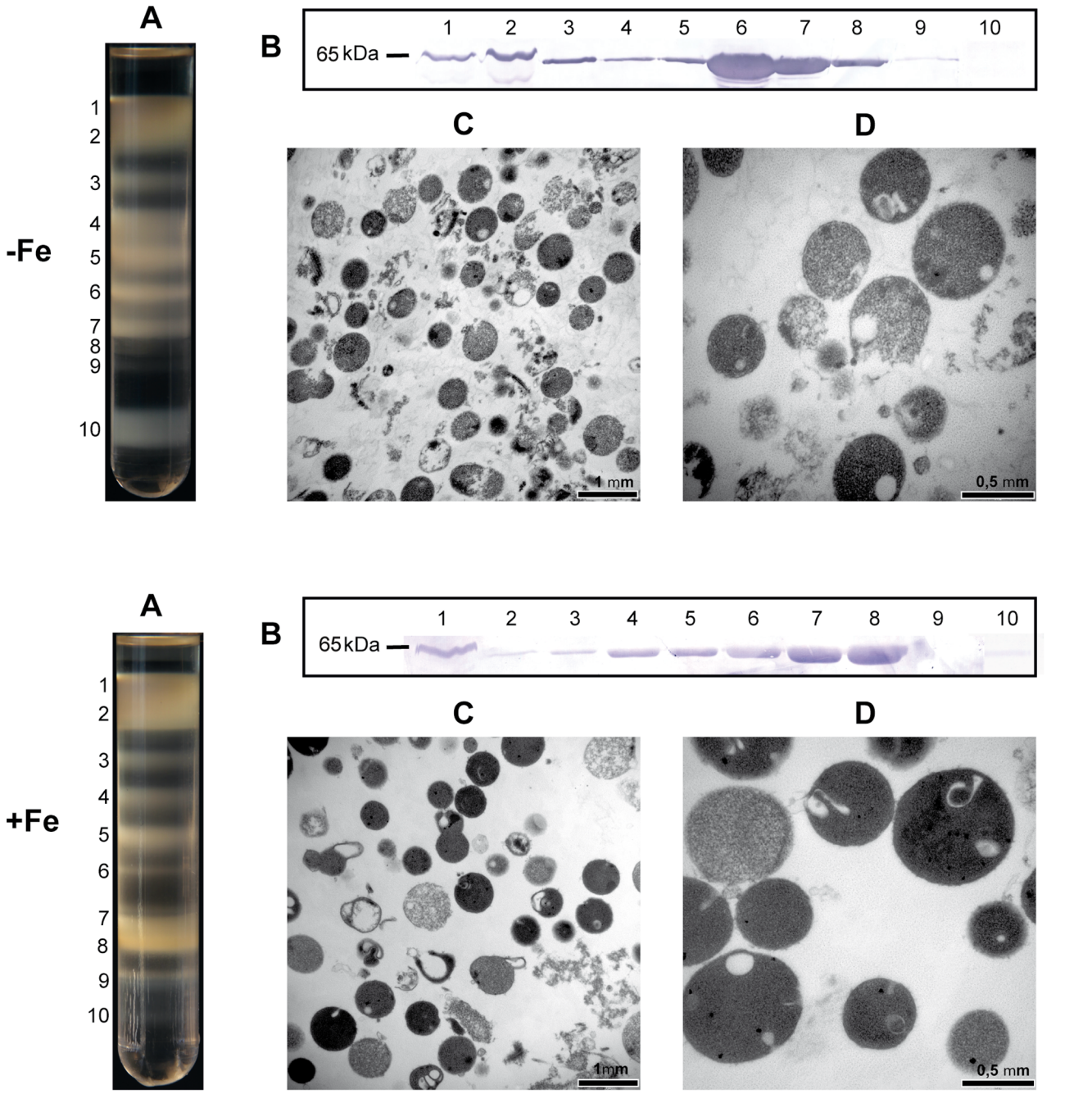

Figure 1. Isolation of hydrogenosomal fractions from *T. vaginalis* cells grown under iron-enriched (+Fe) and iron-depleted (−Fe) conditions. (A) The fraction enriched in hydrogenosomes was further fractionated with an Optiprep density gradient. (B) Analysis of Optiprep fractions by Western blotting using an antibody against hydrogenosomal malic enzyme. (C–D) Transmission electron microscopy of fraction #7, which was chosen for proteomic analysis.
doi:10.1371/journal.pone.0065148.g001

non-hydrogenosomal localization was confirmed experimentally [13,26]. However, we included proteins and their paralogues that were not recognized by the above-mentioned tools but were experimentally identified as hydrogenosomal proteins by others [13,14,26]. Using this approach, we selected 179 proteins (Table S2). We used relatively stringent criteria to eliminate all probable contaminants, and therefore, the final number of putative genuine hydrogenosomal proteins was considerably lower than that previously published by Schneider et al. [14]. Nevertheless, we identified several new paralogues of known hydrogenosomal proteins (e.g., ferredoxins, Nfu and Isd11) and proteins that had been overlooked by previous analyses [13,14], such as frataxin and HydE (Table S2). Altogether, of the 179 proteins identified as likely to be hydrogenosomal, we obtained a fold change of at least 2.0 for 58 proteins; 31 of these proteins were upregulated, and 27 were downregulated under iron-deficient conditions (Table 1).

Table 1. Significantly regulated proteins in iron depleted conditions.

DOWNREGULATED			UPREGULATED		
Accession No.	**Annotation**	**Fold change**	**Accession No.**	**Annotation**	**Fold change**
TVAG_230580	Pyruvate:ferredoxin oxidoreductase BI	−37,4	TVAG_469020	HydG-1	10,4
TVAG_254890	Pyruvate:ferredoxin oxidoreductase E	−16,9	TVAG_146780	Nfu-4	8,7
TVAG_242960	Pyruvate:ferredoxin oxidoreductase BII	−13,5	TVAG_479680	2-nitropropane dioxygenase precursor	5,4
TVAG_310050	[Fe] hydrogenase-3	−9,0	TVAG_451860	Nfu-3	4,7
TVAG_265760	FAD/FMN-binding family protein-4	−8,8	TVAG_253630	Hsp70 mitochondrial type-3	3,5
TVAG_292710	Ferredoxin 4	−6,6	TVAG_008840	Nfu-2	3,2
TVAG_064490	Rubrerythrin-1	−6,4	TVAG_055320	IscA2-2	3,2
TVAG_154730	Iron-sulfur flavoprotein (ISF3)	−6,3	TVAG_044500	Nfu-1.	3,1
TVAG_399860	Ferredoxin 2	−5,9	TVAG_361540	IscA2-3	2,8
TVAG_198110	Pyruvate:ferredoxin oxidoreductase A	−5,4	TVAG_329200	HydE-2	2,7
TVAG_049140	Superoxide dismutase [fe], putative	−5,3	TVAG_282580	Conserved unknown protein	2,6
TVAG_183790	Malic enzyme F	−4,8	TVAG_412560	OsmC-2	2,5
TVAG_076510	Serine palmitoyltransferase	−4,2	TVAG_048590	Thioesterase family protein	2,5
TVAG_412220	Malic enzyme D.	−3,8	TVAG_344280	Conserved unknown protein	2,5
TVAG_296220	Complex 1, Tvh21	−3,6	TVAG_342900	Flavine reductase	2,4
TVAG_037570	[Fe] hydrogenase-2 (64 kDa)	−3,3	TVAG_060450	Acetyltransferase-1	2,3
TVAG_395550	Acetate:succinate CoA transferase-3	−3,2	TVAG_385350	Thioredoxin	2,3
TVAG_466790	Pyruvate:ferredoxin oxidoreductase F	−3,0	TVAG_456770	IscA2-1	2,3
TVAG_181350	Conserved unknown protein	−2,9	TVAG_242760	Isd11-1	2,2
TVAG_133030	Complex 1, Tvh47	−2,9	TVAG_182340	Mge (GrpE) protein −1	2,2
TVAG_003900	Ferredoxin 1	−2,8	TVAG_183850	Arginine deiminase −3	2,1
TVAG_416100	Malic enzyme C	−2,4	TVAG_370860	Tim17/22/23C	2,1
TVAG_047890	Succinyl-CoA synthetase, alpha	−2,3	TVAG_177600	Glycine cleavage system H protein	2,1
TVAG_182620	[Fe] Hydrogenase-1 (50 kDa)	−2,3	TVAG_381290	Hsp20-3	2,0
TVAG_340290	Malic enzyme H	−2,1	TVAG_277380	Ind-4 (P-Loop ATPase)	2,0
TVAG_104250	Hmp35 -2	−2,1	TVAG_205390	HydF	2,0
TVAG_351540	FAD/FMN-binding family protein-3	−2,0	TVAG_086470	Thioredoxin	2,0
			TVAG_433130	Hsp70 mitochondrial type-6	2,0
			TVAG_467820	Arginine deiminase -1	2,0
			TVAG_318670	Succinyl-CoA synthetase, alpha	2,0
			TVAG_109540	Serine hydroxymethyltransferase	2,0

doi:10.1371/journal.pone.0065148.t001

Iron-sulfur Cluster Assembly

Hydrogenosomes of *T. vaginalis* possess machinery required for the formation of FeS clusters, which is homologous to the mitochondrial ISC system [27–29]. Iron depletion caused the increased expression of almost all known components involved in hydrogenosomal ISC assembly machinery; however, some of these components did not reach the cut-off limit (Fig. 2, Table 1). All three detected paralogues of the scaffold protein IscA-2 and four detected copies of Nfu scaffolds were significantly upregulated; however, the expression of a single copy of IscU, which is believed to act as a principal scaffold, did not show iron-dependent regulation (Table 1). This may suggest that *Trichomonas* uses the alternative scaffolds IscA and Nfu preferentially over IscU. Unlike mitochondria, which possess two types of IscA homologues (Isa1 and Isa2), only IscA-2-encoding genes were identified in the *T. vaginalis* genome [19]. Mitochondrial Isa1 and Isa2, together with Iba57, are specifically required for the maturation of aconitase and activation of SAM enzymes [30]. In hydrogenosomes, no aconitase is present; nevertheless, the SAM enzyme HydE is essential for hydrogenase maturation ([28] see below). Therefore, one additional anticipated function of hydrogenosomal IscA-2 might be the activation of HydE. Another protein that most likely fulfills the function of a scaffold is P-loop NTPase Ind1, which is specifically required for the assembly of respiratory complex I in mitochondria [32]. Four homologues of Ind1 were detected in the hydrogenosomal proteome, which correlates with the presence of a highly reduced (two subunit) form of complex I within the organelle [10,33]. One of the Ind1 proteins was significantly upregulated under −Fe conditions. Similarly, a single homologue of Isd11, an accessory protein of cysteine desulfurase (IscS) [34], was significantly upregulated under −Fe conditions, while the upregulation of the second detected copy of this protein and IscS itself was not significant. Consistent with the previous study of Sutak et al. [28], our study detected only IscS-2, and IscS-1 was not found, suggesting that only one of the two gene copies is expressed. Of the components that act late in FeS protein

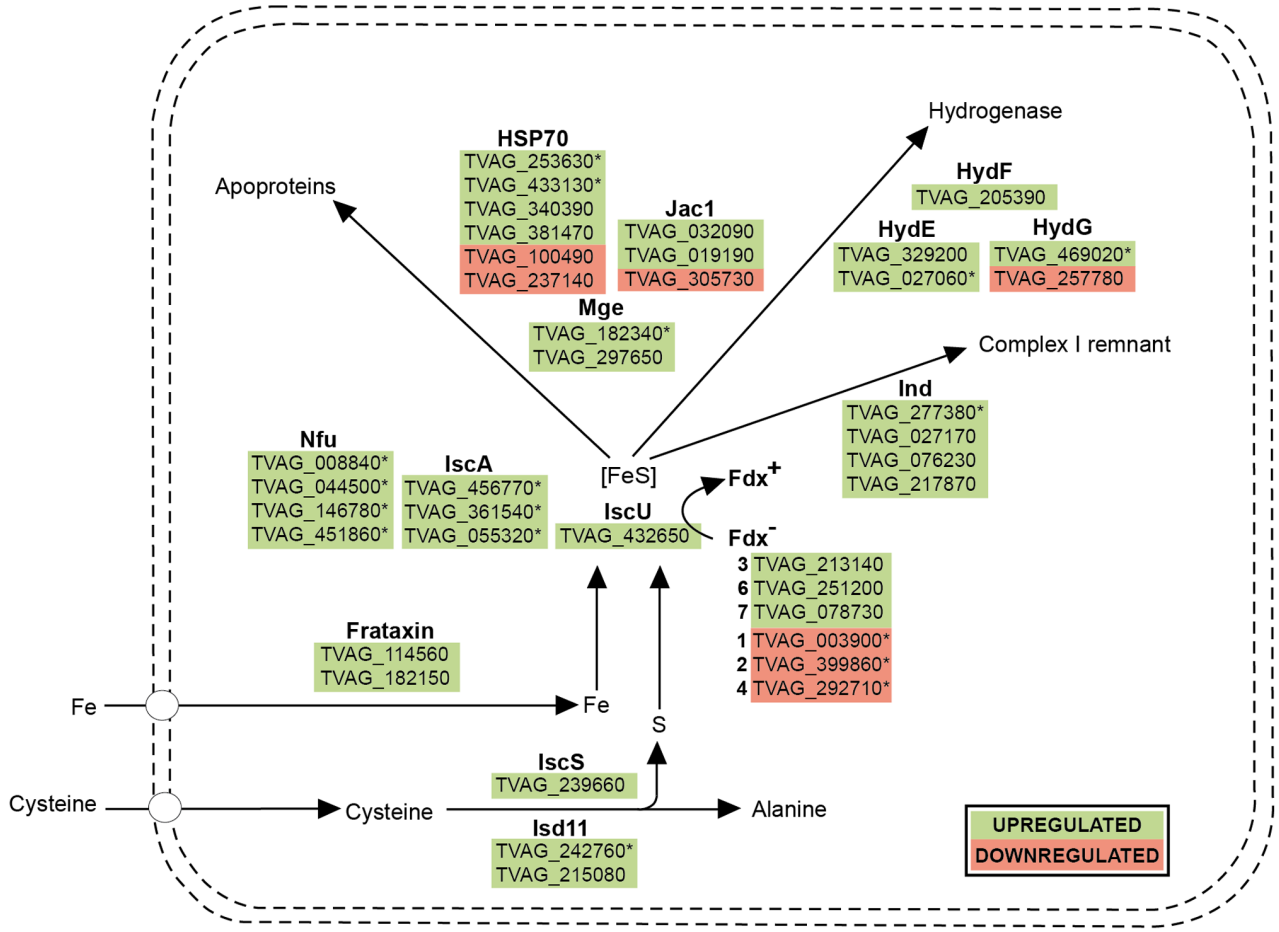

Figure 2. Proteins of the iron-sulfur cluster assembly machinery identified in this study. Gene IDs marked with an asterisk denote proteins that were significantly regulated in response to iron availability.
doi:10.1371/journal.pone.0065148.g002

biogenesis and ensure the transfer of the nascent FeS cluster to the target apoprotein, two homologues of the chaperone HSP70 and one nucleotide exchange factor Mge1 (GrpE) were significantly upregulated under -Fe conditions.

Hydrogenosomal Hyd machinery, which consists of the three proteins HydE, HydF and HydG, is essential for maturation of the H cluster, the active site of [FeFe] hydrogenase [31,35]. Interestingly, one paralogue of each component was upregulated under –Fe conditions, and moreover, HydG-1 showed the highest fold change between the two iron conditions (Table 1).

The observed upregulation of virtually all ISC components under iron limitation suggests the existence of a common regulatory mechanism. Multifarious Myb-like regulatory machinery has been shown to regulate the iron-dependent expression of hydrogenosomal malic enzyme; one of the identified myb regulatory elements was named MRE2f [16,17,36]. In our recent study, we found the MRE2f motif in the 5′untranslated regions of IscS-2 (TVAG_239660) and IscA2 (TVAG_456770) [18], suggesting that these genes might be regulated through the Myb system. However, the mode of regulation of the remaining ISC components remains unclear.

Energy Metabolism

Iron restriction resulted in the decreased expression of all enzymes involved in hydrogenosomal carbohydrate metabolism. These enzymes are encoded by multiple genes in *T. vaginalis*. Our proteomic analysis detected virtually all gene products (Fig. 3, Table 1); however, only one or several paralogues of a particular enzyme were significantly downregulated (Table 2). Two crucial FeS enzymes in the pathway, PFO and [FeFe]-hydrogenase, as well as the non-FeS malic enzyme, were among the most downregulated proteins. Three paralogues of PFO displayed downregulation one order of magnitude higher than all of the other proteins participating in energy metabolism (fold changes of −37.4, −16.9 and −13.5 for PFO BI, BII and E, respectively, Table 1). Only one of the detected paralogues was significantly downregulated in the following cases: both subunits of the respiratory complex I remnant, acetate:succinate-CoA transferase (ASCT) and heterodimeric succinyl-CoA synthase (SCS), of which only the α subunit showed significant downregulation under -Fe conditions.

Taken at face value, it appears that the above-described changes in the expression of proteins involved in iron-sulfur cluster assembly and energy metabolism are adaptive and aimed at minimizing the negative effects of iron shortage. While the pathway of hydrogenosomal pyruvate catabolism, in which abundant FeS proteins operate, is downregulated to lower the need for iron supply, the ISC system is strengthened, apparently to increase the efficiency of FeS cluster formation, which is needed for vital housekeeping proteins.

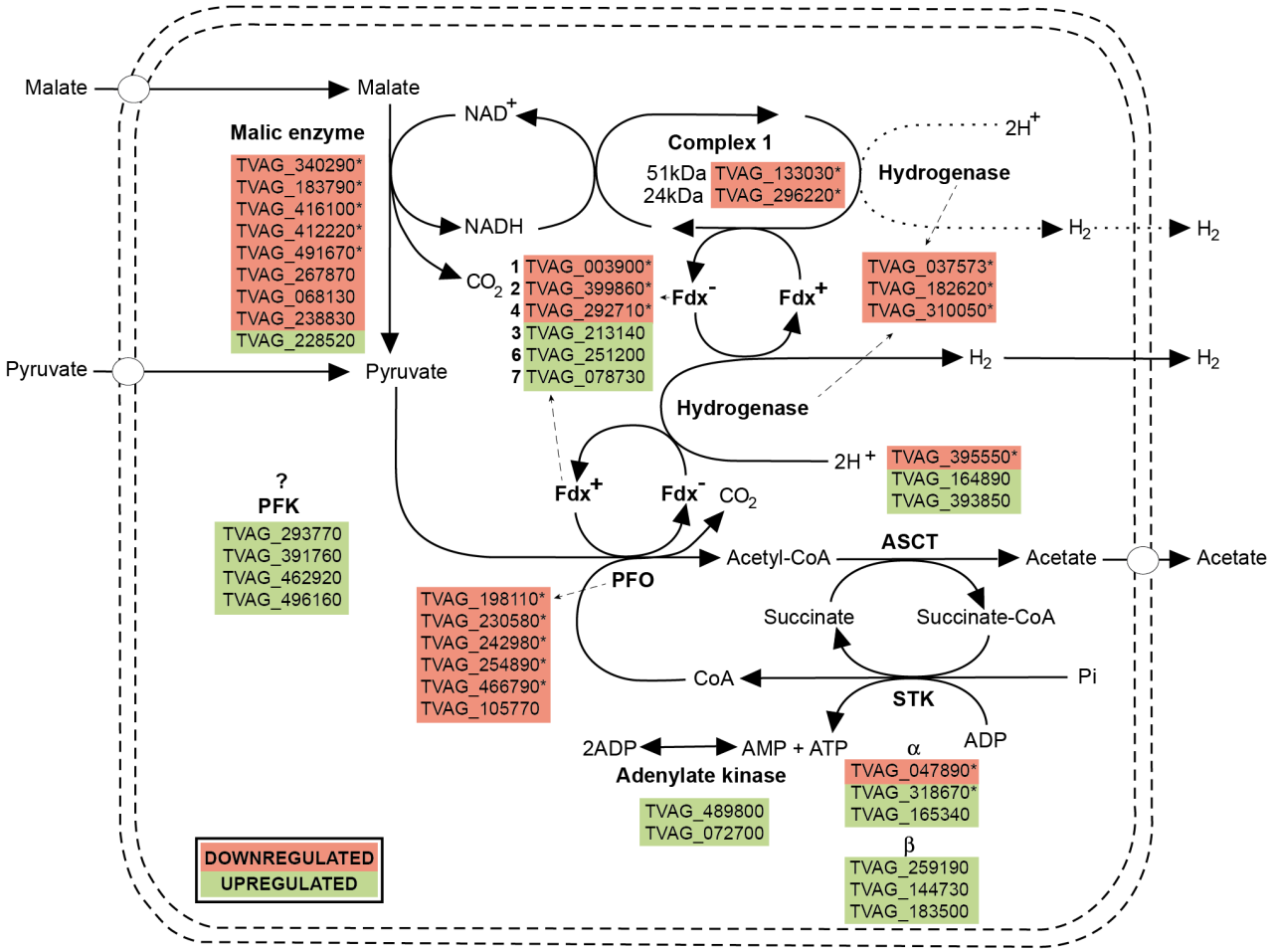

Figure 3. Proteins of hydrogenosomal energy metabolism identified in this study. Gene IDs marked with an asterisk denote proteins that were significantly regulated in response to iron availability.
doi:10.1371/journal.pone.0065148.g003

Oxygen Detoxification System

Although *T. vaginalis* inhabits oxygen-poor environments, it is well adapted to survive periods of relative aerobiosis. The parasite possesses a number of defense mechanisms that provide protection against oxidative damage to vulnerable cellular components, among which the hydrogenosomal enzymes PFO and hydrogenase are particularly oxygen sensitive. The spectrum of proteins that are able to play a role in hydrogenosomal oxygen and reactive oxygen species (ROS) detoxification seems to be unexpectedly broad [34,11,9,14]. We detected several proteins that are possibly involved in oxygen and ROS defense whose expression was influenced by iron availability. Two thioredoxins and one protein with similarity to bacterial OsmC proteins were upregulated, while rubrerythrin and superoxide dismutase were downregulated under -Fe conditions (Table 1). Thioredoxins and thioredoxin peroxidases are components of the ubiquitous peroxiredoxin system, which provides protection against peroxides similar to bacterial-type OsmC proteins, which are believed to act upon organic hydroperoxides [37,38] (the function of the OsmC homologue in *T. vaginalis* is nevertheless unknown). It is noteworthy that while the above three upregulated proteins are non-Fe enzymes whose activity is based on cysteine residues, rubrerythrin and superoxide dismutase, which are downregulated under iron limitation, are both Fe-containing (but not FeS cluster-containing) proteins.

In addition, one of the two detected paralogues of bacterial-type FeS flavoproteins, which are likely involved in oxygen and hydrogen peroxide detoxification, was also downregulated (Table 1). In contrast, flavodiiron oxygen reductase, the terminal oxidase of the hydrogenosome [12], was not affected under -Fe conditions.

The Differential Regulation of Paralogous Gene Expression

The iron-dependent changes in the level of hydrogenosomal proteins determined in this study corresponded well with previous transcriptomic investigations of iron-dependent gene expression based on DNA microarray (TvArray V2.0) and comparative EST analyses (Fig. 4) [18]. The only exception observed was the α-SCS subunit (TVAG 318670), which was significantly upregulated at the proteomic level but downregulated with the EST approach under -Fe conditions. Importantly, the proteomic analysis extended the list of iron-regulated hydrogenosomal proteins, as a limited set of hydrogenosomal protein-coding transcripts was detected by DNA microarray and/or identified among *T. vaginalis* ESTs [18]. The proteomic analysis also confirmed and further elaborated a previous striking observation [18]; i.e., the differential regulation of individual copies of multi-member gene families, with some paralogues being regulated in response to changed iron

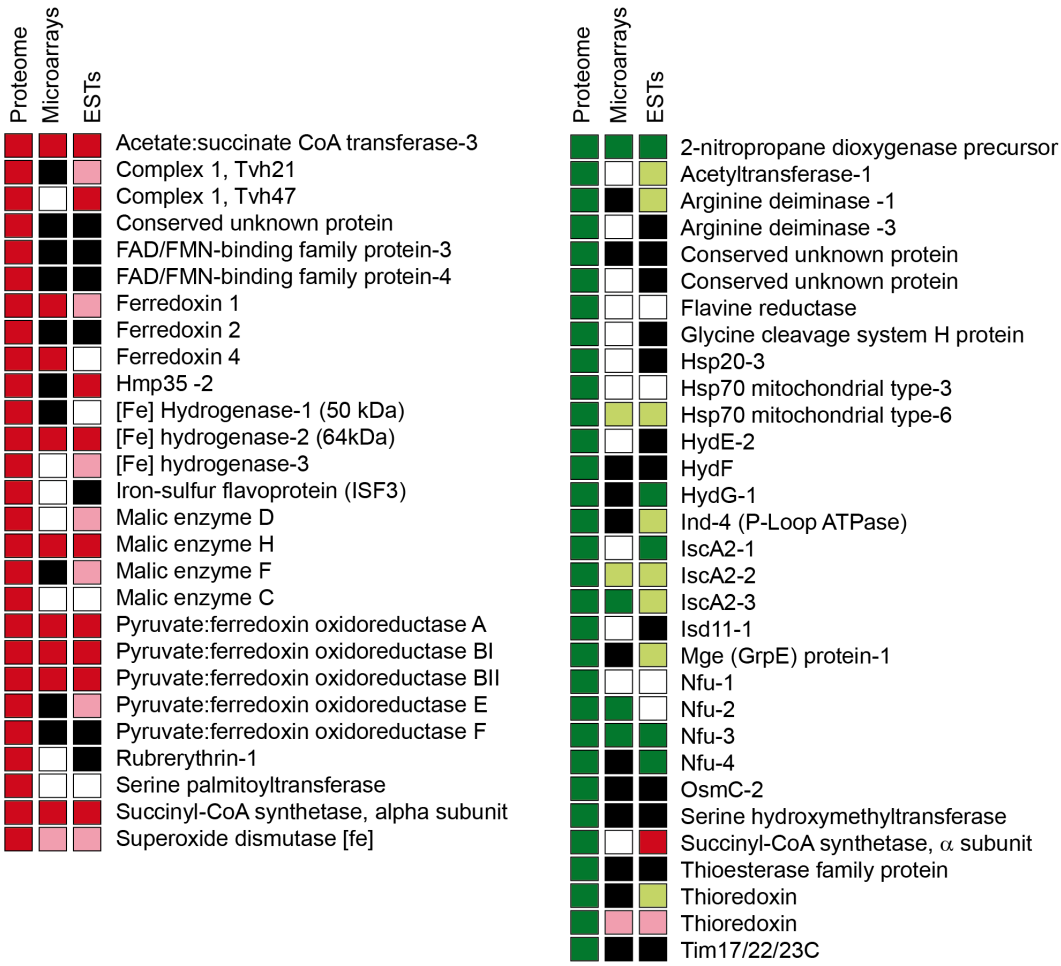

Figure 4. Comparison between iron-regulated proteins determined with the proteomic approach and the expression of corresponding genes studied by DNA microarrays and comparative EST analysis [18]. Red square, significant upregulation under high iron; pink square, insignificant upregulation under high iron; green square; significant upregulation under low iron; light green square, insignificant upregulation under low iron; empty square, no change in the transcript level; black square, a gene that was not included in the analysis.
doi:10.1371/journal.pone.0065148.g004

concentration and others unaffected. For example, seven distinct paralogues of [2Fe-2S] ferredoxin ensure electron transport in *T. vaginalis* hydrogenosomes. Three of the paralogues (ferredoxin 1, 2 and 4) showed significant downregulation under -Fe conditions, while three paralogues (ferredoxin 3, 6, and 7) appeared to be upregulated, although their fold changes did not reach the cut-off limit (Table S1). It could be speculated that ferredoxins share the trend of regulation with the pathway in which they are involved. Therefore, we suggest that downregulated ferredoxin paralogues are involved in energy metabolism, while those that are upregulated may participate in ISC assembly. For the hydrogenase maturase HydG, the HydG-1 paralogue displayed high upregulation, with a fold change of 10.4, while the other paralogue HydG-2 showed insignificant downregulation, with a fold change of -1.6 under -Fe conditions. The observed difference in the expression of HydG paralogues may reflect their different functions or requirement for different environmental signals. Indeed, the differential expression of individual genes of multigene families was reported for *T. vaginalis* upon interaction with fibronectin [39]. For example, there are seven paralogues of thioredoxin peroxidases in the *T. vaginalis* genome [19]; of these, a single paralogue, TVAG_484570, was shown to be upregulated in parasites bound to fibronectin [39], while two different paralogues (TVAG_038090 and TVAG_455310) were significantly upregulated in cells grown under -Fe conditions (Table S1). Previous genome analyses revealed that the majority of *T. vaginalis* genes, including those coding for hydrogenosomal proteins, are present in multiple copies [13,14,19]. Although the reason for expansion of the *T. vaginalis* genome is not clear, it is tempting to speculate that gene multiplication together with an ability of the parasite to regulate individual genes upon different environmental stimuli provided an advantage to the parasite in its efficient response to continuous challenges in the host environment caused by factors such as the immune system, physiological changes during the menstrual cycle, iron availability and adverse microbial community.

In conclusion, the combination of transcriptomic [18] and proteomic data from trichomonads cultivated under different iron conditions presented in this work provides a basis for the study of the iron-dependent expression of individual genes that belong to multigene families, which apparently plays an important role in *T. vaginalis* cells living in rapidly changing environments.

Supporting Information

Figure S1 Enzymatic activities of hydrogenosomal marker malic enzyme and lysosomal marker acid

phosphatase in subcellular fractions from Optiprep density gradient from iron rich and iron depleted culture.
(TIF)

Table S1 Complete list of proteins identified in the hydrogenosomes of Trichomonas vaginalis including likely contaminants, putative membrane proteins and hypothetical proteins.
(XLS)

Table S2 Bona fide hydrogenosomal proteins including putative membrane proteins.
(XLS)

Author Contributions

Conceived and designed the experiments: NCB PJ IH JT. Performed the experiments: NCB LH PJ MŠ PR MM. Analyzed the data: NCB LH PJ IH JT. Wrote the paper: NCB LH IH JT.

References

1. Crichton R (2009) Iron Metabolism: From Molecular Mechanisms to Clinical Consequences (Google eBook). John Wiley & Sons.
2. Weinberg ED (2009) Iron availability and infection. Biochim Biophys Acta 1790: 600–605.
3. Sutak R, Lesuisse E, Tachezy J, Richardson DR (2008) Crusade for iron: iron uptake in unicellular eukaryotes and its significance for virulence. Trends Microbiol 16: 261–268.
4. Johnston VJ, Mabey DC (2008) Global epidemiology and control of *Trichomonas vaginalis*. Curr Opin Infect Dis 21: 56–64.
5. World health organisation (2011) Global Prevalence and incidence of Selected Curable Sexually Transmitted Infections. Available: http://www.who.int/docstore/hiv/GRSTI/006.htm. Accessed 2013 May 5.
6. Hrdý I, Tachezy J, Müller M (2008) Metabolism of Trichomonad Hydrogenosomes. In: Tachezy J, editor. Hydrogenosomes and Mitosomes: Mitochondria of Anaerobic Eukaryotes. Berlin: Heidelberg: Springer-Verlag. 113–144.
7. Gorrell TE (1985) Effect of culture medium iron content on the biochemical composition and metabolism of *Trichomonas vaginalis*. J Bacteriol 161: 1228–1230.
8. Vanáčová S, Rasoloson D, Rázga J, Hrdý I, Kulda J, et al. (2001) Iron-induced changes in pyruvate metabolism of *Tritrichomonas foetus* and involvement of iron in expression of hydrogenosomal proteins. Microbiology 147: 53–62.
9. Lehker MW, Alderete JF (1992) Iron regulates growth of *Trichomonas vaginalis* and the expression of immunogenic trichomonad proteins. Mol Microbiol 6: 123–132.
10. Hrdy I, Hirt RP, Dolezal P, Bardonova L, Foster PG, et al. (2004) Trichomonas hydrogenosomes contain the NADH dehydrogenase module of mitochondrial complex I. Nature 432: 618–622.
11. Pütz S, Gelius-Dietrich G, Piotrowski M, Henze K (2005) Rubrerythrin and peroxiredoxin: two novel putative peroxidases in the hydrogenosomes of the microaerophilic protozoon *Trichomonas vaginalis*. Mol Biochem Parasitol 142: 212–223.
12. Smutna T, Goncalves VL, Saraiva LM, Tachezy J, Teixeira M, et al. (2009) Flavodiiron protein from *Trichomonas vaginalis* hydrogenosomes: the terminal oxygen reductase. Eukaryot Cell 8: 47–55.
13. Rada P, Doležal P, Jedelský PL, Bursac D, Perry AJ, et al. (2011) The core components of organelle biogenesis and membrane transport in the hydrogenosomes of *Trichomonas vaginalis*. PLoS ONE 6: e24428.
14. Schneider RE, Brown MT, Shiflett AM, Dyall SD, Hayes RD, et al. (2011) The *Trichomonas vaginalis* hydrogenosome proteome is highly reduced relative to mitochondria, yet complex compared with mitosomes. Int J Parasitol 41: 1421–1434.
15. Peterson KM, Alderete JF (1984) Iron uptake and increased intracellular enzyme activity follow host lactoferrin binding by *Trichomonas vaginalis* receptors. J Exp Med 160: 398–410.
16. Ong SJ, Hsu HM, Liu HW, Chu CH, Tai JH (2006) Multifarious transcriptional regulation of adhesion protein gene ap65–1 by a novel Myb1 protein in the protozoan parasite *Trichomonas vaginalis*. Eukaryot Cell 5: 391–399.
17. Hsu HM, Ong SJ, Lee MC, Tai JH (2009) Transcriptional regulation of an iron-inducible gene by differential and alternate promoter entries of multiple Myb proteins in the protozoan parasite *Trichomonas vaginalis*. Eukaryot Cell 8: 362–372.
18. Horváthová L, Safaríková L, Basler M, Hrdy I, Campo NB, et al. (2012) Transcriptomic identification of iron-regulated and iron-independent gene copies within the heavily duplicated *Trichomonas vaginalis* genome. Genom Biol Evol 4(10): 1017–29.
19. Carlton JM, Hirt RP, Silva JC, Delcher AL, Schatz M, et al. (2007) Draft genome sequence of the sexually transmitted pathogen *Trichomonas vaginalis*. Science (New York, NY) 315: 207–212.
20. De Jesus JB, Ferreira MA, Cuervo P, Britto C, e Silva-Filho FC, et al. (2006) Iron modulates ecto-phosphohydrolase activities in pathogenic trichomonads. Parasitol Int 55: 285–290.
21. De Jesus JB, Cuervo P, Junqueira M, Britto C, Silva-Filho FCE, et al. (2007) A further proteomic study on the effect of iron in the human pathogen *Trichomonas vaginalis*. Proteomics 7: 1961–1972.
22. Nägele E, Vollmer M, Hörth P, Vad C (2004) 2D-LC/MS techniques for the identification of proteins in highly complex mixtures. Expert Rew Proteomics 1: 37–46.
23. Diamond LS (1957) The establishment of various trichomonads of animals and man in axenic cultures. J Parasitol 43: 488–490.
24. Drmota T, Proost P, Weyda F, Ranst M Van, Kulda J, et al. (1996) Iron-ascorbate cleavable malic enzyme from hydrogenosomes of *Trichomonas vaginalis*: purification and characterization. Mol Biochem Parasitol 83: 221–234.
25. Šmíd O, Matušková A, Harris SR, Kučera T, Novotný M, et al. (2008) Reductive evolution of the mitochondrial proscessing peptidase of the unicellular parasites *Trichomonas vaginalis* and *Giardia intestinalis*. PLoS pathogens 4: e1000243.
26. Zimorski V, Major P, Hoffmann K, Brás XP, Martin WF, et al. (2013) The N-terminal sequences of four major hydrogenosomal proteins are not essential for import into hydrogenosomes of *Trichomonas vaginalis*. J Eukar Microbiol 60: 89–97.
27. Tachezy J, Sánchez LB, Müller M (2001) Mitochondrial type iron-sulfur cluster assembly in the amitochondriate eukaryotes *Trichomonas vaginalis* and *Giardia intestinalis*, as indicated by the phylogeny of IscS. Mol Biol Evol 18: 1919–1928.
28. Sutak R, Dolezal P, Fiumera HL, Hrdy I, Dancis A, et al. (2004) Mitochondrial-type assembly of FeS centers in the hydrogenosomes of the amitochondriate eukaryote *Trichomonas vaginalis*. Proc Natl Acad Sci USA 101: 10368–10373.
29. Hjort K, Goldberg AV, Tsaousis AD, Hirt RP, Embley TM (2010) Diversity and reductive evolution of mitochondria among microbial eukaryotes. Philos Trans R Soc B 365: 713–727.
30. Gelling C, Dawes IW, Richhardt N, Lill R, Mühlenhoff U (2008) Mitochondrial Iba57p is required for Fe/S cluster formation on aconitase and activation of radical SAM enzymes. Mol Cel Biol 28: 1851–1861.
31. Pütz S, Dolezal P, Gelius-Dietrich G, Bohacova L, Tachezy J, et al. (2006) Fe-hydrogenase matureses in the hydrogenosomes of *Trichomonas vaginalis*. Eukaryot Cell 5: 579–586.
32. Bych K, Kerscher S, Netz DJA, Pierik AJ, Zwicker K, et al. (2008) The iron-sulphur protein Ind1 is required for effective complex I assembly. EMBO J 27: 1736–1746.
33. Dyall SD, Yan W, Delgadillo-Correa MG, Lunceford A, Loo JA, et al. (2004) Non-mitochondrial complex I proteins in a hydrogenosomal oxidoreductase complex. Nature 431: 1103–1107.
34. Pandey A, Yoon H, Lyver ER, Dancis A, Pain D (2011) Isd11p protein activates the mitochondrial cysteine desulfurase Nfs1p protein. J Biol Chem 286: 38242–38252.
35. Mulder DW, Boyd ES, Sarma R, Lange RK, Endrizzi JA, et al. (2010) Stepwise [FeFe]-hydrogenase H-cluster assembly revealed in the structure of HydA(DeltaEFG). Nature 465: 248–251.
36. Ong SJ, Hsu HM, Liu HW, Chu CH, Tai JH (2007) Activation of multifarious transcription of an adhesion protein ap65–1 gene by a novel Myb2 protein in the protozoan parasite *Trichomonas vaginalis*. J Biol Chem 282: 6716–6725.
37. Coombs GH, Westrop GD, Suchan P, Puzova G, Hirt RP, et al. (2004) The amitochondriate eukaryote *Trichomonas vaginalis* contains a divergent thioredoxin-linked peroxiredoxin antioxidant system. J Biol Chem 279: 5249–5256.
38. Lesniak J, Barton WA, Nikolov DB (2003) Structural and functional features of the *Escherichia coli* hydroperoxide resistance protein OsmC. Protein Sci 12: 2838–2843.
39. Huang PJ, Lin WC, Chen SC, Lin YH, Sun CH, et al. (2012) Identification of putative miRNAs from the deep-branching unicellular flagellates. Genomics 99: 101–107.

8.2 Transcriptomic identification of iron-regulated and iron-independent gene copies within the heavily duplicated *Trichomonas vaginalis* genome.

GBE

Genome Biology and Evolution

SMBE

Transcriptomic Identification of Iron-Regulated and Iron-Independent Gene Copies within the Heavily Duplicated *Trichomonas vaginalis* Genome

Lenka Horváthová[1], Lucie Šafaříková[1], Marek Basler[2], Ivan Hrdý[1], Neritza B. Campo[1], Jyh-Wei Shin[3], Kuo-Yang Huang[4], Po-Jung Huang[5], Rose Lin[4], Petrus Tang[4,5,*], and Jan Tachezy[1,*]

[1]Department of Parasitology, Faculty of Science, Charles University in Prague, Prague 2, Czech Republic

[2]Department of Microbiology and Immunobiology, Harvard Medical School

[3]Department of Parasitology, National Cheng Kung University, Tainan, Taiwan

[4]Department of Parasitology, Molecular Regulation and Bioinformatics Laboratory, Chang Gung University, Kweishan, Taoyuan, Taiwan

[5]Bioinformatics Center, Chang Gung University, Kweishan, Taoyuan, Taiwan

*Corresponding author: E-mail: petang@mail.cgu.edu.tw, tachezy@natur.cuni.cz.

Accepted: September 3, 2012

Abstract

Gene duplication is an important evolutionary mechanism and no eukaryote has more duplicated gene families than the parasitic protist *Trichomonas vaginalis*. Iron is an essential nutrient for *Trichomonas* and plays a pivotal role in the establishment of infection, proliferation, and virulence. To gain insight into the role of iron in *T. vaginalis* gene expression and genome evolution, we screened iron-regulated genes using an oligonucleotide microarray for *T. vaginalis* and by comparative EST (expressed sequence tag) sequencing of cDNA libraries derived from trichomonads cultivated under iron-rich (+Fe) and iron-restricted (−Fe) conditions. Among 19,000 ESTs from both libraries, we identified 336 iron-regulated genes, of which 165 were upregulated under +Fe conditions and 171 under −Fe conditions. The microarray analysis revealed that 195 of 4,950 unique genes were differentially expressed. Of these, 117 genes were upregulated under +Fe conditions and 78 were upregulated under −Fe conditions. The results of both methods were congruent concerning the regulatory trends and the representation of gene categories. Under +Fe conditions, the expression of proteins involved in carbohydrate metabolism, particularly in the energy metabolism of hydrogenosomes, and in methionine catabolism was increased. The iron–sulfur cluster assembly machinery and certain cysteine proteases are of particular importance among the proteins upregulated under −Fe conditions. A unique feature of the *T. vaginalis* genome is the retention during evolution of multiple paralogous copies for a majority of all genes. Although the origins and reasons for this gene expansion remain unclear, the retention of multiple gene copies could provide an opportunity to evolve differential expression during growth in variable environmental conditions. For genes whose expression was affected by iron, we found that iron influenced the expression of only some of the paralogous copies, whereas the expression of the other paralogs was iron independent. This finding indicates a very stringent regulation of the differentially expressed paralogous genes in response to changes in the availability of exogenous nutrients and provides insight into the evolutionary rationale underlying massive paralog retention in the *Trichomonas* genome.

Key words: gene duplication, iron, microarrays, EST analysis.

Introduction

Gene duplications are important in evolution (Lynch and Conery 2000), and no genome has more recently duplicated genes than the parasitic flagellate *Trichomonas vaginalis*, the causative agent of trichomoniasis (Carlton et al. 2007; Cui et al. 2010). Trichomoniasis is the most common sexually transmitted infection of nonviral origin in humans. Although trichomoniasis is usually self-limiting in males, it causes serious health problems for female patients, including an increased risk of cervical cancer, pelvic inflammatory disease, infertility, and transmission of the HIV (Laga et al. 1993; Zhang and Begg 1994; Viikki et al. 2000; Moodley et al. 2002). Trichomoniasis during pregnancy is associated with low birth weight, the

premature rupture of membranes and preterm birth (Cotch et al. 1997). The establishment of a *T. vaginalis* infection as well as infections by other pathogenic microorganisms is dependent on the efficient acquisition of essential nutrients such as iron, from the host environment. Trichomonads can utilize various host iron-containing proteins such as lactoferrin, transferrin, ferritin, hemoglobin, and low-molecular-weight-iron complexes (Sutak et al. 2008). Iron is required for critical housekeeping functions such as proteosynthesis, genome duplication, and energy fixation. A significant portion of the trichomonad energy metabolism takes place in hydrogenosomes, whose function is particularly dependent on iron (Gorrell 1985; Vanácová et al. 2001). These specific mitochondria-related organelles contain a number of FeS proteins that catalyze key steps in ferredoxin-linked electron transport, hydrogen production, and ATP synthesis at the level of substrate phosphorylation (Hrdy et al. 2004). The formation of FeS clusters in the catalytic centers of apoproteins is mediated by the hydrogenosomal iron–sulfur cluster (ISC) assembly machinery, which consists of approximately 10 proteins, of which cysteine desulfurase (IscS) and the molecular scaffold protein IscU are the main components (Tachezy et al. 2001; Sutak, Dolezal, et al. 2004. Iron is also required for the functions of cytosolic and nuclear FeS proteins such as Rli1p, which is a protein essential for ribosome biogenesis and function (Kispal et al. 2005; Yarunin et al. 2005). This protein is highly conserved in eukaryotes, including *T. vaginalis* (Smíd et al. 2008).

In addition to housekeeping functions, iron affects specific host–pathogen interactions associated with the virulence of the parasite. Experiments performed in vitro have shown that iron regulates the cytoadherence of *T. vaginalis* to target cells (Mundodi et al. 2006) as well as the expression of cysteine proteinases (Sommer et al. 2005; Solano-González et al. 2007; Kummer et al. 2008), ecto-ATPases and ecto-phosphatases (De Jesus et al. 2006), and it increases trichomonad resistance to complement-mediated lysis (Alderete et al. 1995). Iron-dependent enhancement of experimental infections in mice was demonstrated with the related bovine parasite *Tritrichomonas foetus* (Kulda et al. 1999). However, little is known about the mechanisms underlying the iron-dependent regulation of these processes. Positive iron regulation at the transcriptional level was observed for the expression of some hydrogenosomal proteins, including malic enzyme (ME) and pyruvate:ferredoxin oxidoreductase (PFOR) (Vanácová et al. 2001). A detailed study of the iron-dependent regulation of hydrogenosomal ME, which may alternatively be present on the cell surface as the adhesin (AP65–1) (Hirt et al. 2007), led to the identification of Myb recognition elements and novel Myb proteins that appear to be components of a multifarious regulatory machinery in *T. vaginalis* (Ong et al. 2006, 2007). Two cysteine proteases, TVCP4 and TVCP12, were recently reported to be regulated at the posttranscriptional level by an iron-responsive element/iron response protein-like system (Solano-González et al. 2007; Torres-Romero and Arroyo 2009).

We combined cDNA microarray analysis with an expressed sequence tag (EST) approach to map iron-regulated genes and to reconstruct iron-regulated pathways in *T. vaginalis*. Our data revealed numerous iron-responsive genes that are involved in several essential pathways, particularly in cytosolic glycolysis and extended glycolysis in hydrogenosomes, as well as genes that encode components of the FeS cluster assembly machinery. Moreover, iron affected the expression of many genes with unknown functions.

Materials and Methods

Cell Cultures

Axenic cultures of *T. vaginalis* strain T1 were grown in trypticase–yeast extract–maltose medium supplemented with 10% heat-inactivated horse serum, pH 6.2 (Diamond 1957). Iron-rich medium (+Fe) and iron-restricted medium (−Fe) were supplemented with 100 μM Fe-nitrilotriacetate; and 50 μM 2-2-dipyridyl (Sigma), respectively. The cells were subcultured daily in +Fe and −Fe media for 5 days prior to experiment.

cDNA Library Construction and DNA Sequencing

RNA isolation kit (Pharmacia) was used to extract the total RNA from cells grown under +Fe and −Fe conditions, and contaminating genomic DNA was digested with DNase I. PolyA+ RNA was isolated using a PolyA+ tract mRNA isolation kit (Promega). Complementary DNA was synthesized using a ZAP–cDNA synthesis kit after priming with oligo-dT. The cDNA was then directionally cloned into the EcoRI and XhoI sites of the Uni-ZAP XR vector (Stratagene). Single and well-separated plaques were cored out from agar plates and transferred to 96-well microtiter plates containing SM buffer. The phage stocks were used as templates for cDNA insert amplification with T3 and T7 primers (1 nM for each primer). The amplified products were separated in 1.5% agarose gels, and clones that yielded single polymerase chain reaction (PCR)-amplified bands were collected for sequencing. Single-pass sequencing from the 5′-end of the cDNA insert was initiated with a T3 primer using the ABI PRISM BigDye Terminator Cycle Sequencing Kit (Applied Biosystems). The sequencing products were resolved and analysed on an ABI PRISM 377 (Applied Biosystems) or a MEGABACE DNA Sequencer (GE). The nucleotide sequences obtained were processed with the Phred/Phrap/Consed package (http://www.phrap.org/phredphrapconsed.html).

Functional Annotations and Sequence Analysis

BLAST tools were used to compare the assembled sequence contigs to known *Trichomonas* mRNAs, putative open-reading-frames from the *T. vaginalis* G3 genome (Carlton et al. 2007) and NCBI's nonredundant (nr) nucleotide (*E* value =

10^{-15}) and protein database. Genes were functionally annotated based on the Interpro and Gene Ontology databases. Contigs with identity greater than 60% of their length were annotated and assigned to KEGG pathways.

Putative coding regions from the EST data were collected from BLASTX alignments, and the codon usage bias was calculated. A Perl script was also written to locate poly-A tails and to search 10–35 bp upstream for putative mRNA poly-adenylation signals; the script allowed one mismatch and two mismatches from the sequence AAUAAA. Putative signal sequences and transmembrane domains in the coding regions were identified by SignalP 3.0 and TMHMM 2.0 (http://www.cbs.dtu.dk/services/), respectively. Putative *Trichomonas* protein kinases and peptidases were identified by sequence comparison with datasets downloaded from the KinBase (http://www.kinase.com) and the MEROPS (http://merops.sanger.ac.uk) databases, respectively.

Microarray Sample Preparation

RNA from trichomonads grown in +Fe and −Fe conditions was isolated using a QuickPrep Total RNA Extraction Kit (Amersham Biosciences) according to the manufacturer's instructions. The total RNA was further purified using an RNeasy CleanUp Kit (Qiagen). The RNA concentration and purity were determined using a NanoDrop ND-1000 spectrophotometer (NanoDrop Technologies). The integrity of the RNA was checked by agarose gel electrophoresis. The same RNA samples were used in parallel experiments for cDNA microarray analysis and quantitative real-time PCR (qRT-PCR). cDNA probes were synthesized using 2 μg of total RNA and primers labeled with Cy3 and Cy5, respectively, according to the manufacturer's instructions (3DNA Array 900 Expression Array Detection Kit, Genisphere). Four independent RNA samples (biological replicates) from *T. vaginalis* strain T1 grown under +Fe and −Fe conditions were compared. A dye–swap design was used to prevent dye-associated effects on cDNA synthesis.

Microarray Analysis

A *T. vaginalis* customized cDNA microarray (TvArray V2.0) was implemented by the Molecular Regulation and Bioinformatics Laboratory, Chang Gung University, Taiwan. The TvArray chip contained PCR products amplified from 7,688 EST clones with an average GC content of 38.36% and an average length of 384 bp. The cDNA inserts were fabricated on GAPS™ II Coated Slides (Corning. USA). The microarrays were prehybridized in Coplin chambers using a solution containing 1% bovine serum albumine, 1% sodium dodecyl sulfate, and 3X saline sodium citrate buffer (1X SSC consists of 0.15 M NaCl with 0.015 M sodium acetate). The slides were incubated at 50°C for 30 min, washed with water and isopropanol and dried by centrifugation at 90 × g for 3 min. Hybridization with the cDNA hybridization mix and washes were performed following the protocol for the 3DNA Array 900 Expression Array Detection Kit (Genisphere). cDNA hybridizations were performed in a VersArray Hybridization Chamber (Bio-Rad) at 60°C overnight. Hybridizations with fluorescent 3DNA reagents were performed in the same chamber at 60°C for 4 h. After the final washing step, the slides were dried by centrifugation at 90 × g for 3 min and scanned using the GenePix 4200A scanner (Axon). GenePix Pro 5.1 software was used to determine the average signal intensity and the local background for each spot. The Cy3/Cy5 fluorescence ratios were Log 2 transformed and normalized by LOWESS normalization method in the TIGR microarray data analysis system version 2.19 (Saeed et al. 2003). In total, 10 independent hybridizations using samples from 4 independent cultures and RNA extractions were performed and data of the independent experiments were combined. We used MeV v4.8.1 to determine significantly regulated genes. One-class Student *t* test was performed and *P* values were based on all 1,024 possible permutations (cut-off was 0.01) and the proportion of false significant genes was set to not exceed 10 genes.

The results of all experiments are available in the ArrayExpress database (http://www.ebi.ac.uk/arrayexpress/) under the array design name TvArray v1.0.

qRT-PCR Analysis

Oligonucleotide primers (supplementary table S1, Supplementary Material online) were designed using Primer Designer software v1.01 (Scientific and Education software). The primers were tested prior to qRT-PCR analysis using DNA as a template, and single amplicons of the proper size were sequenced. The RT reaction contained 1 μg of total RNA, 500 ng of Oligo(dT) 15 Primer (Invitrogen), 5 mM DTT (Invitrogen), 2 U of RNasin (Invitrogen), 10 U of SuperScriptII reverse transcriptase (Invitrogen), and 500 μM each of dATP, dCTP, dGTP, and dTTP. The reactions were incubated at 42°C for 50 min followed by 15 min at 70°C. For qRT-PCR, 1 μl of cDNA was amplified in a 25 μl reaction mixture containing each gene-specific primer at 50 nM and 12.5 μl of iQTM SYBR green Supermix (Bio-Rad). All reactions were performed in triplicate using a RotorGene 2000 Real-Time PCR cycler (Corbett Life Science). The expression levels of each gene were normalized to those of the housekeeping gene β-tubulin, expression of which is not affected by the availability of iron. Relative quantitative values were obtained by the comparative threshold cycle ($2^{-\Delta\Delta C_T}$) method as described by (Livak and Schmittgen 2001).

Analysis of 5′ Untranslated Regions

An application based on the NetBeans Platform (http://platform.netbeans.org) was developed to search for MRE-like motifs in 300 bp of the upstream regions of all iron-regulated genes. We searched for the MRE eukaryotic consensus (C/T)AACG(G/T) and the specific MREs of the ME gene as described

by Hsu et al. (2009): MRE1/MRE2r (A[A/T/C/G]AACGAT, CGATA, AACGATA, and TAACGA) and MRE2f (TATCGT and TATCGTC).

Results and Discussion

Microarray Analysis

To investigate changes in gene expression caused by iron availability, trichomonads were grown in media supplemented with 100 μM Fe-nitrilotriacetate (iron-rich conditions, +Fe) or with the iron chelator 2,2-dipyridyl (50 μM; iron-restricted conditions, −Fe). To estimate timeframe for cultivation prior to RNA isolation, we monitored enzymatic activities of PFOR and ME (Rasoloson et al. 2002) as their expression is known to be affected by iron availability in trichomonads (Vanácová et al. 2001). The activities of both enzymes decreased during 24 h cultivation under −Fe conditions and then remained stable (supplementary fig. S1, Supplementary Material online). Thus, to assure ultimate effect of iron on trichomonads, we cultivated the cells for 5 days under +Fe/−Fe conditions prior to each experiment. The total RNA was then isolated from both treatment groups and hybridized onto DNA microarray slides containing PCR products amplified from 7,688 EST clones representing 4,950 unique *T. vaginalis* genes. A direct pairwise comparison strategy was used to identify differentially expressed genes. Altogether, 10 independent hybridizations were performed using samples from four independent experiments. Genes whose expression ratios changed by a factor of at least 1.3 and had *P* values lower than 0.01 were considered to be significantly regulated by iron. In total, 195 genes met this criterion that represent approximately 4% of unique genes; 117 and 78 genes were upregulated in cells cultivated under +Fe and −Fe conditions, respectively (fig. 1 and supplementary table S2*a*, Supplementary Material online). The distribution of genes into fold change categories is given in supplementary table S2*b*, Supplementary Material online. The complete dataset including genes expression of which was not affected by iron was deposited in the ArrayExpress database (http://www.ebi.ac.uk/arrayexpress/) under the array design name TvArray v1.0.

To verify the cut-off limit and to validate the microarray data, we selected 15 genes for qRT-PCR analyses. The selection included genes that were not affected by iron (ferredoxin 6, IscS-2), genes with moderate changes in expression (−1.42- to 1.67-fold change) and genes with a greater than 2-fold change in expression (hydrogenase, alcohol dehydrogenase, and PFOR) according to the microarray data (table 1). In each instance, the qRT-PCR confirmed regulation trends observed in the microarray analysis. The ratios between paired samples (fold change) determined by qRT-PCR were, however, greater than the fold change obtained for the same gene by microarray analysis. These results are consistent with those of Yuen et al. (2002) and Dallas et al. (2005), who showed that microarray analysis underestimates the changes in gene expression compared with the more qRT-PCR assay, although correlations between microarray and qRT-PCR data are generally strong. The list of genes that met the cut-off limit 1.3 in our study included majority of genes coding for proteins that were showed previously to be affected by iron on protein level in *T. vaginalis* and related parasite *T. foetus* such as PFOR, hydrogenosomal ME, hydrogenase, ferredoxin, cytosolic malate dehydrogenase, and cysteine protease (Vanácová et al. 2001; De Jesus et al. 2007; Dolezal et al. 2007) that further supports validity of the microarray analysis.

Comparative EST Analysis

As a second technique to identify differentially expressed genes, we employed a comparative EST approach (Lee et al. 1995). 10,042 and 9,032 ESTs were sequenced from two distinct cDNA libraries that were derived from trichomonads grown under +Fe and −Fe conditions, respectively. The relative frequency (RF) of an EST was calculated as the number of ESTs per 10,000 clones. The upregulation index was calculated as the difference between the RF under +Fe conditions and the RF under −Fe conditions. The distribution of unique genes to upregulation index categories is summarized in supplementary table S2*d*, Supplementary Material online. The upregulation index values ranged from 1 to 70, which was considerably higher than the range of the fold change based on microarray analysis. Consequently we used higher cut-off limit: a gene was considered to be significantly upregulated if the upregulation index was greater than or equal to five. This criterion met 336 genes (∼5%) out of a total number of 6,381 unique genes that were generated by the assembly of the ESTs. Of those genes, 165 were upregulated under +Fe conditions, and 171 were upregulated under −Fe conditions (supplementary table S2*c*, Supplementary Material online). A representation of the gene categories that were affected by iron availability is shown in figure 2.

Major Iron-Regulated Pathways

Glycolysis

The energy metabolism of *T. vaginalis* relies on fermentative carbohydrate catabolism in the cytosol that is extended to malate or pyruvate degradation in the hydrogenosome (Müller et al. 2012). At least one (but usually several) of multiple gene copies encoding glycolytic proteins showed significant iron-dependent regulation (fig. 3 and supplementary table S3, Supplementary Material online), with similar results obtained from both methods (microarray and EST analysis). The enzymes that supply the glycolytic pathway with substrates (glucokinase, glycogen phosphorylase, and phosphoglucomutase) and the successive glycolytic enzymes were significantly upregulated under +Fe conditions. A striking exception was the upregulation of one of the four detected glyceraldehyde-3-phosphate dehydrogenase (GAPDH) genes

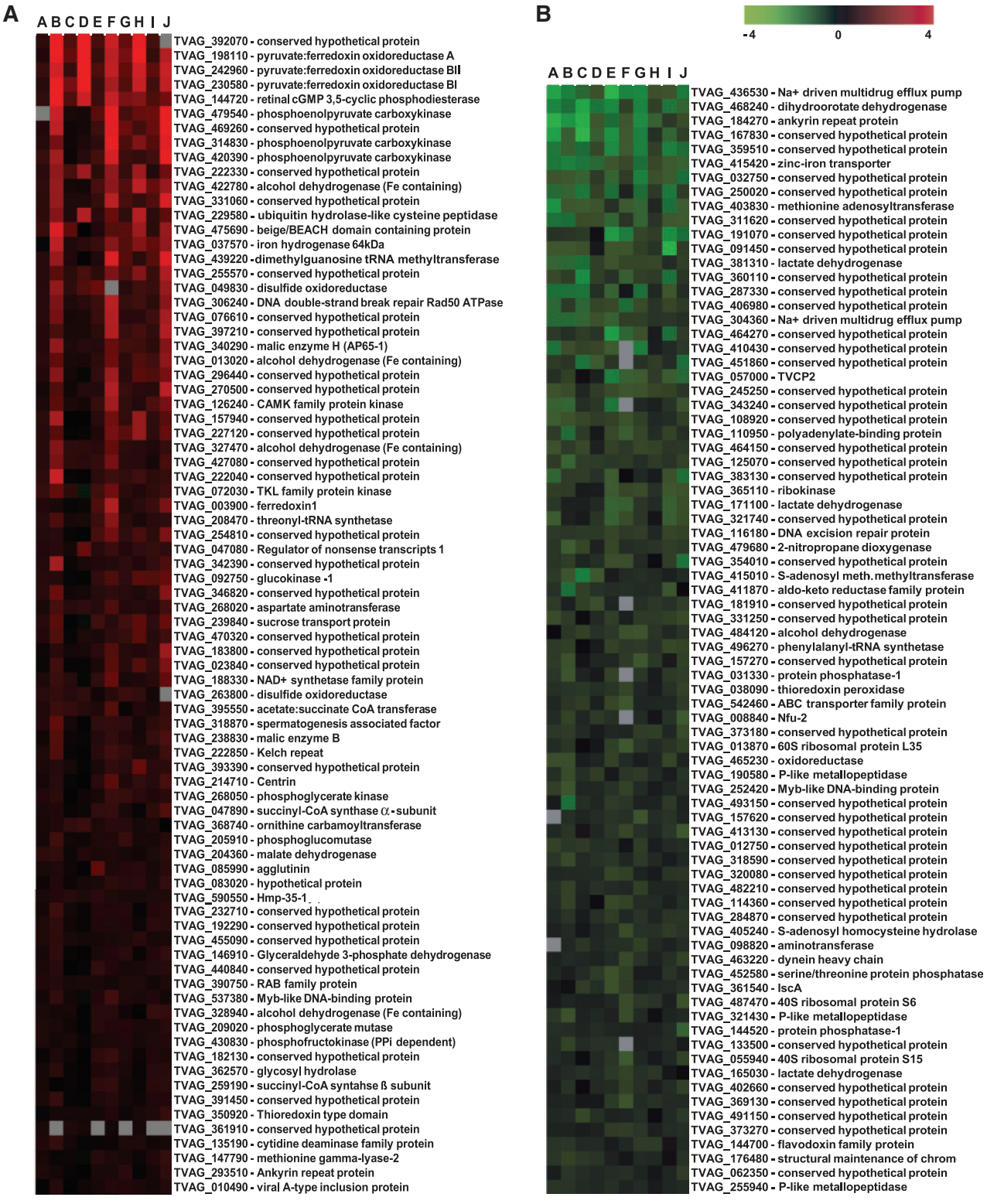

Fig. 1.—Heatmap visualization of iron-regulated genes based on microarray analysis. Results of 10 experiments are given in columns A–J. (*A*) genes upregulated in +Fe conditions; (*B*) genes upregulated in −Fe conditions.

Table 1

Fold Changes Detected by qRT-PCR in Comparison with Results of Microarray Analysis

TrichDB 1.2 Accession No.	Annotation	Microarrays Upregulation Rate*	Fold Change Detected by qRT-PCR**
TVAG_239660	IscS-2	NSC	NSC
TVAG_251200	Ferredoxin 6	NSC	NSC
TVAG_129940	IBP39	1.11	1.88
TVAG_348330	Glycogen phosphorylase	1.24	1.95
TVAG_281070	Phosphofructokinase	1.31	4.62
TVAG_292710	Ferredoxin 4	1.33	2.89
TVAG_104250	Hmp-35-2	1.56	2.28
TVAG_238830	Malic enzyme B	1.67	2.51
TVAG_198110	PFO A	4.01	24.96
TVAG_037570	Iron hydrogenase 64 kDa	2.48	109.64
TVAG_422780	Alcohol dehydrogenase	2.57	31.44
TVAG_165030	Malate dehydrogenase	−1.33	−1.62
TVAG_381311	Lactate dehydrogenase	−1.81	−5.02
TVAG_361540	IscA-2	−1.36	−2.26
TVAG_008840	NfU-2	−1.42	−1.47

NOTE.—NSC, no significant change of gene expression.
*$P \leq 0.01$.
**$P \leq 0.05$.

(TVAG_366380) under −Fe conditions according to the EST analysis, as the other three GAPDH genes were upregulated under +Fe conditions (fig. 3 and supplementary table S3, Supplementary Material online). It is tempting to speculate that GAPDH TVAG_366380 gene copy encodes protein with the function distinct from other paralogs. Multifunctional character of GAPDH was reported in macrophages where GAPDH serves as a surface receptor that is upregulated upon iron depletion (Rawat et al. 2012). Interestingly, *T. vaginalis* possesses two types of phosphofructokinase (PFK) (Liapounova et al. 2006) Inorganic pyrophosphate (PPi)-dependent PFK catalyzes reversible phosphorylation of fructose-6-phosphate in the cytosol (Mertens et al. 1998). More recently, putative ATP-dependent PFK has been identified in proteome of hydrogenosomes (Rada et al. 2011). Two of the three genes that encode the PPi-dependent PFK and one of two genes for the ATP-dependent PFK were upregulated under +Fe conditions (supplementary table S3, Supplementary Material online). The most significant changes in iron-dependent gene expression were associated with the pathways that follow the conversion of phosphoenolpyruvate (PEP), the branch-point of carbohydrate metabolism. The enzymes that catalyze the formation of malate from PEP via oxaloacetate (PEP carboxykinase and malate dehydrogenase) were considerably upregulated under +Fe conditions (fig. 3). In contrast, the pathway that converts malate to lactate was upregulated under −Fe conditions. This pathway involves cytosolic NADP-dependent ME and NADH-dependent lactate dehydrogenase (fig. 3). These findings indicate that under +Fe conditions, malate preferentially enters the hydrogenosome and serves as a substrate for hydrogenosomal energy metabolism. However, under −Fe, when hydrogenosomal metabolism is ceased, malate is metabolized in the cytosol via pyruvate to lactate. Thus, the ability to switch between hydrogenosomal and cytosolic malate metabolism seems to be important for the ability of trichomonads to quickly adapt to changes in iron availability in their environment. Similar changes in carbohydrate metabolism were reported in *T. vaginalis* that had impaired hydrogenosomal metabolism because of the induction of metronidazole resistance (Kulda et al. 1993).

Besides lactate, *T. vaginalis* also produces low amount of ethanol (Cerkasovová et al. 1986). In our dataset, we identified two types of alcohol dehydrogenases (ADHs) that differ in the metal ion present in the active site of the enzyme. Notably, four of five genes coding for the iron-containing ADH were upregulated under +Fe conditions, whereas one gene was upregulated under −Fe conditions together with one of two genes coding for the zinc-containing ADH (fig. 3). In the related organism *T. foetus*, acetaldehyde that is reduced by ADH to ethanol is formed from pyruvate by the enzyme pyruvate decarboxylase (Sutak, Tachezy, et al. 2004). However, pyruvate decarboxylase activity was not detected in *T. vaginalis,* and the gene encoding this enzyme was not identified in the genome (Carlton et al. 2007). Thus, the pathway responsible for the formation of acetaldehyde remains unclear.

Hydrogenosomal Energy Metabolism

Iron increased the transcription of all critical enzymes in hydrogenosomal carbohydrate catabolism; at least one copy of each gene was significantly upregulated (fig. 4 and supplementary table S3, Supplementary Material online). PFOR and ME, which are the enzymes that catalyze the oxidative decarboxylation of the hydrogenosomal substrates pyruvate and malate, respectively, were the most highly upregulated enzymes of the pathway. Three genes encoding PFOR (PFOR-A, BI and BII) displayed the highest upregulation observed in the microarray analysis (4.01, 3.71, and 3.64, respectively), and also had high upregulation scores determined by the EST analysis (32, 18, and 9, respectively) (supplementary table S2*a* and *c*, Supplementary Material online). The gene coding for ME-H was the most highly upregulated according to the EST analysis, with an upregulation index value of 63 (supplementary table S2c, Supplementary Material online). The re-oxidation of NADH resulting from ME activity is mediated by heterodimeric NADH dehydrogenase (remnant of respiratory complex I). The 51 kDa subunit of this enzyme was significantly upregulated under +Fe conditions according to EST analysis, but the upregulation of the 24 kDa subunit did not reach the cut-off limit. Electrons generated by PFOR are transferred via ferredoxin to the hydrogenase responsible for the synthesis of molecular hydrogen. The genes that code for ferredoxin-1 and the 64 kDa [Fe]-hydrogenase were upregulated under +Fe

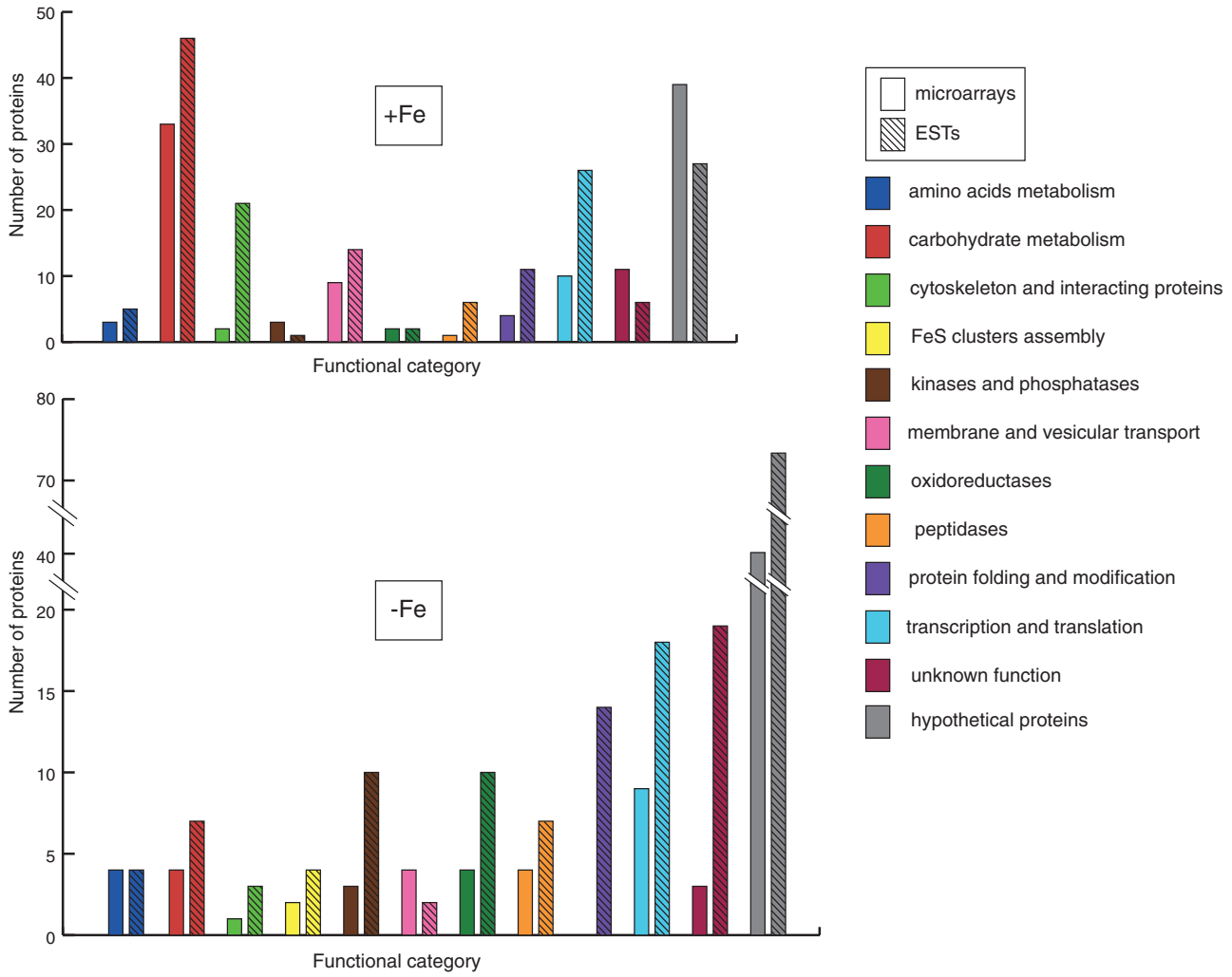

Fig. 2.—Classification of iron-regulated genes by functional category. Numbers of genes that were upregulated under iron-rich (+Fe) and iron-restricted (−Fe) conditions. Results of microarray and EST analysis are represented by open and hatched bars, respectively. Color code of functional categories is given in the legend.

conditions. Finally, the acetyl-CoA that is generated by PFOR activity is used in two steps of ATP synthesis: the reactions catalyzed by acetate:succinate-CoA transferase (ASCT) and heterodimeric succinyl-CoA synthase (SCS). One of the four ASCT genes and all of the genes that encode SCS subunits showed significant upregulation under +Fe conditions.

FeS Cluster Assembly

The biosynthesis of the ISCs that are necessary for the maturation of FeS proteins is an indispensable process that occurs in the hydrogenosomes of *T. vaginalis*. In contrast to the components of energy metabolism, the ISC assembly machinery appeared to be upregulated under −Fe conditions (fig. 4 and supplementary table S3, Supplementary Material online). Our screen detected genes that encode two paralogs of the scaffold protein IscA, three Nfu paralogs, and the cysteine desulfurase IscS-2. Frataxin was previously shown to be upregulated under −Fe conditions using a nuclear run-on assay (Dolezal et al. 2007). This trend was also observed in our analysis, but the cut off limit was not reached (EST upregulation index −2). Interestingly, −Fe conditions also caused a significant increase in the expression of the hydrogenase maturase (Hyd–G) that is required for the assembly of the hydrogenase-specific H cluster (Putz et al. 2006). Altogether, these results suggest a common regulatory mechanism for the genes that encode the multiple components of the ISC assembly machinery that are upregulated under −Fe conditions. This regulation might be related to the sensing of an increased cellular demand for FeS cluster synthesis during −Fe conditions.

Hydrogenosomal Membrane Proteins

Hydrogenosomes are surrounded by two membranes that possess a specific set of proteins that facilitate the exchange

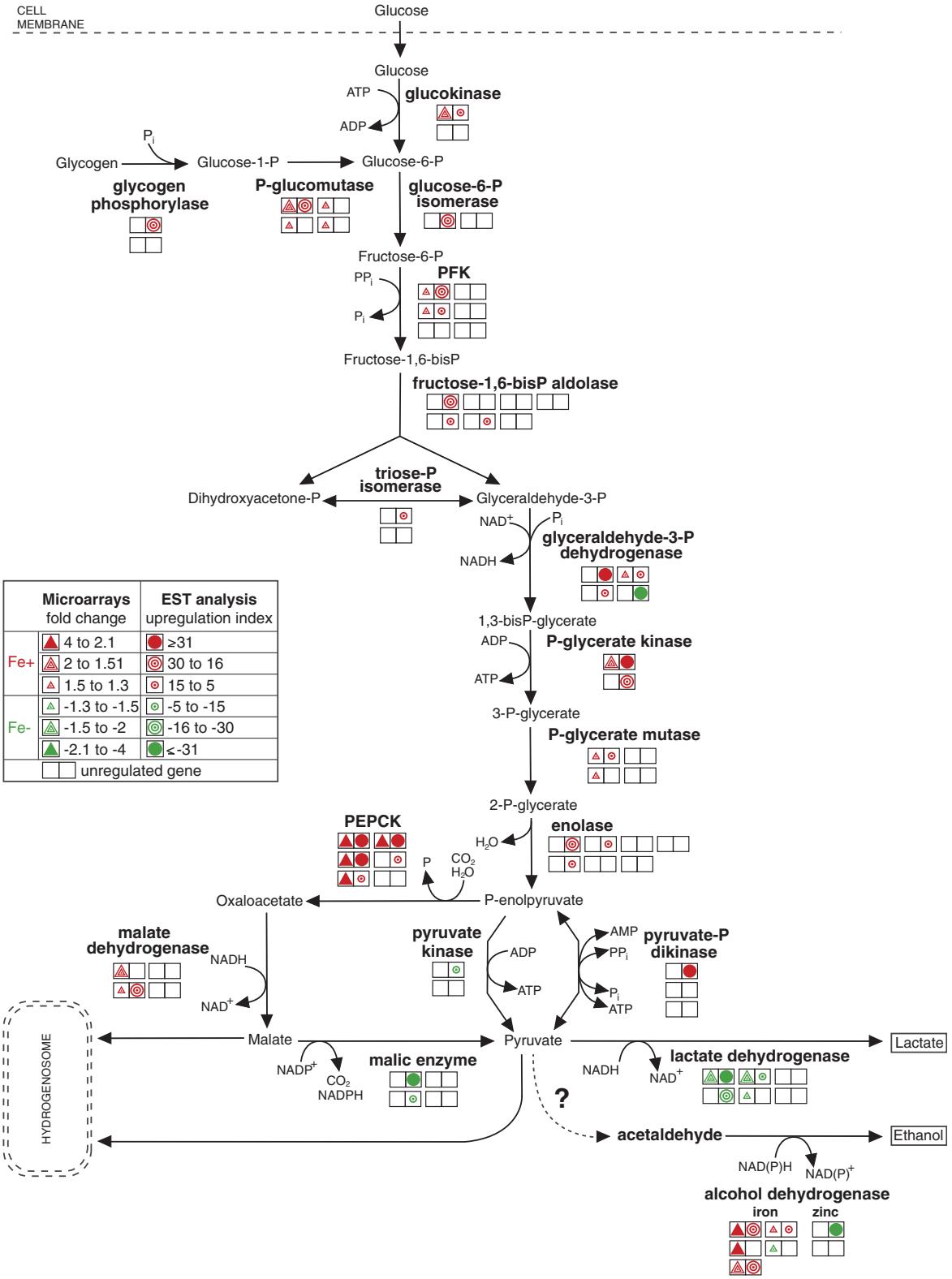

Fig. 3.—Iron-dependent regulation of genes encoding enzymes in glycolytic pathway. Each double square represents a single gene copy. Triangles represent the results of the microarray analysis, and circles represent the results of the EST analysis. Upregulation under +Fe and −Fe conditions is indicated by red and green colors, respectively. The empty squares represent detected, but unregulated gene copies.

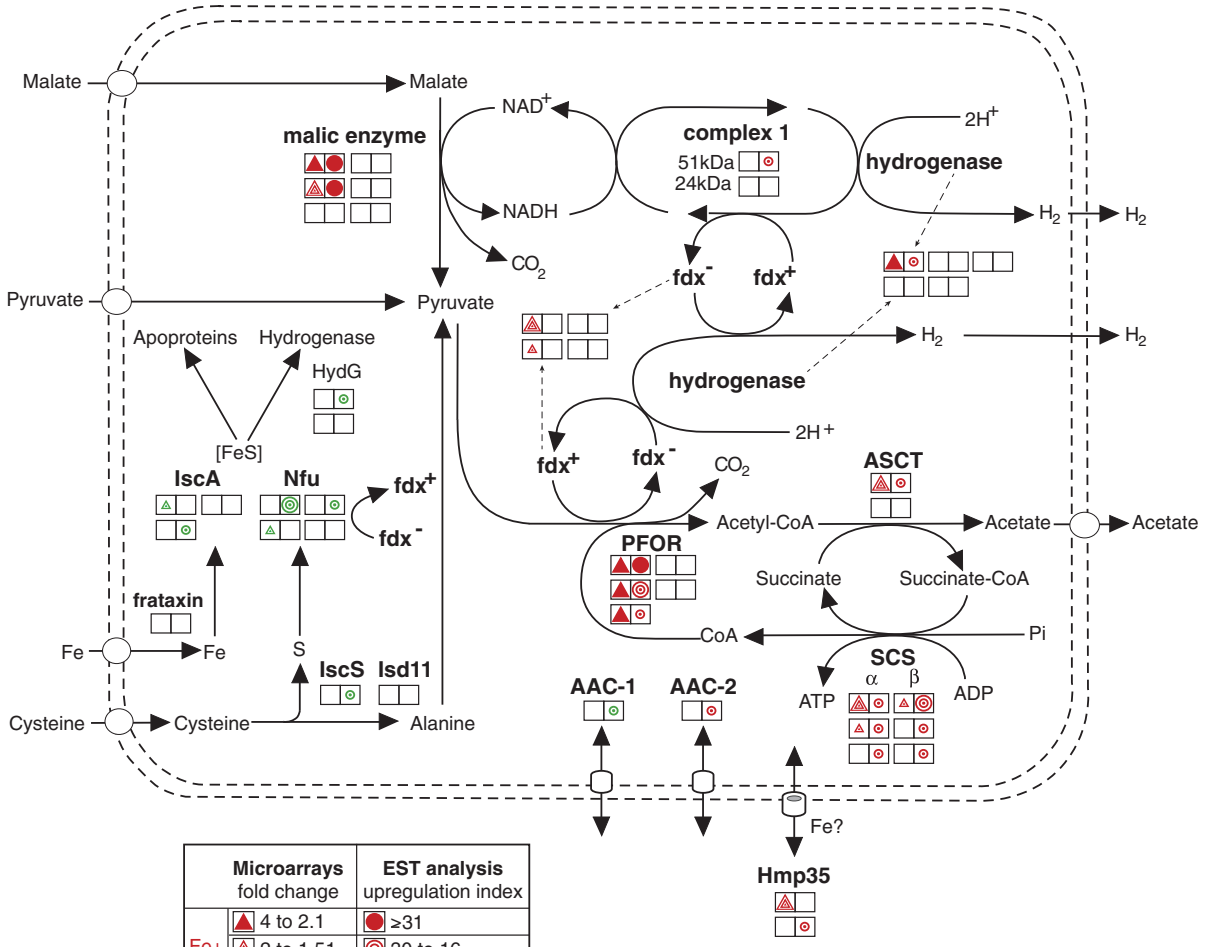

Fig. 4.—Iron-dependent regulation of hydrogenosomal metabolism. Each double square represents a single gene copy. Triangles represent the results of the microarray analysis, and circles represent the results of the EST analysis. Upregulation under +Fe and −Fe conditions is indicated by red and green colors, respectively. The empty squares represent detected, but unregulated gene copies.

of metabolites between the cytosol and organelles. We detected four hydrogenosomal membrane proteins [two Hmp35 and two ADP/ATP carriers (AACs)] that were differentially expressed in response to iron availability (supplementary table S3, Supplementary Material online). Hmp35, which is a unique form of a β-barrel protein that is localized to the outer hydrogenosomal membrane, was significantly upregulated under +Fe conditions. Hmp35 is a cysteine-rich protein with the cysteine residues clustered near the C terminus, where they form a metal-binding motif (Dyall et al. 2003; Rada et al. 2011). These structural properties, together with the observed upregulation of the protein under +Fe conditions, allow us to speculate that Hmp35 may be involved in iron transport. Five members of the mitochondrial carrier protein family (MCF) that serve as AACs in the inner hydrogenosomal membrane have been identified (Dyall et al. 2000; Rada et al. 2011). In this study, two of these proteins showed significant iron-dependent regulation: AAC-1 was upregulated under −Fe conditions, whereas AAC-2 was upregulated under +Fe conditions (fig. 4 and supplementary table S3, Supplementary Material online). As described earlier, active hydrogenosomal energy metabolism is dependent on iron. Under these conditions, a portion of the ATP synthesized in the hydrogenosomes is directly used by processes such as ISC assembly and HSP-70–dependent protein transport and maturation. Some ATP could also be exported by AACs to the cytosol in exchange for ADP as in mitochondria. However, ATP is also required for hydrogenosomal functions under iron-limiting conditions when the expression of enzymes necessary for ATP synthesis is ceased.

Thus, ATP might be imported from the cytosol by AACs. The expression of AAC-1 is increased under −Fe conditions, which renders it the most likely candidate for the transportation of ATP into hydrogenosomes.

Amino Acid Metabolism

The arginine dihydrolase pathway contributes to energy metabolism in *T. vaginalis* (Yarlett et al. 1996). Two components of the pathway, ornithine carbamoyltransferase and carbamate kinase, were significantly upregulated under +Fe conditions (supplementary table S3, Supplementary Material online), whereas arginine deiminase, which was recently shown to be localized in hydrogenosomes (Morada et al. 2011), was not regulated by iron availability.

Methionine can be directly degraded to α-ketobutyrate, ammonia, and thiols or converted to homocysteine. These two metabolic pathways appear to be regulated by iron in opposing manners. Methionine degradation is catalyzed by the unique enzyme methionine γ-lyase (McKie et al. 1998). We found that one of the two genes that encode this enzyme was upregulated under +Fe conditions. In contrast, genes that encode three components of the homocysteine-forming pathway (methionine adenosyltransferase, *S*-adenosyl methionine-dependent methyltransferase, and *S*-adenosyl homocysteine hydrolase) appear to be upregulated under −Fe conditions (fig. 5 and supplementary table S3, Supplementary Material online).

Proteases

Multiple proteinases have been found in *T. vaginalis* (Carlton et al. 2007), and many of them have been implicated in the virulence of the parasite (Dailey et al. 1990; Ramon-Luing et al. 2010). The expression of 16 genes coding for cysteine proteases and metallopeptidases was found to be regulated by iron, and 9 of these genes were upregulated under −Fe conditions (supplementary table S3, Supplementary Material online). De Jesus et al. (2007) used comparative proteomics to show that CP3 and the legumain-like cysteine proteinase-1(LEGU1) are downregulated under −Fe conditions, and their results are consistent with upregulation of these proteins that we observed with EST under +Fe conditions. Kummer et al. (2008) isolated an extracellular protein fraction from *T. vaginalis* that they called CP30 and that contained CP2, CP3, CP4, and CPT, and they demonstrated that trichomonads grown under −Fe conditions had increased CP30 fraction protease activity. These results are consistent with the increased transcription of CP2 observed in our experiments (supplementary table S3, Supplementary Material online), whereas opposite trend we obtained for CP3 and CPT (supplementary table S3, Supplementary Material online).

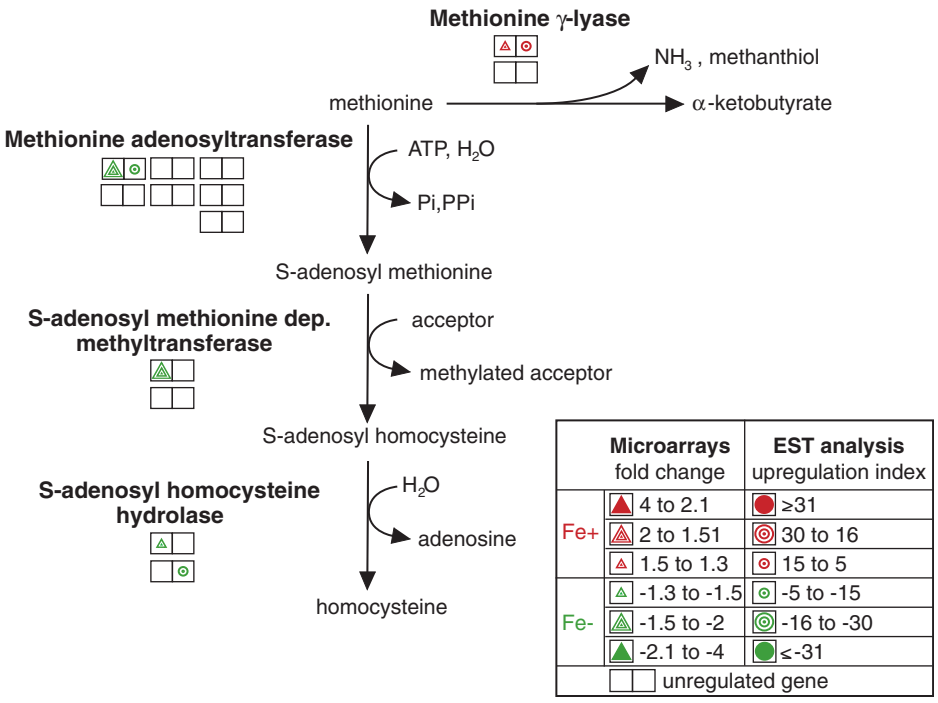

Fig. 5.—Iron-regulated genes involved in methionine metabolism. Each double square represents a single gene copy. Triangles represent the results of the microarray analysis, and circles represent the results of the EST analysis. Upregulation under +Fe and −Fe conditions is indicated by red and green colors, respectively. The empty squares represent detected, but unregulated gene copies.

Table 2
Iron-Regulated Genes That Contain Both MRE1/MRE2r and MRE2f in Their Upstream Regions

TrichDB 1.2 Accession No.	Annotation	MRE1/MRE2r	MRE2f
+Fe		**ANAACGATA**	**TATCGT**
		−111/−103	**−59/−54**
TVAG_422780	Alcohol dehydrogenase	−136/−129	−37/−32
		CGATA	**TATCGT**
		−107/−103	**−59/−54**
TVAG_035180	Arp2/3 complex subunit	−300/−296	−45/−40
TVAG_218790	Conserved hypothetical protein	−230/−226	−110/−105
TVAG_405900	Phosphoglucomutase	−286/−282	−199/−194
		TAACGA	**TATCGTC**
		−110/−105	**−59/−53**
TVAG_072120	Conserved hypothetical protein	−173/−168	−19/−13
−Fe		**CGATA**	**TATCGT**
		−107/−103	**−59/−54**
TVAG_383370	Conserved hypothetical protein	−114/−110	−81/−76
TVAG_474980	Thioredoxin reductase	−151/−147	−107/−102

Note.—The numbers indicate position of the sequence motifs of translation start site. Values in bold indicate position of the motifs in the 5′-UTR of ME (Ong et al. 2006).

Regulation of Transcription

Proteins that are involved in the regulation of transcription and translation, including ribosomal proteins and proteins that affect DNA metabolism, constitute approximately 10% of the iron-regulated genes (fig. 2 and supplementary table S3, Supplementary Material online). Of particular interest are the Myb-like transcription factors, which are exceptionally abundant in the *T. vaginalis* genome and have been suggested to be major regulators of gene transcription (Hsu et al. 2009). In our dataset, we detected the expression of 97 Myb-like DNA-binding proteins, five of which were significantly regulated by iron. One gene was upregulated under +Fe conditions, and four genes were upregulated under −Fe conditions (supplementary table S3, Supplementary Material online). To date, four *T. vaginalis* Myb-like proteins have been characterized (Ong et al. 2006, 2007; Hsu et al. 2009; Smith et al. 2011). It was demonstrated that the temporal and iron-inducible transcription of the ME is regulated by the synergistic or antagonistic actions of three proteins that can selectively bind to two discrete Myb protein recognition sites in the 5′-untranslated regions (5′-UTR) of the ME gene. Myb1 and Myb2, that play the roles of a repressor and an activator, respectively, are able to bind to both sites with affinities that differ over time and according to iron availability (Ong et al. 2006, 2007). Myb3 activates basal and prolonged iron-inducible transcription by binding solely to the MRE1 site (Hsu et al. 2009). In the *T. vaginalis* genome, there are three genes that encode Myb-3-like proteins, and all three products contain conserved base-contacting amino acids. Hsu et al. (2009) showed that the gene copy TVAG_475500 is upregulated under +Fe conditions. In our screen, we detected a second copy (TVAG_252420) that was upregulated under −Fe conditions. We also identified a Myb2 gene; however, under our experimental conditions, Myb2 was not regulated by iron, which contradicts the findings of Ong et al. (2007).

Because MRE sites were demonstrated to be essential for the iron-dependent regulation of ME, we searched 300 bp of the 5′-UTR of all iron-regulated genes detected in our screen for the presence of MRE motifs. We found numerous genes that had upstream sequences containing the MRE eukaryotic consensus sequence (C/T)AACG(G/T) or specific MRE-like sites similar to those found in the ME gene (supplementary table S4, Supplementary Material online). The genes that contain both MRE1/MRE2r and MRE2f in their upstream regions, and that have the motifs in the same order as in ME upstream region, are listed in table 2. Interestingly, the 5′-UTR of the genes that encode ADH, hypothetical protein TVAG_383310 and thioredoxin reductase contain both elements at positions similar to those in the 5′-UTR sequence of the ME gene (table 2), which suggests a similar multifarious Myb-mediated regulation of transcription.

Conclusions

The 160 Mb *T. vaginalis* genome is the largest protozoan genome that has been sequenced thus far (Carlton et al. 2007). A unique feature of the *Trichomonas* genome among all sequenced eukaryotes is the massive expansion of many gene families and the retention of multiple copies for almost

all genes (Cui et al. 2010). The mechanistic origins and biological functions of these multiple gene copies are yet unknown, but it is clear that they provided abundant starting material for evolutionary innovation while also contributing to the genetic robustness of the organism (Li et al. 2010). Indeed, because the *T. vaginalis* genome appears to be haploid, genetic redundancy might be particularly important to buffer gene mutations. Moreover, the differential expression of paralogous copies could be necessary for optimal growth in response to various environmental conditions (Giaever et al. 2002). We demonstrated that iron, a critical nutrient for *T. vaginalis*, has broad effects on the parasite's trancriptome, which is consistent with the observation that iron modulates trichomonad growth, metabolic fluxes, and virulence phenotypes such as cytoadherence (Mundodi et al. 2006). However, we found that in most cases iron regulated the expression of a single gene or a portion of the gene copies, whereas the expression of other paralogous copies of the gene was iron independent.

The strongest iron-dependent upregulation we observed was for ME and PFOR, enzymes that play critical roles in hydrogenosomal energy metabolism and that are known to exhibit iron-dependent changes in protein expression and enzyme activity (Vanacova et al. 2001; Leitsch et al. 2009. However, we also found that there were four gene copies for ME, and two for PFOR, whose expression was not iron dependent. Of all major enzymes involved in hydrogenosomal energy metabolism, only SCS, which mediates the final step of ATP synthesis, appears to be an exception in that the expression of all copies of both SCS subunits was iron dependent. Further studies of expression profiles for cells grown under various conditions such as the absence of external glucose, temperature or oxygen stress, the induction of the amoeboid form or comparison with nonpathogenic forms should lead to further insights as to how individual copies among the myriad trichomonad gene families have come to fall under differential iron regulation during evolution.

Supplementary Material

Supplementary figure S1 and tables S1–S4 are available at *Genome Biology and Evolution* online (http://www.gbe.oxfordjournals.org/).

Acknowledgments

The authors thank M. Marcinčiková for technical support and J. Horváth for the development of the sequence motif searching software. This work was supported by the Czech Ministry of Education grants [MSM0021620858, LC07032] to J.T. and the Charles University GAUK 179/2006/B-BIO/PrF to L.Š. The *T. vaginalis* EST sequencing project was supported by the Chang Gung Memorial Hospital research grant [SMRPD33002] to P.T.

Literature Cited

Alderete JF, Provenzano D, Lehker MW. 1995. Iron mediates *Trichomonas vaginalis* resistance to complement lysis. Microb Pathog. 19:93–103.

Carlton JM, et al. 2007. Draft genome sequence of the sexually transmitted pathogen *Trichomonas vaginalis*. Science 315:207–212.

Cerkasovová A, Novák J, Cerkasov J, Kulda J, Tachezy J. 1986. Metabolic properties of *Trichomonas vaginalis* resistant to metronidazole under anaerobic conditions. In: Kulda J, Cerkasov J, editors. Trichomonads and trichomoniasis, Vol. 2. Prague: Acta Universitatis Carolinae Biologica. p. 505–512.

Cotch MF, et al. 1997. *Trichomonas vaginalis* associated with low birth weight and preterm delivery. The Vaginal Infections and Prematurity Study Group. Sex Transm Dis. 24:353–360.

Cui J, Das S, Smith TF, Samuelson J. 2010. *Trichomonas* transmembrane cyclases result from massive gene duplication and concomitant development of pseudogenes. PLoS Negl Trop Dis. 4:e782.

Dailey DC, Chang TH, Alderete JF. 1990. Characterization of *Trichomonas vaginalis* haemolysis. Parasitology 101(Pt 2):171–175.

Dallas PB, et al. 2005. Gene expression levels assessed by oligonucleotide microarray analysis and quantitative real-time RT-PCR—how well do they correlate? BMC Genomics 6:59.

De Jesus JB, et al. 2006. Iron modulates ecto-phosphohydrolase activities in pathogenic trichomonads. Parasitol Int. 55:285–290.

De Jesus JB, et al. 2007. A further proteomic study on the effect of iron in the human pathogen *Trichomonas vaginalis*. Proteomics 7: 1961–1972.

Diamond LS. 1957. The establishment of various trichomonads of animals and man in axenic cultures. J Parasitol. 43:488–490.

Dolezal P, et al. 2007. Frataxin, a conserved mitochondrial protein, in the hydrogenosome of *Trichomonas vaginalis*. Eukaryot Cell. 6: 1431–1438.

Dyall SD, et al. 2000. Presence of a member of the mitochondrial carrier family in hydrogenosomes: conservation of membrane-targeting pathways between hydrogenosomes and mitochondria. Mol Cell Biol. 20: 2488–2497.

Dyall SD, et al. 2003. *Trichomonas vaginalis* Hmp35, a putative pore-forming hydrogenosomal membrane protein, can form a complex in yeast mitochondria. J Biol Chem. 278:30548–39561.

Giaever G, et al. 2002. Functional profiling of the *Saccharomyces cerevisiae* genome. Nature 418:387–391.

Gorrell TE. 1985. Effect of culture medium iron content on the biochemical composition and metabolism of *Trichomonas vaginalis*. J Bacteriol. 161:1228–1230.

Hirt RP, Noel CJ, Sicheritz-Ponten T, Tachezy J, Fiori PL. 2007. *Trichomonas vaginalis* surface proteins: a view from the genome. Trends Parasitol. 23:540–547.

Hrdy I, et al. 2004. *Trichomonas* hydrogenosomes contain the NADH dehydrogenase module of mitochondrial complex I. Nature 432: 618–622.

Hsu HM, Ong SJ, Lee MC, Tai JH. 2009. Transcriptional regulation of an iron-inducible gene by differential and alternate promoter entries of multiple Myb proteins in the protozoan parasite *Trichomonas vaginalis*. Eukaryot Cell. 8:362–372.

Kispal G, et al. 2005. Biogenesis of cytosolic ribosomes requires the essential iron-sulphur protein Rli1p and mitochondria. EMBO J. 24: 589–598.

Kulda J, Poislova M, Suchan P, Tachezy J. 1999. Iron enhancement of experimental infection of mice by *Tritrichomonas foetus*. Parasitol Res. 85:692–699.

Kulda J, Tachezy J, Cerkasovova A. 1993. In vitro induced anaerobic resistance to metronidazole in *Trichomonas vaginalis*. J Eukaryot Microbiol. 40:262–269.

Kummer S, et al. 2008. Induction of human host cell apoptosis by *Trichomonas vaginalis* cysteine proteases is modulated by parasite exposure to iron. Microb Pathog. 44:197–203.
Laga M, et al. 1993. Non-ulcerative sexually transmitted diseases as risk factors for HIV-1 transmission in women: results from a cohort study. AIDS 7:95–102.
Lee NH, et al. 1995. Comparative expressed-sequence-tag analysis of differential gene expression profiles in PC-12 cells before and after nerve growth factor treatment. Proc Natl Acad Sci U S A. 92: 8303–8307.
Leitsch D, et al. 2009. *Trichomonas vaginalis:* metronidazole and other nitroimidazole drugs are reduced by the flavin enzyme thioredoxin reductase and disrupt the cellular redox system. Implications for nitroimidazole toxicity and resistance. Mol Microbiol. 72:518–536.
Li J, Yuan Z, Zhang Z. 2010. The cellular robustness by genetic redundancy in budding yeast. PLoS Genet. 6:e1001187.
Liapounova NA, et al. 2006. Reconstructing the mosaic glycolytic pathway of the anaerobic eukaryote *Monocercomonoides*. Eukaryot Cell. 12: 2138–2146.
Livak KJ, Schmittgen TD. 2001. Analysis of relative gene expression data using real-time quantitative PCR and the 2(-Delta Delta C(T)) method. Methods 25:402–408.
Lynch M, Conery JS. 2000. The evolutionary fate and consequences of duplicate genes. Science 290:1151–1155.
McKie AE, Edlind T, Walker J, Mottram JC, Coombs GH. 1998. The primitive protozoon *Trichomonas vaginalis* contains two methionine gamma-lyase genes that encode members of the gamma-family of pyridoxal 5′-phosphate-dependent enzymes. J Biol Chem. 273: 5549–5556.
Mertens E, et al. 1998. The pyrophosphate-dependent phosphofructokinase of the protist, *Trichomonas vaginalis*, and the evolutionary relationships of protist phosphofructokinases. J Mol Evol. 47(6):739–750.
Moodley P, Wilkinson D, Connolly C, Moodley J, Sturm AW. 2002. *Trichomonas vaginalis* is associated with pelvic inflammatory disease in women infected with human immunodeficiency virus. Clin Infect Dis. 34:519–522.
Morada M, et al. 2011. Hydrogenosome-localization of arginine deiminase in *Trichomonas vaginalis*. Mol Biochem Parasitol. 176:51–54.
Mundodi V, Kucknoor AS, Chang TH, Alderete JF. 2006. A novel surface protein of *Trichomonas vaginalis* is regulated independently by low iron and contact with vaginal epithelial cells. BMC Microbiol. 6:6.
Müller M, et al. 2012. Biochemistry and evolution of anaerobic energy metabolism in eukaryotes. Microbiol Mol Biol Rev. 76:444–495.
Ong SJ, Hsu HM, Liu HW, Chu CH, Tai JH. 2007. Activation of multifarious transcription of an adhesion protein ap65-1 gene by a novel Myb2 protein in the protozoan parasite *Trichomonas vaginalis*. J Biol Chem. 282:6716–6725.
Ong SJ, Hsu HM, Liu HW, Chu CH, Tai JH. 2006. Multifarious transcriptional regulation of adhesion protein gene ap65-1 by a novel Myb1 protein in the protozoan parasite *Trichomonas vaginalis*. Eukaryot Cell. 5:391–399.
Putz S, et al. 2006. Fe-hydrogenase maturases in the hydrogenosomes of *Trichomonas vaginalis*. Eukaryot Cell. 5:579–586.
Rada P, et al. 2011. The core components of organelle biogenesis and membrane transport in the hydrogenosomes of *Trichomonas vaginalis*. PloS One. 6:e24428.
Ramon-Luing LA, et al. 2010. Immunoproteomics of the active degradome to identify biomarkers for *Trichomonas vaginalis*. Proteomics 10:435–444.
Rasoloson D, et al. 2002. Mechanisms of in vitro development of resistance to metronidazole in *Trichomonas vaginalis*. Microbiology 148(Pt 8): 2467–2477.
Rawat P, Kumar S, Sheokand N, Raje CI, Raje M. 2012. The multifunctional glycolytic protein glyceraldehyde-3-phosphate dehydrogenase (GAPDH) is a novel macrophage lactoferrin receptor. Biochem Cell Biol. 90(3):329–338.
Saeed AI, et al. 2003. TM4: a free, open-source system for microarray data management and analysis. Biotechniques 34:374–378.
Smith AJ, et al. 2011. Novel core promoter elements and a cognate transcription factor in the divergent unicellular eukaryote *Trichomonas vaginalis*. Mol Cell Biol. 31:1444–1458.
Smíd O, et al. 2008. Reductive evolution of the mitochondrial processing peptidases of the unicellular parasites *Trichomonas vaginalis* and *Giardia intestinalis*. PLoS Pathogens. 4:e1000243.
Solano-González E, et al. 2007. The trichomonad cysteine proteinase TVCP4 transcript contains an iron-responsive element. FEBS Lett. 581:2919–2928.
Sommer U, et al. 2005. Identification of *Trichomonas vaginalis* cysteine proteases that induce apoptosis in human vaginal epithelial cells. J Biol Chem. 280:23853–23860.
Sutak R, Dolezal P, et al. 2004. Mitochondrial-type assembly of FeS centers in the hydrogenosomes of the amitochondriate eukaryote *Trichomonas vaginalis*. Proc Natl Acad Sci U S A. 101: 10368–10373.
Sutak R, Lesuisse E, Tachezy J, Richardson DR. 2008. Crusade for iron: iron uptake in unicellular eukaryotes and its significance for virulence. Trends Microbiol. 16:261–268.
Sutak R, Tachezy J, Kulda J, Hrdy I. 2004. Pyruvate decarboxylase, the target for omeprazole in metronidazole-resistant and iron-restricted *Tritrichomonas foetus*. Antimicrob Agents Chemother. 48: 2185–2189.
Tachezy J, Sánchez LB, Müller M. 2001. Mitochondrial type iron-sulfur cluster assembly in the amitochondriate eukaryotes *Trichomonas vaginalis* and *Giardia intestinalis*, as indicated by the phylogeny of IscS. Mol Biol Evol. 18:1919–1928.
Torres-Romero JC, Arroyo R. 2009. Responsiveness of *Trichomonas vaginalis* to iron concentrations: evidence for a post-transcriptional iron regulation by an IRE/IRP-like system. Infect Genet Evol. 9: 1065–1074.
Vanácová S, et al. 2001. Iron-induced changes in pyruvate metabolism of *Tritrichomonas foetus* and involvement of iron in expression of hydrogenosomal proteins. Microbiology 147:53–62.
Viikki M, Pukkala E, Nieminen P, Hakama M. 2000. Gynaecological infections as risk determinants of subsequent cervical neoplasia. Acta Oncol. 39:71–75.
Yarlett N, Martinez MP, Moharrami MA, Tachezy J. 1996. The contribution of the arginine dihydrolase pathway to energy metabolism by *Trichomonas vaginalis*. Mol Biochem Parasitol. 78:117–125.
Yarunin A, et al. 2005. Functional link between ribosome formation and biogenesis of iron-sulfur proteins. EMBO J. 24:580–588.
Yuen T, Wurmbach E, Pfeffer RL, Ebersole BJ, Sealfon SC. 2002. Accuracy and calibration of commercial oligonucleotide and custom cDNA microarrays. Nucleic Acids Res. 30:e48.
Zhang ZF, Begg CB. 1994. Is *Trichomonas vaginalis* a cause of cervical neoplasia? Results from a combined analysis of 24 studies. Int J Epidemiol. 23:682–690.

Associate editor: Bill Martin

8.3 The core components of organelle biogenesis and membrane transport in the hydrogenosomes of *Trichomonas vaginalis*.

OPEN ACCESS Freely available online

PLoS one

The Core Components of Organelle Biogenesis and Membrane Transport in the Hydrogenosomes of *Trichomonas vaginalis*

Petr Rada[1], Pavel Doležal[1], Petr L. Jedelský[1,2], Dejan Bursac[3¤], Andrew J. Perry[3], Miroslava Šedinová[1], Kateřina Smíšková[1], Marian Novotný[1], Neritza Campo Beltrán[1], Ivan Hrdý[1], Trevor Lithgow[3], Jan Tachezy[1]*

1 Department of Parasitology, Charles University in Prague, Faculty of Science, Prague, Czech Republic, **2** Laboratory of Mass Spectrometry, Charles University in Prague, Faculty of Science, Prague, Czech Republic, **3** Department of Biochemistry & Molecular Biology, Monash University, Melbourne, Australia

Abstract

Trichomonas vaginalis is a parasitic protist of the Excavata group. It contains an anaerobic form of mitochondria called hydrogenosomes, which produce hydrogen and ATP; the majority of mitochondrial pathways and the organellar genome were lost during the mitochondrion-to-hydrogenosome transition. Consequently, all hydrogenosomal proteins are encoded in the nucleus and imported into the organelles. However, little is known about the membrane machineries required for biogenesis of the organelle and metabolite exchange. Using a combination of mass spectrometry, immunofluorescence microscopy, *in vitro* import assays and reverse genetics, we characterized the membrane proteins of the hydrogenosome. We identified components of the outer membrane (TOM) and inner membrane (TIM) protein translocases include multiple paralogs of the core Tom40-type porins and Tim17/22/23 channel proteins, respectively, and uniquely modified small Tim chaperones. The inner membrane proteins TvTim17/22/23-1 and Pam18 were shown to possess conserved information for targeting to mitochondrial inner membranes, but too divergent in sequence to support the growth of yeast strains lacking Tim17, Tim22, Tim23 or Pam18. Full complementation was seen only when the J-domain of hydrogenosomal Pam18 was fused with N-terminal region and transmembrane segment of the yeast homolog. Candidates for metabolite exchange across the outer membrane were identified including multiple isoforms of the β-barrel proteins, Hmp35 and Hmp36; inner membrane MCF-type metabolite carriers were limited to five homologs of the ATP/ADP carrier, Hmp31. Lastly, hydrogenosomes possess a pathway for the assembly of C-tail-anchored proteins into their outer membrane with several new tail-anchored proteins being identified. These results show that hydrogenosomes and mitochondria share common core membrane components required for protein import and metabolite exchange; however, they also reveal remarkable differences that reflect the functional adaptation of hydrogenosomes to anaerobic conditions and the peculiar evolutionary history of the Excavata group.

Citation: Rada P, Doležal P, Jedelský PL, Bursac D, Perry AJ, et al. (2011) The Core Components of Organelle Biogenesis and Membrane Transport in the Hydrogenosomes of *Trichomonas vaginalis*. PLoS ONE 6(9): e24428. doi:10.1371/journal.pone.0024428

Editor: Bob Lightowlers, Newcastle University, United Kingdom

Received May 30, 2011; **Accepted** August 9, 2011; **Published** September 15, 2011

Funding: This work was supported by grants from the Czech Ministry of Education (MSM0021620858, LC07032), Czech Science Foundation (P305/10/0651), and Australian Research Council. AP is a National Health and Medical Research Council Postdoctoral Fellow, and TL is an Austrailian Research Council Federation Fellow. The funders had no role in study design, data collection and analysis, decision to publish, or preparation of the manuscript.

Competing Interests: The authors have declared that no competing interests exist.

* E-mail: tachezy@natur.cuni.cz

¤ Current address: The Walter and Eliza Hall Institute of Medical Research, Melbourne, Australia

Introduction

Hydrogenosomes are highly divergent forms of mitochondria adapted for ATP synthesis under anaerobic conditions with the concomitant production of molecular hydrogen [1]. These organelles are present in pathogenic and free-living unicellular eukaryotes that inhabit oxygen-poor environments [2]. In the course of the mitochondria-to-hydrogenosome transition, aspects of typical mitochondrial energy metabolism were lost, including the classic pyruvate dehydrogenase complex, the citric acid cycle and the elaborate membrane-associated respiratory chain. Given the absence of genes encoding the membrane subunits of respiratory complexes, which are invariably coded by the mitochondrial genome (e.g., cytochrome oxidase subunit Cox1 and cytochrome b), perhaps this is the reason that hydrogenosomal genomes were relinquished [3,4]. To synthesize ATP, hydrogenosomes have gained specific pathways that metabolize pyruvate or malate to acetate and CO_2 and hydrogen in a process accompanied by substrate-level phosphorylation [1].

One of the major mitochondrial functions is to supply other cellular compartments with metabolic energy. The evolution of ADP/ATP carriers (AACs) provided a means to mediate the export of ATP across the mitochondrial inner membrane in exchange for ADP. The function of AACs is coupled with a specific family of porins called voltage-dependent anion channels (VDACs) that passively allow a nucleotide flux across the outer membrane [5]. In addition to AACs, the mitochondrial inner membrane possesses up to 55 distinct carriers that belong to a large mitochondrial carrier protein family (MCF) [6–11]. These carriers facilitate the exchange of a wide variety of metabolites to connect cytosolic and

mitochondrial metabolism [12,13]. MCFs and VDACs are nuclearly encoded proteins that are synthesized in the cytosol and targeted to a translocase in the outer mitochondrial membrane (TOM) complex. The TOM complex is the main gate for the entry of mitochondrial proteins into the intermembrane space, where they are further sorted according to their final destination. The porin precursors that are targeted to the outer membrane are assembled by sorting and assembly machinery (SAM complex). The AACs and other MCFs are assembled by a protein translocase in the inner mitochondrial membrane (TIM) complex. In many eukaryotes, there are two distinct TIM complexes [14,15] that are built from distinct members of the Tim17/Tim22/Tim23 family of proteins. In this case, the MCFs are assembled by the TIM22 complex [16–19], whereas proteins transferred into the matrix are assembled by the TIM23 complex in a process catalyzed by the presequence translocase-associated motor (PAM) complex.

Our knowledge about the proteins in hydrogenosomal membranes that facilitate protein transport and the exchange of metabolites is in its infancy. The most-studied hydrogenosomes are those in the human pathogen, *Trichomonas vaginalis*, for which the complete genome sequence is available [20]. However, only two hydrogenosomal membrane proteins, i.e., Hmp31 and Hmp35, have been described in this organism thus far. Hmp31 is a MCF member and serves as an AAC carrier localized in the inner hydrogenosomal membrane [21–24]. The cysteine-rich Hmp35 protein is predicted to form pores but has no known homologs; its precise function is unknown. Despite the paucity of knowledge on membrane proteins, a number of proteins have been localized in the matrix of hydrogenosomes. The targeting of matrix proteins is dependent on N-terminal cleavable presequences [25,26] or internal targeting signals [27]. The presequences are removed in the hydrogenosomal matrix by a dimeric hydrogenosomal processing peptidase that shares a common origin with the mitochondrial processing peptidase, MPP [26].

To gain insight into the processes mediating the exchange of metabolites and the protein import machinery in *T. vaginalis* hydrogenosomes, we established a proteomics survey of the organelle. We sought to determine how many outer membrane porins and inner membrane MCF-like carriers are present in the hydrogenosomes, what the spectrum of other hydrogenosomal multitopic and monotopic membrane proteins is, and whether any components of the protein import machinery have been overlooked by previous bioinformatic-only searches [14,20]. The proteomic approach, together with bioinformatics, biochemical assays and fluorescence microscopy, allowed the identification and validation of an unusually large number of β-barrel proteins, including several paralogs of Tom40, Sam50 and Hmp35, whereas the spectrum of inner membrane carriers was apparently limited to the AAC types of MCF. Two selected components of the inner membrane translocase, Tim17-22-23A and Pam18, were identified, and their efficient assembly into yeast mitochondrial membranes suggests the conservation of membrane targeting signals for these inner membrane proteins. However, the extreme divergence of four hydrogenosomal Tim17-22-23 family proteins obscures the determination of whether distinct TIM23 and TIM22 complexes are both present in the hydrogenosomes. Lastly, we identified two small Tim chaperones with previously unseen modifications that adapt them to function in the unique anaerobic conditions of the hydrogenosomes in *T. vaginalis*.

Results

Identification of hydrogenosomal membrane proteins of diverse topologies

Hydrogenosomes were purified by differential and Percoll-gradient centrifugation from a lysate of *T. vaginalis*, and membrane proteins were extracted from the purified hydrogenosomes using Triton X-114. The extracted proteins were separated by 1D SDS-PAGE (Fig. 1), the gel lane was cut into 47 slices, and each slice was submitted to nanoLC MS/MS analysis (Table S1). The sequences of the identified proteins were analyzed by a range of bioinformatic tools designed for the detection of conserved domains using multiple sequence alignments and hidden Markov models, structure predictions, and predictions of subcellular localization (Tables 1A,1B and S2). We identified 68 putative membrane proteins; we annotated 17 of these as components of protein import machinery, including key components of the outer membrane TOM and inner membrane TIM complexes. In addition, 11 polytopic transmembrane proteins and 44 integral monotopic proteins were identified, as judged by transmembrane prediction algorithms (see the Materials and Methods). The most abundant proteins observed by electrophoresis after Triton X-114 extraction included eight integral membrane proteins: ADP/ATP carrier-1, ADP/ATP carrier-2, Hmp35-2, Hmp36-1, Sam50, hypothetical proteins TVAG_455090 and TVAG_440200, and pyruvate:ferredoxin oxidoreductase, in addition to the most abundant soluble protein in the hydrogenosome, i.e., malic enzyme (Fig. 1).

To validate the proteomic and sequence analysis, we chose 26 of these putative hydrogenosomal membrane proteins and tested their localization using the expression of epitope-tagged constructs in *T. vaginalis* (Fig. 2 and Table 1,2). Immunofluorescent microscopy revealed the colocalization of tagged proteins and the hydrogenosomal marker protein, malic enzyme. The membrane proteins were often observed at the peripheral rings surrounding the hydrogenosomal matrix labeled by the anti-malic enzyme antibody.

The proteomic survey identified the products of 63 genes that were either previously annotated as encoding 'hydrogenosomal proteins' with known matrix localization or novel hydrogenosomal

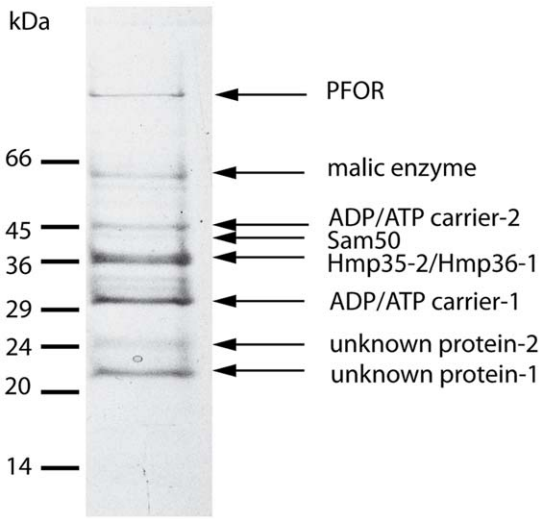

Figure 1. Proteins extracted by Triton-X114 from hydrogenosomal membranes. The most abundant proteins observed by electrophoresis after Triton X-114 extraction included seven integral membrane proteins (ADP/ATP carrier-1, ADP/ATP carrier-2, Hmp35-2, Hmp36-1, Sam50, unknown protein-1 TVAG_455090, and unknown protein-2 TVAG_440200), an integral monotopic proteins (pyruvate:ferredoxin oxidoreductase, PFOR), and malic enzyme, which is the dominant hydrophobic protein in hydrogenosomes.
doi:10.1371/journal.pone.0024428.g001

Table 1. Putative membrane proteins identified in *T. vaginalis* hydrogenosomes.

Identification		Structure		Cell localization			Signal
Accession number	Name	TMHMM	MEMSAT3	TargetP	PsortII	Exp. Local.	
		TM No.	TM No.		mit%		
Protein import machinery							
TVAG_399510	Tom40-1	0	0	O	17.4%	NV	β
TVAG_332970	Tom40-2	0	0	O	*		β
TVAG_450220	Tom40-3	0	0	O	17.4%	H	β
TVAG_123100	Tom40-4	0	0	O	4.3%	NV	β
TVAG_341190	Tom40-5	0	0	O	8.7%	H	β
TVAG_195900	Tom40-6	0	0	O	4.3%	H	β
TVAG_178100	Sam50	0	0	O	17.4%	H	β
TVAG_287510	small Tim9-10A	0	0	O	8.7%	H	
TVAG_026080	small Tim9-10B	0	0	O	4.3%	H	
TVAG_198350	Tim17/22/23A	0	0	O	8.7%	H	
TVAG_061900	Tim17/22/23B	2	0	O	17.4%	H	
TVAG_370860	Tim17/22/23C	0	0	O	26.1%	H	
TVAG_379950	Tim17/22/23D	3	0	O	8.7%		
TVAG_447580	Tim17-like	0	0	M	4.3%		
TVAG_008790	Tim44	0	0	M	17.4%	H	
TVAG_470110	Pam16	0	0	O	17.4%	H	
TVAG_436580	Pam18	0	1	O	13.0%	H	Δ
beta-barrel proteins							
TVAG_146920	Porin-1	0	0	O	4.3%		β
TVAG_340380	Porin-2	0	0	O	21.7%		β
TVAG_590550	Hmp-35-1	0	0	O	8.7%	H[50]	β
TVAG_104250	Hmp-35-2	0	0	O	8.7%	H	β
TVAG_031860	Hmp-36-1	0	0	O	4.3%		
TVAG_216170	Hmp-36-2	0	0	O	8.7%		
Integral polytopic proteins							
TVAG_237680	ADP/ATP carrier-1, Hmp-31	0	5	O	26.1%	H[21]	
TVAG_051820	ADP/ATP carrier-2	0	6	O	34.8%	H	
TVAG_164560	ADP/ATP carrier-3	0	4	O	8.7%		
TVAG_196220	ADP/ATP carrier-4	0	5	O	13.0%		
TVAG_262210	ADP/ATP carrier-5	0	5	O	13.0%		
TVAG_039960	Unknown	6	6	S	11.1%	H	
TVAG_455090	Unknown	2	1	O	17.4%	H	
TVAG_489980	Unknown	6	3	O	4.3%		
TVAG_127990	Unknown	2	2	O	21.7%		
TVAG_440200	Unknown	3	2	O	4.3%		
TVAG_136450	Unknown	0	2	O	8.7%		
TVAG_192370	Unknown	2	1	O	11.1%	H	

doi:10.1371/journal.pone.0024428.t001

matrix proteins, such as alanine aminotransferase, phosphofructokinase, hybrid cluster proteins, and Ind-1 (Tables S3A-C), and the protein products of 45 genes that were previously annotated as encoding 'hypothetical proteins' with unclear localization (Tables S4C and S4D). The hydrogenosomal preparation also contained 52 proteins annotated as being found in other cellular locations; some of these identified proteins may represent contamination by other membranes (e.g., the ABC transporter, MFS transporter and vacuolar proton ATPase) or cytoplasmic adherence on the hydrogenosomes (e.g., cytosolic HSP70 and cytoskeletal proteins), whereas many were simply inferred to be located elsewhere based on minimal sequence similarity to proteins from other eukaryotes (Tables S3A–C and S4A–D).

Polytopic proteins of the mitochondrial carrier family

Multiple transmembrane domains were predicted in 12 of the identified proteins. Of these, five were classified as MCF members: one of these proteins is Hmp31 [21], and the other four have not

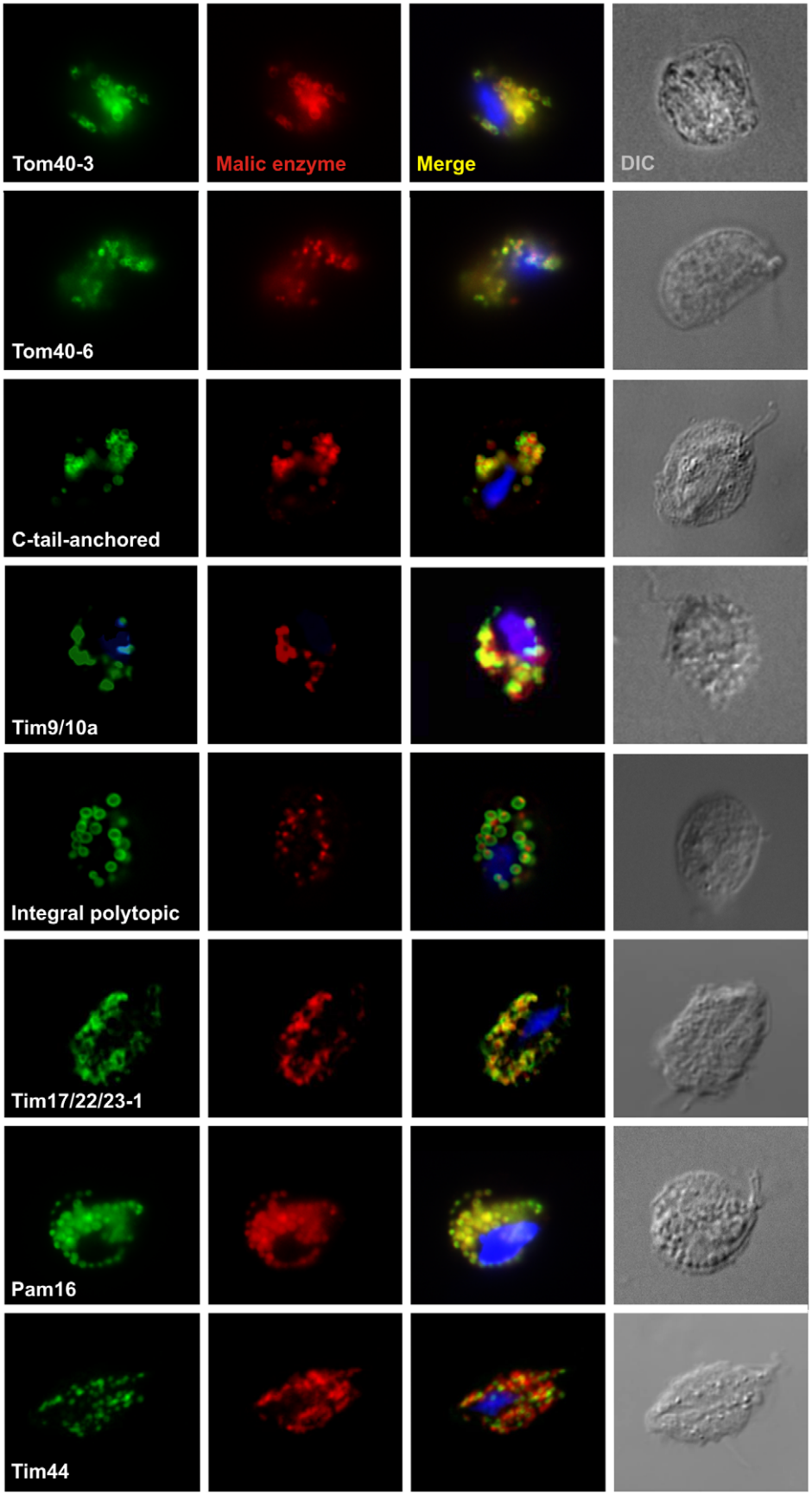
Tom40-3
Malic enzyme
Merge
DIC
Tom40-6
C-tail-anchored
Tim9/10a
Integral polytopic
Tim17/22/23-1
Pam16
Tim44

Figure 2. Immunofluorescent microscopy of *T. vaginalis* strains expressing selected membrane proteins. Hemagglutinin-tagged proteins were visualized using an anti-hemagglutinin mouse monoclonal antibody (in green). The matrix protein, malic enzyme, was visualized using a rabbit polyclonal anti-malic antibody (in red). The nucleus was stained with DAPI (blue). DIC, differential interference contrast. Tom40-3 (TVAG_450220), Tom40-6 (TVAG_195900), C-tail-anchored (TVAG_277930), Tim9/10a (TVAG_287510), integral polytopic (TVAG_455090), Tim17/22/23-1 (TVAG_198350), Pam16 (TVAG_470110), Tim44 (TVAG_008790).
doi:10.1371/journal.pone.0024428.g002

been previously studied and have no obvious orthologs in other organisms. It was predicted that all five of the hydrogenosomal MCF proteins contain the characteristic six transmembrane alpha-helices. As with all carrier proteins, in these five hydrogenosomal proteins, the odd-numbered helices contain P-X-[DE]-X-X-[KR] signature motifs that, in the context of the three-dimensional structure, surround the pore and determine the substrate specificity of the carrier [28] (Fig. 3). An ADP-ATP exchange activity has been determined for Hmp31 in *Trichomonas gallinae*, and the other carrier proteins we identified in hydrogenosomes have sequence motifs (such as the RRRMMM signature; Fig. S1) that suggest that they also mediate nucleotide exchange.

Single-spanning and C-tail-anchored proteins

According to the structure predictions, 33 putative hydrogenosomal proteins were classified as integral monotopic proteins with a single hydrophobic transmembrane domain (TMD). Of these proteins, 21 contain a TMD located in the middle of the protein, with N- and C-terminal flanking regions (single-spanning proteins), whereas 12 proteins have characteristics of C-tail anchored proteins (Table 2). The genes corresponding to the single-spanning proteins and C-tail-anchored proteins were previously annotated as encoding 'hypothetical proteins' with no significant homology in other organisms.

C-tail-anchored proteins consist of a large functional domain exposed to the cytosol and a short C-terminal transmembrane segment that is flanked at both ends by positively charged residues [29–31]. The predicted transmembrane segments of the hydrogenosomal C-tailed proteins are 19–23 amino acid residues in length, which is somewhat longer than those found in mitochondrial proteins. This increased length may reflect differences in the thickness of the lipid bilayer in the outer membranes of each organelle. The C-terminal ends that follow the transmembrane segments are 2–16 amino acid residues in length and contain 2–7 positively charged residues (Fig. S2).

To validate the predicted topology of the C-tailed anchored protein TVAG_ 277930, we added a C-terminal HA tag and expressed the modified protein in *T. vaginalis*. We then confirmed that the expressed protein was targeted to hydrogenosomes by immune-fluorescent microscopy (Table 2). Hydrogenosomes from this transformed strain were isolated and treated with trypsin. Although proteolysis did not affect the mobility of the matrix protein, pyruvate:ferredoxin oxidoreductase, which is protected by the hydrogenosomal membranes (Fig. 4), proteolysis resulted in a shift of Tta1 mobility on SDS-PAGE from 36 kDa to ~14 kDa. This result is consistent with the expected cleavage of the ~22 kDa domain facing the cytosol, with the C-terminal domain and epitope-tag protected from trypsinolysis by the outer membrane. The C-terminal domain of this C-tail anchored protein was degraded only when Triton X-100 was added to solubilize the outer membrane (Fig. 4).

Mitochondrial porins and other outer membrane β -barrel proteins

Tom40, an essential component of the TOM complex, is the main gate for membrane proteins imported into the mitochondria [16]. Tom40 is a β-barrel protein and, together with VDAC, belongs to the Pfam family, PF01459, whose members are also referred to as the 'mitochondrial porins' [32]. Recent structural studies have shown that the β-barrels of the mitochondrial porins are assembled from 19 beta-strands [33,34]. In hydrogenosomal preparations, we identified 8 proteins that we designate as mitochondrial porins because they have sequence features of the PF01459 family, and secondary structure predictions using the PSI-PRED algorithm suggest that all 8 of the sequences contain 19 transmembrane beta strands (Fig. S3). The very last beta strand of all of the known mitochondrial outer membrane β-barrel proteins contains a beta signal motif, PxGxxHxH, where P stands for polar amino acid residue, G for glycine and H for hydrophobic acid. The signal is recognized by the SAM complex to facilitate the assembly of these proteins in the outer membrane [35]. All eight of the *T. vaginalis* mitochondrial porins contain this conserved motif (Fig. S3).

To distinguish whether the identified β-barrel proteins represent Tom40 or VDAC homologs, we performed independent HMM-based searches of predicted *T. vaginalis* proteins based on *T. vaginalis* genome sequences. Tom40 and VDAC HMMs were built from the protein sequences of an identical set of species. The Tom40 HMM search identified 6 of the 8 mitochondrial porins, which we therefore named Tom40-(1 through 6). No sequences were matched using the VDAC-specific HMM search under the HMMER 2 default parameters. It remains possible that one or more of the remaining mitochondrial porins functions as a VDAC and has a sequence that is too highly diverged to be aligned with the VDAC sequences from other eukaryotes.

Given that the TOM complex is a multi-subunit molecular machine built around a Tom40 channel, we tested whether *T. vaginalis* Tom40 was also found as a part of a high-molecular-weight complex. We engineered a strain of *T. vaginalis* to express a HA-tagged version of Tom40-3 and verified that the protein was localized to hydrogenosomes (Fig. 5A). Hydrogenosomes were isolated from the transformed parasites, gently solubilized by 0.5% Triton X-100 and analyzed by gel filtration. Immunoblotting of the elution profile revealed a major peak of Tom40-3 present as oligomers of ~230 kDa, with a smaller population of Tom40-3 in a complex of ~590 kDa (Fig. 5B). These results are consistent with the mitochondrial porin, Tom40-3, being a subunit of a protein complex that assists hydrogenosomal protein import.

Hmp35 (hydrogenosomal membrane protein 35) is a unique form of a β-barrel protein identified in hydrogenosomes. The proteomic assessment of the hydrogenosomes identified what appears to be a second isoform of Hmp35 (Hmp35-2) and another two related proteins that are distinguished by a C-terminal extension (Hmp36-1 and Hmp36-2). The Hmp35 and Hmp36 proteins are encoded from four different genes in *T. vaginalis*; excluding the C-terminal extension, their DNA sequences are sufficiently similar to strongly indicate very recent gene duplications and a likely functional redundancy of the proteins. Previously, Hmp35 was predicted to be predominantly composed of beta sheets [36], and current PSIPRED predictions (Fig. S4) indicate that the polypeptide chain is arranged in up to 19 beta sheets, plus one alpha helix positioned in the middle of the protein sequence between beta sheets 10 and 11. We therefore extend the suggestion by Dyall et al. [36] to conclude that the Hmp35 and Hmp36 family of proteins are outer membrane β-barrels. A

Table 2. Putative membrane proteins identified in *T. vaginalis* hydrogenosomes (continued).

Identification		Structure		Cell localization			Signal
Accession number	Name	TMHMM	MEMSAT3	TargetP	PsortII	Exp. Local.	
		TM No.	TM No.		mit%		
Integral monotopic C-tail-anchored proteins							
TVAG_090120	C-tail-1	1	1	O	13.0%		Ct
TVAG_190830	C-tail-2	1	0	O	13.0%		Ct
TVAG_458060	C-tail-3	1	1	O	4.3%		Ct
TVAG_272350	C-tail-4	1	0	O	13.0%	H	Ct
TVAG_240680	C-tail-5	1	1	O	13.0%		Ct
TVAG_137270	C-tail-6	1	1	O	8.7%		Ct
TVAG_277930	C-tail-7	1	1	O	13.0%	H	Ct
TVAG_283120	C-tail-8	1	1	O	13.0%	H	Ct
TVAG_174010	C-tail-9	1	1	O	13.0%		Ct
TVAG_369980	C-tail-10	1	1	O	4.3%	H	Ct
TVAG_393390	C-tail-11	1	1	O	*		Ct
TVAG_211970	C-tail-12	1	0	O	13.0%		Ct
Integral monotopic single spanning proteins							
TVAG_032990	Unknown	0	1	O	21.7%		
TVAG_080160	Unknown	0	1	O	13.0%		
TVAG_094480	Unknown	1	1	O	17.4%		
TVAG_152710	Unknown	0	1	O	13.0%		
TVAG_178320	Unknown	0	1	O	8.7%		
TVAG_182990	Unknown	0	1	O	21.7%		
TVAG_210010	Unknown	0	1	O	*		
TVAG_218130	Unknown	1	1	S	*		
TVAG_225560	Unknown	1	0	O	21.7%		
TVAG_251750	Unknown	1	1	O	4.3%		
TVAG_252220	Unknown	0	1	O	*		
TVAG_295140	Unknown	0	1	O	*		
TVAG_331680	Unknown	1	1	S	11.1%		
TVAG_333160	Unknown	1	1	O	22.2%		
TVAG_337270	Unknown	0	1	O	26.1%		
TVAG_341690	Unknown	0	1	O	*		
TVAG_370950	Unknown	0	1	M	21.7%		
TVAG_403380	Unknown	0	1	O	33.3%		
TVAG_413430	Unknown	0	1	O	13.0%		
TVAG_425430	Unknown	0	1	O	8.7%		
TVAG_423530	Unknown	1	2	O	17.4%	H	

Proteins were manually annotated based on searches in TrichDB, Uniprot, and PFAM A+B (Table S2). Protein structure was predicted using TMHMM and MEMSAT3; subcellular location was predicted using TargetP and PsortII. TM No., number of predicted transmembrane α-helixes. M, predicted location in mitochondria. S - predicted proteins of secretory pathway; O, predicted location in other compartments; Mit%, probability percentage of mitochondrial location; *, mitochondrial location was not predicted; Exp. Local., experimental location; H, localization of HA-tagged proteins was confirmed in *T. vaginalis* hydrogenosomes by immunofluorescence microscopy; NV, transformed *T. vaginalis* strain was not viable. Signal: Δ indicates N-terminal targeting sequence identified by Hunter; β indicates presence of beta signal of beta-barrel proteins for insertion into the outer membrane of mitochondria; Ct, C-tail anchor detected [Fig. S2].

doi:10.1371/journal.pone.0024428.t002

distinguishing feature of the Hmp35-1 and Hmp35-2 proteins is their cysteine-rich character, including a C-terminal domain that features the metal-binding motif, $CX_6CCX_2CX_9HX_{15}CCXHXX_2C$ [36]. The Hmp36-1 and Hmp36-2 proteins both lack this C-terminal cysteine-rich domain, and Hmp36-1 and Hmp36-2 contain only 2 and 5 cysteine residues, respectively. Although the last predicted beta-strand of Hmp35-1 and Hmp35-2 shows a match to the beta-signal motif, this motif is not clear in Hmp36-1 and Hmp36-2.

Small TIM chaperones associated with hydrogenosomal membranes

Integral membrane proteins of the outer and inner membranes of mitochondria are assembled into the membranes with the assistance of a group of ~10 kDa chaperones called small TIMs. These chaperones are localized within the intermembrane space and are also found associated with membranes, reflecting their role in the delivery of nascent imported membrane proteins [37–39].

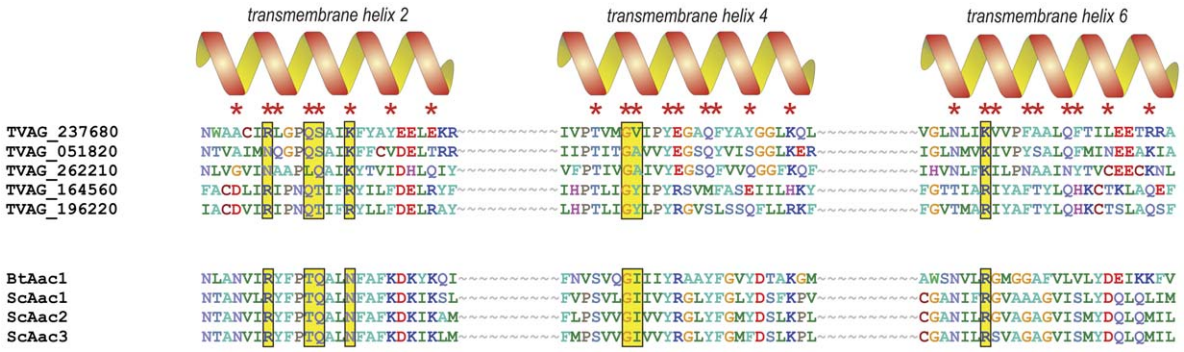

Figure 3. The amino acid sequences of six putative hydrogenosomal carrier proteins were aligned with the sequences of 33 mitochondrial carriers from *Saccharomyces cerevisiae* and that of the AAC1 carrier from *Bos taurus* (Pebay-Peyroula et al., 2003), according to the method of Kunji and Robinson (2006). The substrate specificity of the carrier is determined by the amino acid residues of the even-numbered transmembrane helixes facing the transport pore (red stars). The residues in direct contact with the substrate are highlighted in yellow boxes. Only the even-numbered helixes of the most similar homologs are shown, indicating that TVAG_237680, TVAG_051820, TVAG_262210, TVAG_164560 and TVAG_196220 belong to the group of adenine nucleotide carriers. The corresponding residues of TVAG_197670 do not resemble any of the specificity motifs (Kunji and Robinson, 2006). BtAac1 and ScAac1, ScAac2 and ScAac3 are adenine nucleotide carriers from *Bos taurus* and *Saccharomyces cerevisiae*, respectively.
doi:10.1371/journal.pone.0024428.g003

Sequence classifications have demonstrated that there are four small TIM families: Tim8, Tim9, Tim10 and Tim13 [40]. These families reflect the structural characteristics required to form hetero-hexameric functional chaperones of the type $Tim8_3$:$Tim13_3$ or $Tim9_3$:$Tim10_3$. In the hydrogenosomal membrane fraction, we identified two small TIM proteins that share 93% sequence identity (Fig. 6). The main difference between these paralogs is at position 12, where either a negatively-charged glutamic acid (TvTim9/10a) or positively charged lysine (TvTim9/10b) is present. A comparative analysis of the hydrogenosomal small TIMs is made difficult by sequence divergence, but the highest sequence identity for TvTim9/10a and TvTim9/10b was found with Tim9 of *S. cerevisiae*. An extraordinarily distinguishing feature of both hydrogenosomal proteins is the absence of the defining conserved twin cysteine motif, $CX_3CX_nCX_3C$: TvTim9-10a and TvTim9-10b retain only a single cysteine (Cys25) (Fig. 6).

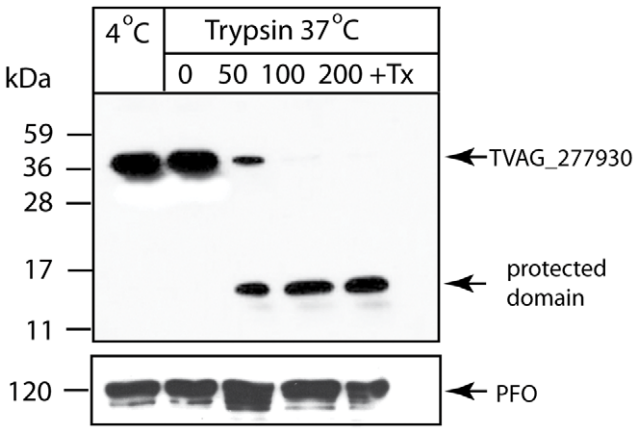

Figure 4. Expression of the C-tail anchored protein, TVAG_277930, in the hydrogenosomal outer membrane. Hydrogenosomes were isolated from a *T. vaginalis* strain expressing TVAG_277930 with a C-terminal hemagglutinin tag and incubated for 30 min at 4°C and 37°C with 0, 50, 100 or 200 μg/ml trypsin or μg/ml trypsin plus 0.5% Triton X-100 (Tx). Samples were analyzed by SDS-PAGE and immunoblotting using a mouse monoclonal anti-HA tag and anti-PFO antibodies. Pyruvate:ferredoxin oxidoreductase (PFO) was used as a control matrix proteins.
doi:10.1371/journal.pone.0024428.g004

Proteins of the Tim17/22/23 family and the hydrogenosomal TIM complexes

The key components of the inner membrane translocase complexes, TIM23 and TIM22, belong to the Tim17/Tim22/Tim23 protein family. These proteins typically possess four transmembrane domains and an amino acid signature called the PRAT motif [41]. As characterized in yeast, the Tim17 and Tim23 proteins constitute the TIM23 complex that translocates proteins into the matrix, whereas the protein called Tim22 forms a distinct TIM22 complex to facilitate the import of MCFs and other multitopic proteins. The proteomics survey identified two hydrogenosomal proteins, TvTim17/22/23-1 and TvTim17/22/23-2, which match significantly with the Tim17/22/23 family in the PFAM database ($E = 1{,}7^{-18}$ and $E = 2{,}3^{-14}$; respectively). In

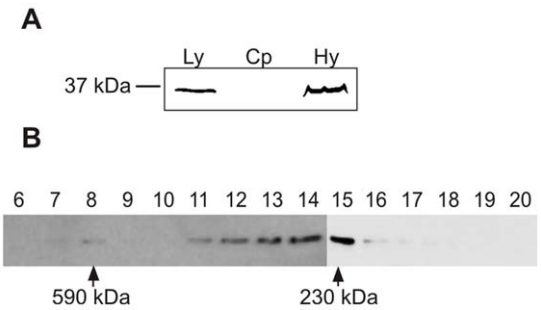

Figure 5. Cellular localization and gel filtration chromatography of trichomonad Tom40-3. (A) Total cell lysates (Ly) and cytosolic (Cp) and hydrogenosomal fractions (Hy) were prepared from trophozoites expressing an HA-tagged Tom40-3 (TVAG_450220) and analyzed by SDS-PAGE and immunoblotting using a mouse monoclonal anti-HA tag antibody. (B) Size exclusion chromatography of Tom40-3. Hydrogenosomes were solubilized in gel filtration running buffer containing 0.5% TX-100 and centrifuged, and the supernatant was subjected to gel filtration on a Superdex-200 column. Fractions of 500 μl (6-20) were analyzed by immunoblotting. Estimated sizes of the components of the putative trichomonad Tom40 complex are marked with arrows.
doi:10.1371/journal.pone.0024428.g005

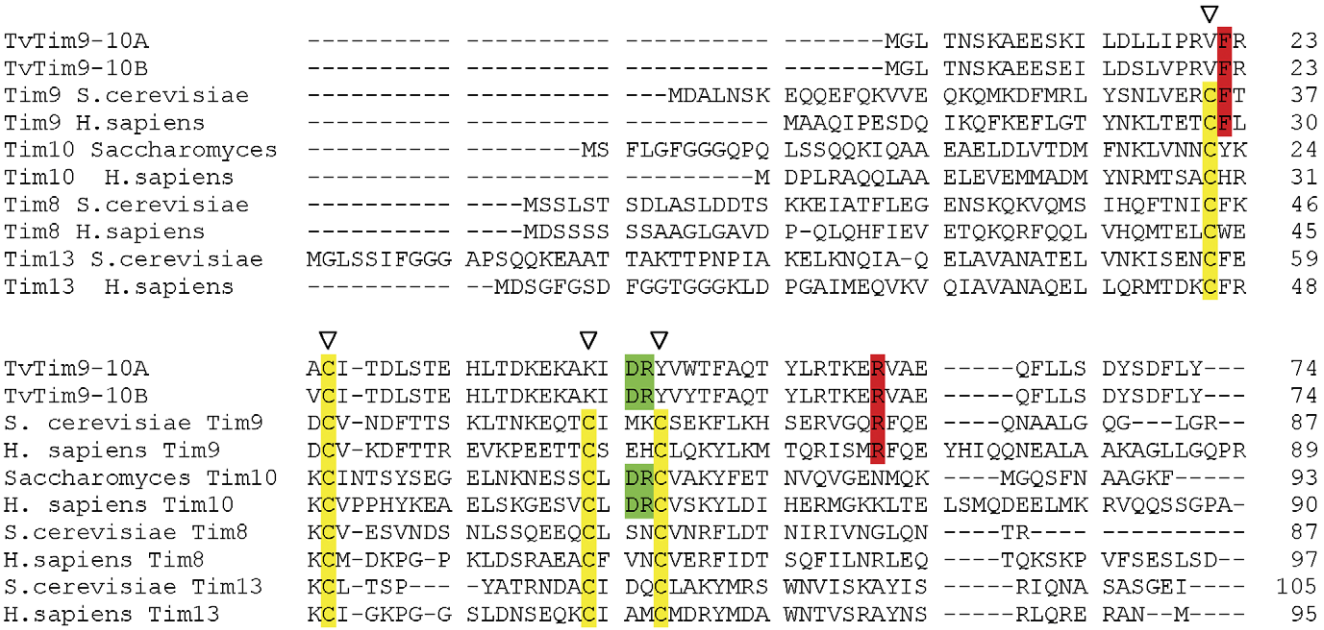

Figure 6. Sequence alignment of the *Trichomonas vaginalis* small Tims, TvTim9-10A (TVAG_287510) and TvTim9-10B (TVAG_026080) against the sequences of *S. cerevisiae* and human members of four small Tim families. Tim9: *S. cerevisiae*, O74700; *H. sapiens*, Q9Y5J7. Tim10: *S. cerevisiae*, P87108; *H. sapiens*, P62072. Tim8: *S. cerevisiae*, P57744; *H. sapiens*, O60220. Tim13: *S. cerevisiae*, P53299; *H. sapiens*, AAF15101. The conserved cysteine residues are marked by arrowheads (▽) and highlighted in yellow. The conserved Tim9 residues are highlighted in red, and conserved Tim10 residues are highlighted in green.
doi:10.1371/journal.pone.0024428.g006

addition, we found three other hydrogenosomal membrane proteins with some overall sequence similarity to the family but with insignificant matches ($E>7{,}2^{-6}$) (Table 1). We refer to these three proteins as TvTimC, TvTimD and TvTim-like. The PRAT domain was partially conserved in TvTim17/22/23-1 and TvTim17/22/23-2, and it was conserved to a lesser extent in TvTimC and TvTim D and was absent in the TvTim-like protein. We suggest that TvTim17/22/23-1 and TvTim17/22/23-2 should be considered as candidate TIM complex subunits and that TvTimC and TvTimD should be considered as potential candidates (Fig. 7). We note also that TvTim17/22/23-1 possesses positively charged residues at its C-terminus (Lys130 and Lys131) and negatively charged residues at its N-terminus (Glu26 and Glu27), which are features of Tim23 [42]. However, limited conservation of the hydrogenosomal proteins in any of the Tim17, Tim22 and Tim23 subfamilies prevents a determination of their functional equivalence based on sequence alone. Consistent with this sequence divergence, the expression of TvTim17/22/23-1 or TvTim17/22/23-2 failed to support the growth of yeast strains lacking Tim17, Tim22 or Tim23 (Fig. S5A, B, C).

To test whether these hydrogenosomal proteins possess the information required for assembly into the inner membrane of yeast mitochondria, we measured the import of TvTim17/22/23-1 into mitochondria isolated from yeast. A time-dependent incorporation of the radiolabeled protein was observed (Fig. 8A), indicating that TvTim17/22/23-1 was imported across the outer membrane. The treatment of the mitochondria in hypo-osmotic buffer before the addition of proteinase K (PK) revealed the presence of a TvTim17/

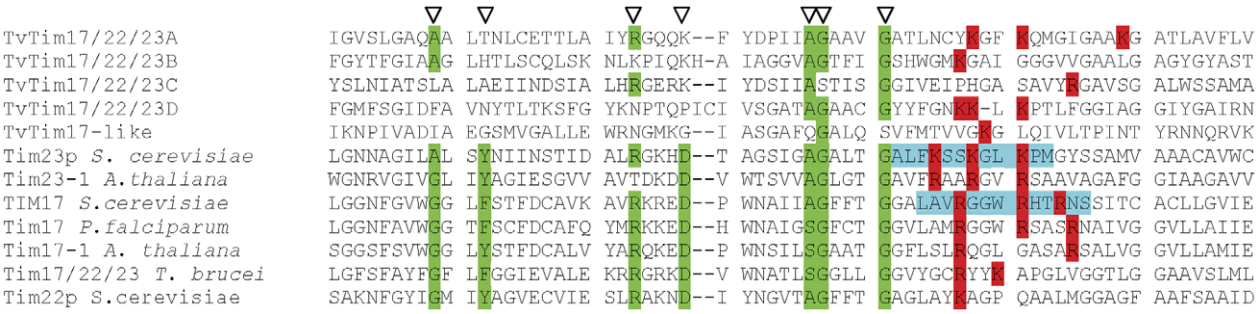

Figure 7. Alignment of the *T. vaginalis* Tim17/22/23 PRAT domains against eukaryotic orthologs. Organism names and accession numbers are as follows: *T. vaginalis* TvTim17/22/23A, TVAG_198350; TvTim17/22/23B, TVAG_061900; TvTim17/22/23C, TVAG_370860; TvTim17/22/23D, TVAG_379950; TvTim17-like, TVAG_447580; *A. thaliana* Tim23-1, AAR26373; *S. cerevisiae*, Tim17, CAA89438; *P. falcparum*, putative Tim17, XP_001348502; *A. thaliana*, Tim17-1, AAO63303; *T. brucei* Tim17/22/23 CBH18364; *S. cerevisiae* Tim22p NP_010064. Consensus PRAT sequence: G/$AX_2F/YX_{10}RX_3DX_6$ G/A/SGX_3G. Conserved residues are marked by arrowheads and highlighted in green. Experimentally verified internal targeting signals are in blue. Positively charged residues at the C-terminus are in red.
doi:10.1371/journal.pone.0024428.g007

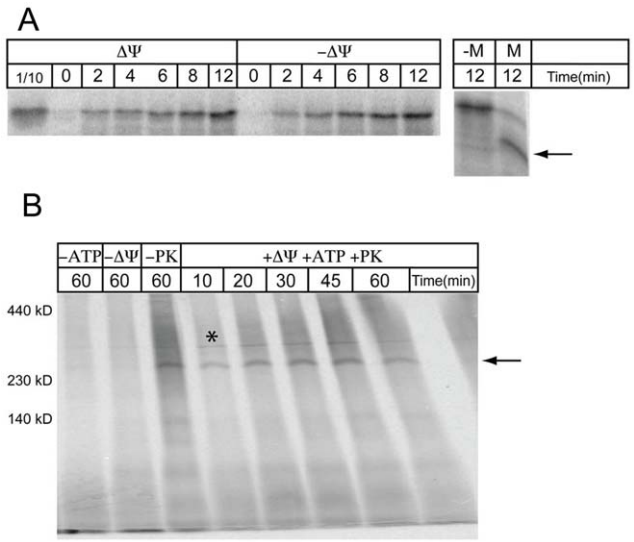

Figure 8. *In vitro* import and topology of TvTim17/22/23-1. (A) *In vitro* synthesized, [S^{35}]-radiolabeled TvTim17/22/23-1 was incubated with isolated yeast mitochondria at 25°C for the indicated time, treated with 25 μg/mL proteinase K to degrade surface-associated proteins and analyzed by SDS PAGE and autoradiography. After incubation with the [S^{35}]-radiolabeled TvTim17/22/23-1 for 12 minutes, yeast mitochondria were exposed to proteinase K in import buffer (see the Material and Methods) with a hypo-osmotic buffer (10 mM MOPS – "M") or import buffer alone ("-M") and resolved by SDS PAGE. The arrow indicates the fragment of TvTim17/22/23-1 protected by the inner mitochondrial membrane. Proteins were detected by autoradiography. Δψ, the reaction as described proceeding in the presence of transmembrane potential; -Δψ, the reaction as described when the transmembrane potential was dissipated by the addition of 1 nM valinomycine. (B) *In vitro* synthesized, [S^{35}]-radiolabeled TvTim17/22/23-1 was incubated with isolated yeast mitochondria at 25°C for the indicated time. Proteins were then treated with 25 μg/mL proteinase K to degrade surface-associated proteins or incubated in the absence of externally added ATP (-ATP) when the transmembrane potential was dissipated by the addition of 1 nM valinomycine (-Δψ) or without PK treatment (-PK). One species was detected (~280 kD) (arrow). (*), abundant respiratory chain complex radiolabeled by free [S^{35}] methionine.
doi:10.1371/journal.pone.0024428.g008

22/23-1 fragment that was ~3 kDa smaller than the full-length protein, indicating that TvTim17/22/23-1 was incorporated into the inner membrane (and, thereby, largely protected from PK). Whereas no effect on the translocation of TvTim17/22/23-1 across the outer membrane was observed when the membrane potential (Δψ) was dissipated by valinomycine (Fig. 8A), the incorporation of TvTim17/22/23-1 into a high molecular complex (over 230 kDa) was observed, but only when TvTim17/22/23-1 was incubated with energized mitochondria (Fig. 8B). Thus, the translocation of TvTim17/22/23-1 across the outer membrane is independent of Δψ, whereas its insertion into the inner membrane complex depends on Δψ. These properties conform to those observed for Tim17/22/23 proteins from yeast [43].

Presequence translocase-associated motor (PAM)

The final step of preprotein import across the inner membrane requires the function of the matrix-exposed PAM complex, which consists of two soluble matrix proteins, mtHsp70 and Mge1, and 3 essential membrane components (Tim44, Pam16, and Pam18). A complete set of putative membrane PAM components was identified in hydrogenosomes, and the membrane proteins, TvPam16, TvPam18 and TvTim44, localize to hydrogenosomes when expressed in *T. vaginalis* with a C-terminal HA tag (Table 1). The protein sequence of TVAG_436580 (TvPam18) conforms to the sequence characteristics of HMM for the Pam18 family (Fig. S6) [44]. The characteristic features of Pam16, which forms a subcomplex with Pam18, were identified in protein sequence TVAG_470110 (TvPam16), and the conserved hypothetical protein, TVAG_008790, is a candidate Tim44 (Table 1 and Figs. S7 and S8). It is noteworthy that the N-terminal domains of Tim44 vary in length and structure depending on the species [45], with the TvTim44 N-terminal domain consisting of 144 residues with a predicted hydrogenosomal targeting presequence (Fig. S8).

We sought to determine whether TvPam18 functions in the PAM complex in yeast. First, we tested whether [^{35}S]-labeled TvPam18 accumulated in yeast mitochondria in a time-dependent manner and behaved as an inner membrane protein (Figs. 9A and B). To assess the topology of the imported TvPam18, yeast mitochondria were sequentially treated by proteinase K and a hypo-osmotic buffer. When the outer membrane was ruptured, the intermembrane space protein, Cyb2, was degraded, but TvPam18

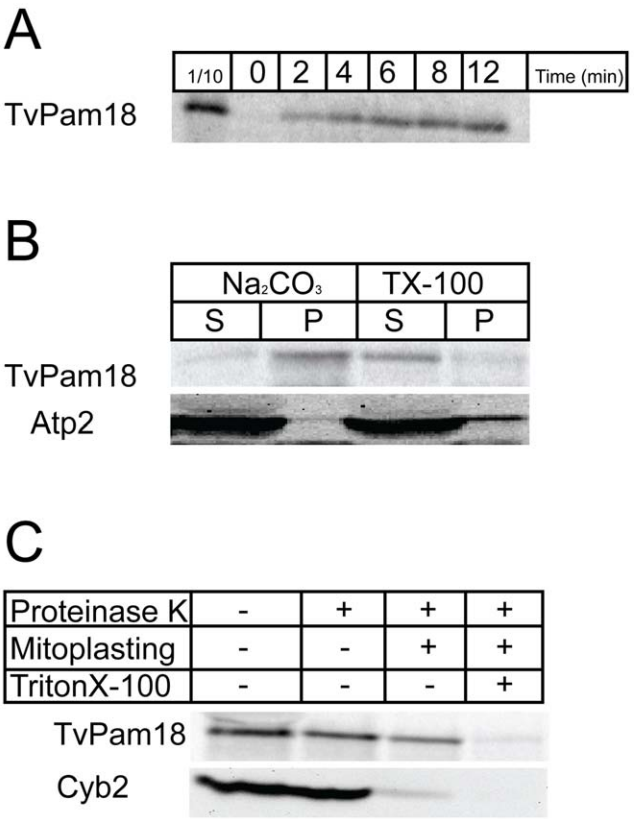

Figure 9. *In vitro* import and the topology of TvPam18. (A) *In vitro* synthesized, [S^{35}]-radiolabeled TvPam18 was incubated with isolated yeast mitochondria at 25°C for the indicated time, treated with 25 μg/ml proteinase K to degrade surface-associated proteins and analyzed by SDS PAGE and autoradiography. (B) After incubation with [S^{35}]-radiolabeled TvPam18 for 30 minutes, yeast mitochondria were treated with sodium carbonate (pH 11.5) and Triton X-100 and centrifuged at 100,000× g. Samples were resolved by SDS-PAGE, and the proteins were detected by western blotting and autoradiography. (S) soluble fraction; (P) insoluble fraction. (C) After incubation with [S^{35}]-radiolabeled TvPam18 or GiPam18 for 30 minutes, yeast mitochondria were exposed to proteinase K in import buffer, hypo-osmotic buffer (10 mM MOPS – "M") or 1% Triton X-100 ("TX") and resolved by SDS PAGE. Proteins were detected by western blotting or autoradiography.
doi:10.1371/journal.pone.0024428.g009

was not affected (Fig. 9C). However, when the outer and inner membranes were lysed by Triton X-100, TvPam18 was degraded. Thus, TvPam18 assumes the same topology as the ScPam18 yeast protein does in mitochondria, with an N-terminal transmembrane domain in the inner mitochondrial membrane and its J-domain located in the mitochondrial matrix.

To test whether TvPam18 can function in place of ScPam18, chimeric ScPam18-TvPam18 constructs were expressed in a heterozygous mutant yeast, Pam18/Δ*pam18* (Fig. 10). The heterozygous diploid cells were induced to sporulate, and the tetrads were dissected onto rich media plates. Because PAM18 is an essential gene, the Δ*pam18* haploid progeny should not form viable colonies on the dissection plates. Cells transformed with the plasmid encoding ScPam18 served as a control and showed four viable colonies from each tetrad (Fig. 10D). When TvPam18 was expressed, only two spores germinated to form colonies of haploid cells, indicating that TvPam18 was not able to restore full PAM function in yeast (Fig. 10A). Furthermore, the addition of the specific yeast intermembrane space domain to TvPam18 (ScIMSTvPam18) was not sufficient to bring TvPam18 into the correct context to function in yeast (Fig. 10B). Full complementation was seen only when the yeast N-terminal region and transmembrane segment were fused with the TvPam18 J-domain (ScNTvJPam18) (Fig. 10C). The growth rate and viability of wild-type and cells complemented with ScNTvJPam18 were indistinguishable at 25-30°C when the cells were grown on a fermentable (glucose) or non-fermentable (lactate) carbon source (Fig. S9A), and the efficiency of protein import into the mitochondria where the PAM complex was restored with ScNTvJPam18 was indistinguishable from the activity of ScPam18 (Fig. S9B).

Discussion

Mitochondria are surrounded by two distinct membranes, across which metabolites are exchanged to coordinate metabolic pathways in the cytosol with those that act within the organelle. Both the outer membrane and inner membrane possess a specific set of membrane proteins that facilitate this metabolite exchange as well as machineries for protein import, interactions with various cellular structures and other diverse functions. Our analysis of hydrogenosomal membrane proteins revealed the presence of membrane transporters, including major core components required for organelle biogenesis that are functional homologs of the mitochondrial systems, thus extending support for the common evolutionary origin of mitochondria and hydrogenosomes from an ancestral endosymbiont. However, our analysis also revealed remarkable distinctions in the membrane proteome of hydrogenosomes (Fig. 11A, B).

Outer membrane proteins in hydrogenosomes

The outer hydrogenosomal membrane has proteins of at least two distinct architectures: β-barrel proteins and α-helical, monotopic proteins of tail-anchored topology. Proteins of the mitoporin family of β-barrel proteins include Tom40 (a protein transport pore) and VDAC (a metabolite pore). The proteome of hydrogenosomes includes multiple paralogs of the Tom40-type of sequence. Although hydrogenosomes do not have an obvious VDAC, Tom40-type channels can serve as metabolite channels in the outer membrane [46,47]; it is possible that one or more of these 'Tom40' sequences functions as a metabolite pore.

Hydrogenosomes also have four isoforms of a β-barrel protein, Hmp35/Hmp36. Neither BLAST searches nor structural homology detection engines detected Hmp35 or Hmp36 homologs in any other available genome sequence. The functions of Hmp35 and Hmp36 are not known, but Hmp35 possesses a cysteine motif, $CX_6CCX_2CX_9HX_{15}CCXHXX_2C$, in its C-terminal region that could function to coordinate metal ions [48], and it is possible that Hmp35 might function in metal ion transport. The transported metal ions may include the iron that is essential for the function of hydrogenosomal FeS proteins [49] and that accumulates within these organelles [50]. Consistent with this idea, we observed increased expression of Hmp35 in *T. vaginalis* grown on iron-rich media, whereas the expression of Hmp36 was not affected (unpublished results).

The α-helical C-tail-anchored proteins are the second category of proteins found in the outer hydrogenosomal membrane. An outer membrane topology was confirmed for Tta1, which was selected from the 12 proteins with characteristics of C-tail-anchored proteins. In mitochondria, the C-tail-anchored proteins include important components of the outer mitochondrial membrane, such as Tom5, Tom6, Tom7, cytochrome b_5, Fis1

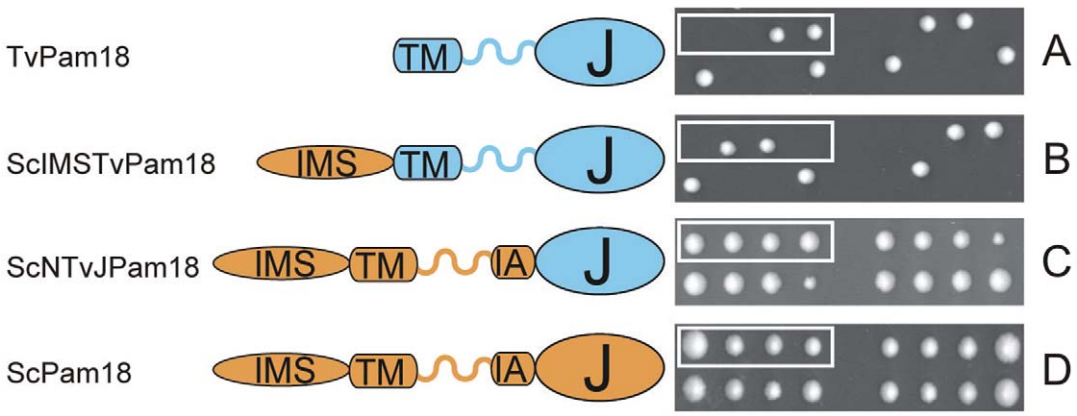

Figure 10. The J-domain of *Trichomonas vaginalis* TvPam18 can substitute for the J-domain of yeast ScPam18. Yeast Pam18/Δ*pam18* cells were transformed with plasmids carrying wild-type or modified Pam18 sequences. Cells were sporulated, and the tetrads were dissected onto YPD plates. Two viable colonies indicate no complementation by the candidate protein; four viable colonies indicate successful complementation by the candidate sequence. (A) TvPam18, wild-type *Trichomonas vaginalis* Pam18 sequence; (B) ScIMSTvPam18, ScPam18 IMS domain fused to wild-type TvPam18; (C) ScNTvJPam18, ScPam18 J-domain replaced by TvPam18 J-domain; (D) ScPam18, wild-type yeast Pam18 sequence; Orange, ScPam18 sequence; Blue, TvPam18 sequence; TM, transmembrane domain; IMS, intermembrane space domain; IA, interaction arm; J, J-domain.
doi:10.1371/journal.pone.0024428.g010

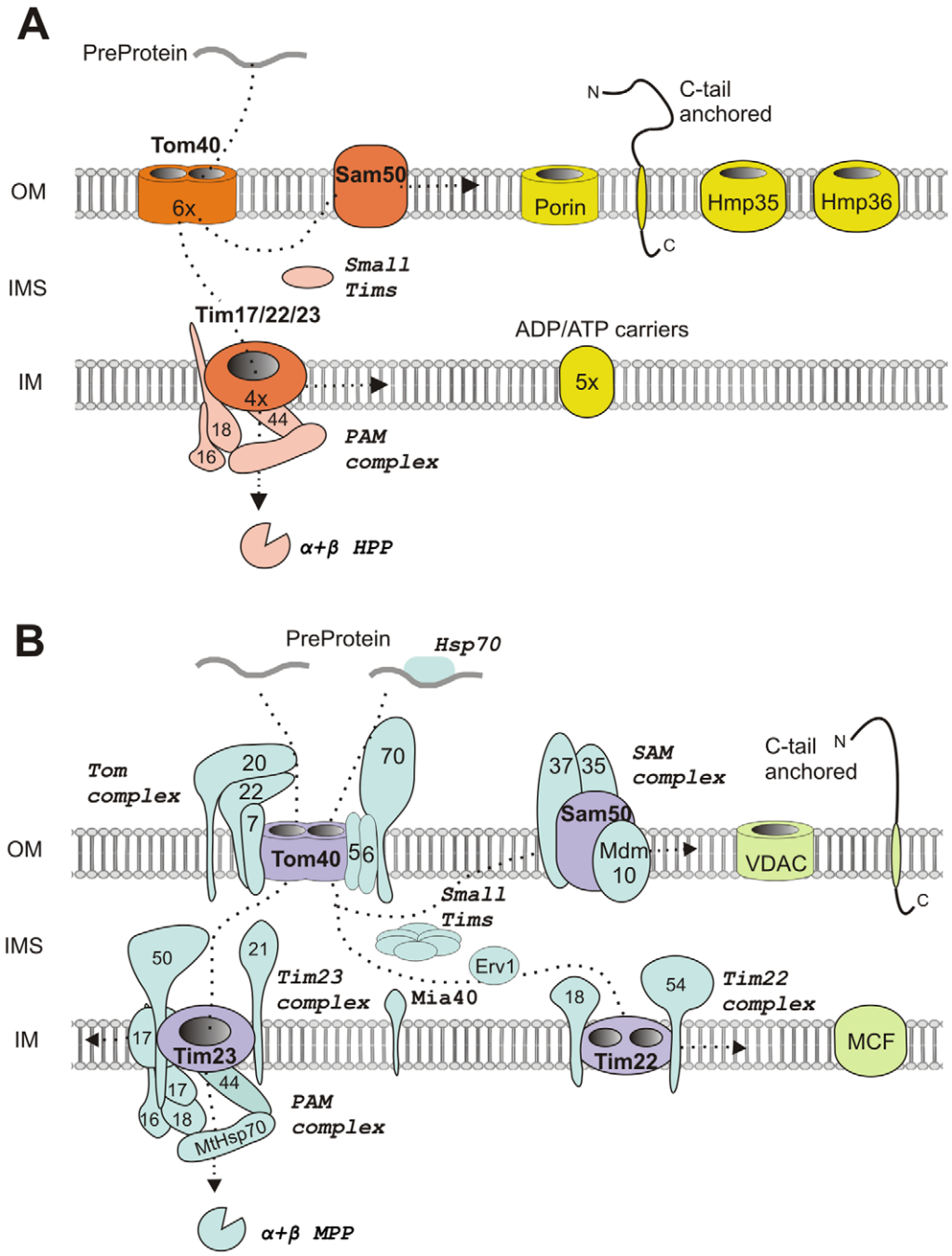

Figure 11. Comparison of the protein machineries of the outer and inner membranes of *T. vaginalis* hydrogenosomes (A) and *S. cerevisiae* mitochondria (B). *T. vaginalis* and *S. cerevisiae* belong to two distinct eukaryotic supergroups: Excavata and Opisthokonta, respectively. Excavates are exclusively unicellular and are often parasitic eukaryotes, whereas opisthokonts include both unicellular and multicellular organisms, such as fungi and animals. *T. vaginalis* hydrogenosomes and yeast mitochondria share core components of the outer and inner membranes (Tom40, Sam50, Tim17/22/23, and PAM machinery), although the protein sequences are extremely divergent. The associated components, such as Tom20 and Tom70, and the inner membrane component, Mia40, were not identified in the hydrogenosomes or other excavates, suggesting that these components were not present in the last common mitochondrial ancestor, although a secondary loss cannot be excluded. Conversely, the absence of Erv1 and the reduction of the small Tims family to a single type of highly modified TvTim9/10 most likely reflect the specific adaptation of hydrogenosomes to anaerobic conditions. The assembly of ADP/ATP within the inner hydrogenosomal membrane and the identification of divergent small Tims and Tim17/22/23 proteins indicate that a functional TIM22 complex is present; however, sequence divergence prevented the prediction of whether the Tim17/22/23 proteins form a single multifunctional channel or distinct TIM23 and TIM22 complexes. In addition to the TOM/TIM machineries, the hydrogenosomes possess a conserved pathway for the assembly of inner membrane C-tail anchored proteins. (A) The core components of the hydrogenosomal protein import machinery are shown in orange, and the subunits of the PAM machinery and the hydrogenosomal processing peptidase, HPP, are in pink. The putative components of the metabolite exchange system and C-tail-anchored protein are shown in yellow. (B) The core components of the mitochondrial protein import machinery are shown in purple, and associated components are depicted in blue. VDACs, C-tail-anchored proteins and MCFs (mitochondrial carrier family) are shown in green.
doi:10.1371/journal.pone.0024428.g011

and VAMP-1B [29,31]. A single C-tail-anchored protein, VAP, was recently identified in the mitosomes of the related excavate, *Giardia intestinalis* [51]. The hydrogenosomal C-tail-anchored proteins revealed no homology with any known mitochondrial protein in other organisms. Surprisingly, given the topology of many mitochondrial proteins in fungi, animals and plants [16,52], including the receptors of the TOM complex, Tom70 and Tom20, none of the hydrogenosomal membrane proteins that we identified contained N-terminal signal-anchor sequences.

The inner membrane proteome in the hydrogenosomes of *T. vaginalis*

The inner mitochondrial membrane possesses a large variety of α-helical, single-spanning or polytopic proteins that are required for (i) protein transport across the inner membrane (TIM complex), (ii) the exchange of metabolites (MCF), and (iii) respiratory chain function. The hydrogenosomal inner membrane proteome seems to be less complex. We identified candidate core subunits of a TIM complex and the complete PAM machinery. However, all of the hydrogenosomal proteins that matched with the Tim17/22/23 family in the PFAM database were too divergent to allow the determination of their functional equivalents that correspond to any of the Tim17, Tim22 and Tim23 subfamilies, and their expression failed to support the growth of yeast strains lacking Tim17, Tim22 or Tim23. The hydrogenosomal MCF protein, Hmp31, was efficiently targeted into the inner membrane of *S. cerevisiae* mitochondria, and conversely, when yeast AAC was expressed in *T. vaginalis*, it was integrated into a hydrogenosomal membrane [21]. These data, together with the identification and characterization of the TvTim17/22/23 proteins, indicate that hydrogenosomes possess a functional equivalent of the TIM22 complex. However, it remains to be established whether the assembly of hydrogenosomal AACs is mediated by a specialized TIM22 complex as required for the assembly of metabolite carrier proteins in yeast, humans and (most likely) plants [52]. Another possibility is that *T. vaginalis* has a single inner membrane translocase for the assembly of membrane proteins and the translocation of matrix components. Such a situation would not be unprecedented, as a single gene coding for a Tim17/22/23 protein has been identified in the genomes of *Trypanosoma brucei* [15] and microsporidians [53], which strongly suggests the presence of a single multifunctional TIM complex in these protists.

The adaptation of hydrogenosomes to function in oxygen-poor or anaerobic environments is likely the major factor that resulted in the remarkable differences between the hydrogenosomal membrane machineries and the mitochondrial systems. These adaptations include the complete loss of inner membrane complexes of the respiratory chain, including the components generating a transmembrane electrochemical potential. In mitochondria, the membrane potential is essential to activate the Tim23 channel and exerts an electrophoretic effect on the positively charged N-terminal targeting signals of transported proteins. It is not clear how a membrane potential is generated in hydrogenosomes or whether the membrane potential is necessary for protein translocation into hydrogenosomes, although a requirement for a small potential has been suggested [25]. Such a fundamental difference in the character of the inner membrane might explain the observed divergence of hydrogenosomal TIM components, together with modifications of the corresponding substrates. Indeed, it has been demonstrated that hydrogenosomal targeting signals of matrix proteins possess a considerably lower negative charge than mitochondrial targeting presequences [26].

Metabolite transport across the hydrogenosomal membranes

A remarkable difference was observed with respect to the limited spectrum of MCF proteins. Mitochondrial carriers are considered to be a unique eukaryotic invention that allows metabolic communication between the organelles and the cytosol [6–11]. A spectrum of MCFs that are specialized for the transport of various substrates is conserved across all eukaryotic groups, from the excavate, *T. brucei*, which has at least twenty-five carriers proteins [15], to humans, with forty-four MCF members [20]. Hydrogenosomal membranes have five MCFs that appear to be paralogs of Hmp31, which facilitates the transport of ADP and ATP across the inner hydrogenosomal membrane [21,24]. The presence of only a single MCF-type AAC in the hydrogenosomal inner membrane most likely reflects the reduction of metabolic pathways, such as the pyruvate dehydrogenase-dependent conversion of pyruvate, the citric acid cycle, citrulline synthesis, and lipid breakdown, for which various MCF proteins are required [6]. However, there are several hydrogenosomal pathways that are dependent on substrate import or for which a metabolite exchange could be expected. The hydrogenosomal energetic metabolism is based on the import of pyruvate and malate, whereas acetate is released as a metabolic end product [1]. The hydrogenosomal localization of two components of the glycine cleavage system [54], arginine deiminase [55], and aminotransferase (this study) strongly suggests a requirement for amino acid exchange. Transporters for these substrates remain to be identified; however, they are unlikely to be of MCF types.

In addition to functional adaptations, some of the peculiarities in the hydrogenosomal membrane proteome might reflect the distant evolutionary history of *T. vaginalis* and other model organisms, such as *S. cerevisiae* and vertebrates (Figure 11). A case in point comes from the analysis of the TOM complex. The core TOM complex components have been found in all eukaryotic lineages, suggesting their presence in a common mitochondrial ancestor [14]. However, the phylogenetic distribution of the additional components that optimize the function of the TOM complex is lineage-specific. In *S. cerevisiae*, the TOM complex comprises seven components (Tom70, Tom40, Tom22, Tom20, Tom7, Tom6, and Tom5) [16]. In *T. vaginalis*, we did not identify Tom20 or Tom70, which function as receptors for N-terminal and inner targeting signals, although both types of signals are conserved in this organism [25,27]. The absence of these components seems to be common to the eukaryotic group, Excavata [56], to which trichomonads belong, as they have not been identified in the related protists, *Giardia intestinalis*, *Trypanosoma brucei* or *Naegleria gruberii* [51,57] (unpublished results), or in plants [14,58,59]. Although there may be a large number of membrane proteins (58%) in the hydrogenosomes of *T. vaginalis* without known functional domains, whether these components represent highly divergent homologs of known systems that were not recognized or represent novel systems will require further functional investigations.

Materials and Methods

Cell cultivation

T. vaginalis strain T1 (kindly provided by J.-H. Tai. Institute of Biomedical Sciences, Taipei, Taiwan) was grown in Diamond's Tryptone-Yeast extract-Maltose medium (TYM) with 10% (v/v) heat-inactivated horse serum at 37°C.

Extraction of membrane proteins in Triton X-114

Highly purified hydrogenosomes were obtained from cell lysates by differential and Percoll-gradient centrifugation [60]. Membrane proteins were isolated using Triton X-114 as previously described [61]. Briefly, hydrogenosomes were solubilized for 1 hour on ice with 2% (w/v) Triton® X-114 (Sigma) in Tris buffer (150 mM NaCl, 10 mM Tris·HCl and 1 mM EDTA, pH 7.4) at a ratio of 1 mg of hydrogenosomal pellet to 4 ml of the buffer. Solubilized hydrogenosomes were centrifuged at 20,00× g for 20 minutes (min) at 4°C. The pellet was discarded, and the supernatant was incubated for 3 min at 37°C. The Triton X-114 phase was separated from the aqueous phase by centrifugation for 1 min at 13,000× g. The aqueous supernatant with soluble proteins was discarded, and the Triton X-114 phase containing the membrane proteins was redissolved in 10 volumes of Tris buffer at 4°C. The ensuing extraction of the Triton-X114 phase at 37°C and solubilization in ice-cold Tris buffer was repeated twice. Proteins in the final Triton X-114 phase were precipitated by the addition of 10 volumes of ice-cold acetone and air-dried.

SDS-PAGE and liquid chromatography

Proteins were separated by 1D SDS PAGE and digested in-gel (slices) by trypsin; subsequently, the tryptic peptides were separated by reverse-phase nano liquid chromatography. The Triton X-114-extracted proteins were solubilized in sample buffer (20% glycerol, 4% SDS, 0.02% bromophenol blue and 125 mM Tris·HCL, pH 7.4) and separated on a 12% gel by SDS PAGE. The gel was stained with Coomassie Brilliant Blue R-250, and the lanes with separated proteins were cut to 1-mm wide slices. Each slice was transferred to a separate microtube, and the proteins were subjected to in-gel tryptic digestion using sequencing-grade modified trypsin (Promega) as described previously [62]. The tryptic peptides were separated by liquid chromatography using an Ultimate 3000 HPLC system (Dionex). The peptide samples, diluted in 0.3% TCA with 10% ACN, were loaded onto a PepMap 100 C18 RP column (3-µm particle size, 15-cm length, 75-µm internal diameter; Dionex) at a flow rate of 300 nl per minute. The peptides were eluted by a 45-min linear gradient of 5–80% (v/v) ACN in 0.1% (v/v) TCA over a period of 45 min. The eluate (60 nl) was mixed 1:3 with matrix solution (20 mg/ml a-cyano-4-hydroxycinnamic acid in 80% ACN) prior to spotting onto MALDI target plates using a Probot microfraction collector (Dionex).

Mass spectrometry and MS/MS data analysis

Spectra were acquired using a 4800 Plus MALDI TOF/TOF analyzer (Applied Biosystems/MDS Sciex) equipped with an Nd:YAG laser (355 nm) with a firing rate of 200 Hz. All of the spots were measured in the MS mode, and up to 10 of the strongest precursors were selected for MS/MS, which was performed with a collision energy of 1 kV and an operating pressure of collision cell set to 10^{-6} Torr. Peak lists from the MS/MS spectra were generated using GPS Explorer v. 3.6 (Applied Biosystems/MDS Sciex) and searched by local Mascot v. 2.1 (Matrix Science) against annotated proteins in the TrichDB database (http://trichdb.org/trichdb/). Database search criteria were as follows: enzyme - trypsin; taxonomy - *Trichomonas vaginalis*; fixed modification - carbamidomethylation; variable modification - methionine oxidation; peptide tolerance −120 ppm, allowing one missed cleavage; and MS/MS tolerance −0.2 Da.

Protein sequence analysis

All of the identified protein sequences were manually annotated based on searches in the TrichDB (http://trichdb.org/trichdb/), Uniprot Protein knowledgebase (http://www.uniprot.org/), NCBI (http://blast.ncbi.nlm.nih.gov/Blast.cgi) and Pfam (http://pfam.sanger.ac.uk/search) databases. The protein sequences (<1000 residues) were submitted (*i*) against a 90% redundancy-reduced NCBI nr database by means of simple pair-wise alignment Psi-BLAST for 8 iterations at an e-value cutoff of 10^{-3} and (*ii*) against the Pfam 23.0 A+B database of families represented by multiple sequence alignments and hidden Markov models (HMMs) at an e-value of 0.044.

TargetP and SignalP, based on the combination of artificial neural networks and hidden Markov models, respectively (http://www.cbs.dtu.dk/services/), together with PsortII (http://psort.ims.u-tokyo.ac.jp/), were used to predict the subcellular location.

An application based on the NetBeans Platform (Hunter) was used to predict the subcellular localization of proteins according to their N-terminal amino acid sequence, as previously described [26]. The following parameters were used: (i) the presequence start motif - ML[ACGQRSTV] or MS[ILV] or MIS or MTL; (ii) a cleavage site motif - R.F[TKILFSAGQ] or R[AFNESG][TYILFSAGQ] or K[AFNESG][TYILFSAGQ] or K.F[TKILFSAGQ]. The secondary structure and topology of alpha-helix integral membrane proteins was predicted using two bioinformatic tools: TMHMM (http://www.cbs.dtu.dk/services/) and Memsat3 (http://bioinf.cs.ucl.ac.uk/memsat/).To determine members of protein families, a hidden Markov model analysis was performed according to the method of Likic et al. [63].

Selectable transformation of *T. vaginalis* and immunofluorescence microscopy

Selected genes were amplified by PCR from *T. vaginalis* genomic DNA and inserted into the TagVag2 plasmid. Cells were transformed and selected as described previously [64]. *T. vaginalis* cells expressing recombinant proteins with a C-terminal hemagglutinin (HA) tag were identified with a mouse anti-HA mAb [60]. The malic enzyme was detected with a rabbit anti-malic enzyme polyclonal antibody [65]. A secondary AlexaFluor-488 (green) donkey anti-mouse antibody and AlexaFluor-594 (red) donkey anti-rabbit antibody were used for the visualization of the target proteins. Cells were observed using an OLYMPUS Cell-R, IX81 microscope system, and images were processed using ImageJ 1.41e software (http://rsb.info.nih.gov/ij/).

Structural modeling

The model of TvTim44 (residues 144–326) was built using the human Tim44 structure (PDB ID: 2cw9) [66] as a template. The alignment was constructed by MUSCLE [67] and manually edited. The 3D structure model of TvTim 44 was built using Modeller 9v7 [68]. The quality of the final model was checked using What Check [69] and ProSA-web services [70]. The electrostatic potential on the solvent-accessible surface of TvTim44 was calculated using APBS 1.3 [71].

Sequential proteolytic degradation, protein extraction and protein import into *Saccharomyces cerevisiae* mitochondria

Mutant yeast strains and their corresponding wild-type control strains were grown in parallel in YPLac medium at 30°C. The mitochondria were isolated by differential centrifugation, and protein import assays were performed as previously described [72]. BN PAGE analysis following the import of the precursor proteins was performed according to a previously described method [72]. Sequential proteolytic degradation following the import of radiolabeled precursors and protein extraction was performed as described previously [73].

Functional complementation

Functional complementation of yeast mutants was performed by transfection of a heterologous-protein encoding plasmid into Δ*pam18*/Pam18, Δ*tim17*/Tim17, Δ*tim22*/Tim22, or Δ*tim23*/Tim23 cells. To cause the yeast to sporulate, the cells were grown in rich media at 30°C to mid-log phase, isolated by centrifugation, and then transferred to a 1% potassium acetate solution and incubated with shaking at 25°C for 3 to 4 days. The resulting tetrads were dissected onto YPD plates and incubated at 30°C.

Growth and viability analysis

Yeast cells with a disrupted *pam18* gene and carrying the pScPam18 or pScNTvJPam18 construct were grown to a mid-logarithmic growth phase ($0.6< OD_{600}<0.8$) in rich media and diluted to an OD_{600} of 0.2. Each cell suspension was then further diluted in 7 five-fold steps in sterile double-distilled water, and 5 µl of the last 6 diluted cell suspensions was spotted onto media plates. The plates were incubated at 25°C, 30°C or 37°C until colonies were visible.

Sequential proteolytic degradation of C-tail anchored proteins targeted to hydrogenosomes

Aliquots of Percoll-purified intact hydrogenosomes (3 mg) were resuspended in 1 ml of ST buffer (250 mM sucrose, 10 mM Tris, pH 7.4, 0.5 mM KCl, 50 µg/ml TLCK and 10 µg/ml leupeptin). Trypsin was added to final concentrations of 50–200 µg/ml, and the samples were incubated on ice or in a water bath at 37°C for 30 min. After incubation, soybean trypsin inhibitor was added (5 mg/ml), and the samples were analyzed by immunoblotting using a monoclonal mouse anti-HA antibody and an anti-pyruvate:ferredoxin oxidoreductase antibody (kindly provided by Patricia Johnson, UCLA, USA and Guy Brugerolle, University of Clermont Ferrand, France, respectively).

Gel size analysis of Tom40

Approximately 30 mg of Percoll-purified hydrogenosomes were solubilized in 0.5 ml of ice-cold gel size running buffer (150 mM NaCl, Tris [pH 8.0], 0.5 mM $MgCl_2$, 5% ethylene glycol, 50 µg/ml TLCK and 10 µg/ml leupeptin) with 0.5% Triton X-100 on ice for 1 hour. Solubilized hydrogenosomes were centrifuged at 13,000× g for 10 min. The supernatant was loaded onto a Superdex 200 10/300 GL column (GE healthcare; equilibrated with Gel Filtration Standards©, BioRad) and separated using a flow rate of 0.5 ml/min. Fractions (500 µl) were collected, and the proteins were extracted using TCA-methanol/chloroform and analyzed by immunoblotting using a monoclonal mouse anti-HA antibody.

References for the supporting information are available as a separate document in References S1.

Supporting Information

Figure S1 Mitochondrial carrier proteins in *Trichomonas vaginalis*. Sequence alignment of *Trichomonas vaginalis* mitochondrial carrier homologs ADP/ATP carrier 1 (Hmp31, TVAG_237680) AAC-2 (TVAG_051820), AAC-3 (TVAG_164560), AAC-4 (TVAG_197670) and AAC-5 (TVAG_262210) and bovine mitochondrial AAC (NP_777083). Solid lines above the alignment represent alpha-helixes, as deduced from the structure of the bovine AAC [1]. The signature motif of the AAC protein family is shown in box.
(TIF)

Figure S2 The C-terminal domains of putative C-tailed anchored proteins identified in *T. vaginalis* hydrogenosomal membranes. Predicted transmembrane domains (TMD) are highlighted in yellow. Positively charged residues are in red, and negatively charged residues are in green. AA TMD indicates the number of amino acids in the TMD.
(DOC)

Figure S3 Protein sequence alignment of candidate porin_3 family proteins in hydrogenosomal membranes. The secondary structure of all of the protein sequences, as predicted by PSIPRED, is shown above the protein alignment. Predicted beta-strands are in green, and predicted alpha helixes are in purple. The presence of the beta-signal is highlighted in red.
(PDF)

Figure S4 Sequence alignment of *Trichomonas vaginalis* β-barrel proteins, Hmp35 and Hmp36. Cysteines and histidines of the putative metal binding motif, $CX_6CCX_2CX_9HX_{15}$-$CCXHXX_2$ C, are highlighted in yellow. Hmp35-1 (TVAG_590550), Hmp35-2 (TVAG_104250), Hmp36-1 (TVAG_031860) and Hmp36-2 (TVAG_216170).
(PDF)

Figure S5 *Trichomonas vaginalis* TvTim17-22-23A and TvTim17-22-23B cannot substitute for Tim17, Tim22 and Tim23 in *Saccharomyces cerevisiae*. Yeast Tim17/Δ*tim17*, Tim22/Δ*tim22* or Tim23/Δ*tim23* cells were transformed with plasmids carrying TvTim17-22-23A (A), TvTim17-22-23B (B) or TvTim17-22-23A, respectively, where key residues were mutated to restore the PRAT motif (T97Y D112K) (C). Cells were sporulated, and the tetrads were dissected onto YPD plates. Two viable colonies indicate no complementation by the candidate protein, whereas four viable colonies indicate successful complementation by the candidate sequence.
(PDF)

Figure S6 Alignment of *T. vaginalis* Pam16 and Pam18 against eukaryotic orthologs. The diagnostic features identified in TvPam18 are (i) a J-domain at the C-terminus of the protein with a typical arrangement of three helixes and a short linker with a conserved HPDXGGS sequence motif connecting helixes II and III. The invariant HPD tripeptide is critical for the stimulation of the ATPase activity of Hsp70 by Pam18. (ii) A transmembrane α-helix that is close to the N-terminus. TvPam18 also contains a short N-terminal extension that is predicted to be a targeting presequence and a short N-terminal intermembrane space domain. However, TvPam18 does not contain a conserved interaction arm in front of helix I, which was structurally defined by [2] as one of the means by which Pam18 interacts with Pam16. The Pam16 protein family contains a degenerate J-domain with homology to Pam18 that lacks the HPD tripeptide in the linker motif; thus, it is unable to stimulate the ATPase activity of Hsp70. In TvPAM16, HPD is replaced by a D90, L91, E92 tripeptide, whereas the GGS motif of the linker is conserved. Importantly, TvPam16 contains a conserved L99 in the J-like domain that corresponds to L97 in the yeast ortholog. This residue has been shown to mediate an essential interaction between the Pam16 J-like domain and the J domain of Pam 18 that stabilizes the heterodimer [3]. A second characteristic feature predicted in TvPam16 is an N-terminal hydrophobic domain that is required for the interaction of Pam18:Pam16 heterodimer with the TIM23 translocon. The J-like domain of TvPam16 is underlined. Helical structures of the J-like domain (in red) were predicted by PSIPRED (http://bioinf.cs.ucl.ac.uk/psipred/). Arrowheads indicate the degenerate HPD motif of Pam16 between helixes II and III. The HPD motif of Pam18 is boxed. The leucine and asparagine residues essential for the Pam16-Pam18 interaction are marked with a star. Organisms and accession numbers: *T. vaginalis*,

TVAG_470110; *S. cerevisiae*, Pam16, P42949; *H. sapiens*, Pam16, Q9Y3D7; *D. discoideum*, Pam16, XP_640279; *E. cuniculi*, Pam16, ECU11_0700; *T. vaginalis*, Pam18, TVAG_436580; *S. cerevisiae*, Pam18, Q07914; *H. sapiens*, NP_660304.
(PDF)

Figure S7 Alignment of the Tim44 domain of *T. vaginalis* against eukaryotic and bacterial orthologs. Conserved hydrophobic residues that form the large hydrophobic pocket of Tim44 are highlighted in yellow [4,5]. The conserved proline mutation, which causes familial oncocytic thyroid carcinoma, is in red [6]. Organisms and accession numbers: *Saccharomyces cerevisiae*, Q01852; *Schizosaccharomyces pombe*, NP_595905; *Phytophora infestans*, XP_002997475; *Tribolium castaneum*, XP_975336; *Homo sapiens*, NP_006342; *Caenorhabiditis elegans*, O02161; *Caulobacter crestentus*, AAK25703.
(PDF)

Figure S8 Tim44 is a peripheral membrane protein exposed at the matrix side of the inner membrane that provides a molecular scaffold for the assembly of the import motor [7]. The BLAST algorithm (NCBI BLAST, reference) using the PDB database of macromolecular structures detected a sequence similarity between the C-terminal part of TVAG_008790 and the C-terminal part of yeast Tim44 ($E = 6^{-4}$). This result was further supported by recognition of the C-terminal Tim44 domain by PFAM ($E = 7^{-3}$) and HHsenser ($E = 1^{-4}$) (Table S2). The structure of the C-terminal part of human Tim44 [8] was used to build the model of the C-terminal part of TVAG_008790 (residues 144-326). The resulting structure shows that all of the secondary structures present in human Tim44 appear in TvTim44 (Fig. 8B). The C-terminus of TvTim44 can form a large characteristic pocket with the conserved hydrophobic residues (Fig. 8C and Fig. S7 alignment) that were suggested to participate in the binding of Tim44 to the inner membrane [8]. A significant difference can be observed at position 225 of TvTim44, where an Arg replaces a hydrophobic Leu or Phe in orthologous species (Fig. S7 alignment). The positively charged domain of human Tim44 implicated in the binding of cardiolipins (residues 289-295) is not well conserved in TvTim44, although calculations of the electrostatic potential of TvTim44 also suggest a positive charge in this area (Fig. 8D charge identification). The low conservation of this domain likely reflects an absence of cardiolipin in *Trichomonas vaginalis* [9].
(PDF)

Figure S9 ScNTvJPam18 can support wild-type rates of cell viability and *in vitro* protein import. (A) Equal cell numbers of wild-type or complemented yeast were serially diluted onto medium containing glucose or lactic acid as a carbon source and incubated at 25°C, 30°C or 37°C. (B) Mitochondria from wild-type and complemented cells were isolated and incubated at 25°C with [^{35}S]-labeled precursors for the indicated time, treated with 25 µg/ml proteinase K to degrade the surface-associated proteins, and analyzed by SDS-PAGE and digital autoradiography.
(PDF)

References S1 References for the supporting information figures and tables.
(DOC)

Table S1 Complete list of proteins identified by nanoLC MS/MS in four independent experiments.
(DOC)

Table S2 Identification of hydrogenosomal proteins using TrichDB (http://trichdb.org/trichdb/), Uniprot (http://www.uniprot.org/), and PFAM A+B (http://pfam.sanger.ac.uk/) searches.
(DOC)

Table S3 Putative matrix proteins identified in *T. vaginalis* hydrogenosome.
(DOC)

Table S4 List of putative non-hydrogenosomal proteins.
(DOC)

Acknowledgments

We thank Michael Dagley for comments on prediction of mitochondrial porins.

Author Contributions

Conceived and designed the experiments: PR PD DB TL IH JT. Performed the experiments: PR PD PJ DB MS KS IH NCB. Analyzed the data: PR TL JT. Contributed reagents/materials/analysis tools: AP PJ MN. Wrote the paper: PR PD PJ DB TL JT.

References

1. Hrdy I, Tachezy J, Müller M (2008) Metabolism of trichomonad hydrogenosomes. In: Tachezy J, ed. Hydrogenosomes and Mitosomes:Mitochondria of Anaerobic Euakryotes. Berlin, Heidelberg: Springer-Verlag. pp 114–145.
2. Hjort K, Goldberg AV, Tsaousis AD, Hirt RP, Embley TM (2010) Diversity and reductive evolution of mitochondria among microbial eukaryotes. Phil Trans Roy Soc B-Biol Sci 365: 713–727.
3. Clemens DL, Johnson PJ (2000) Failure to detect DNA in hydrogenosomes of *Trichomonas vaginalis* by nick translation and immunomicroscopy. Mol Biochem Parasitol 106: 307–313.
4. Adams KL, Palmer JD (2003) Evolution of mitochondrial gene content: gene loss and transfer to the nucleus. Mol Phylogenet Evol 29: 380–395.
5. Crompton M (1999) The mitochondrial permeability transition pore and its role in cell death. Biochem J 341(Pt 2): 233–249.
6. Kunji ER (2004) The role and structure of mitochondrial carriers. FEBS Lett 564: 239–244.
7. el Moualij B, Duyckaerts C, Lamotte-Brasseur J, Sluse FE (1997) Phylogenetic classification of the mitochondrial carrier family of *Saccharomyces cerevisiae*. Yeast 13: 573–581.
8. Palmieri F (2004) The mitochondrial transporter family (SLC25): physiological and pathological implications. Pflugers Arch 447: 689–709.
9. Palmieri F, Pierri CL (2010) Mitochondrial metabolite transport. Essays Biochem 47: 37–52.
10. Picault N, Hodges M, Palmieri L, Palmieri F (2004) The growing family of mitochondrial carriers in *Arabidopsis*. Trends Plant Sci 9: 138–146.
11. Palmieri F, Bisaccia F, Capobianco L, Dolce V, Fiermonte G, et al. (1996) Mitochondrial metabolite transporters. Biochim Biophys Acta 1275: 127–132.
12. Belenkiy R, Haefele A, Eisen MB, Wohlrab H (2000) The yeast mitochondrial transport proteins: new sequences and consensus residues, lack of direct relation between consensus residues and transmembrane helices, expression patterns of the transport protein genes, and protein-protein interactions with other proteins. Biochim Biophys Acta 1467: 207–218.
13. Millar AH, Heazlewood JL (2003) Genomic and proteomic analysis of mitochondrial carrier proteins in *Arabidopsis*. Plant Physiol 131: 443–453.
14. Dolezal P, Likic V, Tachezy J, Lithgow T (2006) Evolution of the molecular machines for protein import into mitochondria. Science 313: 314–318.
15. Schneider A, Bursac D, Lithgow T (2008) The direct route: a simplified pathway for protein import into the mitochondrion of trypanosomes. Trends Cell Biol 18: 12–18.
16. Chacinska A, Koehler CM, Milenkovic D, Lithgow T, Pfanner N (2009) Importing mitochondrial proteins: machineries and mechanisms. Cell 138: 628–644.
17. Koehler CM (2004) New developments in mitochondrial assembly. Annu Rev Cell Dev Biol 20: 309–335.
18. Gabriel K, Pfanner N (2007) The mitochondrial machinery for import of precursor proteins. Methods Mol Biol 390: 99–117.
19. Neupert W, Herrmann JM (2007) Translocation of proteins into mitochondria. Annu Rev Biochem 76: 723–749.

20. Carlton JM, Hirt RP, Silva JC, Delcher AL, Schatz M, et al. (2007) Draft genome sequence of the sexually transmitted pathogen *Trichomonas vaginalis*. Science 315: 207–212.
21. Dyall SD, Koehler CM, Delgadillo-Correa MG, Bradley PJ, Plumper E, et al. (2000) Presence of a member of the mitochondrial carrier family in hydrogenosomes: conservation of membrane-targeting pathways between hydrogenosomes and mitochondria. Mol Cell Biol 20: 2488–2497.
22. van der Giezen M, Slotboom DJ, Horner DS, Dyal PL, Harding M, et al. (2002) Conserved properties of hydrogenosomal and mitochondrial ADP/ATP carriers: a common origin for both organelles. EMBO J 21: 572–579.
23. Voncken F, Boxma B, Tjaden J, Akhmanova A, Huynen M, et al. (2002) Multiple origins of hydrogenosomes: functional and phylogenetic evidence from the ADP/ATP carrier of the anaerobic chytrid *Neocallimastix* sp. Mol Microbiol 44: 1441–1454.
24. Tjaden J, Haferkamp I, Boxma B, Tielens AG, Huynen M, et al. (2004) A divergent ADP/ATP carrier in the hydrogenosomes of *Trichomonas gallinae* argues for an independent origin of these organelles. Mol Microbiol 51: 1439–1446.
25. Bradley PJ, Lahti CJ, Plumper E, Johnson PJ (1997) Targeting and translocation of proteins into the hydrogenosome of the protist *Trichomonas*: similarities with mitochondrial protein import. EMBO J 16: 3484–3493.
26. Smid O, Matuskova A, Harris SR, Kucera T, Novotny M, et al. (2008) Reductive evolution of the mitochondrial processing peptidases of the unicellular parasites *Trichomonas vaginalis* and *Giardia intestinalis*. PLoS Pathog 4: e1000243.
27. Mentel M, Zimorski V, Haferkamp P, Martin W, Henze K (2008) Protein import into hydrogenosomes of *Trichomonas vaginalis* involves both N-terminal and internal targeting signals: a case study of thioredoxin reductases. Eukaryot Cell 7: 1750–1757.
28. Robinson AJ, Kunji ER (2006) Mitochondrial carriers in the cytoplasmic state have a common substrate binding site. Proc Natl Acad Sci USA 103: 2617–2622.
29. Egan B, Beilharz T, George R, Isenmann S, Gratzer S, et al. (1999) Targeting of tail-anchored proteins to yeast mitochondria in vivo. FEBS Lett 451: 243–248.
30. Isenmann S, Khew-Goodall Y, Gamble J, Vadas M, Wattenberg BW (1998) A splice-isoform of vesicle-associated membrane protein-1 (VAMP-1) contains a mitochondrial targeting signal. Mol Biol Cell 9: 1649–1660.
31. Horie C, Suzuki H, Sakaguchi M, Mihara K (2002) Characterization of signal that directs C-tail-anchored proteins to mammalian mitochondrial outer membrane. Mol Biol Cell 13: 1615–1625.
32. Pusnik M, Charriere F, Maser P, Waller RF, Dagley MJ, et al. (2009) The single mitochondrial porin of *Trypanosoma brucei* is the main metabolite transporter in the outer mitochondrial membrane. Mol Biol Evol 26: 671–680.
33. Hiller S, Garces RG, Malia TJ, Orekhov VY, Colombini M, et al. (2008) Solution structure of the integral human membrane protein VDAC-1 in detergent micelles. Science 321: 1206–1210.
34. Bayrhuber M, Meins T, Habeck M, Becker S, Giller K, et al. (2008) Structure of the human voltage-dependent anion channel. Proc Natl Acad Sci USA 105: 15370–15375.
35. Kutik S, Stojanovski D, Becker L, Becker T, Meinecke M, et al. (2008) Dissecting membrane insertion of mitochondrial beta-barrel proteins. Cell 132: 1011–1024.
36. Dyall SD, Lester DC, Schneider RE, Delgadillo-Correa MG, Plumper E, et al. (2003) *Trichomonas vaginalis* Hmp35, a putative pore-forming hydrogenosomal membrane protein, can form a complex in yeast mitochondria. J Biol Chem 278: 30548–30561.
37. Curran SP, Leuenberger D, Schmidt E, Koehler CM (2002) The role of the Tim8p-Tim13p complex in a conserved import pathway for mitochondrial polytopic inner membrane proteins. J Cell Biol 158: 1017–1027.
38. Curran SP, Leuenberger D, Oppliger W, Koehler CM (2002) The Tim9p-Tim10p complex binds to the transmembrane domains of the ADP/ATP carrier. EMBO J 21: 942–953.
39. Koehler CM (2004) The small Tim proteins and the twin Cx3C motif. Trends Biochem Sci 29: 1–4.
40. Gentle IE, Perry AJ, Alcock FH, Likic VA, Dolezal P, et al. (2007) Conserved motifs reveal details of ancestry and structure in the small TIM chaperones of the mitochondrial intermembrane space. Mol Biol Evol 24: 1149–1160.
41. Rassow J, Dekker PJ, van WS, Meijer M, Soll J (1999) The preprotein translocase of the mitochondrial inner membrane: function and evolution. J Mol Biol 286: 105–120.
42. Murcha MW, Lister R, Ho AYY, Whelan J (2003) Identification, expression, and import of components 17 and 23 of the inner mitochondrial membrane translocase from *Arabidopsis*. Plant Physiology 131: 1737–1747.
43. Kaldi K, Bauer MF, Sirrenberg C, Neupert W, Brunner M (1998) Biogenesis of Tim23 and Tim17, integral components of the TIM machinery for matrix-targeted preproteins. EMBO J 17: 1569–1576.
44. Dolezal P, Smid O, Rada P, Zubacova Z, Bursac D, et al. (2005) *Giardia* mitosomes and trichomonad hydrogenosomes share a common mode of protein targeting. Proc Natl Acad Sci USA 102: 10924–10929.
45. Clements A, Bursac D, Gatsos X, Perry AJ, Civciristov S, et al. (2009) The reducible complexity of a mitochondrial molecular machine. Proc Natl Acad Sci USA 106: 15791–15795.
46. Budzinska M, Galganska H, Karachitos A, Wojtkowska M, Kmita H (2009) The TOM complex is involved in the release of superoxide anion from mitochondria. J Bioenerg Biomembr 41: 361–367.
47. Kmita H, Budzinska M (2000) Involvement of the TOM complex in external NADH transport into yeast mitochondria depleted of mitochondrial porin1. Biochim Biophys Acta 1509: 86–94.
48. Borden KL, Boddy MN, Lally J, O'Reilly NJ, Martin S, et al. (1995) The solution structure of the RING finger domain from the acute promyelocytic leukaemia proto-oncoprotein PML. EMBO J 14: 1532–1541.
49. Vanacova S, Rasoloson D, Razga J, Hrdy I, Kulda J, Tachezy J (2001) Iron-induced changes in pyruvate metabolism of *Tritrichomonas foetus* and involvement of iron in expression of hydrogenosomal proteins. Microbiology-SGM 147: 53–62.
50. Suchan P, Vyoral D, Petrak J, Sut'ak R, Rasoloson D, et al. (2003) Incorporation of iron into *Tritrichomonas foetus* cell compartments reveals ferredoxin as a major iron-binding protein in hydrogenosomes. Microbiology-SGM 149: 1911–1921.
51. Jedelsky PL, Dolezal P, Rada P, Pyrih J, Smid O, et al. (2011) The minimal proteome in the reduced mitochondrion of the parasitic protist *Giardia intestinalis*. PLoS One 6: e17285.
52. Carrie C, Murcha MW, Whelan J (2010) An in silico analysis of the mitochondrial protein import apparatus of plants. BMC Plant Biology 10.
53. Burri L, Williams BA, Bursac D, Lithgow T, Keeling PJ (2006) Microsporidian mitosomes retain elements of the general mitochondrial targeting system. Proc Natl Acad Sci USA 103: 15916–15920.
54. Mukherjee M, Brown MT, McArthur AG, Johnson PJ (2006) Proteins of the glycine decarboxylase complex in the hydrogenosome of *Trichomonas vaginalis*. Eukaryot Cell 5: 2062–2071.
55. Morada M, Smid O, Hampl V, Sutak R, Lam B, et al. (2011) Hydrogenosome-localization of arginine deiminase in *Trichomonas vaginalis*. Mol Biochem Parasitol 176: 51–54.
56. Simpson AG, Roger AJ (2004) The real 'kingdoms' of eukaryotes. Curr Biol 14: R693–R696.
57. Panigrahi AK, Ogata Y, Zikova A, Anupama A, Dalley RA, et al. (2009) A comprehensive analysis of *Trypanosoma brucei* mitochondrial proteome. Proteomics 9: 434–450.
58. Perry AJ, Hulett JM, Likic VA, Lithgow T, Gooley PR (2006) Convergent evolution of receptors for protein import into mitochondria. Curr Biol 16: 221–229.
59. Murcha MW, Elhafez D, Lister R, Tonti-Filippini J, Baumgartner M, et al. (2007) Characterization of the preprotein and amino acid transporter gene family in *Arabidopsis*. Plant Physiol 143: 199–212.
60. Sutak R, Dolezal P, Fiumera HL, Hrdy I, Dancis A, et al. (2004) Mitochondrial-type assembly of FeS centers in the hydrogenosomes of the amitochondriate eukaryote *Trichomonas vaginalis*. Proc Natl Acad Sci USA 101: 10368–10373.
61. Bordier C (1981) Phase-separation of integral membrane-proteins in Triton X-114 solution. J Biol Chem 256: 1604–1607.
62. Honys D, Renak D, Fecikova J, Jedelsky PL, Nebesarova J, et al. (2009) Cytoskeleton-associated large RNP complexes in tobacco male gametophyte (EPPs) are associated with ribosomes and are involved in protein synthesis, processing, and localization. J Proteome Res 8: 2015–2031.
63. Likic VA, Dolezal P, Celik N, Dagley M, Lithgow T (2010) Using hidden markov models to discover new protein transport machines. Methods Mol Biol 619: 271–284.
64. Hrdy I, Hirt RP, Dolezal P, Bardonova L, Foster PG, et al. (2004) *Trichomonas* hydrogenosomes contain the NADH dehydrogenase module of mitochondrial complex I. Nature 432: 618–622.
65. Drmota T, Proost P, Van Ranst M, Weyda F, Kulda J, et al. (1996) Iron-ascorbate cleavable malic enzyme from hydrogenosomes of *Trichomonas vaginalis*: purification and characterization. Mol Biochem Parasitol 83: 221–234.
66. Handa N, Kishishita S, Morita S, Akasaka R, Jin ZM, et al. (2007) Structure of the human Tim44 C-terminal domain in complex with pentaethylene glycol: ligand-bound form. Acta Crystallogr Sec D-Biol Crystallogr 63: 1225–1234.
67. Edgar RC (2004) MUSCLE: multiple sequence alignment with high accuracy and high throughput. Nucleic Acids Res 32: 1792–1797.
68. Sali A, Blundell TL (1993) Comparative protein modeling by satisfaction of spatial restraints. J Mol Biol 234: 779–815.
69. Rodriguez R, Chinea G, Lopez N, Pons T, Vriend G (1998) Homology modeling, model and software evaluation: three related resources. Bioinformatics 14: 523–528.
70. Wiederstein M, Sippl MJ (2007) ProSA-web: interactive web service for the recognition of errors in three-dimensional structures of proteins. Nucleic Acids Res 35: W407–W410.
71. Baker NA, Sept D, Joseph S, Holst MJ, McCammon JA (2001) Electrostatics of nanosystems: Application to microtubules and the ribosome. Proc Natl Acad Sci USA 98: 10037–10041.
72. Chan NC, Lithgow T (2008) The peripheral membrane subunits of the SAM complex function codependently in mitochondrial outer membrane biogenesis. Mol Biol Cell 19: 126–136.
73. Bursac D, Lithgow T (2009) Jid1 is a J-protein functioning in the mitochondrial matrix, unable to directly participate in endoplasmic reticulum associated protein degradation. FEBS Lett 583: 2954–2958.

8.4 The minimal proteome in the reduced mitochondrion of the parasitic protist *Giardia intestinalis*.

OPEN ACCESS Freely available online

PLoS one

The Minimal Proteome in the Reduced Mitochondrion of the Parasitic Protist *Giardia intestinalis*

Petr L. Jedelský[1,2], Pavel Doležal[1], Petr Rada[1], Jan Pyrih[1], Ondřej Šmíd[1], Ivan Hrdý[1], Miroslava Šedinová[1], Michaela Marcinčiková[1], Lubomír Voleman[1], Andrew J. Perry[3], Neritza Campo Beltrán[1], Trevor Lithgow[3], Jan Tachezy[1]*

1 Department of Parasitology, Faculty of Science, Charles University in Prague, Prague, Czech Republic, **2** Laboratory of Mass Spectrometry, Faculty of Science, Charles University in Prague, Prague, Czech Republic, **3** Department of Biochemistry & Molecular Biology, Monash University, Clayton Campus, Melbourne, Australia

Abstract

The mitosomes of *Giardia intestinalis* are thought to be mitochondria highly-reduced in response to the oxygen-poor niche. We performed a quantitative proteomic assessment of *Giardia* mitosomes to increase understanding of the function and evolutionary origin of these enigmatic organelles. Mitosome-enriched fractions were obtained from cell homogenate using Optiprep gradient centrifugation. To distinguish mitosomal proteins from contamination, we used a quantitative shot-gun strategy based on isobaric tagging of peptides with iTRAQ and tandem mass spectrometry. Altogether, 638 proteins were identified in mitosome-enriched fractions. Of these, 139 proteins had iTRAQ ratio similar to that of the six known mitosomal markers. Proteins were selected for expression in *Giardia* to verify their cellular localizations and the mitosomal localization of 20 proteins was confirmed. These proteins include nine components of the FeS cluster assembly machinery, a novel diflavo-protein with NADPH reductase activity, a novel VAMP-associated protein, and a key component of the outer membrane protein translocase. None of the novel mitosomal proteins was predicted by previous genome analyses. The small proteome of the *Giardia* mitosome reflects the reduction in mitochondrial metabolism, which is limited to the FeS cluster assembly pathway, and a simplicity in the protein import pathway required for organelle biogenesis.

Citation: Jedelský PL, Doležal P, Rada P, Pyrih J, Šmíd O, et al. (2011) The Minimal Proteome in the Reduced Mitochondrion of the Parasitic Protist *Giardia intestinalis*. PLoS ONE 6(2): e17285. doi:10.1371/journal.pone.0017285

Editor: Bob Lightowlers, Newcastle University, United Kingdom

Received November 8, 2010; **Accepted** January 26, 2011; **Published** February 24, 2011

Funding: This work was supported by the Czech Ministry of Education (MSM0021620858, LC07032) and the Czech Science Foundation grants 204/05/H023 (P.J.) and 204/06/0947 (J.T.) and the Australian Research Council (T.L.). The funders had no role in study design, data collection and analysis, decision to publish, or preparation of the manuscript.

Competing Interests: The authors have declared that no competing interests exist.

* E-mail: tachezy@gmail.com

Introduction

Mitochondria are eukaryotic organelles that are thought to have evolved from an alpha-proteobacterial endosymbiont about two billion years ago. The loss of bacterial autonomy and transition of the endosymbiont to a "protomitochondrion" were associated with a reduction in the number of genes in the endosymbiont genome; these genes were either transferred to the nuclear genome or lost. While the genome of the extant alpha-proteobacterium *Rickettsia prowazekii* contains 834 protein-coding genes [1], the largest number of genes (67 protein-coding genes) in a mitochondrial genome is found in *Reclinomonas americana* [2], with only three protein-coding genes present in the *Plasmodium falciparum* mitochondrial genome [3]. Paradoxically, the reduction of the mitochondrial genome did not lead to a reduction of the organellar proteome [4]. The acquisition of a mechanism for mitochondrial import at the earliest stage of the endosymbiont-to-protomitochondrion transition allowed the recruitment of the proteins of endosymbiotic origin that were now encoded in the nucleus, and the import of proteins of other origins [5]. Contemporary mitochondrial proteomes contain hundreds of proteins, up to 1100 proteins in the mouse [6].

Mitosomes are the most highly reduced forms of mitochondria, having completely lost their genomes and dramatically reduced their proteomes. Mitosomes have also lost many of the typical mitochondrial functions, such as respiration, the citric acid cycle, and ATP synthesis. Biosynthesis of FeS clusters is the only mitochondrial function seen to be retained by at least some mitosomes [7]. Mitosomes have become established independently in diverse groups of unicellular eukaryotes (protists); many of them once considered to be amitochondrial because they lack organelles with the expected mitochondrial morphology [8].

Organisms with mitosomes live under oxygen-limiting conditions, like the human intestinal parasites *Giardia intestinalis* [9] and *Entamoeba histolytica* [10], or are intracellular parasites like the microsporidians *Encephalitozoon cuniculi* and *Trachipleistophora hominis* [11,12] and the apicomplexan *Cryptosporidium parvum* [13]. Mitosomes are tiny ovoid organelles enclosed by two membranes. Unlike mitochondria, the inner membrane of mitosomes does not form cristae. The morphology of the mitosome is reminiscent of the hydrogenosome, another form of mitochondrion that is present in some anaerobic protists, such as *Trichomonas vaginalis*. Unlike mitosomes, however, hydrogenosomes are metabolically active organelles that produce ATP by substrate level phosphorylation [14].

The limited knowledge of mitosomal proteomes has been gained mainly from analyses of genome sequences and localization studies of a few model mitosomal proteins [9,11,15–21]. The only published proteomics study that focused on mitosomes was that

recently reported for the amoeba *E. histolytica*, identifying a unique sulfate activation pathway [22]. To increase our understanding of the function and origin of these enigmatic organelles, we established a large-scale proteomic approach to analyze the mitosomes of *Giardia intestinalis*. This organism was selected because *Giardia intestinalis* is a common human intestinal pathogen, its genome sequence has been published [23,24], and it is considered to be among the most basal eukaryotes [25]. Moreover, previous analysis of the *G. intestinalis* genome provided little new information pertaining to the putative mitosomal proteome [24], so there are substantial gaps in our knowledge of the structure and function of this essential organelle. Here, we quantitatively analyzed the presence of isobarically-tagged proteins in mitosome enriched fractions. This technique allowed us to discriminate the mitosomal proteins from those of contaminating cellular structures. Combined with an exhaustive bioinformatics analysis, this strategy identified 139 putative mitosomal proteins; 20 of which were experimentally confirmed to be localized in mitosomes. Our results revealed that the proteome of the *G. intestinalis* mitosome is selectively reduced and houses a single metabolic pathway for FeS cluster assembly, a novel diflavin protein with NADPH reductase activity, a minimal protein import machinery and proteins that may be important for the interaction of mitosomes with other cellular compartments.

Results and Discussion

Identification of putative mitosomal proteins by isobaric tagging

Mitosome-enriched fractions were separated from a *Giardia* homogenate by preparative centrifugation using a discontinuous Optiprep (iodixanol) gradient [26]. This method produced five dense organellar fractions (Fig. 1A). The mitosomal marker protein IscU was particularly enriched in fraction #4 and to a lesser extent in fraction #3 (Fig. 1B). Electron microscopy confirmed the presence of mitosomes in both fractions; however, co-fractionating vesicles of similar densities were also found (data not shown).To discriminate between putative mitosomal proteins and those of contaminating cellular structures, we compared the relative distribution of each protein in fractions #3 and #4. Because the mitosomal proteins necessarily co-fractionate (i.e. being contained within mitosomes) during gradient centrifugation, each of the *bona fide* mitosomal protein should display similar distribution ratios [27]. To this end, the proteins of fractions #3 and #4 were digested in parallel with trypsin and each peptide population was labeled with a distinct iTRAQ reagent and then combined. The isobaric mass characteristics of the iTRAQ reagents means the differentially-labeled peptides from fractions #3 and #4 form a single peak in the MS scan for protein identification. MS/MS analysis of the iTRAQ-labelled peptides liberates the isotope-encoded reporter ions, the ratio of which can reflects the distribution of the protein across the two fractions. In our analysis, the pooled peptides were analyzed by tandem mass spectrometry after subsequent separation with isoelectric focusing and nano-liquid chromatography (nano-LC MS/MS). The iTRAQ ratio was then calculated for each protein, and the proteins were sorted according to the relative distributions in the fractions (Fig. 2).

Validating the methodology, mitosomal markers (IscS, IscU, [2Fe2S] ferredoxin, Cpn60, Hsp70 and glutaredoxin 5) [28] clustered together with similar iTRAQ ratios (Fig. 2). Proteins with ratios between the lowest and highest values for the markers were considered to be candidate mitosomal proteins. We also extended this window on both sides by half of the distance between the limiting markers and included all proteins in this extended window (Fig. 2). In total, we identified 638 proteins (Table S1), with 139 of these proteins meeting the defined criteria for mitosomal proteins (Tables 1–7). Each of the 139 mitosomal candidates was assigned to a probable function based on current annotations in the GiardiaDB, PSI BLAST searches in the NCBI nr database, and motif and domain searches in the Pfam database. Three additional bioinformatics tools were used to predict cellular localization (PsortII, TargetP 1.1 and SignalP 3.0), and two web-based programs were used to predict alpha-helical transmembrane region segments (TMHMM and Memsat3) (Tables S2–S4, summary is given in Tables 1–7). The candidate proteins were clustered into 13 groups according to their predicted functions (Tables 1–7, Fig. 3). The proteomic data confirmed the validity of 250 hypothetical genes predicted from the complete genome sequence of *Giardia* [24]; 40 of these formed the largest group of candidate mitosomal proteins.

Evolution-inspired orthology phylogenetic profiling

Previous phylogenetic analyses of known mitosomal proteins have generally confirmed their alpha-proteobacterial origin [28–30]. On this premise, we compared the genomes of *G. intestinalis* and *Rickettsia typhi* using the orthology phylogenetic profile tool at GiardiaDB (http://www.orthomcl.org/cgi-bin/OrthoMclWeb.cgi) to identify proteins of alpha-proteobacterial ancestry in the *G. intestinalis* genome. The phylogenetic profiling yielded 106 candidate genes that were analyzed with the topology prediction algorithms described above (Table S5). Based on these analyses, six additional proteins: acetyl CoA acetyl transferase, CDP-diacylglycerol-glycerol-3-phosphate 3-phosphatidyltransferase, guanylate kinase, J-protein HesB, thioredoxin reductase, and thymidylate kinase were added to the set of candidate mitosomal proteins identified by our proteomics approach (Tables 1–7).

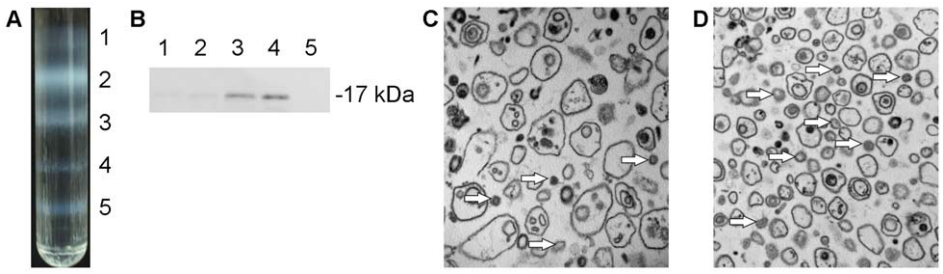

Figure 1. Isolation of mitosome-rich fractions. (A) Trophozoites were disrupted and centrifuged to remove unbroken cells, nuclei and cytoskeletal residue. The high-speed pellet was resuspended in sucrose buffer, layered onto an Optiprep density gradient, and centrifuged overnight. Five distinct fractions were obtained. (B) Fractions were collected and analyzed by SDS-PAGE and Western blot. The mitosomal marker GiIscU was detected in fractions #3 and #4 using a polyclonal rabbit antibody. (C–D) Electron microscopy of subcellular fractions. Fraction #3 (C) contains numerous vesicles of variable sizes, while fraction #4 (D) contains vesicles of more homogeneous sizes. Arrows indicate mitosomes.
doi:10.1371/journal.pone.0017285.g001

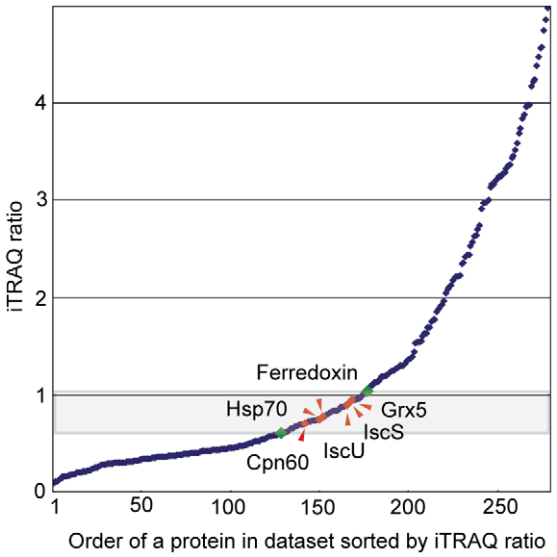

Figure 2. iTRAQ ratios define protein subcellular localization. Proteins in fractions #3 and #4 isolated on the Optiprep gradient were labeled with the iTRAQ-114 and iTRAQ-115 reagents, respectively, analyzed by LC MS/MS, and sorted according to the iTRAQ ratios. Mitosomal marker proteins (red diamonds) fall into a narrow range of iTRAQ ratios. Green diamondsdindicate the zone of proteins considered as mitosomal candidates (mitosomal distribution, MiD).
doi:10.1371/journal.pone.0017285.g002

Experimental validation of protein subcellular localization

The cellular localization of the selected candidate proteins was observed by stable episomal expression in *Giardia*. To establish the morphology of subcellular localizations by this approach, we first observed the localization of five marker proteins: cytosolic enolase, two proteins from the endoplasmic reticulum (Hsp70 and protein disulfide isomerase 5), mitosomal Hsp70 and glutaredoxin (Fig. 4A). We added to these markers of known location, three proteins of untested location with iTRAQ ratios outside that of the mitosomal range: glutamate dehydrogenase, copine and peroxiredoxin. Glutamate dehydrogenase and copine were associated with cytoskeletal structures, while peroxiredoxin localizes to the endoplasmic reticulum network. This strategy was used to test the sub-cellular localization of 44 selected proteins. Of these 20 expressed fluorescent fusions that were found in the mitosomes (Tables 1–7). By way of example, four of these: VAP, Pam16, Cpn10 and unknown proteins GL50803_9296 and GL50803_ 14939 are shown in Fig. 4B.

Iron-sulfur cluster assembly

Proteins involved in FeS cluster assembly formed the most prominent functional group within the predicted mitosomal proteins. These included components required for the formation of transient FeS clusters on the molecular scaffold (IscS, IscU, Nfu) (Fig. S1) and components that have been proposed to transfer the transient FeS clusters to target apoproteins, including IscA (Fig. S2), the monothiol glutaredoxin 5, chaperone Hsp70 and its co-chaperones the J-protein HscB (Fig. S3) and nucleotide exchange factor GrpE (Fig. S4). The identification of the FeS cluster assembly machinery in the mitosomal proteome is consistent with the ability of the mitosome-enriched fraction to catalyze the formation of FeS clusters on a ferredoxin apoprotein [9]. However, when we compared the FeS cluster machinery of *Giardia* mitosomes to that of *S. cerevisiae* and *Trypanosoma brucei* mitochondria, we found that several mitochondrial components were absent from the mitosomes (Table 8).

A striking deviation from other eukaryotes is the absence of frataxin in *Giardia* mitosomes. Frataxin is invariably present in eukaryotes that contain the ISC-type FeS cluster assembly machinery. The presence of frataxin in mitosomes was found in *E. cuniculi* [17], and genes encoding frataxin are present in the genomes of *C. parvum* and the diplomonad *Spironucleus vortens*, a close relative of *Giardia*. We failed to identify frataxin in the genomes of three *G. intestinalis* strains in the GiardiaDB, using either BLAST searches or the motif search tool.

Two IscA-like proteins, IscA1 (Isa1) and IscA2 (Isa2) are present in virtually all mitochondria [31] and are thought to act as scaffold proteins for transient FeS clusters [32–34] and/or serve as iron donors [35]. Interestingly, the *Giardia* mitosome contains only a single IscA-2 type protein (Fig. S2), while IscA-1 is absent. The same situation was found in hydrogenosomes of *Trichomonas vaginalis* (Table 8). No genes encoding IscA were found in the genomes of other organisms with mitosomes. The observed distributions of IscA therefore suggest that IscA-1 was lost in mitosomes and hydrogenosomes together with a specific set of mitochondrial FeS proteins, while IscA-2 was retained in *Giardia* mitosomes to function either in the maturation of specific FeS protein(s) or as an iron transporter [35].

The mitosomes did not contain Ind1 or Iba57. In mitochondria, these proteins are required for the formation of FeS clusters on specific substrates. Ind1 is a P-loop NTPase that is required for the maturation of FeS proteins of the multi-subunit respiratory complex I [36,37]. Homologues of Ind1 are also present in the hydrogenosomes of *T. vaginalis* (Table 8), which contain a highly reduced form of complex I with only two FeS catalytic subunits [38]. The selective absence of Ind1 in the mitosomes of *Giardia* (Table 8) is thus consistent with the absence of complex I and highlights the specific role of Ind1 in the biogenesis of this respiratory complex. Iba57 forms a complex with the scaffold protein IscA (Isa1p and Isa2p in yeast), which plays a specific role in [4Fe4S] cluster assembly of aconitase-type proteins and the functional activation of mitochondrial radical-SAM FeS proteins [39]. As in the case of Ind1, the absence of Iba57 likely reflects the absence of the respective substrate proteins in mitosomes.

Pyridine nucleotide-driven electron transport in mitosomes

The formation of FeS clusters requires reducing equivalents, which are provided by a short electron chain consisting of the [2Fe2S] ferredoxin and ferredoxin:$NADP^+$ reductase (FNR) [40]. The presence of this chain has been predicted in the mitosomes of *C. parvum* and *E. cuniculi*; however, [2Fe2S] ferredoxin, but not FNR, was found in *Giardia* mitosomes (Table 1). We identified a distinct protein with a possible redox activity named GiOR-1 (GL50803_91252), which is currently annotated in the GiardiaDB as an inducible nitric oxide synthase. This protein consists of a flavodoxin-like FMN-binding domain that is connected to a cytochrome p450 reductase-like domain, including a FAD binding pocket and an NADP(H) binding site (Fig. S5). These two domains are present in the C-termini of various oxidoreductases, such as cytochrome p450 reductase and nitric oxide synthase, and serve as electron donors (Fig. S5). GiOR-1 does not contain an N-terminal domain that determines the specific functions of known oxidoreductases.

The architecture of GiOR-1 resembles that of the recently identified protein Tah18 in *Saccharomyces cerevisiae* [41,42]. Tah18 was shown to form a complex with Dre2 in the cytosol, where it participates in cytosolic FeS cluster assembly [43]. Under oxidative stress, the Dre2-Tag18 complex was destabilized, and Tah18 relocalized from the cytosol to the mitochondria. This behavior has been shown to be associated with apoptotic events.

Table 1. Putative mitosomal proteins classified by predicted function: Iron-sulfur cluster assembly, chaperones, redox mechanism and protein translocation and processing.

Accession number	Annotation	Identification		Localization					Structure		
		MASCOT	Coverage	MiD	SignalP	Target P	Psort II	Exp Ver.	MEMSAT3	SGP	TMHMM
		score	peptides				% mito		TM No.		TM No.
Iron-sulfur cluster assembly											
GL50803_14519	IscS, cysteine desulfurase	296	4	Y	N	O		M	0	#	0
GL50803_15196	IscU	243	5	Y	N	M	17%	M	0	#	0
EAA38809	Nfu	60	2	Y	N	M	39%	M	1		0
GL50803_14821	IscA	198	3	Y	N	O	35%	M	0	#	0
GL50803_2013	Glutaredoxin 5	249	3	Y	N	O	13%	M	0	#	0
Molecular chaperones											
GL50803_14581	mitochondrial type HSP70	404	7	Y	N	O	13%	M	0	#	0
GL50803_1376	GrpE	29	1	Y	N	M	39%	M	0	#	0
GL50803_17030	DnaJ protein, Jac1	*	*	*	N	O	35%	M	0	#	0
GL50803_9751	DnaJ protein, Type III	34	1	Y	N	O	13%	M	1		1
GL50803_103891	Cpn60	336	6	Y	N	O		M	0	#	0
GL50803_29500	Cpn10	68	1	Y	Y	O	9%	M	0	#	0
Redox mechanism											
GL50803_27266	[2Fe-2S] ferredoxin	182	2	Y	N	M	48%	M	0	#	0
GL50803_91252	GiOR-1, oxidoreductase	40	1	N	N	O	13%	M	0	#	0
GL50803_15897	GiOR-2, oxidoreductase	*	*	*	N	O	21%	O	0	#	0
GL50803_9827	Thioredoxin reductase	*	*	*	N	M	13%	O	0	#	0
GL50803_9719	NADH oxidase	271	5	Y	N	O	9%	**	0	#	0
GL50803_16076	Peroxiredoxin 1	293	5	Y	N	O	9%		0	#	0
Protein translocation and processing											
GL50803_17161	Tom40	208	2	Y	N	O	13%	M	0	#	0
XP_002364144	Pam18	68	1	Y	N	M	30%	M	0	#	0
GL50803_19230	Pam16	35	1	Y	N	O	13%	M	0	#	0
GL50803_9478	GPP, processing peptidase	30	1	Y	N	O	4%	M	0	#	0

Mascot score, Mascot total ion score for the identified protein. Coverage, number of unique peptides per identified protein. MiD, mitosomal distribution. Proteins are marked "Y" if their distributions in fractions #3 and #4 of the Optiprep gradient (measured by the iTRAQ ratio) were within the range between Cpn10 and IscU and the window that extended in both directions by half of the distance between these markers. Proteins with ratios outside of this range are indicated with "N". TargetP and PsortII were used to predict the subcellular location of *Giardia* proteins. S, secretory; N, non-secretory; M, mitochondrial; O, other. Exp. ver., experimental verification of protein localization using the pONDRA expression vector. The recombinant tagged proteins were localized by fluorescence microscopy. M, mitosome; ER, endoplasmic reticulum; O, other; ? inconclusive. MEMSAT3 and TMHMM were used to predict transmembrane domains. SGP, predicted soluble proteins are marked with number sign (#). Asterisk (*) is used where no data were available. (**) transformed *Giardia* did not express the recombinant tagged protein.
doi:10.1371/journal.pone.0017285.t001

Searches for a Dre2 homologue in *Giardia* were unsuccessful. However, we identified a second paralogue of Tah18 named GiOR-2 (GL50803_15897, Fig. S5). The expression of tagged GiOR-1 and GiOR-2 in *G. intestinalis* confirmed that the GiOR-1 is localized to the mitosome, but GiOR-2 was found in numerous vesicles that did not correspond to mitosomes (Fig. 4C). To assess the oxidoreductase activity of GiOR-1, recombinant GiOR-1 was produced in *Escherichia coli* and isolated as a yellow protein, which is expected for diflavin oxidoreductases. GiOR-1 efficiently transferred electrons from NADPH to dichlorophenolindolphenol, whereas an about 30 fold lower activity was measured using NADH as the electron donor (Table 9). Low specific activities were observed also with methyl viologen and oxygen as electron acceptors (Table 9). No activity was observed when GiOR-1 was assayed with *G. intestinalis* mitosomal ferredoxin as a possible native electron acceptor. These results suggest that GiOR-1 does not act directly as a ferredoxin reductase in mitosomes, however, its ability to utilize NADPH as an electron donor indicates that pyridine nucleotides are involved in mitosomal electron transport.

Molecular chaperones in the mitosomal matrix: protein folding and assembly

A single mitosomal Hsp70, three J-protein co-chaperones and the nucleotide exchange factor GrpE were identified in the mitosomes. The J-proteins included HscB, an orthologue of yeast Jac1 (Fig. S3)that has a predicted role in FeS cluster biogenesis [44], and Pam18/Tim14, which is required for translocation of proteins across the mitochondrial inner membrane [45]. The third J-protein also contains an N-terminal DnaJ domain (type III family); however, its function cannot be inferred from domain structure or phylogenetic profiling. We also identified the chaperonins Cpn60 and Cpn10 (Fig. S6), that function in folding and assembly of newly-imported proteins [46,47] (Table 1).

Table 2. Putative mitosomal proteins classified by predicted function: transporters and proteins known to operate in endoplasmic reticulum and tramsport vesicles.

Accession number	Annotation	Identification		Localization					Structure		
		MASCOT	Coverage	MiD	SignalP	Target P	Psort II	Exp Ver.	MEMSAT3	SGP	TMHMM
		score	peptides				% mito		TM No.		TM No.
Transporters											
GL50803_114777	major facilitator superfamily mfs_1	658	8	N	N	M	4%	ER	10		12
GL50803_17296	major facilitator superfamily mfs_1	32	1	Y	N	M		**	7		10
GL50803_17342	major facilitator superfamily mfs_1	151	3	Y	N	M		**	10		12
GL50803_87446	ABC transporter, A family, putative	554	7	Y	N	O		**	4		7
GL50803_3470	ABC transporter, A family, putative	95	2	Y	N	M		**	6		7
GL50803_17165	ABC transporter, A family, putative	113	2	Y	N	O	4%		8		7
GL50803_21411	ABC transporter, A family, putative	429	10	Y	N	S			0		14
ER, vesicle transport											
GL50803_5744	Sec61-alpha	175	3	Y	N	M	22%	ER	10		9
GL50803_16906	Phosphatidate cytidylyltransferase	48	2	Y	N	M	9%	ER	7		8
GL50803_14200	Molybdenum cofactor sulfurase	56	1	Y	N	O	22%	ER	2		1
GL50803_14670	Protein disulfide isomerase PDI3	69	1	Y	Y	S	22%		1		0
GL50803_8064	Protein disulfide isomerase PDI5	58	1	Y	Y	S	13%	ER	1		1
GL50803_17121	ER Hsp70 (Bip)	1626	24	Y	Y	S	11%	ER	0	#	1
GL50803_15204	Endosomal cargo receptor 3	95	2	Y	Y	S			1		1
GL50803_14469	R-SNARE 3	45	1	Y	N	O			1		2
GL50803_8559	Vacuolar ATP synthase 16 kDa proteolipid subunit	90	1	Y	N	O	11%		4		4
GL50803_7532	Vacuolar ATP synthase catalytic subunit A	146	2	Y	N	O	17%		1		0
GL50803_13000	Vacuolar ATP synthase subunit d	342	5	Y	N	O	13%		1		0
GL50803_23833	Vacuolar protein sorting 35	26	1	Y	N	O	11%		1		0
GL50803_18470	Vacuolar proton-ATPase subunit, putative	608	8	Y	N	O	4%		6		6
GL50803_96670	Potassium-transporting ATPase alpha chain 1	473	9	Y	N	O	4%		10		8

Mascot score, Mascot total ion score for the identified protein. Coverage, number of unique peptides per identified protein. MiD, mitosomal distribution. Proteins are marked "Y" if their distributions in fractions #3 and #4 of the Optiprep gradient (measured by the iTRAQ ratio) were within the range between Cpn10 and IscU and the window that extended in both directions by half of the distance between these markers. Proteins with ratios outside of this range are indicated with "N". TargetP and PsortII were used to predict the subcellular location of *Giardia* proteins. S, secretory; N, non-secretory; M, mitochondrial; O, other. Exp. ver., experimental verification of protein localization using the pONDRA expression vector. The recombinant tagged proteins were localized by fluorescence microscopy. M, mitosome; ER, endoplasmic reticulum; O, other; ? inconclusive. MEMSAT3 and TMHMM were used to predict transmembrane domains. SGP, predicted soluble proteins are marked with number sign (#). Asterisk (*) is used where no data were available. (**) transformed *Giardia* did not express the recombinant tagged protein.
doi:10.1371/journal.pone.0017285.t002

Protein import

We identified four components that are potentially involved in transporting proteins across the mitosomal membranes: a homologue of a mitochondrial Tom40, which would form a general import pore in the outer mitosomal membrane, and the three essential components of the PAM (presequence translocase-associated motor) complex: Pam18, Pam16 (Fig. S7) and mHsp70. Pam18 and Pam16 form an intimate complex that anchors a population of the matrix Hsp70 to the inner membrane and regulates its activity to drive protein translocation across the inner

Table 3. Putative mitosomal proteins classified by predicted function: protein modification, cztosceletal and motor proteins.

Accession number	Annotation	Identification		Localization				Structure		
		MASCOT	Coverage	MiD	SignalP	Target P	Psort II	MEMSAT3	SGP	TMHMM
		score	peptides				% mito	TM No.		TM No.
Protein modification										
GL50803_8587	Kinase, AGC NDR	22	1	Y	N	O	4%	0	#	0
GL50803_14223	Kinase, NEK	124	2	Y	N	O	13%	0	#	0
GL50803_16824	Kinase, NEK	87	2	Y	N	O		0	#	0
GL50803_17510	Kinase, NEK	25	1	Y	N	O	17%	0	#	0
GL50803_5375	Kinase, NEK	46	1	Y	N	O	17%	0	#	0
GL50803_11775	Kinase, NEK-frag	50	2	Y	N	O	17%	0	#	0
GL50803_7183	Kinase, NEK-frag	22	1	Y	N	O	13%	0	#	0
GL50803_8805	Kinase, SCY1	159	2	Y	N	O	11%	1		0
GL50803_7110	Ubiquitin	360	5	Y	N	O	17%	0	#	0
Cytoskeletal and motor proteins										
GL50803_11654	Alpha-1 giardin	934	17	Y	N	O	13%	1		0
GL50803_7796	Alpha-2 giardin	478	8	Y	N	O	17%	1		0
GL50803_5649	Alpha-10 giardin	294	5	Y	N	O	9%	1		0
GL50803_15097	Alpha-14 giardin	643	9	Y	N	O	4%	0	#	0
GL50803_112079	Alpha-tubulin	394	7	Y	N	O		0	#	0
GL50803_136020	Beta tubulin	841	13	Y	N	O		0	#	0
GL50803_42285	Ciliary dynein heavy chain 11	23	1	Y	N			1		0
GL50803_93736	Dynein heavy chain	29	1	Y	N		13%	0		0
GL50803_16993	FtsJ cell division protein, putative	24	1	Y	N	O	17%	0	#	0
GL50803_102101	Kinesin-3	85	1	Y	N	O	26%	0	#	0
GL50803_21444	Spindle pole protein, putative	63	2	Y	N	O	22%	0	#	0
GL50803_8589	Suppressor of actin 1	81	2	Y	N	O	11%	3		2

Mascot score, Mascot total ion score for the identified protein. Coverage, number of unique peptides per identified protein. MiD, mitosomal distribution. Proteins are marked "Y" if their distributions in fractions #3 and #4 of the Optiprep gradient (measured by the iTRAQ ratio) were within the range between Cpn10 and IscU and the window that extended in both directions by half of the distance between these markers. Proteins with ratios outside of this range are indicated with "N". TargetP and PsortII were used to predict the subcellular location of *Giardia* proteins. S, secretory; N, non-secretory; M, mitochondrial; O, other. Exp. ver., experimental verification of protein localization using the pONDRA expression vector. The recombinant tagged proteins were localized by fluorescence microscopy. M, mitosome; ER, endoplasmic reticulum; O, other; ? inconclusive. MEMSAT3 and TMHMM were used to predict transmembrane domains. SGP, predicted soluble proteins are marked with number sign (#). Asterisk (*) is used where no data were available. (**) transformed *Giardia* did not express the recombinant tagged protein.

doi:10.1371/journal.pone.0017285.t003

membrane [48]. Typically, it functions together with a TIM complex that forms the translocation pore for protein passage across the membrane. In representative organisms from all lineages of eukaryotes, the TIM complex is built from one or two proteins of the Tim17/22/23 family [49]. Surprisingly, we find no evidence for a member of this protein in our proteomics data, and sensitive hidden Markov model searches detected no related sequences in the *Giardia* genome (unpublished, see Methods). In eukaryotes, the Sec61 channel catalyzes protein transport across the endoplasmic reticulum [2], while a highly-related protein called SecY is the translocation channel in the inner membrane of bacteria, including the alpha-proteobacteria from which mitochondria are derived. Interestingly, *Reclinomonas americana* encodes a bacterial-type SecY protein translocation channel in its mitochondrial genome [50], and our proteomics analysis detected what appeared to be contamination of the mitosomal membranes with GiSecY/Sec61. We expressed a tagged version of this protein in *Giardia* but it localized to the endoplasmic reticulum, as expected for a cognate Sec61, rather than to the mitosomes. The nature of the mitosomal inner membrane protein translocation channel remains unknown, and yet must exist given that at least 17 of the proteins detected in the mitosomal proteome are likely to reside in the matrix.

We suggest that Tim23/17/22 protein(s) have been secondarily lost from *Giardia*, given that the these proteins appear to be derived from components of the ancestral endosymbiont [48] and are present in all other groups of eukaryotes including other members of the Excavata [51], particularly *T. vaginalis* (TrichDB, http://trichdb.org/trichdb; our unpublished data). Because there is evidence to suggest that *T. vaginalis* and *G. intestinalis* share a common ancestor [44,52], the absence of a Tim23 homologue in *Giardia* likely reflects the overall simplification of the organelle than a primitive trait. Why has the TIM complex been replaced? In addition to a reliance on ATP hydrolysis mediated by the PAM motor, the TIM complex is powered by the membrane potential through its physical association with the respiratory complexes III and IV [53,54]. *Giardia* mitosomes do not generate a large membrane potential, as shown by their inability to accumulate the routinely used mitochondrial probes that are sensitive to the membrane potential (e.g., mitotrackers, JC-1, our observations). Perhaps any membrane potential that is present, is insufficient to support the function of a TIM23 translocase.

Table 4. Putative mitosomal proteins classified by predicted function: various metabolic processes, lipid metabolism.

Accession number	Annotation	Identification		Localization					Structure		
		MASCOT	Coverage	MiD	SignalP	Target P	Psort II	Exp Ver.	MEMSAT3	SGP	TMHMM
		score	peptides				% mito		TM No.		TM No.
Various metabolic processes											
GL50803_7203	Guanylate kinase	*	*	*	N	M	65%	O	0	#	0
GL50803_3287	Acetyl-CoA acetyltransferase	*	*	*	N	M	22%	O	0	#	0
GL50803_8163	Manganese-dependent inorganic pyrophosphatase, putative	25	1	Y	N	O	22%		0	#	0
GL50803_6497	Metal-dependent hydrolase	30	1	Y	N	O	13%		1		0
GL50803_10311	Ornithine carbamoyltransferase	665	8	Y	N	O	9%		1		0
GL50803_14993	Pyrophosphate-fructose 6-phosphate 1-phosphotransferase alpha subunit	56	1	Y	N	M	35%		1		0
GL50803_15380	CDC8 Thymidylate kinase	*	*	*	N	O	35%	O	0	#	0
Lipid metabolism											
GL50803_9062	Long chain fatty acid CoA ligase 5	279	3	Y	N	O	22%	**	0	#	0
GL50803_21118	Long chain fatty acid CoA ligase 5	25	1	Y	N	O	26%		0	#	0
GL50803_113892	Long chain fatty acid CoA ligase, putative	224	4	Y	N	O	26%		0	#	0
GL50803_7259	CDP-diacylglycerol-glycerol-3-phosphate 3-phosphatidyltransferase	43	1	N	N	M	22%		6		2

Mascot score, Mascot total ion score for the identified protein. Coverage, number of unique peptides per identified protein. MiD, mitosomal distribution. Proteins are marked "Y" if their distributions in fractions #3 and #4 of the Optiprep gradient (measured by the iTRAQ ratio) were within the range between Cpn10 and IscU and the window that extended in both directions by half of the distance between these markers. Proteins with ratios outside of this range are indicated with "N". TargetP and PsortII were used to predict the subcellular location of *Giardia* proteins. S, secretory; N, non-secretory; M, mitochondrial; O, other. Exp. ver., experimental verification of protein localization using the pONDRA expression vector. The recombinant tagged proteins were localized by fluorescence microscopy. M, mitosome; ER, endoplasmic reticulum; O, other; ? inconclusive. MEMSAT3 and TMHMM were used to predict transmembrane domains. SGP, predicted soluble proteins are marked with number sign (#). Asterisk (*) is used where no data were available. (**) transformed *Giardia* did not express the recombinant tagged protein.
doi:10.1371/journal.pone.0017285.t004

Interaction of mitosomes with other cellular compartments

In the *Giardia* mitosomes, we identified a VAMP (vesicle-associated membrane protein)-associated protein, VAP (Table 6). VAPs are involved mainly in membrane trafficking and lipid metabolism. They provide membrane anchors for various lipid binding proteins on the surfaces of the endoplasmic reticulum and Golgi complex [53] and physically interact with SNARE proteins, with FFAT-motif containing lipid transport proteins and microtubules. Like other VAPs, the *Giardia* VAP protein contains an N-terminal domain that includes the VAP consensus sequence [55], a central coiled-coil domain and a C-terminal transmembrane domain with the putative dimerization motif GxxxG (Fig. S8). The presence of a VAP protein has not been reported in mitochondria or other mitosomes so far. In *Giardia*, GiVAP was found within the set of hypothetical proteins with distribution value corresponding to mitosomal proteins (Table 6) and its mitosomal localization was experimentally confirmed (Fig. 4B).

Hypothetical proteins

The set of mitosomal candidates contains 40 proteins annotated as hypothetical proteins. We selected six proteins with high mitochondrial score (Tables 6–7) for the verification of their subcellular localization. Three proteins were confirmed to reside in mitosomes (Table 6, Fig 4): (i) putative VAP (GL50803_15985) that is discussed above, (ii) hypothetical protein GL50803_14939 that contains two predicted transmembrane domains (residues 13–35 and 102–124), and (iii) a putative soluble globular protein GL50803_9296. The latter two proteins seem to be unique for giardia as no orthologues were identified in available databases. Two other hypothetical proteins (GL50803_16596 and GL50803_4768) were observed in the cytosol and in association with kinetosomes, respectively (Table 6, data not shown). The cellular localization of hypothetical protein GL50803_12999 remains inconclusive. Although the protein co-localized with IscU in some vesicles, it was not observed in typical rod-like structure between nuclei (data not shown).

Origin of mitosomes and perspectives

Mitosomes are thought to have evolved several times in different eukaryotic lineages through the reduction of ancestral mitochondria. For example, microsporidians are intracellular parasites allied with Fungi; whereas Fungi typically possess fully equipped mitochondria with large proteomes (>850 proteins) [11,56], only twenty to thirty proteins have been identified from genome analysis of *E. cuniculi* as having similarity to *bona fide* mitochondrial proteins of *Saccharomyces cerevisiae* [15,18,21]. Apicomplexan parasites related to *Plasmodium* also include

Table 5. Putative mitosomal proteins classified by predicted function: miscellaneous.

Accession number	Annotation	Identification		Localization					Structure		
		MASCOT	Coverage	MiD	SignalP	Target P	Psort II	Exp Ver.	MEMSAT3	SGP	TMHMM
		score	peptides				% mito		TM No.		TM No.
Miscellaneous											
GL50803_11953	Coatomer alpha subunit (WD40)	31	1	Y	N	O			0	#	0
GL50803_88765	Cytosolic HSP70	22	1	Y	N	O	4%		1		0
GL50803_112312	Elongation factor 1-alpha	424	10	Y	N	O	4%		1		0
GL50803_12102	Elongation factor 1-gamma	158	3	Y	N	M	13%		1		0
GL50803_28379	Multidrug resistance-associated protein 1	210	4	Y	N	O			0		10
GL50803_16313	Pescadillo (ribosome biogenesis)	52	1	Y	N	M	17%	**	0	#	0
GL50803_15380	CDC8 Thymidylate kinase	*	*	*	N	O	35%	O	0	#	0
GL50803_16354	Protein 21.1	25	1	Y	N	O	4%		0	#	0
GL50803_17288	Protein 21.1	54	2	Y	N	O	4%		0		0
GL50803_23492	Protein 21.1	130	1	Y	N	O	30%		1		0
GL50803_86855	Protein 21.1	22	1	Y	N	O	9%		0	#	0
GL50803_88245	Protein 21.1	23	1	Y	N	O	17%		0	#	0
GL50803_21662	Coiled-coil protein	31	1	N	N	M		**	0	#	0
GL50803_16152	Coiled-coil protein	57	2	Y	N	O			0	#	0
GL50803_8564	Coiled-coil protein	74	3	Y	N	O			0		0
GL50803_9515	Coiled-coil protein	61	2	Y	N	O			0	#	0
GL50803_40244	P24, putative	53	1	Y	N	O	13%		1		1
GL50803_6430	14-3-3 protein	78	2	Y	N	O	13%		1		0
GL50803_8903	Copine I	190	4	Y	N	O	44%	O	0	#	0
GL50803_14225	CXC-rich protein	494	8	Y	Y	S			0		1
GL50803_17476	CXC-rich protein	255	7	Y	Y	S	4%		0		1
GL50803_113656	Cysteine protease	73	2	Y	Y	S			1		1
GL50803_103454	High cysteine membrane protein Group 1	1038	14	Y	Y	S			1		1
GL50803_17328	High cysteine membrane protein Group 2	113	3	Y	Y	S			0		1
GL50803_91099	High cysteine membrane protein Group 2	65	1	Y	Y	S	13%		0	#	1
GL50803_114042	High cysteine membrane protein Group 4	330	5	Y	Y	S			1		1
GL50803_11359	Ribosomal protein S4	31	1	Y	N	O	17%		1		0
GL50803_17411	TCP-1 chaperonin subunit gamma	24	1	Y	N	O			1		0

Mascot score, Mascot total ion score for the identified protein. Coverage, number of unique peptides per identified protein. MiD, mitosomal distribution. Proteins are marked "Y" if their distributions in fractions #3 and #4 of the Optiprep gradient (measured by the iTRAQ ratio) were within the range between Cpn10 and IscU and the window that extended in both directions by half of the distance between these markers. Proteins with ratios outside of this range are indicated with "N". TargetP and PsortII were used to predict the subcellular location of *Giardia* proteins. S, secretory; N, non-secretory; M, mitochondrial; O, other. Exp. ver., experimental verification of protein localization using the pONDRA expression vector. The recombinant tagged proteins were localized by fluorescence microscopy. M, mitosome; ER, endoplasmic reticulum; O, other; ? inconclusive. MEMSAT3 and TMHMM were used to predict transmembrane domains. SGP, predicted soluble proteins are marked with number sign (#). Asterisk (*) is used where no data were available. (**) transformed *Giardia* did not express the recombinant tagged protein.

doi:10.1371/journal.pone.0017285.t005

organisms with mitosomes, such as *Cryptosporidium parvum* and *Cryptosporidium hominis*. Based on genomic analyses, 37–54 proteins have been predicted to reside in these mitosomes [19], of which 18 were detected by mass spectrometry in whole *C. parvum* sporozoites [25].

An intriguing question concerns the nature of the mitochondrial progenitor from which mitosomes of *G. intestinalis* have evolved. *Giardia* is a member of the Excavate group, which has recently been re-considered to belong to the basal groups of eukaryotes based on its mechanism of cytochrome c and c1 biogenesis

Table 6. Putative mitosomal proteins classified by predicted function: miscellaneous - continued; hypothetical proteins.

Accession number	Annotation	Identification		Localization					Structure		
		MASCOT	Coverage	MiD	SignalP	Target P	Psort II	Exp Ver.	MEMSAT3	SGP	TMHMM
		score	peptides				% mito		TM No.		TM No.
GL50803_10330	Tenascin precursor	330	4	Y	Y	S	11%		0	#	0
GL50803_16477	Tenascin-37	178	4	Y	Y	S	17%		1		0
GL50803_16833	Tenascin-like	96	2	Y	Y	S			0	#	0
GL50803_13561	Translation elongation factor	36	1	Y	N	O	13%		1		0
GL50803_15889	UDP-N-acetylglucosamine-dolichyl-phosphateN-acetylglucosamine-phosphotransferase	36	1	Y	Y	S	4%		10		7
GL50803_11521	VSP	198	3	Y	Y	S			1		1
GL50803_137618	VSP	530	9	Y	N	O	4%		2		1
GL50803_11470	VSP with INR	220	3	Y	N	O			2		1
GL50803_6733	Zinc finger domain	55	1	Y	N	S	22%		4		4
Hypothetical proteins											
GL50803_12999	Hypothetical protein	414	5	Y	Y	M		?	2		2
GL50803_14939	Hypothetical protein	133	2	Y	Y	M	30%	M	1		2
GL50803_15985	Hypothetical protein (VAP, VAMP associated protein)	35	1	Y	N	M	13%	M	1		1
GL50803_16596	Hypothetical protein	177	3	N	N	M	30%	O	0	#	0
GL50803_4768	Hypothetical protein	21	1	Y	N	M	57%	O	0	#	0
GL50803_9296	Hypothetical protein	178	4	Y	Y	M	57%	M	0	#	0
GL50803_11237	Hypothetical protein	24	1	Y	N	O	9%		1		0
GL50803_11557	Hypothetical protein	41	1	Y	N	O	17%		1		0
GL50803_11866	Hypothetical protein	25	1	Y	N	O	22%		0	#	0
GL50803_13288	Hypothetical protein	35	1	Y	N	O	9%		1		0
GL50803_13413	Hypothetical protein	95	2	Y	N	O	11%		2		2
GL50803_137685	Hypothetical protein	200	4	Y	N	S			13		9
GL50803_137746	Hypothetical protein	25	1	Y	N	O			0	#	0
GL50803_13922	Hypothetical protein	1121	14	Y	Y	S			1		1
GL50803_14164	Hypothetical protein	23	1	Y	N	O	13%		0	#	0
GL50803_14278	Hypothetical protein	31	1	Y	N	O	13%		0	#	0
GL50803_14660	Hypothetical protein	105	2	Y	N	O	35%		1		0

Mascot score, Mascot total ion score for the identified protein. Coverage, number of unique peptides per identified protein. MiD, mitosomal distribution. Proteins are marked "Y" if their distributions in fractions #3 and #4 of the Optiprep gradient (measured by the iTRAQ ratio) were within the range between Cpn10 and IscU and the window that extended in both directions by half of the distance between these markers. Proteins with ratios outside of this range are indicated with "N". TargetP and PsortII were used to predict the subcellular location of *Giardia* proteins. S, secretory; N, non-secretory; M, mitochondrial; O, other. Exp. ver., experimental verification of protein localization using the pONDRA expression vector. The recombinant tagged proteins were localized by fluorescence microscopy. M, mitosome; ER, endoplasmic reticulum; O, other; ? inconclusive. MEMSAT3 and TMHMM were used to predict transmembrane domains. SGP, predicted soluble proteins are marked with number sign (#). Asterisk (*) is used where no data were available. (**) transformed *Giardia* did not express the recombinant tagged protein.
doi:10.1371/journal.pone.0017285.t006

[25,57]. These and other data have placed the root of eukaryotes between Excavata and Euglenozoa, a group of protists that includes trypanosomatids [58]. In this respect, there is an apparent simplicity in the protein import machinery of the *Giardia* mitosomes that deserves attention (Fig. 5). The proteomics analysis detected in mitosomes a protein recently shown to be Tom40, the protein translocation channel across the outer membrane [25,59]. The current model for the evolution of the TOM complex posits that Tom40 was derived from a beta-barrel protein in the endosymbiont's outer membrane, perhaps of an usher or autotransporter type protein translocase [60]. Because two other proteins: Tom7 and Tom22, have been found in representative species of all other eukaryotic groups [58], the model further suggests that the first TOM complex was composed of Tom40, Tom22 and Tom7. Our proteomics finds no evidence of Tom7 or Tom22 in mitosomes, and sensitive hidden Markov model searches likewise fail to find any proteins encoded in the *Giardia* genome with similarity to Tom7 or Tom22 [25,57]. Whether reflecting a secondary gene loss or the ancestral condition, GiTom40 would appear to be a selectively simple protein translocase. In addition to Tom40, mitochondria contain one other member of the mitochondrial porin family, the voltage-

Table 7. Putative mitosomal proteins classified by predicted function: hypothetical proteins – continued.

Accession number	Annotation	Identification		Localization				Structure		
		MASCOT	Coverage	MiD	SignalP	Target P	Psort II	MEMSAT3	SGP	TMHMM
		score	peptides				% mito	TM No.		TM No.
GL50803_14845	Hypothetical protein	69	2	Y	N	O	4%	0	#	0
GL50803_15084	Hypothetical protein	22	1	Y	N	O		0	#	0
GL50803_16424	Hypothetical protein	117	3	Y	N	O	26.1%	0	#	0
GL50803_16430	Hypothetical protein	32	1	Y	N	O	9%	1		0
GL50803_16998	Hypothetical protein	24	1	Y	N	O	17%	0	#	0
GL50803_17236	Hypothetical protein	69	1	Y	N	M		10		10
GL50803_1937	Hypothetical protein	75	2	Y	N	S		2		2
GL50803_23389	Hypothetical protein	33	1	Y	N	O		4		6
GL50803_28962	Hypothetical protein	39	1	Y	Y	S	4%	1		1
GL50803_29327	Hypothetical protein	111	2	Y	N	O	17%	1		0
GL50803_3021	Hypothetical protein	21	1	Y	N	O	13%	0	#	0
GL50803_32999	Hypothetical protein	98	3	Y	N	O	13%	0	#	0
GL50803_3491	Hypothetical protein	25	1	Y	N	O	30%	1		0
GL50803_6617	Hypothetical protein	350	5	Y	Y	S		1		1
GL50803_7188	Hypothetical protein	926	11	Y	Y	S	13%	3		1
GL50803_7242	Hypothetical protein	69	1	Y	N	O	22%	3		3
GL50803_7244	Hypothetical protein	144	3	Y	N	O	11%	4		3
GL50803_94658	Hypothetical protein	27	1	Y	N	O	13%	0	#	0
GL50803_9503	Hypothetical protein	206	3	Y	N	O	9%	0	#	0
GL50803_9780	Hypothetical protein	333	5	Y	Y	S	11%	0	#	0
GL50803_9861	Hypothetical protein	137	2	Y	N	O	4%	0	#	0
GL50803_10016	Hypothetical protein	265	5	Y	Y	S	22%	1		0
GL50803_111809	Hypothetical protein	34	1	Y	N	O		0	#	0

Mascot score, Mascot total ion score for the identified protein. Coverage, number of unique peptides per identified protein. MiD, mitosomal distribution. Proteins are marked "Y" if their distributions in fractions #3 and #4 of the Optiprep gradient (measured by the iTRAQ ratio) were within the range between Cpn10 and IscU and the window that extended in both directions by half of the distance between these markers. Proteins with ratios outside of this range are indicated with "N". TargetP and PsortII were used to predict the subcellular location of *Giardia* proteins. S, secretory; N, non-secretory; M, mitochondrial; O, other. Exp. ver., experimental verification of protein localization using the pONDRA expression vector. The recombinant tagged proteins were localized by fluorescence microscopy. M, mitosome; ER, endoplasmic reticulum; O, other; ? inconclusive. MEMSAT3 and TMHMM were used to predict transmembrane domains. SGP, predicted soluble proteins are marked with number sign (#). Asterisk (*) is used where no data were available. (**) transformed *Giardia* did not express the recombinant tagged protein.
doi:10.1371/journal.pone.0017285.t007

dependent anion channels (VDAC), which serve to exchange metabolites [61]. The absence of VDAC in *Giardia* mitosomes might reflect the disappearance of many of the metabolic pathways, and the concomitant decrease in metabolite flux across the outer membrane. It is likely that the *Giardia* Tom40, in addition to importing proteins, exchanges ions and small metabolites across the outer mitosomal membrane as has been demonstrated for the yeast Tom40 in mutants lacking VDAC [44,62–64].

Another surprising result, one that can only be explained by a secondary gene loss, is the absence of the outer membrane protein Sam50 in *Giardia*. Sam50 is a component of the SAM (sorting and assembly machinery) complex, which is required for the assembly of both Tom40 and VDAC [48,65]. The apparent absence of Sam50 from the *Giardia* genome and from our proteomics data is unique among eukaryotes. A putative Sam50 homologue has been predicted in the genomes of all eukaryotes, including trypanosomatids [58,65] and mitosome- and hydrogenosome-containing protists (*C. parvum*, *E. cuniculi*, *E. histolytica* and *T. vaginalis*) [66]. Numerous phylogenetic and functional analyses indicate that Sam50 was derived from the Omp85/BamA protein present in the outer membrane of the ancestral, alpha-proteobacterial endosymbiont and it must, therefore, have been present in the earliest mitochondria [44]. It is not clear how *Giardia* Tom40 is assembled within the outer membrane without the assistance of the SAM complex. It is known that even in yeast Tom40 mediates the import of new molecules of Tom40 into mitochondria [67] and it is tempting to speculate that the *Giardia* Tom40 is capable of mediating its own import and membrane insertion, given the highly simplified nature of the TOM complex in mitosomes.

Our proteomics data support the hypothesis that ISC assembly is an important and possibly the only biosynthetic function of *Giardia* mitosomes. Previous phylogenic analyses have indicated that the ISC assembly machinery was obtained from the alpha-proteobacterial endosymbiont; nearly complete ISC assembly machinery is present from trypanosomatids to higher eukaryotes. Therefore, the absence of certain components, such as IscA-1, Iba57, and Ind, in the mitosomal machines (Table 8) is apparently due to a secondary loss of specific target proteins. Noteworthy, we did not identify any proteins that would carry FeS clusters in *Giardia* mitosomes, except for components of the FeS cluster assembly machinery itself. It seems likely then that the main role of

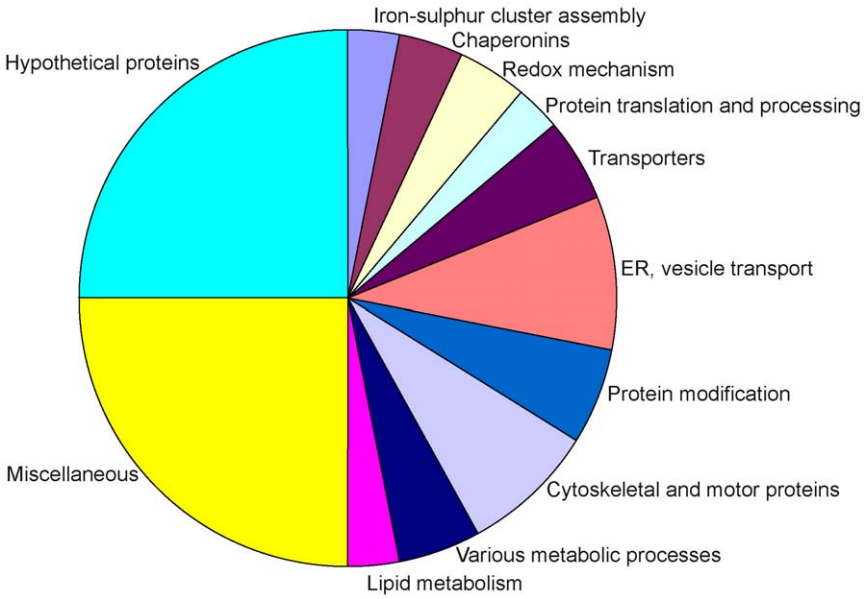

Figure 3. Classification of the identified proteins according to function. Functions were assigned based upon *Giardia*DB annotations, PSI-BLAST analysis and searches of the Pfam database (Tables 1, 2, 3, 4, 5, 6 and 7, Tables S2–S3).
doi:10.1371/journal.pone.0017285.g003

mitosomes could be to export preassembled FeS clusters, or other compounds that are essential for the biogenesis of FeS proteins, to other cellular compartments. In mitochondria, the export of these enigmatic compounds is dependent on the membrane ABC "half-transporter" Atm1 [68] and sulfhydryl oxidase Erv1 [69]. In the mitosome-enriched fraction, we identified four ABC half-transporters by mass spectrometry, and another candidate was predicted based on phyletic profiling of the *G. intestinalis* genome (Table 2). However, compared to other Atm1 homologues, these candidates lack the x-loop with the conserved arginine, which is essential for known Atm1 transporters (Fig. S9). No protein with homology to Erv1 was found by proteomics or by analysis of the *Giardia* genome.

Another remaining question pertains to the source of ATP that is required for the multiple processes identified in mitosomes including FeS cluster assembly and export, organelle division, protein import and protein folding. In *E. histolytica*, it has been shown that a mitochondrial carrier family (MCF) protein localizes to mitosomes and exchanges ATP and ADP across the inner membrane, effecting the import ATP into mitosomes [20]. *E. cuniculi* mitosomes contain a distinct bacterial nucleotide transporter that may fulfill the same function [23,24]. However, our proteomic analysis did not revealed a candidate nucleotide transporter in the mitosomes of *Giardia* leaving open the question of ATP acquisition.

In conclusion, using iTRAQ-based mass spectrometry and bioinformatics we identified 139 candidate mitosomal proteins. Mitosomal localization was confirmed experimentally for 20 of 44 proteins tested, suggesting the complete mitosomal proteome of *Giardia* to be of the order of 50-100 proteins. Previous genome analyses failed to predict any of the novel mitosomal proteins identified here [70]; only by combining quantitative mass spectrometry and bioinformatics were these novel proteins identified. The small proteome of the *G. intestinalis* mitosome indicates a marked reduction in mitochondrial metabolic activity and reduced requirements for organelle biogenesis. These do not mirror the reductions seen in the mitosomal proteome of *Cryptosporidium*, supporting the view that lineage-specific reductions produce organelles with distinct metabolic pathways and specific "short-cut" pathways for biogenesis. Our findings provide new insight into aspects of mitochondrial evolution and the basis from which to begin reconstructing the details of precisely how these organelles are built and replicated to support *Giardia* growth and division.

Methods

Cell culture and fractionation

G. intestinalis strain WB (American Type Culture Collection) was grown in TYI-S-33 medium supplemented with 10% heat-inactivated bovine serum and 0.1% bovine bile [9]. Trophozoites were freeze-detached, washed in PBS and collected by centrifugation. Cells were then resuspended in hypotonic buffer (12 mM MOPS, pH 7.4) and incubated for 15 minutes. The cells were then pelleted at 680× g for 15 minutes, resuspended in the same buffer with DNase I (40 µg/mL) and homogenized by 10 passages through a 25G needle. After homogenization, the isotonicity was immediately restored with the addition of an equal volume of 500 mM sucrose in MOPS buffer. The homogenate was then treated with trypsin (200 µg/mL) for 10 minutes at 37°C to release the organelles from the cytoskeleton. Proteases inhibitors were then added (5 mg/mL of soybean trypsin inhibitor, leupeptin and TLCK), and the homogenate was diluted and centrifuged for 20 minutes at 2760× g to remove cellular debris. The collected supernatant was centrifuged using a Beckman rotor Ti 50 at 20,000 rpm for 30 minutes. After centrifugation, the pellet was collected and washed in SM buffer (250 mM sucrose and 12 mM MOPS, pH 7.4). Next, the pellet was resuspended in 0.5 mL of SM buffer and layered onto a discontinuous density OptiPrep (Axis-Shield PoC AS, Oslo, Norway) gradient, which consisted of 1 ml each of 15%, 20%, 25%, 30% and 50% OptiPrep diluted in 12 mM MOPS buffer. The gradient was centrifuged for 24 h in a Beckman SW 40 rotor at 120,000× g at 4°C. Fractions (1 mL each) were collected, washed and analyzed by immunoblot using a polyclonal rabbit anti-IscU antibody [71,72].

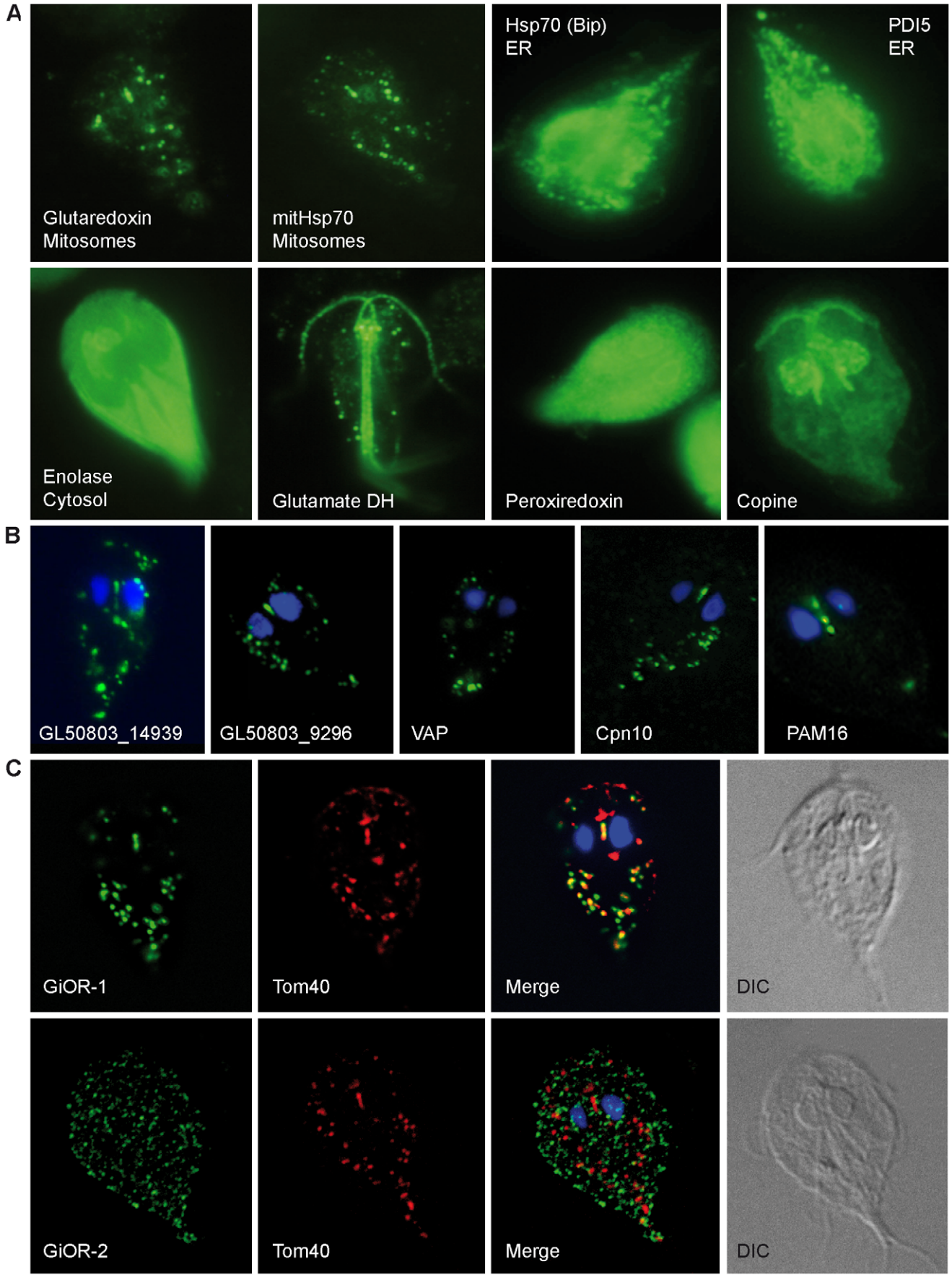
A
Glutaredoxin
Mitosomes
mitHsp70
Mitosomes
Hsp70 (Bip)
ER
PDI5
ER
Enolase
Cytosol
Glutamate DH
Peroxiredoxin
Copine
B
GL50803_14939
GL50803_9296
VAP
Cpn10
PAM16
C
GiOR-1
Tom40
Merge
DIC
GiOR-2
Tom40
Merge
DIC

Figure 4. Sub-cellular localization of selected proteins in *Giardia*. Transformed *G. intestinalis* cells with episomally-expressed HA-tagged proteins. (A) Marker proteins were stained using a mouse anti-HA antibody (green). Grx5, glutaredoxin 5; ER, endoplasmic reticulum; glutamate DH, glutamate dehydrogenase. (B) Predicted mitosomal proteins (GL50803_14939, GL50803_9296, VAP, Cpn10, Pam16) were stained using a mouse anti-HA antibody (green). (C) Cellular localization of tagged diflavin proteins GiOR-1 and GiOR-2 stained with mouse anti HA antibody (green). Tom40 was detected by polyclonal rabbit anti-Tom40 antibody (red).
doi:10.1371/journal.pone.0017285.g004

Mass spectrometry analysis

Samples of two selected fractions (100 µg of total protein each) were precipitated with acetone at −20°C for 2 hours and then pelleted at 13,000× g for 15 min. The proteins were trypsin digested and labeled with sample-specific iTRAQ reagents according to the manufacturer's protocol (Applied Biosystems). Labeled samples were mixed and precipitated with acetone. The pellet was dissolved in 2 M urea in HPLC grade water, and the solution was subjected to IEF using 7 cm immobilized pH 3–10 gradient strips (Bio-Rad) for 20,000 VHrs. The strips were cut into 2-mm wide slices, and peptides were extracted using 50% ACN with 1% TFA. Extracted peptides were then separated using an Ultimate 3000 HPLC system (Dionex) coupled to a Probot micro-fraction collector (Dionex). The samples were loaded onto a PepMap 100 C18 RP column (3 µm particle size, 15 cm long, 75 µm internal diameter; Dionex) and separated with a gradient of 5% (v/v) ACN and 0.1% (v/v) TFA to 80% (v/v) ACN and 0.1% (v/v) TFA over 60 min at a flow rate of 300 nl/min. The eluate was mixed 1:3 with matrix solution (20 mg/mL α-cyano-4-hydroxycinnamic acid in 80% ACN) prior to spotting onto a MALDI target. Spectra were acquired using a 4800 Plus MALDI TOF/TOF analyzer (Applied Biosystems/MDS Sciex) equipped with a Nd:YAG laser (355 nm, 200 Hz firing rate). All spots were measured in MS mode; up to 10 of the strongest precursors were selected for MS/MS analysis, which was performed using collision energy of 1 kV and operating pressure of the collision cell of 10^{-6} Torr. Peak lists from the MS/MS spectra were generated using GPS Explorer v. 3.6 (Applied Biosystems/MDS Sciex) subtraction of baseline enabled with peak width 50, smoothing with Savitsky-Golay algorithm of polynomial order of four and three points across peak, minimum signal to noise (S/N) 3, local noise window 250 m/z, cluster area S/N optimization enabled with S/N threshold 5. Spectra were searched with locally installed Mascot v. 2.1 (Matrix Science) against the *Giardia*DB release 1.3 annotated protein database (4892 sequences, 2663813 residues) and *GiardiaDB* release 1.2 Open Reading Frame translations greater than 50 amino acids (85612 sequences, 9633221 residues). The database search criteria were as follows: trypsin; one missed cleavage site allowed; fixed modifications iTRAQ 4-plex on *N*-terminal- and lysine ε-amino group, methylthiolation of cysteine; variable modification methionine oxidation; peptide mass tolerance of 100 ppm; MS/MS tolerance of 0.2 Da; maximum peptide rank of 1, minimum ion score C.I. (peptide) of 95%.

Table 8. Comparison of iron-sulfur cluster assembly machineries in organisms with mitosomes (*Giardia intestinalis*, *Cryptosporidium parvum*, and *Encephalitozoon cuniculi*), hydrogenosomes (*Trichomonas vaginalis*), and mitochondria (*Trypanosoma brucei*, *Saccharomyces cerevisiae*).

Name	*G. intestinalis*	*C. parvum*	*E. cuniculi*	*T. vaginalis*	*T. brucei*	*S. cerevisiae*
IscS (Nfs)	•	•	•	••	•	•
Isd11	○	○	•	••	•••	•
Nfu	•	○	○	•••	•••	•
IscU (Isu)	•	•	•	•	•	••
IscA1(Isa1)	○	○	○	○	•	•
IscA2 (Isa2)	•	○	○	••••	•	•
Iba57	○	○	○	○	•	•
Ind	○	○	○	•••	•	•
Grx5	•	○	•	○	•	•
Ferredoxin (Yah1)	•	•	•	•••••••	••	•
FOR (Arh1)	○	•	•	○	•	•
Frataxin (Yfh1)	○	•	•	••	•	•
HSP70	•	•	•	•••	••	•♦♦
Dna-J (Jac1)	•	•	•	••	•	•
GrpE	•	•	•	••	•	•
Atm1	○	•	•	○	•	•
Erv1	○	○	•	○	•	•

Filled circles indicate the presence of protein exhibiting homology to the known component of mitochondrial iron-sulfur cluster assembly machinery identified by BLAST searches. Empty circles indicates absence of homologous protein. Mitochondria of *S. cerevisiae* possess three distinct Hsp70 of which Ssq1 is devoted for FeS cluster assembly (filled circle), while Ssc1, and Ecm10 have other fuctions (diamonds). Other eukaryotes possess multifunctional Hsp70. IscS, cysteine desulfurase; Isd11, IscS binding protein; Nfu, IscU, IscA, a scafold proteins; Iba57, IscA binding protein required for [4Fe4S] cluster assembly; Ind, P-loop NTPaseb required for assembly of respiratory complex I; Grx5, glutaredoxin 5; ferredoxin, [2Fe2S] ferredoxin that transport electrons; FOR, ferredoxin oxidoreductase; frataxin, iron binding protein; Hsp70, chaperone; DnaJ, GrpE, co-chaperones; Atm1, ABC half trasnporter; Erv1, sulfhydryl oxidase. Names of proteins used for *S. cerevisiae* orthologs are in brackets.
doi:10.1371/journal.pone.0017285.t008

Table 9. Activity of mitosomal diflavin oxidoreductase GiOR-1.

Substrate	Specific activity [$\mu g.min^{-1}.mg^{-1}$]	Standard deviation
NADPH	0	
NADPH+DCIP	9,053	0,111
NADH + DCIP	0,269	0,034
NADPH + MV	0,450	0,205
NADPH + O_2	0,144	0,042
NADPH+ferredoxin	0	

Electron donors: NADPH, NADH.
Electron acceptors: DCIP, dichlorophenol-indolephenol; MV, methyl viologen; O_2, aerobic conditions; ferredoxin, recombinant *G. intestinalis* [2Fe2S]ferredoxin.
doi:10.1371/journal.pone.0017285.t009

Bioinformatics

Bioinformatics searches based on simple pair-wise alignment Psi-BLAST and hidden Markov models (HMMs) were applied to verify the automatic protein annotations and estimate their functions. Protein sequences (<1000 residues) were submitted (*i*) against a 90% redundancy reduced NCBI nr database for 8 iterations at an e-value cutoff of 10^{-3} and (*ii*) against Pfam 23.0 A+B database of families represented by multiple sequence alignments and hidden Markov models at an e-value of 0.044 (http://pfam.sanger.ac.uk/search). Where noted in the text, tailored HMM libraries were used to search for components of the protein import machinery [16].

Programs based on a combination of artificial neural networks (TargetP) and hidden Markov models (SignalP, both http://www.cbs.dtu.dk/services/) together with PsortII (http://psort.ims.u-tokyo.ac.jp/) were used to predict the subcellular localizations of the proteins. The secondary structures and topologies of alpha-helical integral membrane proteins were predicted using two bioinformatics tools: TMHMM, a program based on hidden Markov models (http://www.cbs.dtu.dk/services/), and Memsat3 (http://bioinf.cs.ucl.ac.uk/memsat/).

Transformation of *G. intestinalis* and immunofluorescence

Selected genes were amplified by PCR from genomic *Giardia* DNA and inserted into the pONDRA plasmid [73]. Table S6 contains a list of primers that were used for subcloning of genes into expression vector. Cells were transformed and selected as described previously [16]. *G. intestinalis* cells expressing the recombinant proteins fused to a hemagglutinin tag (HA) at the C-terminus were fixed and stained for immunofluorescence microscopy with a mouse monoclonal anti-HA antibody. A secondary AlexaFluor-488 (green) donkey anti-mouse antibody was used.

Preparation of recombinant proteins and enzyme assay

The coding region of GiOR-1 and [2Fe2S]ferredoxin was subcloned into pET42b and pET3a (Invitrogen), respectively and

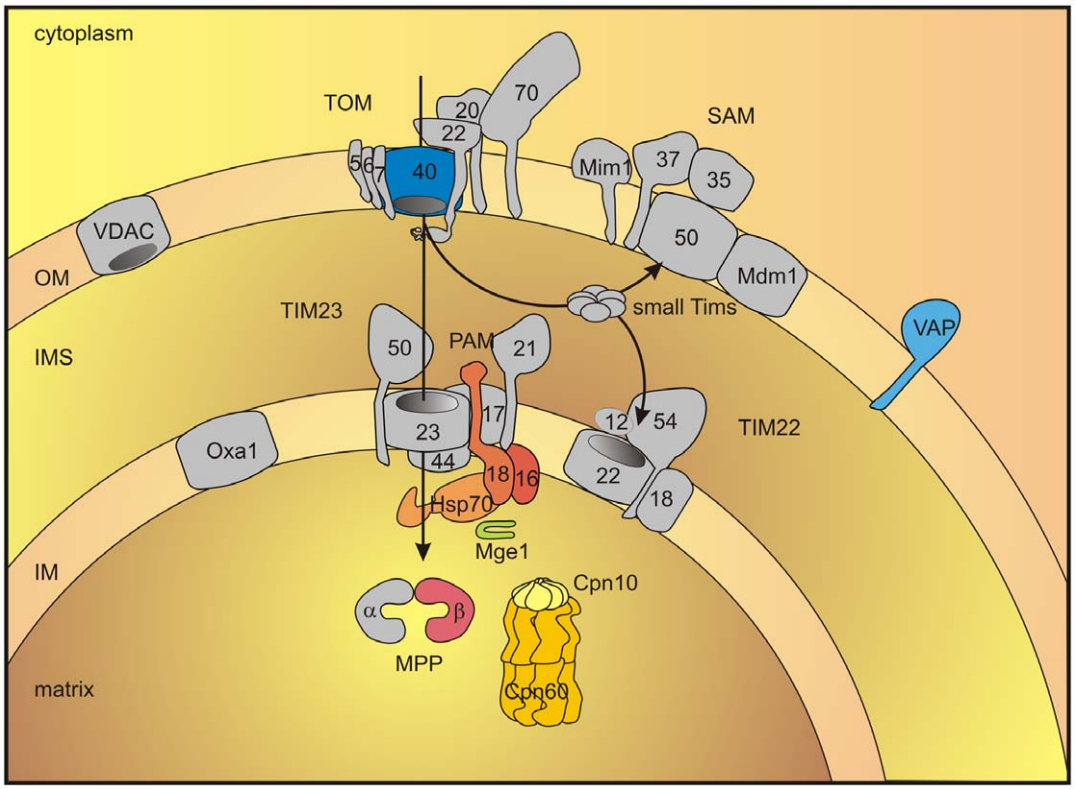

Figure 5. Schematic representation of protein import pathway in the mitosome of *G. intestinalis*. Components identified in mitosome are highlighted by color. Components that are known to participate in the protein import into mitochondria of animals and fungi are shown in grey colour. OM, outer membrane; IMS, intermembrane space; IM, inner membrane; TOM, translocase of outer membrane; SAM, sorting and assembly machinery; TIM, translocase of inner membrane; PAM, presequence translocase-associated motor; VAP, VAMP (vesicle-associated membrane protein)-associated protein; VDAC, voltage-dependent anion channel; MPP, mitochondrial processing peptidase.
doi:10.1371/journal.pone.0017285.g005

expressed in *Escherichia coli* BL21. The bacteria were induced with 0,5 mM IPTG (isopropyl-β-D-thiogalactopyranoside) and grown at 37°C in LB medium. For expression of GiOR-1, the LB medium was supplemented with 250 μM flavin adenine dinucleotide (FAD) and 250 μM flavin mononucleotide (FMN), whereas the LB medium supplemented with 400 μM ferric ammonium citrate was used for expression of ferredoxin. After induction, the cells were incubated overnight at 4°C. The harvested cells were homogenized, and soluble fraction was obtained by centrifugation at 250,000× g, 1 h, 4°C. The his-tagged GiOR-1was affinity purified under native conditions using a Ni-NTA column (Qiagen) according to manufacture's protocol. Ferredoxin was isolated by gel filtration chromatography using a BioLogic HR system (BioRad).

Enzyme activity of GiOR-1 was assayed spectrophotometrically at 25°C in anaerobic cuvettes under nitrogen atmosphere. The activity was monitored as a rate of NADPH or NADH (0,25 mM) oxidation in the presence of dichlorophenol-indolephenol (0,1 mM) or ferredoxin at 340 nm, or as a rate of methyl viologen (2 mM) reduction at 600 nm. NADPH oxidase activity was measured under aerobic conditions at 340 nm. The enzymatic activity was determined in phosphate buffer (100 mM KH_2PO_4/KOH, 150 mM NaCl, pH 7,4). Protein concentration was determined according to Lowry method.

Supporting Information

Figure S1 Sequence alignment of Giardia Nfu against ekaryotic and prokaryotic orthologues. Conserved thioredoxin-like CXXC motif is shown in green. Giardia, *Giardia intestinalis* EAA38809; Trichomonas, *Trichomonas vaginalis*, TVAG_146780; Trypanosoma, *Trypanosoma brucei*, XP_845796; Leishmania, *Leishmania infantum*, XP_001470367; Toxoplasma, *Toxoplasma gondii*, XP_002371042; Plasmodium, *Plasmodium falciparum*, CAX64255; Saccharomyces, *Saccharomyces cerevisiae*, NP_012884; Homo, *Homo sapiens*, AAI13695; Rickettsia, *Rickettsia prowazekii*, NP_221029; Stigmatella, *Stigmatella aurantiaca*, ZP_01463912.
(PDF)

Figure S2 Sequence alignment of *Giardia* IscA against eukaryotic and bacterial orthologs. The conserved cysteine residues are highlited in yellow. Organism names and accession numbers: Giardia, *Giardia intestinalis* GL50803_14821; Trichomonas, *Trichomonas vaginalis* TVAG_055320; Trypanosoma, *Trypanosoma cruzi* XP_806610; Saccharomyces, *Saccharomyces cerevisiae* Q12425; Homo, *Homo sapiens* NP_919255; Arabidopsis, *Arabidopsis thaliana* NP_179262; Chlamydomonas, *Chlamydomonas reinhardtii* XP_001697636; Rickettsia, *Rickettsia conorii* NP_360365; Escherichia, Escherichia coli CAQ32901; Mycobacterium, *Mycobacterium leprae* NP_301657.
(PDF)

Figure S3 Sequence alignment of *Giardia* Jac1 against eukaryotic and bacterial orthologs. The conserved HSP70 interactin site is highlited in green. Organism names and accession numbers: Giardia, *Giardia intestinalis*, GL50803_17030; Trichomonas, *Trichomonas vaginalis*, TVAG_422630; Trypanosoma, *Trypanosoma brucei*, XP_843770; Leishmania, *Leishmania infantum*, XP_001466207; Plasmodium, *Plasmodium falciparum*, CAX64223; Toxoplasma, *Toxoplasma gondii*, XP_002368309; Naegleria, *Naegleria gruberi*, EFC47366; Saccharomyces, *Saccharomyces cerevisiae*, NP_011497; Homo, *Homo sapiens*, AAN85282; Escherichia, *Escherichia* coli, YP_002408666.
(PDF)

Figure S4 Sequence alignment of *Giardia* Mge1 against eukaryotic (Mge1) and bacterial (GrpE) orthologs. The residues in yellow indicate a GrpE dimer interface. HSP70 binding sites are shown in green (Harrison CJ, Hayer-Hartl M, Di Liberto M, Hartl F, Kuriyan J, Crystal structure of the nucleotide exchange factor GrpE bound to the ATPase domain of the molecular chaperone DnaK, Science 1999, 276:431–435. *Giardia intestinalis*, GL50803_1376; *Homo sapiens*, NP_079472; *Saccharomyces cerevisae*, NP_014875; *Escherichia coli*, NP_417104; *Arabidopsis thaliana*, NP_567757; *Trichomonas vaginalis*, XP_001329309; *Trypanosoma brucei*, XP_845338; *Dictyostelium discoideum*, XP_638912; *Bacillus subtilis*, NP_390426; *Halobacterium sp.*, NP_279548.
(PDF)

Figure S5 Sequence alignment of *G. intestinalis* mitosomal oxidoreductase OR-1 (GL50803_91252), against *G. intestinalis* non-mitosomal paralogue OR-2 (GL50803_15897) and structurally related proteins containing flavodoxin-like FMN-binding domain (conserved residua in blue), FAD binding pocket (residua involved in FAD binding in green) and NADP(H) binding site (residua involved in NADP(H) in red). *Saccharomyces cerevisiae* Tah18, DAA11472; *Homo sapiens* NDOR, NADPH dependent diflavin oxidoreductase, AAH15735; *Rattus norvegicus* NOS, nitric oxide synthase, AAC13747; *Rattus norvegicus* CPR, cytochrome P450 reductase, NP_113764; *Escherichia coli* SiR, sulfite reductase, YP_002330508; *Homo sapiens* MSR, methionine synthase reductase, NP_076915; *Trichomonas vaginalis* Hyd, hydrogenase, TVAG_136330; *Leptospira interrogans* FNR, ferredoxin reductase, YP_003372.
(PDF)

Figure S6 Conserved glycine which is present in all GroES and Cpn10 homologues is shown in green. Hsp60 binding site is shown in yellow (van der Giezen M, León-Avila G, Tovar J. (2005) Characterization of chaperonin 10 (Cpn10) from the intestinal human pathogen *Entamoeba histolytica*. Microbiology 151:3107-15). *Giardia intestinalis* GL50803_29500; *Trichomonas vaginalis* TVAG_191660; *Saccharomyces cerevisiae* NP_014663.1; *Homo sapiens* XP_001118014.1; *Leishmania infantum* XP_001470405.1; *Plasmodium falciparum* PFL0740c; Arabidopsis thaliana NP_563961.1; *Dictyostelium discoideum* XP_636819.1; *Mycobacterium tuberculosis* NP_217935.1; *Escherichia coli* NP_290775.1.
(PDF)

Figure S7 Sequence alignment of *Giardia* Pam16 against eukaryotic Pam 16 orthologues and giardial Pam 18 paralogue. Conserved leucin in an interacting hydrofobic pocket is shown in green (D'Silva PR, Schilke B, Hayashi M, Craig EA (2008) Interaction of the J-protein heterodimer Pam18/Pam16 of the mitochondrial import motor with the translocon of the inner membrane. Mol Biol Cell 19:424-32). The typical HPD motif (in blue) present in Pam18 is degenerated in Pam16, in yellow (Mokranjac D, Bourenkov G, Hell K, Neupert W, Groll M (2006) Structure and function of Tim14 and Tim16, the J and J-like components of the mitochondrial protein import motor. EMBO J 25:4675-85). *Giardia intestinalis* Pam 16 GL50803_19230; *Trichomonas vaginalis* TVAG_470110; *Toxoplasma gondii* XP_002367323.1; *Saccharomyces cerevisiae* NP_012431.1; *Neurospora crassa* XP_960477.1; *Pediculus humanus* XP_002428010.1; *Schistosoma japonicum* CAX74438.1; *Homo sapiens* NP_057153.8; *Mus musculus* NP_079847.1; *Xenopus laevis* NP_001084733.1; *Giardia intestinalis* Pam 18 XP_002364144.
(PDF)

Figure S8 Protein sequence alignment of VAP (VAMP-associated protein) homologues. Domain structure is depicted for each represented sequence according to HHPRED (http://toolkit.tuebingen.mpg.de/). Major sperm protein domain, yellow. Coiled-coil domain in green and dimerization motif GXXXG in red. The *G. intestinalis* VAP contains all protein characteristics as described for human homologue.
(PDF)

Figure S9 Sequence alignment of *Giardia* AbcB transporter against mitochondrial and bacterial orthologs. *Giardia intestinalis* AbcB, GL50803_17315; *Saccharomyces cerevisiae* Atm1, NP_014030; *Saccharomyces cerevisae* Mdl1, NP_013289; *Homo sapiens* AbcB7, NP_004290; *Homo sapiens* AbcB10, NP_036221; *Arabidopsis thaliana* Atm3, NP_200635; *Naegleria gruberi* Atm1,XP_002683195; *Rhodobacter sphaeroides* AbcB, YP_001168064; *Halobacterium sp*. AbcB, NP_279266. Walker A part of a conserved ATP-binding motif in yellow; Q-loop part of a conserved ATP-binding motif in green; ABC signature, a conserved sequence specific for ABC proteins in pink; Walker B part of a conserved ATP-binding motif in blue; D-loop part of a conserved ATP-binding motif in red; H-loop part of a conserved ATP-binding motif in purple; X-loop contains a conserved arginine in AbcB transporters (•), which is not present in Giardia sequence, in cyan (Dawson RJ, Locher KP (2006) Structure of a bacterial multidrug ABC transporter. Nature 443:180-185; Bernard DG, Cheng Y, Zhao Y, Balk J (2009) An allelic mutant series of ATM3 reveals its key role in the biogenesis of cytosolic iron-sulfur proteins in Arabidopsis. Plant Physiol 151: 590-602).
(PDF)

Table S1 Complete list of proteins identified by LC MS/MS in mitosomal fractions labelled by iTRAQ reagents.
(PDF)

Table S2 List of *Giardia* proteins within the mitosomal distribution range (MiD) identified by LC MS/MS.
(PDF)

Table S3 Identification of protein families using PfamA+B databases.
(PDF)

Table S4 Predictions of cellular localization.
(PDF)

Table S5 Orthology phylogenetic profililng. Genomes of *G. intestinalis* and *Rickettsia typhi* were compared using orthology phylogenetic profile tool at GiardiaDB.
(PDF)

Table S6 List of primers that were used for subcloning of genes into expression vector pONDRA to investigate subcellular localization of corresponding gene products in *G. intestinalis*.
(PDF)

Author Contributions

Conceived and designed the experiments: JT PLJ PD IH PR. Performed the experiments: PLJ PD PR JP OŠ MŠ MM LV NCB. Analyzed the data: PLJ PD PR JP AJP JT TL. Wrote the paper: JT PLJ.

References

1. Andersson SG, Zomorodipour A, Andersson JO, Sicheritz-Ponten T, Alsmark UC, et al. (1998) The genome sequence of *Rickettsia prowazekii* and the origin of mitochondria. Nature 396: 133–140.
2. Lang BF, Burger G, O'Kelly CJ, Cedergren R, Golding GB, et al. (1997) An ancestral mitochondrial DNA resembling a eubacterial genome in miniature. Nature 387: 493–497.
3. Vaidya AB, Mather MW (2009) Mitochondrial evolution and functions in malaria parasites. Annu Rev Microbiol 63: 249–267. 10.1146/annurev.micro.091208.073424 [doi].
4. Gabaldon T, Huynen MA (2004) Shaping the mitochondrial proteome. Biochim Biophys Acta 1659: 212–220.
5. Gabaldon T, Huynen MA (2007) From endosymbiont to host-controlled organelle: the hijacking of mitochondrial protein synthesis and metabolism. PLoS Comput Biol 3: e219.
6. Pagliarini DJ, Calvo SE, Chang B, Sheth SA, Vafai SB, et al. (2008) A mitochondrial protein compendium elucidates complex I disease biology. Cell 134: 112–123.
7. Tachezy J, Smid O (2008) Mitosomes in parasitic protists. In: Tachezy J, ed. Hydrogenosomes and Mitosomes: Mitochondria of Anaerobic Eukaryotes. Berlin, Heidelberg: Springer-Verlag. pp 201–230.
8. Cavalier-Smith T (1987) The origin of eukaryotic and archaebacterial cells. Ann N Y Acad Sci 503: 17–54:17–54.
9. Tovar J, Leon-Avila G, Sanchez LB, Sutak R, Tachezy J, et al. (2003) Mitochondrial remnant organelles of *Giardia* function in iron-sulphur protein maturation. Nature 426: 172–176.
10. Tovar J, Fischer A, Clark CG (1999) The mitosome, a novel organelle related to mitochondria in the amitochondrial parasite *Entamoeba histolytica*. Mol Microbiol 32: 1013–1021.
11. Katinka MD, Duprat S, Cornillot E, Metenier G, Thomarat F, et al. (2001) Genome sequence and gene compaction of the eukaryote parasite *Encephalitozoon cuniculi*. Nature 414: 450–453.
12. Williams BAP, Hirt RP, Lucocq JM, Embley TM (2002) A mitochondrial remnant in the microsporidian *Trachipleistophora hominis*. Nature 418: 865–869.
13. Riordan CE, Langreth SG, Sanchez LB, Kayser O, Keithly JS (1999) Preliminary evidence for a mitochondrion in *Cryptosporidium parvum*: Phylogenetic and therapeutic implications. Journal of Eukaryotic Microbiology 46: 52S–55S.
14. Hrdy I, Tachezy J, Müller M (2008) Metabolism of trichomonad hydrogenosomes. In: Tachezy J, ed. Hydrogenosomes and Mitosomes:Mitochondria of Anaerobic Euakryotes. Berlin, Heidelberg: Springer-Verlag. pp 114–145.
15. Abrahamsen MS, Templeton TJ, Enomoto S, Abrahante JE, Zhu G, et al. (2004) Complete genome sequence of the apicomplexan, *Cryptosporidium parvum*. Science 304: 441–445. 10.1126/science.1094786 [doi];1094786 [pii].
16. Dolezal P, Smid O, Rada P, Zubacova Z, Bursac D, et al. (2005) *Giardia* mitosomes and trichomonad hydrogenosomes share a common mode of protein targeting. Proc Natl Acad Sci U S A 102: 10924–10929.
17. Goldberg AV, Molik S, Tsaousis AD, Neumann K, Kuhnke G, et al. (2008) Localization and functionality of microsporidian iron-sulphur cluster assembly proteins. Nature 452: 624–628.
18. Putignani L, Tait A, Smith HV, Horner D, Tovar J, et al. (2004) Characterization of a mitochondrion-like organelle in *Cryptosporidium parvum*. Parasitology 129: 1–18.
19. Sanderson SJ, Xia D, Prieto H, Yates J, Heiges M, et al. (2008) Determining the protein repertoire of *Cryptosporidium parvum* sporozoites. Proteomics 8: 1398–1414.
20. Tsaousis AD, Kunji ER, Goldberg AV, Lucocq JM, Hirt RP, et al. (2008) A novel route for ATP acquisition by the remnant mitochondria of *Encephalitozoon cuniculi*. Nature 453: 553–556. nature06903 [pii];10.1038/nature06903 [doi].
21. Xu P, Widmer G, Wang Y, Ozaki LS, Alves JM, et al. (2004) The genome of *Cryptosporidium hominis*. Nature 431: 1107–1112.
22. Mi-ichi F, Abu YM, Nakada-Tsukui K, Nozaki T (2009) Mitosomes in *Entamoeba histolytica* contain a sulfate activation pathway. Proc Natl Acad Sci U S A 106: 21731–21736. 0907106106 [pii];10.1073/pnas.0907106106 [doi].
23. Franzen O, Jerlstrom-Hultqvist J, Castro E, Sherwood E, Ankarklev J, et al. (2009) Draft genome sequencing of *Giardia intestinalis* assemblage B isolate GS: is human giardiasis caused by two different species? PLoS Pathog 5: e1000560. 10.1371/journal.ppat.1000560 [doi].
24. Morrison HG, McArthur AG, Gillin FD, Aley SB, Adam RD, et al. (2007) Genomic minimalism in the early diverging intestinal parasite *Giardia lamblia*. Science 317: 1921–1926.
25. Cavalier-Smith T (2010) Kingdoms Protozoa and Chromista and the eozoan root of the eukaryotic tree. Biol Lett 6: 342–345.
26. Billington D, Maltby PJ, Jackson AP, Graham JM (1998) Dissection of hepatic receptor-mediated endocytic pathways using self-generated gradients of iodixanol (Optiprep). Anal Biochem 258: 251–258. S0003-2697(98)92561-1 [pii];10.1006/abio.1998.2561 [doi].
27. Dunkley TP, Watson R, Griffin JL, Dupree P, Lilley KS (2004) Localization of organelle proteins by isotope tagging (LOPIT). Mol Cell Proteomics 3: 1128–1134. 10.1074/mcp.T400009-MCP200 [doi];T400009-MCP200 [pii].

28. Smid O, Matuskova A, Harris SR, Kucera T, Novotny M, et al. (2008) Reductive evolution of the mitochondrial processing peptidases of the unicellular parasites *Trichomonas vaginalis* and *Giardia intestinalis*. PLoS Pathog 4: e1000243.
29. Rada P, Smid O, Sutak R, Dolezal P, Pyrih J, et al. (2009) The monothiol single-domain glutaredoxin is conserved in the highly reduced mitochondria of *Giardia intestinalis*. Eukaryot Cell 8: 1584–1591. EC.00181-09 [pii];10.1128/EC.00181-09 [doi].
30. Tachezy J, Sanchez LB, Müller M (2001) Mitochondrial type iron-sulfur cluster assembly in the amitochondriate eukaryotes *Trichomonas vaginalis* and *Giardia intestinalis*, as indicated by the phylogeny of IscS. Molecular Biology and Evolution 18: 1919–1928.
31. Vinella D, Brochier-Armanet C, Loiseau L, Talla E, Barras F (2009) Iron-sulfur (Fe/S) protein biogenesis: phylogenomic and genetic studies of A-type carriers. PLoS Genet 5: e1000497. 10.1371/journal.pgen.1000497 [doi].
32. Krebs C, Agar JN, Smith AD, Frazzon J, Dean DR, et al. (2001) IscA, an alternate scaffold for Fe-S cluster biosynthesis. Biochemistry 40: 14069–14080. bi015656z [pii].
33. Pelzer W, Muhlenhoff U, Diekert K, Siegmund K, Kispal G, et al. (2000) Mitochondrial Isa2p plays a crucial role in the maturation of cellular iron-sulfur proteins. FEBS Lett 476: 134–139. S0014-5793(00)01711-7 [pii].
34. Song D, Tu Z, Lee FS (2009) Human ISCA1 interacts with IOP1/NARFL and functions in both cytosolic and mitochondrial iron-sulfur protein biogenesis. J Biol Chem 284: 35297–35307. M109.040014 [pii];10.1074/jbc.M109.040014 [doi].
35. Ding H, Clark RJ, Ding B (2004) IscA mediates iron delivery for assembly of iron-sulfur clusters in IscU under the limited accessible free iron conditions. J Biol Chem 279: 37499–37504. 10.1074/jbc.M404533200 [doi];M404533200 [pii].
36. Bych K, Kerscher S, Netz DJ, Pierik AJ, Zwicker K, et al. (2008) The iron-sulphur protein Ind1 is required for effective complex I assembly. EMBO J 27: 1736–1746. emboj200898 [pii];10.1038/emboj.2008.98 [doi].
37. Sheftel AD, Stehling O, Pierik AJ, Netz DJ, Kerscher S, et al. (2009) Human ind1, an iron-sulfur cluster assembly factor for respiratory complex I. Mol Cell Biol 29: 6059–6073. MCB.00817-09 [pii];10.1128/MCB.00817-09 [doi].
38. Hrdy I, Hirt RP, Dolezal P, Bardonova L, Foster PG, et al. (2004) *Trichomonas* hydrogenosomes contain the NADH dehydrogenase module of mitochondrial complex I. Nature 432: 618–622.
39. Gelling C, Dawes IW, Richhardt N, Lill R, Mühlenhoff U (2008) Mitochondrial Iba57p is required for Fe/S cluster formation on aconitase and activation of radical SAM enzymes. Mol Cell Biol 28: 1851–1861. MCB.01963-07 [pii];10.1128/MCB.01963-07 [doi].
40. Mühlenhoff U, Richhardt N, Gerber J, Lill R (2002) Characterization of iron-sulfur protein assembly in isolated mitochondria. A requirement for ATP, NADH, and reduced iron. J Biol Chem 277: 29810–29816. 10.1074/jbc.M204675200 [doi];M204675200 [pii].
41. Vernis L, Facca C, Delagoutte E, Soler N, Chanet R, et al. (2009) A newly identified essential complex, Dre2-Tah18, controls mitochondria integrity and cell death after oxidative stress in yeast. PLoS One 4: e4376. 10.1371/journal.pone.0004376 [doi].
42. Zhang Y, Lyver ER, Nakamaru-Ogiso E, Yoon H, Amutha B, et al. (2008) Dre2, a conserved eukaryotic Fe/S cluster protein, functions in cytosolic Fe/S protein biogenesis. Mol Cell Biol 28: 5569–5582. MCB.00642-08 [pii];10.1128/MCB.00642-08 [doi].
43. Walsh P, Bursac D, Law YC, Cyr D, Lithgow T (2004) The J-protein family: modulating protein assembly, disassembly and translocation. EMBO Rep 5: 567–571.
44. Chacinska A, Koehler CM, Milenkovic D, Lithgow T, Pfanner N (2009) Importing mitochondrial proteins: machineries and mechanisms. Cell 138: 628–644. S0092-8674(09)00967-2 [pii];10.1016/j.cell.2009.08.005 [doi].
45. Horwich AL, Fenton WA, Chapman E, Farr GW (2007) Two families of chaperonin: physiology and mechanism. Annu Rev Cell Dev Biol 23: 115–145. 10.1146/annurev.cellbio.23.090506.123555 [doi].
46. Elsner S, Simian D, Iosefson O, Marom M, Azem A (2009) The Mitochondrial Protein Translocation Motor: Structural Conservation between the Human and Yeast Tim14/Pam18-Tim16/Pam16 co-Chaperones. Int J Mol Sci 10: 2041–2053. 10.3390/ijms10052041 [doi].
47. Mokranjac D, Bourenkov G, Hell K, Neupert W, Groll M (2006) Structure and function of Tim14 and Tim16, the J and J-like components of the mitochondrial protein import motor. EMBO J 25: 4675–4685. 7601334 [pii];10.1038/sj.emboj.7601334 [doi].
48. Schneider A, Bursac D, Lithgow T (2008) The direct route: a simplified pathway for protein import into the mitochondrion of trypanosomes. Trends Cell Biol 18: 12–18. S0962-8924(07)00297-8 [pii];10.1016/j.tcb.2007.09.009 [doi].
49. Osborne AR, Rapoport TA, van den Berg B (2005) Protein translocation by the Sec61/SecY channel. Annu Rev Cell Dev Biol 21: 529–550. 10.1146/annurev.cellbio.21.012704.133214 [doi].
50. Clements A, Bursac D, Gatsos X, Perry AJ, Civciristov S, et al. (2009) The reducible complexity of a mitochondrial molecular machine. Proc Natl Acad Sci U S A 106: 15791–15795. 0908264106 [pii];10.1073/pnas.0908264106 [doi].
51. Simpson AG, Inagaki Y, Roger AJ (2006) Comprehensive multigene phylogenies of excavate protists reveal the evolutionary positions of "primitive" eukaryotes. Mol Biol Evol 23: 615–625. msj068 [pii];10.1093/molbev/msj068 [doi].
52. van der Laan M, Meinecke M, Dudek J, Hutu DP, Lind M, et al. (2007) Motor-free mitochondrial presequence translocase drives membrane integration of preproteins. Nat Cell Biol 9: 1152–1159. ncb1635 [pii];10.1038/ncb1635 [doi].
53. Lev S, Ben HD, Peretti D, Dahan N (2008) The VAP protein family: from cellular functions to motor neuron disease. Trends Cell Biol 18: 282–290. S0962-8924(08)00120-7 [pii];10.1016/j.tcb.2008.03.006 [doi].
54. Hanada K, Kumagai K, Yasuda S, Miura Y, Kawano M, et al. (2003) Molecular machinery for non-vesicular trafficking of ceramide. Nature 426: 803–809. 10.1038/nature02188 [doi];nature02188 [pii].
55. Reinders J, Zahedi RP, Pfanner N, Meisinger C, Sickmann A (2006) The complete yeast mitochondrial proteome: Multidimensional separation techniques for mitochondrial proteomics. Journal of Proteome Research 5: 1543–1554.
56. Waller RF, Jabbour C, Chan NC, Celik N, Likic VA, et al. (2009) Evidence of a reduced and modified mitochondrial protein import apparatus in microsporidian mitosomes. Eukaryot Cell 8: 19–26. EC.00313-08 [pii];10.1128/EC.00313-08 [doi].
57. Pusnik M, Charriere F, Maser P, Waller RF, Dagley MJ, et al. (2009) The single mitochondrial porin of *Trypanosoma brucei* is the main metabolite transporter in the outer mitochondrial membrane. Mol Biol Evol 26: 671–680. msn288 [pii];10.1093/molbev/msn288 [doi].
58. Dolezal P, Dagley MJ, Kono M, Wolynec P, Likic VA, et al. (2010) The essentials of protein import in the degenerate mitochondrion of *Entamoeba histolytica*. PLoS Pathog 6: e1000812. 10.1371/journal.ppat.1000812 [doi].
59. Alcock F, Clements A, Webb C, Lithgow T (2010) Evolution. Tinkering inside the organelle. Science 327: 649–650. 327/5966/649 [pii];10.1126/science.1182129 [doi].
60. Macasev D, Whelan J, Newbigin E, Silva-Filho MC, Mulhern TD, et al. (2004) Tom22′, an 8-kDa trans-site receptor in plants and protozoans, is a conserved feature of the TOM complex that appeared early in the evolution of eukaryotes. Mol Biol Evol 21: 1557–1564. 10.1093/molbev/msh166 [doi];msh166 [pii].
61. Kmita H, Budzinska M (2000) Involvement of the TOM complex in external NADH transport into yeast mitochondria depleted of mitochondrial porin1. Biochim Biophys Acta 1509: 86–94. S0005273600002844 [pii].
62. Gentle I, Gabriel K, Beech P, Waller R, Lithgow T (2004) The Omp85 family of proteins is essential for outer membrane biogenesis in mitochondria and bacteria. J Cell Biol 164: 19–24. 10.1083/jcb.200310092 [doi];jcb.200310092 [pii].
63. Kozjak V, Wiedemann N, Milenkovic D, Lohaus C, Meyer HE, et al. (2003) An essential role of Sam50 in the protein sorting and assembly machinery of the mitochondrial outer membrane. J Biol Chem 278: 48520–48523. 10.1074/jbc.C300442200 [doi];C300442200 [pii].
64. Paschen SA, Waizenegger T, Stan T, Preuss M, Cyrklaff M, et al. (2003) Evolutionary conservation of biogenesis of beta-barrel membrane proteins. Nature 426: 862–866. 10.1038/nature02208 [doi];nature02208 [pii].
65. Dolezal P, Likic V, Tachezy J, Lithgow T (2006) Evolution of the molecular machines for protein import into mitochondria. Science 313: 314–318.
66. Gatsos X, Perry AJ, Anwari K, Dolezal P, Wolynec PP, et al. (2008) Protein secretion and outer membrane assembly in Alphaproteobacteria. FEMS Microbiol Rev 32: 995–1009. FMR130 [pii];10.1111/j.1574-6976.2008.00130.x [doi].
67. Kispal G, Csere P, Guiard B, Lill R (1997) The ABC transporter Atm1p is required for mitochondrial iron homeostasis. Febs Letters 418: 346–350.
68. Lange H, Lisowsky T, Gerber J, Mühlenhoff U, Kispal G, et al. (2001) An essential function of the mitochondrial sulfhydryl oxidase Erv1p/ALR in the maturation of cytosolic Fe/S proteins. Embo Reports 2: 715–720.
69. Chan KW, Slotboom DJ, Cox S, Embley TM, Fabre O, et al. (2005) A novel ADP/ATP transporter in the mitosome of the microaerophilic human parasite *Entamoeba histolytica*. Current Biology 15: 737–742.
70. Keister DB (1983) Axenic Culture of Giardia-Lamblia in Tyi-S-33 Medium Supplemented with Bile. Transactions of the Royal Society of Tropical Medicine and Hygiene 77: 487–488.
71. Dagley MJ, Dolezal P, Likic VA, Smid O, Purcell AW, et al. (2009) The protein import channel in the outer mitosomal membrane of *Giardia intestinalis*. Mol Biol Evol 26: 1941–1947. msp117 [pii];10.1093/molbev/msp117 [doi].
72. Likic VA, Dolezal P, Celik N, Dagley M, Lithgow T (2010) Using hidden markov models to discover new protein transport machines. Methods Mol Biol 619: 271–284. 10.1007/978-1-60327-412-8_16 [doi].
73. Sun CH, Chou CF, Tai JH (1998) Stable DNA transfection of the primitive protozoan pathogen *Giardia lamblia*. Mol Biochem Parasitol 92: 123–132.

8.5 Alternative 2-keto acid oxidoreductases in *Trichomonas vaginalis*: artifact of histochemical staining.

Molecular & Biochemical Parasitology 181 (2012) 57–59

Contents lists available at SciVerse ScienceDirect

Molecular & Biochemical Parasitology

Short communication

Alternative 2-keto acid oxidoreductases in *Trichomonas vaginalis*: Artifact of histochemical staining

Věra Zedníková, Neritza Campo Beltrán, Jan Tachezy, Ivan Hrdý*

Department of Parasitology, Charles University in Prague, Viničná 7, 128 44 Prague 2, Czech Republic

ARTICLE INFO

Article history:
Received 20 July 2011
Received in revised form
13 September 2011
Accepted 16 September 2011
Available online 22 September 2011

Keywords:
Trichomonas
Keto acid oxidoreductase
Hydrogenosome
Pyruvate:ferredoxin oxidoreductase
Metronidazole
Nitroblue tetrazolium

ABSTRACT

Trichomonas vaginalis has been reported to possess alternative 2-keto acid oxidoreductases (KORs). These enzymes preferentially used indolepyruvate in a reaction that resembled that of pyruvate:ferredoxin oxidoreductase (PFO). However, the KORs did not reduce ferredoxin and remained active in metronidazole-resistant trichomonads lacking PFO. Therefore, it was proposed that the KORs may help trichomonads to survive in the presence of metronidazole. The KORs were identified using activity staining on native gels (Brown DM, Upcroft JA, Dodd HN, et al. Alternative 2-keto acid oxidoreductase activities in *T. vaginalis*. Mol Biochem Parasitol 1999;98:203–14). In the current study, we showed that the apparent KOR activity was caused by the non-enzymatic reduction of the indicator dye, nitroblue tetrazolium, by indolepyruvate, which is facilitated by Triton X-100 used to prepare the membrane fractions. We could not confirm the presence of KORs in metronidazole-resistant *T. vaginalis*. The low level indolepyruvate-dependent activity that is present in *T. vaginalis* strains sensitive to metronidazole is catalyzed by PFO, which was verified using the pure enzyme. Therefore, our results suggest that alternative 2-keto acid oxidoreductases do not exist in *T. vaginalis*.

Trichomonas vaginalis is a flagellated protist belonging to the supergroup Excavata. It causes the most common non-viral genitourinary infection of humans and has a worldwide annual incidence of up to 170 million cases [1]. *Trichomonas* is an unusual eukaryote that is a fermentative anaerobe with hydrogenosomes instead of typical mitochondria. Hydrogenosomes are mitochondrion-related organelles that lack a genome and form hydrogen by reacting protons with electrons that are derived from metabolized substrates, such as pyruvate and malate. The production of hydrogen is catalyzed by a hallmark hydrogenosomal enzyme, the hydrogenase. The electron donor in this reaction is the reduced form of the electron carrier [2Fe2S] ferredoxin, which is reduced by another typical hydrogenosomal enzyme, pyruvate:ferredoxin oxidoreductase (PFO) [2]. A two-subunit remnant of respiratory complex 1 also donates electrons to ferredoxin by oxidizing NADH [3]. PFO is a Fe–S protein that mediates the oxidative decarboxylation of pyruvate and forms acetyl coenzyme A in a CoA-dependent reaction [4]. Acetyl-CoA serves as a substrate for ATP synthesis via succinyl coenzyme A in reactions that are catalyzed by acetate/succinate CoA transferase and succinate thiokinase [2].

In 1999, new enzymes involved in *T. vaginalis* carbohydrate metabolism were added to the existing list. These enzymes were called alternative 2-keto acid oxidoreductases (KOR1 and KOR2) and were identified using biochemical methods, which showed that KOR1 and KOR2 resided in the membrane (predominantly the hydrogenosomal membrane) fractions [5]. Similar to PFO, these enzymes were reported to utilize 2-keto acids including deaminated forms of aromatic amino acids (indolepyruvate, phenylpyruvate) in a CoA-dependent reaction. However, unlike PFO, KOR1 and KOR2 were found to be equally active in trichomonads that are highly resistant to metronidazole, which is a widely used drug that targets anaerobic pathogenic microorganisms [5]. Laboratory-derived *T. vaginalis* strains with extreme metronidazole resistance (growing in >100 $\mu g\,ml^{-1}$ metronidazole) lack PFO and other hydrogenosomal proteins (hydrogenase, malic enzyme, ferredoxin) and exhibit altered carbohydrate metabolism [6]. By oxidatively decarboxylating pyruvate, PFO generates low-redox-potential electrons that are transferred to the nitro group of metronidazole via ferredoxin, reducing this nitro group to form cytotoxic products, including the reactive nitro-anion radical intermediate. Elimination of the PFO- and ferredoxin-dependent pathway of the reductive activation of metronidazole is a characteristic feature for laboratory-derived *Trichomonas* strains that are resistant to metronidazole. However, the elimination of PFO prevents acetyl coenzyme A formation and consequently ATP synthesis in the hydrogenosomes [7]. The reported presence of alternative 2-keto oxidoreductases in trichomonads was proposed to account for the energy balance while avoiding metronidazole reduction by replacing ferredoxin with an unidentified electron acceptor, to

* Corresponding author. Tel.: +420 221951811; fax: +420 224919704.
E-mail address: hrdy@cesnet.cz (I. Hrdý).

0166-6851/$ – see front matter © 2011 Elsevier B.V. All rights reserved.
doi:10.1016/j.molbiopara.2011.09.005

broaden the spectrum of known catabolic substrates, circumvent the loss of PFO and help resistant trichomonads survive in the presence of the drug [5]. The identification of alternative 2-keto oxidoreductases in trichomonads was based on in-gel activity assays using indolepyruvate as a substrate and nitroblue tetrazolium (NBT) as a reducible acceptor. Tetrazolium dyes are commonly used in assays of the metabolic activity of tissues, cells or isolated proteins that reduce an electron-transporting cofactor (usually NAD^+ or $NADP^+$). This cofactor then reduces the soluble, colorless or weakly colored tetrazolium salt, yielding an intensely dark-colored insoluble formazan [8]. When used with non-denaturing polyacrylamide gels containing separated proteins, this so-called histochemical staining can be used to detect and distinguish a wide variety of redox enzymes that use the same oxidizable substrate but differ in their electrophoretic mobilities. The enzymatic activity is visualized as a colored band that forms in the gel upon its incubation in a suitable buffer containing a substrate, all necessary cofactors and tetrazolium dye.

As presented in the original report, bands corresponding to the suspected indolepyruvate-dependent activity were observed in non-denaturing gels used to separate *T. vaginalis* membrane fractions that had been treated with Triton X-100 (KOR1) followed by 1 M sodium acetate (KOR2). The bands were interpreted as indicating the presence of 2-keto acid oxidoreductases, so far in *T. vaginalis* unknown enzymes. These enzymes were similar to PFO based on their requirement for coenzyme A but differed from PFO based on the electrophoretic mobility, detergent solubility (KOR1), requirement of an electron acceptor other than ferredoxin and maintenance of the enzymatic activity in metronidazole-resistant trichomonads.

A draft of the *T. vaginalis* genome sequence was published in 2007 [9]. While providing an invaluable inventory of the coding potential of *T. vaginalis* (the genome size is estimated to be approximately 160 mega bases), the annotation, among other features, revealed that many *Trichomonas* proteins are coded by multi-gene families. This finding is also valid for the proteins that constitute the core hydrogenosomal catabolic pathway, including PFO, ferredoxin, hydrogenase, malic enzyme and others that are coded by 7–9 distinct genes [9]. With the genome sequence available, we decided to re-address the question of the existence of alternative 2-keto oxidoreductases, because the corresponding proteins/genes have not been identified. We speculated that some of the more divergent PFO-like genes may code for the proteins with the observed activity. We reproduced the described procedure for the preparation of membrane fractions of *T. vaginalis* (strain T1, provided by J.H. Tai, Institute of Biomedical Sciences, Taipei, Taiwan) [5] using the whole-cell lysate or Percoll-purified hydrogenosomes as the starting material [10] because KOR1 activity was proposed to predominantly reside in the hydrogenosomes [5]. The only difference from the described protocol was the use of 0.5% octylglucoside instead of 0.5% dodecylglucoside to wash the membranes obtained from the starting material in the assay buffer (50 mM Hepes, pH 7.5, 200 μM thiamine pyrophosphate, 2.5 mM $MgCl_2$ and 5 mM β-mercaptoethanol) [5]. The supernatant from the octylglucoside wash was discarded, and the resulting pellet (corresponding to 10–20 ml of culture with approximately 3×10^6 cells ml^{-1} or hydrogenosomes that were purified from 2 l of *T. vaginalis* culture) was extracted for 30 min on ice with approximately 400 μl of the assay buffer containing 1% Triton X-100 and then centrifuged at 100 000 × g for 40 min. A total of 10–30 μl of the resulting supernatant was loaded onto a non-denaturing polyacrylamide gel (Laemmli system without SDS, using 5% stacking gel and 9% separating gel, acrylamide:bisacrylamide ratio of 37.5:1). The gel was run with cooling for approximately 4 h, washed and incubated in assay buffer without β-mercaptoethanol as previously described [5]. The staining solution (10 ml) contained 200 μM CoA, 5 mM indolepyruvate and 1 mg ml^{-1} NBT. Within minutes, dark-blue bands with a trailing smear appeared in the gel (Fig. 1, lanes 1, 2). (For interpretation of the references to color in this text, the reader is referred to the web version of the article.) However, the negative control, which lacked the necessary cofactor coenzyme A, produced the same result (Fig. 1, lane 3). Realizing that the color development may not have been the result of enzymatic activity, we performed another control in which the gel was heated at 70 °C for 30 min after the completion of electrophoresis. The staining pattern was identical to that using the non-denatured sample (Fig. 1, lane 4). The enzyme inactivation by this treatment was verified by the complete inactivation of the hydrogenosomal malic enzyme, which is the most abundant hydrogenosomal membrane-associated protein and is easily detected by in-gel activity staining [11,12] (not shown). Additional controls using indifferent protein sample rich in membranes (human red blood cells mixed with Laemmli sample buffer with 1% Triton X-100 and without SDS and reducing agent) or the sample buffer containing only 1% Triton X-100 without any protein produced colored bands in the gel after staining with indolepyruvate (Fig. 1, lanes 5 and 6, respectively). The staining pattern was also dependent on the amount of loaded protein. Less protein yielded sharper bands and reduced the trailing smear (not shown). Controls omitting indolepyruvate in the incubation assay mixture or Triton X-100 in the sample did not display detectable staining (Fig. 1, lanes 7 and 8, respectively). We then set up the reaction in a test tube, mixing NBT (1 mg ml^{-1}) with indolepyruvate (5 mM) in PBS (phosphate-buffered saline, pH 7.4). Upon addition of few microliters of 10% Triton X-100, the mixture rapidly turned violet-brown, demonstrating that the non-enzymatic reduction of NBT yielding formazan is greatly stimulated by Triton X-100. Subsequently, we reviewed the available literature resources and found that the non-enzymatic reduction of tetrazolium salts with indoleacetaldehyde, a compound that contains an indole bicyclic aromatic ring identical to that in indolepyruvate, has been observed in studies using the monoamine oxidase histochemical detection system with tryptamine as a substrate. However, the exact chemistry of this NBT reduction has not been studied [13]. In addition, the enhancing effect of Triton X-100 on tetrazolium salt reduction has been described as well [14,15]. It was proposed that univalently reduced, uncharged tetrazolium radicals rapidly partition into Triton X-100 micelles which greatly increases their local concentration and stimulates the formation of pigmented formazan [14]. Therefore, we inferred that the stained bands in the native gels are caused by the non-enzymatic reduction of NBT by indolepyruvate, which was stimulated by Triton X-100 that was possibly bound to hydrophobic proteins. Triton X-100 alone, which is a nonionic detergent, did not migrate into the gel and promoted formazan formation at the bottom of the sample-loading well (Fig. 1, lane 6).

The previous study claimed that KORs using indolepyruvate as a substrate remained equally active in the highly metronidazole-resistant *T. vaginalis* strain and that the enzymes used methyl viologen, benzyl viologen and NBT as acceptors with equal efficiency [5]. We used the Triton X-100-treated lysate of the *T. vaginalis* strain TV 10-02 MR 100, which lacks PFO [6] and has a similar level of metronidazole resistance as the strain used in the original study, to verify the reported KOR activity with indolepyruvate. We employed the standard, anaerobic spectrophotometric assay with methyl viologen as an acceptor [16]. We were unable to detect any indolepyruvate-dependent activity (not shown). Using the same assay and the lysate from metronidazole-sensitive strain T1, we observed an indolepyruvate- and CoA-dependent reduction of methyl viologen, which amounted to approximately 5% of the activity of PFO with pyruvate (not shown). To verify that this indolepyruvate-dependent activity was catalyzed by the known hydrogenosomal PFO, we used the highly purified enzyme

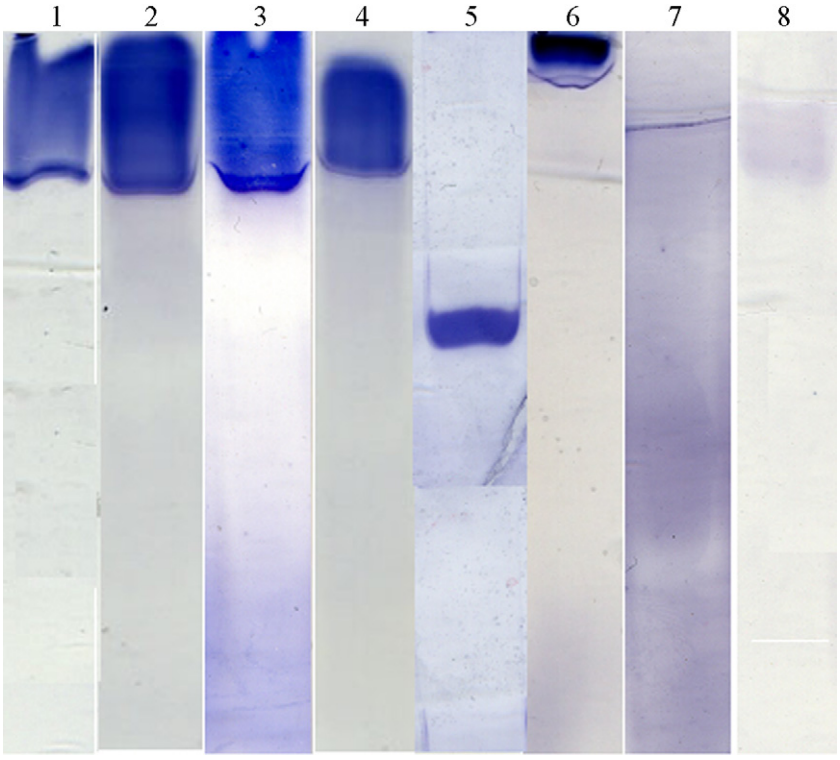

Fig. 1. Non-denaturing polyacrylamide gel electrophoresis of *T. vaginalis* membrane fractions. The gel was developed using the assay buffer (see text for composition) containing 5 mM indolepyruvate, 200 μM CoA and 1 mg ml^{-1} NBT unless specified otherwise. Approximately 15–50 μg of protein was loaded per lane. Lane 1, whole *T. vaginalis* cells that were lysed with 1% Triton X-100. Lane 2, Percoll-purified hydrogenosomes with 1% Triton X-100. Lane 3, Percoll-purified hydrogenosomes with 1% Triton X-100. The incubation mixture did not contain CoA. Lane 4, Percoll-purified hydrogenosomes with 1% Triton X-100. The gel slice was heated at 70 °C for 30 min after electrophoresis and before staining. Lane 5, human red blood cells with 1% Triton X-100. The incubation mixture did not contain CoA. Lane 6, Laemmli sample-loading buffer with 1% Triton X-100 and without protein. Lane 7, Percoll-purified hydrogenosomes with 1% Triton X-100. The incubation mixture did not contain indolepyruvate. Lane 8, Percoll-purified hydrogenosomes without Triton X-100.

[17] in the subsequent assay. Indeed, the purified PFO displayed indolepyruvate-dependent activity, which was 4.5% of the PFO activity with pyruvate (not shown).

In summary, we must conclude that the previously described activities of alternative 2-keto acid oxidoreductases that use indolepyruvate as a preferred substrate were artifacts that were caused by the non-enzymatic conversion of NBT into formazan by indolepyruvate in the presence of Triton X-100 due to the chemistry that has been already described. Likely, no such enzymes exist in *T. vaginalis*, because we were unable to detect this activity in metronidazole-resistant cells lacking PFO using a standard assay with methyl viologen as an acceptor. The low level indolepyruvate-dependent activity that was found in metronidazole-sensitive trichomonads was catalyzed by hydrogenosomal PFO, which has been previously characterized.

Acknowledgements

This work was supported by the grants LC07032 and MSM0021620858 from the Czech Ministry of Education, Youth and Sports.

References

[1] Petrin D, Delgaty K, Bhatt R, et al. Clinical and microbiological aspects of *Trichomonas vaginalis*. Clin Microbiol Rev 1998;11:300–17.
[2] Müller M. The hydrogenosome. J Gen Microbiol 1993;139:2879–89.
[3] Hrdy I, Hirt RP, Dolezal P, et al. Trichomonas hydrogenosomes contain the NADH dehydrogenase module of mitochondrial complex I. Nature 2004;432:618–22.
[4] Williams K, Lowe PN, Leadlay PF. Purification and characterization of pyruvate: ferredoxin oxidoreductase from the anaerobic protozoon *Trichomonas vaginalis*. Biochem J 1987;246:529–36.
[5] Brown DM, Upcroft JA, Dodd HN, et al. Alternative 2-keto acid oxidoreductase activities in *Trichomonas vaginalis*. Mol Biochem Parasitol 1999;98:203–14.
[6] Rasoloson D, Vanacova S, Tomkova E, et al. Mechanisms of in vitro development of resistance to metronidazole in *Trichomonas vaginalis*. Microbiology-SGM 2002;148:2467–77.
[7] Kulda J, Trichomonads. hydrogenosomes and drug resistance. Int J Parasitol 1999;29:199–212.
[8] Berridge MV, Herst PM, Tan AS. Tetrazolium dyes as tools in cell biology: new insights into their cellular reduction. Biotechnol Annu Rev 2005;11:127–52.
[9] Carlton JM, Hirt RP, Silva JC, et al. Draft genome sequence of the sexually transmitted pathogen *Trichomonas vaginalis*. Science 2007;315:207–12.
[10] Sutak R, Dolezal P, Fiumera HL, et al. Mitochondrial-type assembly of FeS centers in the hydrogenosomes of the amitochondriate eukaryote *Trichomonas vaginalis*. Proc Natl Acad Sci U S A 2004;101:10368–73.
[11] Drmota T, Proost P, Van Ranst M, et al. Iron-ascorbate cleavable malic enzyme from hydrogenosomes of *Trichomonas vaginalis*: purification and characterization. Mol Biochem Parasitol 1996;83:221–34.
[12] Hrdy I, Mertens E, Van Schaftingen E. Identification, purification and separation of different isozymes of NADP-specific malic enzyme from Tritrichomonas foetus. Mol Biochem Parasitol 1993;57:253–60.
[13] Glenner GG, Weissbach H, Redfield BG. The histochemical demonstration of enzymatic activity by a nonenzymatic redox reaction – reduction of tetrazolium salts by indolyl-3-acetaldehyde. J Histochem Cytochem 1960;8:258–61.
[14] Liochev SI, Batinic-Haberle I, Fridovich I. The effect of detergents on the reduction of tetrazolium salts. Arch Biochem Biophys 1995;324:48–52.
[15] Nishikimi M. The generation of superoxide anion in the reaction of tetrahydropteridines with molecular oxygen. Arch Biochem Biophys 1975;166:273–9.
[16] Lindmark DG, Müller M. Hydrogenosome, a cytoplasmic organelle of the anaerobic flagellate Tritrichomonas foetus, and its role in pyruvate metabolism. J Biol Chem 1973;248:7724–8.
[17] Smutna T, Goncalves VL, Saraiva LM, et al. Flavodiiron protein from *Trichomonas vaginalis* hydrogenosomes: the terminal oxygen reductase. Eukaryot Cell 2009;8:47–55.

9. Unpublished results

Changes of hydrogenosomal proteomes during development of metronidazole resistance in *Trichomonas vaginalis*

Metronidazole and other derivates of 5-nitroimidazole are the drugs used against the sexually transmitted parasite *T. vaginalis* and other anaerobic and microaerophilic pathogens. Susceptible organisms possess an electron-generating and transport systems involved in the oxidative decarboxylation of pyruvate and ATP synthesis. This pathway is also responsible for reduction of the drug to cytotoxic products including hydroxylamine. Mechanisms of both activation and resistance to metronidazole were described previously and reside in the hydrogenosome, but recently a cytosolic flavin-based mechanism has been proposed. Moreover, different metronidazole resistance mechanisms have been described in other organisms. Nim genes which encode 5-nitroimidazole reductases and NAD(P)H nitroreductases have been associated with metronidazole resistance in *Bacteroides fragilis* and metronidazole activation in *Helicobacter pylori*, respectively (Mendz and Mégraud 2002). The finding of homologues of these genes in the genome of *T. vaginalis* suggests the presence of multiple mechanisms involved in metronidazole activation and metronidazole resistance in this parasite.

In this study we performed the proteomic analysis of the highly purified hydrogenosomal fraction obtained using an Optiprep-sucrose gradient centrifugation. The organelles were isolated from the metronidazole-susceptible parent strain TV10-02 and from the *in vitro* developed resistant derivatives growing with 3, 5 and 100 ug/ml metronidazole (MR3, MR5, and MR100). Hydrogenosomal proteins were digested with trypsin and the peptides were labeled using iTRAQ reagents. The labeled peptides were pooled and after separation using isoelectric focusing and nano-liquid chromatography were analyzed by tandem mass spectrometry (nano-LC MS/MS). From a total of 700 proteins identified, approximately 140 hydrogenosomal proteins were found in all cell lines. Relative quantities of these proteins were compared. Changes in protein expression were not significant (Fold change < 2.0) in MR3 and MR5 strains when compared with parent strain while the highly resistant strain MR100 displayed marked downregulation of the enzymes involved in energy and amino acid metabolism (PFOR, malic enzyme, acetate/succinate CoA transferase and others). In contrast, increased protein levels were observed for key components of ISC

assembly machinery (IscS, IscU, IscA, Nfu and Ferredoxin 7) and for hydrogenase maturases in the MR100 strain. Interestingly, the highest fold change (greater than 38) was observed in two genes coding for the hybrid cluster protein (HCP; originally called "prismane"), that is common in prokaryotes and was initially isolated from the strictly anaerobic sulfate-reducing bacterium *Desulfovibrio vulgaris* (Pierik et al., 1992). HCP is located in the hydrogenosome of *T. vaginalis* and it coordinates two FeS clusters, one of which may be either a [2Fe2S] or a [4Fe4S] in different types of the enzyme, whereas the other is a unique [4Fe-2S-2O] cluster (van den Berg et al., 2000; Macedo et al., 2002). Although widely examined at the biophysical level, little is known about the function of HCP *in vivo*. In prokaryotes, it was reported to be associated with nitrate and nitrite metabolism (Cabello et al., 2004) working as a hydroxylamine reductase (Wolfe et al., 2002), and to be involved in oxidative stress protection (Briolat and Reysset, 2002; Almeida et al., 2006). HCP-coding genes are also present in several unrelated lineages of eukaryotic protists. The exact physiological role of HCP in eukaryotes remains unknown but according with our results, in *T. vaginalis* the protein could be involved in scavenging of cytotoxic metabolites i.e hydroxylamine, formed after metronidazole reduction. These data demonstrate profound changes in the hydrogenosome proteome of highly metronidazole-resistant trichomonads and support the role of hydrogenosomes in the induction of anaerobic resistance to metronidazole.

10. Conclusions

The effect of iron in the gene expression of the human parasite *T. vaginalis* was studied by comparative transcriptomic and proteomic analysis using cells cultured in the presence and absence of iron. The role of iron in the protein expression of *T. vaginalis* was consistent in the results of both analyzes.

Previous studies had shown that iron availability significantly affects the pathogenicity of the parasite and the expression of genes encoding proteins involved in energy metabolism. The aim of these studies was to show in more depth the gene regulation and thus to understand the adaptive capacity of *T. vaginalis* under iron rich and iron restricted conditions. In our first experiment, we observed iron regulation in 308 genes using DNA microarrays and 336 genes

using EST library sequencing. In both methods, it was observed that approximately 50% of the genes were upregulated in iron enriched conditions while the other 50% were upregulated under iron restricted conditions. Genes that showed upregulation in the presence of iron, were those involved in carbohydrate metabolism both in the cytosol and the hydrogenosome, and also the genes involved in the catabolism of methionine. In the absence of iron, there was upregulation of the components of the ISC assembly machinery and various cysteine proteases. It was observed the differential expression of individual copies of the expanded gene group showing that not all of the copies were affected by iron. From this, one could deduce that the gene duplication observed in *T. vaginalis* genome sequence could be a strategy of the parasite to respond and adapt efficiently to the constant changes in its natural habitat.

Proteomic analysis was conducted specifically in hydrogenosomes of *T. vaginalis.* Data was analyzed based on protein expression under iron restricted conditions, for which hydrogenosomes from cells cultured in the presence of iron were taken as a control. The hydrogenosomal proteome confirmed the data obtained in our transcriptomic study. We have identified 179 proteins, of which 58 were differentially expressed. Iron deficiency showed upregulation of proteins involved in ISC assembly machinery and downregulation of proteins involved in carbohydrate metabolism. We confirmed that iron affects the expression of only some of the multiple protein paralogues while the expression of others was iron independent. We can conclude that changes in protein expression in components of the iron-sulfur cluster assembly machinery and energy metabolism are an adaptative mechanism of the parasite in response to the lack of iron. Hydrogenosomal Fe-S proteins with a role in pyruvate catabolism are downregulated to minimize the iron needs while the machinery for ISC assembly maximized its function for the efficient Fe-S clusters formation which is necessary for the core metabolism in the organelle.

In addition, we observed that components involved in oxidative stress protection were affected by iron availability as well. Two thioredoxins and one protein with homology to bacterial OsmC, which was recently found involved in detoxification of peroxides, were upregulated, whereas the Fe-containing proteins, rubrerythrin and superoxide dismutase were downregulated under iron depleted conditions. One paralogue of the bacterial-type FeS flavoprotein with a role in hydrogen peroxide and oxygen detoxification was downregulated too. Interestingly, one of the two detected paralogues of the β-barrel protein Hmp35 was

significantly downregulated under iron restricted conditions. This protein has been detected only in hydrogenosomes of *T. vaginalis* and a role as an iron transporter has been suggested.

In another series of experiments, we compared the protein expression in hydrogenosomes of *T. vaginalis* from a metronidazole-sensitive strain and three strains with *in vitro* developed metronidazole resistance. Protein expression in the highly metronidazole resistant strain (MR100) revealed similar changes when compared with the parent strain as that found in trichomonads that were grown under iron depleted conditions. ISC assembly machinery was upregulated in the MR100 strain whereas the enzymes from the carbohydrate metabolism were downregulated. Interestingly, two paralogues of the hybrid cluster protein (HCP) were identified among the most upregulated proteins in MR100. This protein catalyzes reduction of hydroxylamine and thus it might be involved in the detoxification of toxic products from the nitrogen metabolism including the metronidazole. Another interesting protein is an unknown protein with a RIC and ScdA domain, which was significantly upregulated in MR100. The protein is similar to the bacterial protein FeS_repair_RIC, iron-sulfur cluster repair di-iron protein. The protein in bacteria is stimulated by nitrosative stress and iron starvation. Additionally, RIC protein has homology with the ScdA protein identified in *Staphylococcus aureus*, which participate in cell wall biosynthesis and could be involved in drug resistance by increasing the cell wall permeability or the efflux pumps of active drugs. However, the role of this protein in *T. vaginalis* remain to be elucidated. HCP and the unknown protein with the RIC domain did not reveal a significant regulation under iron depleted conditions.

In a different experiment we have demonstrated that the hydrogenosome of *T. vaginalis* does not possess Alternative 2-keto acid oxidoreductases (KORs) as it was reported in a previous study. It has been suggested that the protein could replace the activity of pyruvate: ferredoxin oxidorreductase (PFOR) in metronidazole-resistant trichomonads. We used a standard assay with methyl viologen as an acceptor but we were unable to detect this activity in metronidazole-resistant cells lacking PFOR. We have concluded that the KOR activity was caused by the non-enzymatic reduction of the indicator dye, nitroblue tetrazolium, by indolepyruvate, which is facilitated by Triton X-100 used to prepare the membrane fractions. Therefore the low level indolepyruvate-dependent activity that is present in *T. vaginalis* strains sensitive to metronidazole is catalyzed by PFOR.

We have carried out an experiment to identify the hydrogenosomal membrane proteins in *T. vaginalis*. The data revealed some homologues of the mitochondrial membrane transporters and other functional components that are necessary for the organelle biogenesis. These findings corroborate a common origin for hydrogenosomes and mitochondria from an ancestral symbiont. However, important differences between the hydrogenosomal and mitochondrial membrane machineries were also observed.

We have identified proteins from the outer membrane of the hydrogenosomes, some of them do not present homology with the mitochondrial counterparts; this is the case of the 12 monotopic C-tailed anchored proteins identified. In addition, components of SAM and TOM complex were found too and 4 isoforms of β-barrel proteins HMP35 and HMP36 which were found exclusively in hydrogenosomes of *T.vaginalis*, so far. A cystein motif at the C- terminus of HMP35 with predicted role in metal transport makes this protein a suitable candidate for iron transport to supply the need of iron for Fe-S cluster formation in the organelle. In the study we did not identify clear homologues of the VDAC protein family; hence the metabolite exchange across the membrane of *T.vaginalis* hydrogenosomes is probably carried out by Tom40. However, it is difficult to distinguish VDAC and Tom40 using just bioinformatic tools, and then it is possible that some proteins named as Tom40 could be actually VDAC proteins. It should be noted that the hydrogenosomal membrane proteins that were identified did not contain N-terminal signal-anchor sequences. These transmembrane segments are present in mitochondrial membrane proteins to anchor the protein in the membrane.

Components of the TIM and PAM complex from inner hydrogenosomal membrane were revealed. Five homologues of the MCF carriers were found but apparently they are all involved in ADP/ATP transport across the membranes, which make as wonder how other metabolites, such as pyruvate or amino acids are transported.

We have identified two small TIMs chaperones in the intermembrane space. The proteins share 93% sequence identity and have been called Tim9/10a and Tim9/10b. The higuest similarity of the hydrogenosomal small TIMs is with Tim 9 of *S. cerevisiae*. Mia40 and Erv1 were not found in the proteome. This is consistent with the analyses of the genome of *T. vaginalis* that did not detected genes coding for these two proteins.

Additionally, 58 unknown membrane proteins were identified, these proteins could be highly divergent from the mitochondrial homologues and this could avoid its recognition by the

bioinformatic tools, although it is possible that these proteins are unique to hydrogenosome of *T. vaginalis*.

The mitosomal proteome of *Giardia intestinalis* revealed an important reduction of the protein content in the organelle by comparison with hydrogenosomes and mitochondria. We have identified 139 proteins using mass spectrometry and 20 of them were experimentally localized in the mitosomes. The analysis revealed the presence of components of the ISC assembly machinery including IscS, IscA, IscU, Nfu and Glutaredoxin. It was shown that just few components of the protein import machineries are present in the mitosomal membranes of *G. intestinalis.* Tom40, Pam 16/18 and molecular chaperones have been identified so far and we could not identified homologues of Sam50, Tim17/22/23 or VDAC protein family. It is a very intriguing matter to know how the organelle assembles Tom40 channel, transport matrix proteins and exchange metabolites in the absence of these components.

Based on these findings it is possible to conclude that ISC assembly machinery is the only known function of the organelle; however any MCF carrier that could be involved in ADP/ATP transport was not found and hence it is not clear how the mitosomes of *G. intestinalis* could obtain the energy necessary for Fe-S cluster assembly, organelle replication and protein import. It is also unclear if the mitosomes export a product necessary for cytosolic Fe-S cluster assembly as in other organisms since Atm1 and Erv1 transporters were not identified. Altogether, our studies significantly contributed to the understanding of the evolution of hydrogenosomes and mitosomes, anaerobic forms of mitochondria in *Trichomonas vaginalis* and *Giardia intestinalis*, respectively. Our results provide basis for the study of the expression of multiple gene families under different environmental conditions and we give clues for the better understanding of the development of metronidazole resistance in anaerobic parasites.

11. References

Akhmanova A, Voncken F, van Alen T, *et al.* (1998) "A hydrogenosome with a genome". *Nature* 396 (6711): 527–8.

Alderete JF, O'Brien JL, Arroyo R, Engbring JA, Musatovova O, Lopez O, Lauriano C, Nguyen J. (1995) Cloning and molecular characterization of two genes encoding

adhesion proteins involved in *Trichomonas vaginalis* cytoadherence.Mol Microbiol.1:69-83.

Allen JF. (2003). The function of genomes in bioenergetic organelles.Philos Trans R Soc Lond B Biol Sci. 358(1429):19-37; discussion 37-8. Review.

Almeida CC, Romão CV, Lindley PF, Teixeira M, Saraiva LM. (2006) The role of the hybrid cluster protein in oxidative stress defense. J Biol Chem.;281(43):32445-50.

Alvarez-Sánchez ME, Solano-González E, Yañez-Gómez C, Arroyo R (2007) Negative iron regulation of the CP65 cysteine proteinase cytotoxicity in *Trichomonas vaginalis*. Microbes Infect. 14-15:1597-605. Epub 2007 Sep 23.

Andersson SG et al. (1998) The genome sequence of *Rickettsia prowazekii* and the origin of mitochondria. Nature 396:133-140

Arroyo R, Alderete JF. (1995) Two *Trichomonas vaginalis* surface proteinases bind to host epithelial cells and are related to levels of cytoadherence and cytotoxicity. Arch Med Res. 3:279-85

Arroyo R, Engbring J, Alderete JF. (1992) Molecular basis of host epithelial cell recognition by *Trichomonas vaginalis*. Mol Microbiol. 7:853-62.

Balk J., R. Lill R., The cell's cookbook for iron–sulfur clusters: recipes for fool's gold? ChemBioChem 5 (2004) 1044–1049.

Barberà MJ, Ruiz-Trillo I, Tufts JY, Bery A, Silberman JD, Roger AJ. (2010). *Sawyeria marylandensis* (Heterolobosea) has a hydrogenosome with novel metabolic properties. Eukaryot Cell. 9(12):1913-24.

Benchimol M. (2000).Ultrastructural characterization of the isolated hydrogenosome in *Tritrichomonas foetus*. Tissue Cell.32(6):518-26.

Benchimol M. (2009). Hydrogenosomes under microscopy. Tissue Cell.41(3):151-68

Bohnert M, Pfanner N, van der Laan M (2007) A dynamic machinery for import of mitochondrial precursor proteins. FEBS Lett. 581(15):2802-10.

Bolliger L et al. (1994) A mitochondrial homolog of bacterial GrpE interacts with mitochondrial hsp70 and is essential for viability. EMBO J 13:1998-2006

Boxma B, de Graaf RM, van der Staay GW, van Alen TA, Ricard G, Gabaldón T, van Hoek AH, Moon-van der Staay SY, Koopman WJ, van Hellemond JJ, Tielens AG, Friedrich T, Veenhuis M, Huynen MA, Hackstein JH. (2005). An anaerobic mitochondrion that produces hydrogen. Nature. 434(7029):74-9.

Bozner P (1997) Immunological detection and subcellular localization of Hsp70 and Hsp60 homologs in *Trichomonas vaginalis*. J Parasitol 83:224-229.

Bradley PJ, Lahti CJ, Plumper E, Johnson PJ (1997) Targeting and translocation of proteins into the hydrogenosome of the protist *Trichomonas*: similarities with mitochondrial protein import. EMBO J 16: 3484–3493.

Briolat V, Reysset G.(2002) Identification of the *Clostridium perfringens* genes involved in the adaptive response to oxidative stress. J Bacteriol. 184(9):2333-43.

Broers CA, Stumm CK, Vogels GD. (1991). Axenic cultivation of the anaerobic free-living ciliate *Trimyema compressum*. *J Protozool*. 38, 507-11.

Broers CAM. (1992). Anaerobic psalteriomonad amoeboflagellates. Thesis, University of Nijmegen, Nijmegen.

Brown DM, Upcroft JA, Dodd HN, Chen N, Upcroft P. (1999) Alternative 2-keto acid oxidoreductase activities in *Trichomonas vaginalis*. Mol Biochem Parasitol. 98(2):203-14.

Brul S, Veltman RH, Lombardo MC, Vogels GD. (1994). Molecular cloning of hydrogenosomal ferredoxin cDNA from the anaerobic amoeboflagellate *Psalteriomonas lanterna*. *Biochim Biophys Acta*. 1183, 544-6

Bui ET, Bradley PJ, Johnson PJ. (1996). A common evolutionary origin for mitochondria and hydrogenosomes. Proc Natl Acad Sci U S A.93(18):9651-6.Cabello P, Pino C, Olmo-Mira MF, Castillo F, Roldán MD, Moreno-Vivián C. (2004) Hydroxylamine assimilation by Rhodobacter capsulatus E1F1. requirement of the hcp gene (hybrid cluster protein) located in the nitrate assimilation nas gene region for hydroxylamine reduction. J Biol Chem. 279(44):45485-94.

Camadro, J. M., and P. Labbe. 1988. Purification and properties of ferrochelatase from the yeast *Saccharomyces cerevisiae*. Evidence for a precursor form of the protein. J. Biol. Chem. 263**:**11675-11682.

Carlier JP, Sellier N, Rager MN, Reysset G. (1997) Metabolism of a 5-nitroimidazole in susceptible and resistant isogenic strains of *Bacteroides fragilis.* Antimicrob Agents Chemother. 1997 Jul; 41(7):1495-9.

Carlton, J.M., Hirt, R.P., Silva, J.C., Delcher, A.L., Schatz, M., Zhao, Q., Wortman, J.R., Bidwell, S.L., Alsmark, U.C., Besteiro, S., Sicheritz-Ponten, T., Noel, C.J., Dacks, J.B., Foster, P.G., Simillion, C., Van de Peer, Y., Miranda-Saavedra, D., Barton, G.J., Westrop, G.D., Müller M., S., Dessi, D., Fiori, P.L., Ren, Q., Paulsen, I., Zhang, H., Bastida-Corcuera, F.D., Simoes-Barbosa, A., Brown, M.T., Hayes, R.D., Mukherjee, M., Okumura, C.Y., Schneider, R., Smith, A.J., Vanácová, S., Villalvazo, M., Haas, B.J., Pertea, M., Feldblyum, T.V., Utterback, T.R., Shu, C.L., Osoegawa, K., de Jong, P.J., Hrdý, I., Horváthová, L., Zubacova, Z., Doležal, P., Malik, S.B., Logsdon, J.M.,

Jr., Henze, K., Gupta, A., Wang, C.C., Dunne, R.L., Upcroft, J.A., Upcroft, P., White, O., Salzberg, S.L., Tang, P., Chiu, C.H., Lee, Y.S., Embley, T.M., Coombs, G.H., Mottram, J.C., Tachezy, J., Fraser-Liggett, C.M., and Johnson, P.J. (2007). Draft genome sequence of the sexually transmitted pathogen *Trichomonas vaginalis*. Science 315, 207-212.

Cavalier-Smith T (2002). "The phagotrophic origin of eukaryotes and phylogenetic classification of Protozoa". *Int. J. Syst. Evol. Microbiol.* 52 (Pt 2): 297–354.

Cavalier-Smith T.1987. Eukaryotes with no mitochondria. Nature. 1987 Mar 26-Apr 1; 326(6111):332-3.

Čerkasov J, Čerkasovová A, Kulda J, Vilhelmová D (1978) Respiration of hydrogenosomesof *Tritrichomonas foetus*. J Biol Chem 253:1207–1214.

Chacinska A, Koehler CM, Milenkovic D, Lithgow T, Pfanner N (2009) Importing mitochondrial proteins: machineries and mechanisms. Cell 138: 628–644.

Chapman A, Cammack R, Linstead D, Lloyd D (1985) The generation of metronidazole radicals in hydrogenosomes isolated from *Trichomonas vaginalis*. J Gen Microbiol. 9:2141-4.

Chapman A, Linstead DJ, Lloyd D (1999) Hydrogen peroxide is a product of oxygen consumption by *Trichomonas vaginalis*. J Biosci 24:339–344

Chen KC, Culbertson NJ, Knapp JS, Kenny GE, Holmes KK.(1982) Rapid method for simultaneous detection of the arginine dihydrolase system and amino acid decarboxylases in microorganisms. J Clin Microbiol. 5:909-19.

Chesson HW, Blandford JM, Pinkerton SD. (2004) Estimates of the annual number and cost of new HIV infections among women attributable to trichomoniasis in the United States. Sexually transmitted diseases. 31(9):547–51.

Clark CG, Roger AJ (1995) Direct evidence for secondary loss of mitochondria in *Entamoeba histolytica*. Proc Natl Acad Sci U S A 92:6518-6521

Clemens DL, Johnson PJ.(2000). Failure to detect DNA in hydrogenosomes of *Trichomonas vaginalis* by nick translation and immunomicroscopy. Mol Biochem Parasitol.106(2):307-13.

Coelho, D. (1997). Metronidazole resistant trichomoniasis successfully treated with paromomysin. Genitourin. Med. 73:397–398.

Coombs GH, Westrop GD, Suchan P, Puzova G, Hirt RP, Embley TM, Mottram JC, Müller S (2004) The amitochondriate eukaryote *Trichomonas vaginalis* contains a divergent thioredoxin-linked peroxiredoxin antioxidant system. J Biol Chem 279:5249–5256

Cotch, M. F. (1990) Carriage of *Trichomonas vaginalis* (Tv) is associated with adverse pregnancy outcome, abstr. 681, p. 199. *In* Program and abstracts of the 30th Interscience Conference on Antimicrobial Agents and Chemotherapy. American Society for Microbiology, Washington, D.C.

Craig EA, Kramer J, Kosic-Smithers J (1987) SSC1, a member of the 70-kDa heat shock protein multigene family of *Saccharomyces cerevisiae*, is essential for growth. Proc Natl Acad Sci USA 84:4156-4160.

Crichton R., (2001). Inorganic biochemistry of iron metabolism. John Wiley & Sons, Ltd.

Cudmore S, Delgaty KL, Hayward-McClelland SF, Petrin DP, Garber E (2004) Treatment of infections caused by metronidazole-resistant *Trichomonas vaginalis*. ClinMicrobiol Rev 17:783–793

Dagley MJ, Doležal P, Likic VA, Smid O, Purcell AW, Buchanan SK, Tachezy J, Lithgow T (2009). The protein import channel in the outer mitosomal membrane of Giardia intestinalis. Mol Biol Evol. 26(9):1941-7

de Graaf RM, Ricard G, van Alen TA, Duarte I, Dutilh BE, Burgtorf C, Kuiper JW, van der Staay GW, Tielens AG, Huynen MA, Hackstein JH. (2011) The organellar genome and metabolic potential of the hydrogen-producing mitochondrion of *Nyctotherus ovalis*. Mol Biol Evol. 28(8):2379-91.

De Jesus JB, Cuervo P, Junqueira M, Britto C, Silva-Filho FC, Soares MJ, Cupolillo E, Fernandes O, Domont GB. (2007) A further proteomic study on the effect of iron in the human pathogen *Trichomonas vaginalis*. Proteomics. 12:1961-72.

Di Matteo, A., F. M. Scandurra, F. Testa, E. Forte, P. Sarti, M. Brunori, and A. Giuffre. 2008. The O_2-scavenging flavodiiron protein in the human parasite *Giardia intestinalis*. J. Biol. Chem. 283**:**4061-4068.

Declerck PJ, Müller M (1987) Hydrogenosomal ATP: AMP phosphotransferase of *Trichomonas vaginalis*. Comp Biochem Physiol B 88:575–580

Docampo R, Moreno SN, Mason RP (1987) Free radical intermediates in the reaction of pyruvate: ferredoxin oxidoreductase in *Tritrichomonas foetus* hydrogenosomes. J Biol Chem 262:12417–12420

Doležal P, Dancis A, Lesuisse E, Šutak R, Hrdý I, Embley TM, Tachezy J.(2007) Frataxin, a conserved mitochondrial protein, in the hydrogenosome of *Trichomonas vaginalis*. Eukaryot Cell. 6(8):1431-8.

Doležal P, Likic V, Tachezy J, Lithgow T. (2006) Evolution of the molecular machines for protein import into mitochondria. *Science*. 313, 314-8.

Doležal P, Smid O, Rada P, Zubácová Z, Bursać D, Suták R, Nebesárová J, Lithgow T, Tachezy J. (2005) *Giardia* mitosomes and trichomonad hydrogenosomes share a common mode of protein targeting. *Proc Natl Acad Sci*. 102, 10924-9.

Doležal P, Vanácová S, Tachezy J, Hrdý I (2004) Malic enzymes of *Trichomonas vaginalis*: two enzyme families, two distinct origins. Gene 329:81–92

Dombrowski, M., W. Brown, and R. Bronsteen. 1987. Intravenous therapy of metronidazole-resistant *Trichomonas vaginalis*. Obstet. Gynecol. 69:524–525.

Drmota T, Proost P, Van Ranst M, Weyda F, Kulda J, Tachezy J (1996) Iron ascorbate cleavable malic enzyme from hydrogenosomes of *Trichomonas vaginalis*: purification and characterization. Mol Biochem Parasitol 83:221–234

D'Silva PD, Schilke B, Walter W, Andrew A, Craig EA (2003) J protein cochaperone of the mitochondrial inner membrane required for protein import into the mitochondrial matrix. Proc Natl Acad Sci USA 100:13839-13844

Dunn, L. L., Suryo Rahmanto, Y., and Richardson, D. R. (2007). Iron uptake and metabolism in the new millennium. Trends in cell biology *17*, 93–100.).

Dunne RL, Dunn LA, Upcroft P, O'Donoghue PJ, Upcroft JA (2003) Drug resistance in the sexually transmitted protozoan *Trichomonas vaginalis*. Cell Res 132:239–249.

Dyall SD, Koehler CM, Delgadillo-Correa MG, Bradley PJ, Plumper E, et al. (2000) Presence of a member of the mitochondrial carrier family in hydrogenosomes: conservation of membrane-targeting pathways between hydrogenosomes and mitochondria. Mol Cell Biol 20: 2488–2497.

Dyall SD et al. (2003) *Trichomonas vaginalis* Hmp35, a putative pore-forming hydrogenosomal membrane protein, can form a complex in yeast mitochondria. J Biol Chem 278:30548-30561

Dyall SD, Brown MT, Johnson PJ. (2004). Ancient invasions: from endosymbionts to organelles. Science. 304(5668):253-7.

Dyall SD, Doležal P. (2008). Protein import into hydrogenosomes and mitosomes. Microbiol Monogr. **9**, 21-74

Dyall SD, Johnson PJ. 2000. Origins of hydrogenosomes and mitochondria: evolution and organelle biogenesis. Curr Opin Microbiol. 3(4):404-11.

Dyer BD. *Metopus*, *Cyclidium* and *Sonderia*: ciliates enriched and cultured from sulfureta of a microbial mat community. (1989). Biosystems. 23, 41-51.

Edwards DI (1993) Nitroimidazole drugs action and resistance mechanisms. II. Mechanisms of resistance. J Antimicrob Chemother 31:201–210.

Ellis JE, Cole D, Lloyd D. (1992). Influence of oxygen on the fermentative metabolism of metronidazole-sensitive and resistant strains of *Trichomonas vaginalis*. Mol Biochem Parasitol.;56(1):79-88.

Ellis JE, Yarlett N, Cole D, Humphreys MJ, Lloyd D (1994) Antioxidant defenses in the microaerophilic protozoan *Trichomonas vaginalis*: comparison of metronidazole resistant and sensitive strains. Microbiol-SGM 140:2489–2494

Embley TM, Martin W. Eukaryotic evolution, changes and challenges. Nature. (2006) Mar 30; 440(7084):623-30. Review.

Esser C, Ahmadinejad N, Wiegand C, Rotte C, Sebastiani F, Gelius-Dietrich G, Henze K, Kretschmann E, Richly E, Leister D, Bryant D, Steel MA, Lockhart PJ, Penny D, Martin W. (2004) A genome phylogeny for mitochondria among alpha-proteobacteria and a predominantly eubacterial ancestry of yeast nuclear genes. Mol Biol Evol.21(9):1643-60. Epub May 21.

Fenchel T & Finlay BJ. 1991. Endosymbiotic methanogenic bacteria in anaerobic ciliates: significance for growth efficiency of the host. J Protozool. 38, 18-22.

Frazier AE et al. (2004) Pam16 has an essential role in the mitochondrial protein import motor. Nat Struct Mol Biol 11:226-233

Gabaldón, T. and Huynen, MA. (2004) Prediction of protein function and pathways in the genome era. Cell. Mol. Life Sci. 61; (78):93044

Garcia AF, Chang TH, Benchimol M, Klumpp DJ, Lehker MW, Alderete JF (2003) Iron and contact with host cells induce expression of adhesins on surface of *Trichomonas vaginalis*. Mol Microbiol. 2003 5:1207-24.

Gardner, A. M., R. A. Helmick, and P. R. Gardner. 2002. Flavorubredoxin, an inducible catalyst for nitric oxide reduction and detoxification *Escherichia coli*. J. Biol. Chem. 2778172-8177.

Garg S, Stölting J, Zimorski V, Rada P, Tachezy J, Martin WF, Gould SB.(2015) Conservation of Transit Peptide-Independent Protein Import into the Mitochondrial and Hydrogenosomal Matrix. Genome Biol Evol.2;7(9):2716-26.

Gelling C, et al. (2008) Mitochondrial Iba57p Is Required for Fe/S Cluster Formation on Aconitase and Activation of Radical SAM Enzymes. *Mol Cell Biol* 28(5):1851-1861.

Germot A, Philippe H, Le Guyader H.1996.Presence of a mitochondrial-type 70-kDa heat shock protein in *Trichomonas vaginalis* suggests a very early mitochondrial endosymbiosis in eukaryotes. Proc Natl Acad Sci U S A. 93(25):14614-7.

Glick BS, Brandt A, Cunningham K, Müller M. S, Hallberg RL, Schatz G (1992) Cytochromes c1 and b2 are sorted to the intermembrane space of yeast mitochondria by a stop-transfer mechanism. Cell 69:809-822

Goldberg AV, et al. *(*2008). Localization and functionality of microsporidian iron-sulphur cluster assembly proteins. *Nature* 452*:*624–628.

Gomes CM, Giuffre A, Forte E, Vicente JB, Saraiva LM, Brunori M, Teixeira M (2002) A novel type of nitric-oxide reductase: *Escherichia coli* flavorubredoxin. J Biol Chem 277:25273–25276

Goodwin A, Kersulyte D, Sisson G, Veldhuyzen van Zanten SJ, Berg DE, Hoffman PS (1998) Metronidazole resistance in *Helicobacter pylori* is due to null mutations in a gene (rdxA) that encodes an oxygen-insensitive NADPH nitroreductase. Mol Microbiol. 28(2):383-93.

Gorrel, T.E. 1985. Effect of culture medium iron content on biochemical composition and metabolism of *Trichomonas vaginalis*. J Bacteriol 161, 1228-1230.

Grossman, J., and R. Galask. 1990. Persistent vaginitis caused by metronidazole-resistant trichomonas. Obstet. Gynecol. 76:521–522.

Hackstein JH, Akhmanova A, Boxma B, Harhangi HR, Voncken FG. 1999. Hydrogenosomes: eukaryotic adaptations to anaerobic environments. Trends Microbiol. 7(11):441-7. Review.

Hackstein JH, Tjaden J, Huynen M. (2006). Mitochondria, hydrogenosomes and mitosomes: products of evolutionary tinkering! Curr Genet.50(4):225-45

Hackstein JH, Yarlett N.Hydrogenosomes and symbiosis.(2006). Prog Mol Subcell Biol. 41:117-42

Haile, D.J., Rouault, T.A., Harford, J.B., Kennedy, M.C., Blondin, G.A., Beinert, H.,Klausner, R.D., 1992. Cellular regulation of the iron-responsive element binding protein: disassembly of the cubane iron-sulfur cluster results in high-affinityRNA-binding. Proc. Natl. Acad. Sci. U.S.A. 89, 11735–11739.

Hardy, P. H., J. B. Hardy, E. E. Nell, D. A. Graham, M. R. Spence, and R. C.Rosenbaum. (1984) Prevalence of six sexually transmitted disease agents among pregnant inner-city adolescents and pregnancy outcome. Lancet ii: 333–337.

Harp, Djana F., Chowdhury, Indrajit (2011). "Trichomoniasis: Evaluation to execution". European Journal of Obstetrics & Gynecology and Reproductive Biology 157 (1): 3–9.

Hashimoto T, Sánchez LB, Shirakura T, Müller M, Hasegawa M. (1998). Secondary absence of mitochondria in *Giardia lamblia* and *Trichomonas vaginalis* revealed by valyl-tRNA synthetase phylogeny. Proc Natl Acad Sci U S A. 95(12):6860-5.

Henze, K. The Proteome of *T. vaginalis* Hydrogenosomes. In: Tachezy, J., editor. Hydrogenosomes and Mitosomes: Mitochondria of Anaerobic Eukaryotes. New York: Springer; 2008. p. 163-78.

Heyworth, R., D. Simpson, G. McNeillage, D. Robertson, and H. Young. 1980. Isolation of *Trichomonas vaginalis* resistant to metronidazole. Lancet ii:476–478.

Hill K et al. (1998) Tom40 forms the hydrophilic channel of the mitochondrial import pore for preproteins. Nature 395:516-521

Hoppins SC, Nargang FE (2004) The Tim8-Tim13 complex of *Neurospora crassa* functions in the assembly of proteins into both mitochondrial membranes. J Biol Chem 279:12396-12405

Horner DS, Hirt RP, Kilvington S, Lloyd D, Embley TM. (1996). Molecular data suggest an early acquisition of the mitochondrion endosymbiont. Proc Biol Sci. 263(1373):1053-9.

Hjort K, Goldberg AV, Tsaousis AD, Hirt RP, Embley TM (2010) Diversity and reductive evolution of mitochondria among microbial eukaryotes. Philos Trans R Soc B 365: 713–727. doi: 10.1098/rstb.2009.0224.

Hofmann B, Hecht HJ, Flohé L (2002) Peroxiredoxins.Biol Chem. 383(3-4):347-64.

Hrdý I, Cammack R, Stopka P, Kulda J, Tachezy J. (2005) Alternative pathway of metronidazole activation in *Trichomonas vaginalis* hydrogenosomes. Antimicrob Agents Chemother. 12:5033-6.

Hrdý I, Hirt RP, Doležal P, Bardonová L, Foster PG, Tachezy J, Embley TM.. (2004) *Trichomonas* hydrogenosomes contain the NADH dehydrogenase module of mitochondrial complex I. Nature. 432, 618-622.

Hrdý I, Müller M (1995a) Primary structure of the hydrogenosomal malic enzyme of *Trichomonas vaginalis* and its relationship to homologous enzymes. J Eukaryot Microbiol 42:593–603

Hrdý I, Müller M. (1995b). Primary structure and eubacterial relationships of the pyruvate:ferredoxin oxidoreductase of the amitochondriate eukaryote *Trichomonas vaginalis.* J Mol Evol. 41(3):388-96.

Hrdý I, Tachezy J, Müller M. (2007) Metabolism of Trichomonad hydrogenosomes. Microbiol Monogr. 9, 113-139

Hsu HM, Ong SJ, Lee MC, Tai JH. (2009) Transcriptional regulation of an iron-inducible gene by differential and alternate promoter entries of multiple Myb proteins in the protozoan parasite *Trichomonas vaginalis*. Eukaryot Cell. 3:362-72.

Jenks PJ, Ferrero RL, Labigne A (1999) The role of the rdxA gene in the evolution of metronidazole resistance in *Helicobacter pylori*. J Antimicrob Chemother. 43(6):753-8.

Jeong JY, Mukhopadhyay AK, Dailidiene D, Wang Y, Velapatiño B, Gilman RH, Parkinson AJ, Nair GB, Wong BC, Lam SK, Mistry R, Segal I, Yuan Y, Gao H, Alarcon T, Brea ML, Ito Y, Kersulyte D, Lee HK, Gong Y, Goodwin A, Hoffman PS, Berg DE (2000). Sequential inactivation of rdxA (HP0954) and frxA (HP0642) nitroreductase genes causes moderate and high-level metronidazole resistance in *Helicobacter pylori*. J Bacteriol. 182(18):5082-90.

Jin S, Kurtz DM, Liu ZJ, Rose J, Wang BC (2002) X-ray crystal structures of reduced rubrerythrin and its azide adduct: a structure-based mechanism for a non-heme diiron peroxidase. J Am Chem Soc 124:9845–9855

Kabíčková H, Kulda J, Čerkasovová A, Němcová H (1988) Metronidazole resistant *Tritrichomonas foetus*: activities of hydrogenosomal enzymes in course of development of anaerobic resistance. Acta Univ Carol Biol 30:513–519

Kai Stefan Dimmer, Stefan Fritz, Florian Fuchs, Marlies Messerschmitt, Nadja Weinbach, Walter Neupert, and Benedikt Westermann (2002) Genetic Basis of Mitochondrial Function and Morphology in *Saccharomyces cerevisiae.* Mol Biol Cell. Mar; 13(3): 847–853.

Karnkowska A, Vacek V, Zubáčová Z, Treitli SC, Petrželková R, Eme L, Novák L, Žárský V, Barlow LD, Herman EK, Soukal P, Hroudová M,Doležal P, Stairs CW, Roger AJ, Eliáš M, Dacks JB, Vlček Č, Hampl V. (2016) A Eukaryote without a Mitochondrial Organelle. Curr Biol. 23;26(10):1274-84.

Kellock, D. J., and C. P. O'Mahoney. (1996). Sexually acquired metronidazole resistant trichomoniasis in a lesbian couple. Genitourin. Med. 72:60–61.

Kirkcaldy, R.D. et al. (2012) *Trichomonas vaginalis* antimicrobial drug resistance in 6 US cities, STD Surveillance Network, 2009–2010. Emerg. Infect. Dis. 18, 939–943.

Kispal G., Csere P., Prohl C., R. Lill R. The mitochondrial proteins Atm1p and Nfs1p are required for biogenesis of cytosolic Fe/S proteins, EMBO J. 18 (1999) 3981–3989.

Kispal G., Sipos K., Lange H, Fekete Z, Bedekovics T., Janáky T., Bassler J., Aguilar Netz D.,, Balk J., Rotte C., Lill R. (2005) Biogenesis of cytosolic ribosomes requires the essential iron-sulphur protein Rli1p and mitochondria. EMBO J. 24:589-598

Kitchener KR, Meshnick SR, Fairfield AS, Wang CC (1984) An iron-containing superoxide dismutase in *Tritrichomonas foetus*. Mol Biochem Parasitol. 12(1):95-9.

Koehler CM (2004) New developments in mitochondrial assembly. Annu Rev Cell Dev Biol 20:309-335.

Kovermann P et al. (2002) Tim22, the essential core of the mitochondrial protein insertion complex, forms a voltage-activated and signal-gated channel. Mol Cell 9:363-373

Kozany C, Mokranjac D, Sichting M, Neupert W, Hell K (2004) The J domain-related cochaperone Tim16 is a constituent of the mitochondrial TIM23 preprotein translocase. Nat Struct Mol Biol 11:234-241

Kozjak V et al. (2003) An essential role of Sam50 in the protein sorting and assembly machinery of the mitochondrial outer membrane. J Biol Chem 278:48520-48523

Kummer S., Hayes GR., Gilbert RO., Beach DH., Lucas JJ. And Singh BN, et al. (2008) Induction of human host cell apoptosis by *Trichomonas vaginalis* cysteine proteases is modulated by parasite exposure to iron. Microb Pathog.; 44:197-203.

Kunji ER (2004) The role and structure of mitochondrial carriers. FEBS Lett 564: 239–244.

Kulda J, Vojtěchovská M, Tachezy J, Demes P, Kunzová E. (1982) Metronidazole resistance of Trichomonas vaginalis as a cause of treatment failure in trichomoniasis--A case report. Br J Vener Dis.; 58(6):394-9

Kulda J (1999) Trichomonads, hydrogenosomes and drug resistance. Int J Parasitol 29:199–212

Kulda J, Cerkasov J, Demes P, Cerkasovová A.(1984) *Tritrichomonas foetus*: stable anaerobic resistance to metronidazole in vitro. Exp Parasitol.1:93-103.

Kulda J, Kabíčková H, Tachezy J, Čerkasovová A, Čerkasov J (1989) Metronidazole resistant trichomonads: mechanisms of in vitro developed anaerobic resistance. In: Lloyd D, Coombs GH, Paget TAP (eds) Biochemistry and molecular biology of anaerobic protozoa. Harwood, London, pp 137–160

Kulda J, Tachezy J, Čerkasovová A. (1993) In vitro induced anaerobic resistance to metronidazole in *Trichomonas vaginalis*. J Eukaryot Microbiol. 3:262-9.

Kutik S, Guiard B, Meyer HE, Wiedemann N, Pfanner N.(2007). Cooperation of translocase complexes in mitochondrial protein import. J Cell Biol. 19;179(4):585-91.

Laga M, Manoka A, Kivuvu M, Malele B, Tuliza M, Nzila N. (1993) Nonulcerative sexually transmitted diseases as risk factors for HIV-1 transmission in women: results from a cohort study. AIDS. 1993; 7:95–102.

Lahti CJ, Bradley PJ, Johnson PJ. (1994). Molecular characterization of the alpha-subunit of *Trichomonas vaginalis* hydrogenosomal succinyl CoA synthetase. Mol Biochem Parasitol. 1994 Aug; 66(2):309-18.

Lahti CJ, d'Oliveira CE, Johnson PJ . (1992). Beta-succinyl-coenzyme A synthetase from *Trichomonas vaginalis* is a soluble hydrogenosomal protein with an amino-terminal sequence that resembles mitochondrial presequences. J Bacteriol.174 (21):6822-30.

Lange H., LisowskyT., Gerber J., Mühlenhoff U., Kispal G.,Lill R., (2001) An essential function of the mitochondrial sulfhydryl oxidase Erv1p/ALR in the maturation of cytosolic Fe/S proteins, EMBO Rep. 2 715–720.

Lange S, Rozario C, Müller M (1994) Primary structure of the hydrogenosomal Adenylate kinase of *Trichomonas vaginalis* and its phylogenetic relationships. Mol Biochem Parasitol 66:297–308.

Lange H., Kispal G., Kaut A., Lill R, A mitochondrial ferredoxin is essential for biogenesis of intra- and extra-mitochondrial Fe/S proteins, Proc. Natl. Acad. Sci. U.S.A. 97 (2000) 1050–1055

Lehker MW., Chang TH., Dailey DC., Alderete JF. (1990) Specific erythrocyte binding is an additional nutrient acquisition system for *Trichomonas vaginalis*. J Exp Med 171(6):2165-70.

Lehker MW, Alderete JF (1992) Iron regulates growth of *Trichomonas vaginalis* and the expression of immunogenic trichomonad proteins. Mol Microbiol 6: 123–132.

Lehker MW, Arroyo R, Alderete JF. (1991) The regulation by iron of the synthesis of adhesins and cytoadherence levels in the protozoan *Trichomonas vaginalis*. J Exp Med. 174:311-8

Leiros HK, Kozielski-Stuhrmann S, Kapp U, Terradot L, Leonard GA, McSweeney SM. (2004) Structural basis of 5-nitroimidazole antibiotic resistance: the crystal structure of NimA from *Deinococcus radiodurans*. J Biol Chem. 53:55840-9. Epub 2004 Oct 18.

Leitsch D, Kolarich D, Binder M, Stadlmann J, Altmann F, Duchêne M. (2009) Trichomonas vaginalis: metronidazole and other nitroimidazole drugs are reduced by the flavin enzyme thioredoxin reductase and disrupt the cellular redox system. Implications for nitroimidazole toxicity and resistance. Mol Microbiol. 72(2):518-36.

Leitsch D, Kolarich D, Duchêne M. (2010) The flavin inhibitor diphenyleneiodonium renders *Trichomonas vaginalis* resistant to metronidazole, inhibits thioredoxin reductase and flavin reductase, and shuts off hydrogenosomal enzymatic pathways. Mol Biochem Parasitol. 171(1):17-24. Leitsch D, Janssen BD, Kolarich D, Johnson PJ, Duchêne M. (2014) *Trichomonas vaginalis* flavin reductase 1 and its role in metronidazole resistance. Mol Microbiol. 91(1):198-208.

Lesniak J, Barton WA, Nikolov DB. (2002) Structural and functional characterization of the Pseudomonas hydroperoxide resistance protein Ohr. EMBO J. 16;21(24):6649-59.

Lesniak J, Barton WA, Nikolov DB (2003) Structural and functional features of the Escherichia coli hydroperoxide resistance protein OsmC. Protein Sci 12:2838-2843

Li Y, Dudek J, Guiard B, Pfanner N, Rehling P, Voos W (2004) The presequence translocase-associated protein import motor of mitochondria. Pam16 functions in an antagonistic manner to Pam18. J Biol Chem 279:38047-38054

Lill R & Muhlenhoff U. (2005) Iron-sulfur-protein biogenesis in eukaryotes. *Trends Biochem. Sci.* 30, 133-141

Lill R, Diekert K, Kaut A, Lange H, Pelzer W, Prohl C, Kispal G. (1999). The essential role of mitochondria in the biogenesis of iron-sulfur proteins. Biol Chem. 380(10):1157-66.

Lill R, Kispal G. (2000). Maturation of cellular Fe-S proteins: an essential function of mitochondria. Trends Biochem Sci. 25(8):352-6. Review.

Lindmark DG, Müller M (1973). "Hydrogenosome, a cytoplasmic organelle of the anaerobic flagellate *Tritrichomonas foetus*, and its role in pyruvate metabolism". *J. Biol. Chem.* 248 (22): 7724–8.

Lindmark DG, Müller M (1974) Superoxide dismutase in the anaerobic flagellates, *Tritrichomonas foetus* and *Monocercomonas* sp. J Biol Chem 249:4634–4637

Lindmark DG, Müller M.(1976a). Antitrichomonad action, mutagenicity, and reduction of metronidazole and other nitroimidazoles. Antimicrob Agents Chemother. 10(3):476-82.

Lindmark DG. (1976b). Acetate production by *Tritrichomonas foetus,* p 15-21. In Van den Bossche H (ed), Biochemistry of parasites and host parasite relationships. Elsevier, Amsterdam, Netherlands.

Linstead D, Cranshaw MA.(1983). The pathway of arginine catabolism in the parasitic flagellate *Trichomonas vaginalis*. Mol Biochem Parasitol. 8(3):241-52.

Linstead DJ, Bradley S (1988) The purification and properties of two soluble reduced nicotinamide:acceptor oxidoreductases from *Trichomonas vaginalis*. Mol Biochem Parasitol 27:125–133

Lloyd D, Hillman K, Yarlett N, Williams AG. (1989). Hydrogen production by rumen holotrich protozoa: effects of oxygen and implications for metabolic control by in situ conditions. J Protozool. 36, 205-13.

Lloyd D, Kristensen B (1985) Metronidazole inhibition of hydrogen production in vivo in drug-sensitive and resistant strains of *Trichomonas vaginalis*. J Gen Microbiol 131:849–853

Lloyd D, Pedersen JZ.(1985) Metronidazole radical anion generation in vivo in *Trichomonas vaginalis*: oxygen quenching is enhanced in a drug-resistant strain. J Gen Microbiol. 1:87-92.

Maarse AC, Blom J, Grivell LA, Meijer M (1992) MPI1, an essential gene encoding a mitochondrial membrane protein, is possibly involved in protein import into yeast mitochondria. EMBO J 11:3619-3628

Macasev D, Whelan J, Newbigin E, Silva-Filho MC, Mulhern TD, Lithgow T (2004) Tom22', an 8-kDa trans-site receptor in plants and protozoans, is a conserved feature of the TOM complex that appeared early in the evolution of eukaryotes. Mol Biol Evol 21:1557-1564.

Macedo S, Mitchell EP, Romão CV, Cooper SJ, Coelho R, Liu MY, Xavier AV, LeGall J, Bailey S, Garner DC, Hagen WR, Teixeira M, Carrondo MA, Lindley P. (2002) Hybrid cluster proteins (HCPs) from Desulfovibrio desulfuricans ATCC 27774 and Desulfovibrio vulgaris (Hildenborough): X-ray structures at 1.25 A resolution using synchrotron radiation. J Biol Inorg Chem. 2002 Apr;7(4-5):514-25.

Maralikova B, et al. *(*2010). Bacterial-type oxygen detoxification and iron-sulfur cluster assembly in amoebal relict mitochondria. *Cell. Microbiol.* 12*:*331–342.

Margulis, L. (1970) Origin of eukaryotic cells; evidence and research implications for a theory of the origin and evolution of microbial, plant, and animal cells on the Precambrian earth. Vol. xxii. New Haven: Yale University Press; p. 349

Martin W, Müller M. (1998). The hydrogen hypothesis for the first eukaryote. Nature. 392(6671):37-41.

Martin W. 2005. The missing link between hydrogenosomes and mitochondria. Trends Microbiol. 13(10):457-9.

Martinez-Caballero S, Grigoriev SM, Herrmann JM, Campo ML, Kinnally KW (2007) Tim17p regulates the twin-pore structure and voltage gating of the mitochondrial protein import complex TIM23. J Biol Chem 282:3584-3593.

Marvin-Sikkema FD, Driessden AJM, Gottschal JC & Prins RA. (1994). Metabolic energy generation in hydrogenosomes of the anaerobic fungus *Neocallimastix*-evidence for a functional relationship with mitochondria. 98, 205-212.

McGonigle S, Dalton JP, James ER (1998) Peroxidoxins: a new antioxidant family. Parasitol Today 14:139–145

McKie, A. E., Edlind, T., Walker, J., Mottram, J. C., and Coombs, G. H. (1998) The Primitive Protozoon *Trichomonas vaginalis* Contains Two Methionine γ-Lyase Genes That Encode Members of the γ-Family of Pyridoxal 5′-Phosphate-dependent Enzymes. J. Biol. Chem. 273, 5549–5556

Meinecke M et al. (2006) Tim50 maintains the permeability barrier of the mitochondrial inner membrane. Science 312:1523-1526.

Meingassner JG, Thurner J. (1979) Strain of *Trichomonas vaginalis* resistant to metronidazole and other 5-nitroimidazoles. Antimicrob Agents Chemother. 2:254-7.

Meisinger C et al. (2001) Protein import channel of the outer mitochondrial membrane: a highly stable Tom40-Tom22 core structure differentially interacts with preproteins, small tom proteins, and import receptors. Mol Cell Biol 21:2337-2348

Melo-Braga MB, da Rocha-Azevedo B, Silva-Filho FC. (2003) *Tritrichomonas foetus*: the role played by iron during parasite interaction with epithelial cells. Exp Parasitol. 2:111-20.

Mendz GL, Mégraud F. (2002) Is the molecular basis of metronidazole resistance in microaerophilic organisms understood? Trends Microbiol. 2002 Aug; 10(8):370-5.

Mentel M, Zimorski V, Haferkamp P, Martin W, Henze K (2008) Protein import into hydrogenosomes of *Trichomonas vaginalis* involves both N-terminal and internal targeting signals: a case study of thioredoxin reductases. Eukaryot Cell 7: 1750–1757.

Mi-ichi F, Yousuf MA, Nakada-Tsukui K, Nozaki T. (2009). Mitosomes in *Entamoeba histolytica* contain a sulfate activation pathway. Proc. Natl. Acad. Sci. U. S. A.106:21731–21736.

Millet CO, Williams CF, Hayes AJ, Hann AC, Cable J, Lloyd D. (2013). Mitochondria-derived organelles in the diplomonad fish parasite Spironucleus vortens. Exp Parasitol. 135(2):262-73.

Moffett M, McGill MI Treatment of trichomoniasis with metronidazole. (1960) Br Med J. 2(5203):910-1.

Mokranjac D et al. (2003a) Tim50, a novel component of the TIM23 preprotein translocase of mitochondria. EMBO J 22:816-825

Morada M, Smid O, Hampl V, Šutak R, Lam B, Rappelli P, Dessì D, Fiori PL, Tachezy J, Yarlett N. (2011) Hydrogenosome-localization of arginine deiminase in *Trichomonas vaginalis*. Mol Biochem Parasitol.176(1):51-4

Moreno-Brito V, Yáñez-Gómez C, Meza-Cervantez P, Avila-González L, Rodríguez MA, Ortega-López J, González-Robles A, Arroyo R. (2005) A *Trichomonas vaginalis* 120 kDa protein with identity to hydrogenosome pyruvate:ferredoxin oxidoreductase is a surface adhesin induced by iron. Cell Microbiol. 2:245-58.

Mühlenhoff U, Lill R. 2000. Biogenesis of iron-sulfur proteins in eukaryotes: a novel task of mitochondria that is inherited from bacteria. Biochim Biophys Acta. 1459(2-3):370-82. Review.

Mukherjee M, Brown MT, McArthur AG, Johnson PJ. (2006a) Proteins of the glycine decarboxylase complex in the hydrogenosome of *Trichomonas vaginalis.* Eukaryot Cell. 5(12):2062-71.

Mukherjee M, Sievers SA, Brown MT, Johnson PJ. (2006b) Identification and biochemical characterization of serine hydroxymethyl transferase in the hydrogenosome of *Trichomonas vaginalis*. Eukaryot Cell. 5(12):2072-8.

Müller M, Gorrell TE. (1983) Metabolism and metronidazole uptake in *Trichomonas vaginalis* isolates with different metronidazole susceptibilities. Antimicrob Agents Chemother. 5:667-73.

Müller M, Lindmark DG (1978) Respiration of hydrogenosomes of *Tritrichomonas foetus*.II. Effect of CoA on pyruvate oxidation. J Biol Chem 253:1215–1218

Müller M, Lindmark DG.(1976) Uptake of metronidazole and its effect on viability in trichomonads and Entamoeba invadens under anaerobic and aerobic conditions. Antimicrob Agents Chemother.9(4):696-700.

Müller M. (1993). The hydrogenosome. J Gen Microbiol. 139(12):2879-89.

Müller M. (1988). Energy metabolism of protozoa without mitochondria. Annu. Rev. Microbiol. 42:465–488.

Müller M. 2003. Energy metabolism. Part I. Anaerobic protozoa*, p* 125–139. *In* Marr JJ*,* Nilsen TW*,* Komuniecki RW *(ed),* Molecular medical parasitology. Academic Press*,* London, United Kingdom*.*

Müller M. 2007. The road to hydrogenosomes*, p* 1–12. *In* Martin WF*,* Müller M *(ed),* Origin of mitochondria and hydrogenosomes*.* Springer-Verlag*,* Heidelberg, Germany.

Müller M, Mentel M, van Hellemond JJ, Henze K, Woehle C, Gould SB, Yu RY, van der Giezen M, Tielens AG, Martin WF (2012). Biochemistry and evolution of anaerobic energy metabolism in eukaryotes. Microbiol Mol Biol Rev. ; 76(2):444-95.

Mundodi, V., Kucknoor, A. S., Chang, T. H., and Alderete, J. F. (2006). A novel surface protein of *Trichomonas vaginalis* is regulated independently by low iron and contact with vaginal epithelial cells. BMC Microbiology 6, 6.

Neupert W (1997) Protein import into mitochondria. Annu Rev Biochem 66:863-917

Nývltová E, Šuták R, Harant K, Šedinová M, Hrdy I, Paces J, Vlček Č, Tachezy J. (2013) NIF-type iron-sulfur cluster assembly system is duplicated and distributed in the mitochondria and cytosol of Mastigamoeba balamuthi. Proc Natl Acad Sci U S A. 30;110(18):7371-6.

Nývltová E, Smutná T, Tachezy J, Hrdý I(2016) OsmC and incomplete glycine decarboxylase complex mediate reductive detoxification of peroxides in hydrogenosomes of Trichomonas vaginalis. Mol Biochem Parasitol. 206(1-2):29-38.

O'Fallon JV, Wright RW Jr, Calza RE. (1991). Glucose metabolic pathways in the anaerobic rumen fungus *Neocallimastix frontalis* EB188. Biochem J. 274 (Pt 2):595-9.

Ong SJ, Huang SC, Liu HW, Tai JH. (2004) Involvement of multiple DNA elements in iron-inducible transcription of the ap65-1 gene in the protozoan parasite *Trichomonas vaginalis*. Mol Microbiol. 6:1721-30.

Ong SJ, Hsu HM, Liu HW, Chu CH, Tai JH.(2006) Multifarious transcriptional regulation of adhesion protein gene ap65-1 by a novel Myb1 protein in the protozoan parasite *Trichomonas vaginalis*. Eukaryot Cell. 2006 Feb; 5(2):391-9.

Ong SJ, Hsu HM, Liu HW, Chu CH, Tai JH. (2007) Activation of multifarious transcription of an adhesion protein ap65-1 gene by a novel Myb2 protein in the protozoan parasite *Trichomonas vaginalis*. J Biol Chem. 2;282(9):6716-25.

Paget TA, Lloyd D. 1990. *Trichomonas vaginalis* requires traces of oxygen and high concentrations of carbon dioxide for optimal growth. Mol Biochem Parasitol. 41(1):65-72.

Pantopoulos K. (2004) Iron metabolism and the IRE/IRP regulatory system: an update. Ann N Y Acad Sci. 1012:1-13.

Paul RG, Williams AG & Butler RD. 1990. Hydrogenosomes in the rumen entodiniomorphid ciliate *Polyplastron multivesiculatum*. J. Gen. Microbiol. 136, 1981-1989.

Payne MJ, Chapman A, Cammack R (1993) Evidence for an [Fe]-type hydrogenase in the parasitic protozoan *Trichomonas vaginalis*. FEBS Lett 317:101–104

Pegg AE (1986) Recent advances in the biochemistry of polyamines in eukaryotes. Biochem J 234:249–262.

Peterson KM, Alderete JF (1984) Iron uptake and increased intracellular enzyme activity follow host lactoferrin binding by*Trichomonas_vaginalis* receptors. J Exp Med. 160(2):398-410.

Petrin D, Delgaty K, Bhatt R, Garber GE. (1998) Clinical and microbiological aspects of *Trichomonas vaginalis.* Clin. Microbiol. Rev. 11:300–317.

Pfanner N, Geissler A (2001) Versatility of the mitochondrial protein import machinery. Nat Rev Mol Cell Biol 2:339-349.

Pierik AJ, Wolbert RB, Mutsaers PH, Hagen WR, Veeger C. (1992) Purification and biochemical characterization of a putative [6Fe-6S] prismane-cluster-containing protein from *Desulfovibrio vulgaris* (Hildenborough). Eur J Biochem. 206(3):697-704.

Putignani L et al. (2004) Characterization of a mitochondrion-like organelle in *Cryptosporidium parvum*. Parasitology 129:1-18

Pütz S, Doležal P, Gelius-Dietrich G, Bohacova L, Tachezy J, Henze K.(2006).Fe-hydrogenase maturases in the hydrogenosomes of *Trichomonas vaginalis.* Eukaryot Cell. 5(3):579-86.

Pütz S, Gelius-Dietrich G, Piotrowski M, Henze K (2005) Rubrerythrin and peroxiredoxin: two novel putative peroxidases in the hydrogenosomes of the microaerophilic protozoon *Trichomonas vaginalis*. Mol Biochem Parasitol 142:212–223

Quon DV, d'Oliveira CE, Johnson PJ. (1992). Reduced transcription of the ferredoxin gene in metronidazole-resistant *Trichomonas vaginalis.* Proc Natl Acad Sci U S A. 89(10):4402-6.

Rada P, et al. 2009. The monothiol single-domain glutaredoxin is conserved in the highly reduced mitochondria of *Giardia intestinalis. Eukaryot. Cell* 8*:*1584–1591.

Rada P, Makki AR, Zimorski V, Garg S, Hampl V, Hrdý I, Gould SB, Tachezy J. (2015) N-Terminal Presequence-Independent Import of Phosphofructokinase into Hydrogenosomes of Trichomonas vaginalis. Eukaryot Cell.14(12):1264-75.

Ragsdale SW, (2003) Pyruvate ferredoxin oxidoreductase and its radical intermediate. Chem Rev. 103(6):2333-46.

Rasoloson D., Tomkova E.**,** Cammack R., Kulda J., Tachezy J. **(**2001). Metronidazole resistant strains of *Trichomonas vaginalis* display increased susceptibility to oxygen. Parasitol. 123: 45-56.

Rasoloson D., Vanácová S., Tomkova E., Hrdý I., Razga J., Tachezy J., Kulda J., (2002). Mechanisms of in vitro development of resistance to metronidazole in *Trichomonas vaginalis*. Microbiol.-SGM**,** 148: 2467-2477.

Regoes A, Zourmpanou D, Leon-Avila G, van der Giezen M, Tovar J, Hehl AB (2005) Protein import, replication and inheritance of a vestigial mitochondrion. J Biol Chem 280:30557-30563

Rehling P et al. (2003) Protein insertion into the mitochondrial inner membrane by a twin-pore translocase. Science 299:1747-1751

Reis IA, Martinez MP, Yarlett N, Johnson PJ, Silva-Filho FC, Vannier-Santos MA. (1999) Inhibition of polyamine synthesis arrests trichomonad growth and induces destruction of hydrogenosomes. Antimicrob Agents Chemother. 43(8):1919-23.

Rhee SG, Chae HZ, Kim K (2005) Peroxiredoxins: a historical overview and speculative preview of novel mechanisms and emerging concepts in cell signaling. Free Radic Biol Med. 38(12):1543-52.

Risgaard-Petersen N, Langezaal AM, Ingvardsen S, Schmid MC, Jetten MS, Op den Camp HJ, Derksen JW, Piña-Ochoa E, Eriksson SP, Nielsen LP, Revsbech NP, Cedhagen T, van der Zwaan GJ. (2006). Evidence for complete denitrification in a benthic foraminifer. Nature. 443(7107):93-6.

Rivera MC, Lake JA. (2004). The ring of life provides evidence for a genome fusion origin of eukaryotes. Nature. 431(7005):152-5.

Rouault TA, Tong WH. (2005) Iron-sulphur cluster biogenesis and mitochondrial iron homeostasis. Nat Rev Mol Cell Biol. 6(4):345-51.

Roy A., Solodovnikova N., Nicholson T., Antholine W, Walden W.E. (2003) A novel eukaryotic factor for cytosolic Fe–S cluster assembly, EMBO J. 22: 4826–4835.

Ryu JS, Choi HK, Min DY, Ha SE, Ahn MH.(2001) Effect of iron on the virulence of *Trichomonas vaginalis*. J Parasitol. 2:457-60.

Santos R, Buisson N, Knight SA, Dancis A, Camadro JM, Lesuisse E (2004) *Candida albicans* lacking the frataxin homologue: a relevant yeast model for studying the role of frataxin. Mol Microbiol 54:507–519.

Saraiva LM, Vicente JB, Teixeira M (2004) The role of the flavodiiron proteins in microbial nitric oxide detoxification. Adv Microb Physiol 49:77–129

Schmid G, Narcisi E, Mosure D, Secor WE, Higgins J, Moreno H. (2001) Prevalence of metronidazole-resistant Trichomonas vaginalis in a gynecology clinic. J Reprod Med 46:545e9.

Schmid, Samuelson and Rowley (2011). Prevalence and incidence of selected sexually transmitted infections, *Chlamydia trachomatis, Neisseria gonorrhoeae,* syphilis and *Trichomonas vaginalis*: methods and results used by WHO to generate 2005 estimates.

Schwebke JR, Burgess D. (2004) Trichomoniasis. Clinical Microbiol. Rev. 17:794–803.

Schwebke JR, Barrientes FJ. (2006) Prevalence of Trichomonas vaginalis isolates with resistance to metronidazole and tinidazole. Antimicrob Agents Chemother 50:4209e10.

Seedorf, H., A. Dreisbach, R. Hedderich, S. Shima, and R. K. Thauer. (2004). F420H2 oxidase (FprA) from *Methanobrevibacter arboriphilus*, a coenzyme F-420-dependent enzyme involved in O_2 detoxification. Arch. Microbiol. 182126-137.

Serwin AB, Koper M. (2013) Trichomoniasis--an important cofactor of human immunodeficiency virus infection. Przegl Epidemiol. 67(1):47-50, 131-4. Review. English, Polish.

Sickmann A, Reinders J, Wagner Y, Joppich C, Zahedi R, Meyer HE, Schönfisch B, Perschil I, Chacinska A, Guiard B, Rehling P, Pfanner N, Meisinger C. (2013). The proteome of *Saccharomyces cerevisiae* mitochondria. Nov 11;100(23):13207-12.

Singh S, Singh G, Sagar N, Yadav PK, Jain PA, Gautam B, Wadhwa G. 2012. Insight into *Trichomonas vaginalis* genome evolution through metabolic pathways comparison. Bioinformation. 8(4):189-95

Sipos K., Lange H., Fekete Z., Ullmann P., Lill R., Kispal G. (2002) Maturation of cytosolic iron–sulfur proteins requires glutathione, J. Biol. Chem. 277, 26944–26949

Smid, O., E. Horakova, V. Vilimova, I. Hrdý, R. Cammack, A. Horvath, J. Lukes, and J. Tachezy. 2006. Knock-downs of iron-sulfur cluster assembly proteins IscS and IscU down-regulate the active mitochondrion of procyclic *Trypanosoma brucei*. J. Biol. Chem. 281**:**28679-28686.

Smid O, Matuskova A, Harris SR, Kucera T, Novotny M, et al. (2008) Reductive evolution of the mitochondrial processing peptidases of the unicellular parasites *Trichomonas vaginalis* and *Giardia intestinalis*. PLoS Pathog 4: e1000243.

Smutná T, Gonçalves VL, Saraiva LM, Tachezy J, Teixeira M, Hrdy I. (2009) Flavodiiron protein from Trichomonas vaginalis hydrogenosomes: the terminal oxygen reductase. Eukaryot Cell. 8(1):47-55.

Solano-González E, Burrola-Barraza E, León-Sicairos C, Avila-González L, Gutiérrez-Escolano L, Ortega-López J, Arroyo R.(2007) The trichomonad cysteine proteinase TVCP4 transcript contains an iron-responsive element. FEBS Lett. 16:2919-28.

Sommer U, Costello C, Hayes G.,Beach D., Gilbert R., Lucas J and Singh B. (2005). Identification of *Trichomonas vaginalis* cysteine proteases that induce apoptosis in human vaginal epithelial cells. J Biol Chem.; 280:23853-23860.

Spence MR, Harwell TS, Davies MC, et al. (1997) The minimum single oral metronidazole dose for treating trichomoniasis: a randomized, blinded study. Obstet Gynecol 89(5 Pt 1):699–703.

Stark, Jennifer R.; Judson, Gregory; Alderete, John F.; Mundodi, Vasanthakrishna; Kucknoor, Ashwini S.; Giovannucci, Edward L.; Platz, Elizabeth A.; Sutcliffe,

Siobhan et al. (2009). "Prospective Study of *Trichomonas vaginalis* Infection and Prostate Cancer Incidence and Mortality: Physicians' Health Study". JNCI Journal of the National Cancer Institute 101 (20): 1406–11.

Stechmann A, Hamblin K, Pérez-Brocal V, Gaston D, Richmond GS, van der Giezen M, Clark CG, Roger AJ.2008. Organelles in *Blastocystis* that blur the distinction between mitochondria and hydrogenosomes. Curr Biol. 18(8):580-5

Steinbüchel A, Müller M. 1986. Anaerobic pyruvate metabolism of *Tritrichomonas foetus* and Trichomonas vaginalis hydrogenosomes. Mol. Biochem. Parasitol. 20:57–65.

Stehling O, Mascarenhas J, Vashisht AA, Sheftel AD, Niggemeyer B, Rösser R, Pierik AJ, Wohlschlegel JA, Lill R. (2013) Human CIA2A-FAM96A and CIA2B-FAM96B integrate iron homeostasis and maturation of different subsets of cytosolic-nuclear iron-sulfur proteins. Cell Metab 18(2):187-98.

Stewart M (2007) Molecular mechanism of the nuclear protein import cycle. Nat Rev Mol Cell Biol 8:195-208

Stuart R (2002) Insertion of proteins into the inner membrane of mitochondria: the role of the Oxa1 complex. Biochim Biophys Acta 1592:79-87

Šutak, R., Lesuisse, E., Tachezy, J., and Richardson, D. R. (2008). Crusade for iron: iron uptake in unicellular eukaryotes and its significance for virulence. Trends in Microbiology *16*, 261–268.

Šutak, R., P. Doležal, H. L. Fiumera, I. Hrdý, A. Dancis, M. Delgadillo-Correa, P. J. Johnson, M. Müller, and J. Tachezy (2004). Mitochondrial-type assembly of FeS centers in the hydrogenosomes of the amitochondriate eukaryote *Trichomonas vaginalis*. Proc. Natl. Acad. Sci. USA 101**:**10368-10373.

Tabor CW, Tabor H (1976) 1,4 -Diaminobutane (putrescine), spermidine, and spermine. Ann Rev Biochem 45:285–306

Tachezy J (2008). Hydrogenosomes and mitosomes:mitochondria of anaerobic eukaryotes. Springer-Verlag, Heidelberg, Germany.

Tachezy J. *(*1999). More on iron acquisition by parasitic protozoa. *Parasitol. Today* 15*:*207

Tachezy J, Kulda J, Tomková E. (1993) Aerobic resistance of *Trichomonas vaginalis* to metronidazole induced in vitro. Parasitology. Pt 1:31-7.

Tachezy J., Kulda J., Bahnikova I., Suchan P., Razga J., Schrevel J. (1996) *Trichomonas foetus* iron acquisition from lactoferrin and transferrin. Exp. Parasitol. 83, 216-228.

Tachezy J., Sánchez L.C., Müller M., 2001**.** Mitochondrial type iron-sulfur cluster assembly in the amitochondriate eukaryotes *Trichomonas vaginalis* and *Giardia intestinalis,as* indicated by the phylogeny of IscS. Mol. Biol. Evol. 18: 1919-1928.

Tadolini B (1988) Polyamine inhibition of lipoperoxidation: the influence of polyamines on iron oxidation in the presence of compounds mimicking phospholipid polar heads. Biochem J 249:33–36.

Tanabe M (1979) *Trichomonas vaginalis*: NADH oxidase activity. Exp Parasitol 48:135–143.

Thin RN, Symonds MA, Booker R, et al. (1979) Double-blind comparison of a single dose and a five-day course of metronidazole in the treatment of trichomoniasis. Br J Vener Dis 55:354–6.

Thomas A. Richards and Mark van der Giezen (2006) Evolution of the Isd11–IscS Complex Reveals a Single α–Proteobacterial Endosymbiosis for All Eukaryotes. *Mol Biol Evol* 23 (7): 1341-1344.

Thong KW, Coombs GH (1987) Comparative study of ferredoxin-linked and oxygen metabolizing enzymes of trichomonads. Comp Biochem Physiol B 87:637–641

Tielens AG, Rotte C, van Hellemond JJ, Martin W. (2002) Mitochondria as we don't know them. Trends Biochem Sci. 27(11):564-72.

Tjaden J, Haferkamp I, Boxma B, Tielens AG, Huynen M, et al. (2004) A divergent ADP/ATP carrier in the hydrogenosomes of *Trichomonas gallinae* argues for an independent origin of these organelles. Mol Microbiol 51: 1439–1446.

Torres-Romero JC, Arroyo R. (2009) Responsiveness of *Trichomonas vaginalis* to iron concentrations: evidence for a post-transcriptional iron regulation by an IRE/IRP-like system. Infect Genet Evol. 2009 6:1065-74.

Tovar J, Leon-Avila G, Sanchez LB, Sutak R, Tachezy J, et al. (2003) Mitochondrial remnant organelles of *Giardia* function in iron-sulphur protein maturation. Nature 426: 172–176..

Tovar J, Fischer A, Clark CG (1999) The mitosome, a novel organelle related to mitochondria in the amitochondrial parasite *Entamoeba histolytica*. Mol Microbiol 32: 1013–1021.

Truscott KN et al. (2003) A J-protein is an essential subunit of the presequence translocase-associated protein import motor of mitochondria. J Cell Biol 163:707-713

Tsai CD, Liu HW, Tai JH. (2002) Characterization of an iron-responsive promoter in the protozoan pathogen *Trichomonas vaginalis*. J Biol Chem. 7: 5153-62

Upcroft P, Upcroft JA (2001) Drug targets and mechanisms of resistance in the anaerobic protozoa. Clin Microbiol Rev 14:150–164.

Upcroft, J.A. et al. (2009) Metronidazole resistance in *Trichomonas vaginalis* from highland women in Papua New Guinea. Sex. Health 6,334–338 50

van Bruggen JJA, Zwart KB, van Assema RM, Stumm CK & Vogels GD. (1984). *Methanobacterium formicium*, an endosymbiont of the anaerobic ciliate *Metopus striatus*. J Mol Biol. 130, 1-7.

van den Berg WA, Hagen WR, van Dongen WM. (2000) The hybrid-cluster protein ('prismane protein') from Escherichia coli. Characterization of the hybrid-cluster protein, redox properties of the [2Fe-2S] and [4Fe-2S-2O] clusters and identification of an associated NADH oxidoreductase containing FAD and [2Fe-2S]. Eur J Biochem. 267(3):666-76.

van der Giezen M, Klaas A Sjollema, Rebekka R.E Artz, Wynand Alkema, Rudolf A Prins. (1997) Hydrogenosomes in the anaerobic fungus *Neocallimastix frontalis* have a double membrane but lack an associated organelle genome. FEBS Letters, 408 2: 147-150.

van der Giezen M (2009) Hydrogenosomes and mitosomes: conservation and evolution of functions. J Eukaryot Microbiol. 56:221–31.

Van der Laan M et al. (2005) Pam17 is required for architecture and translocation activity of the mitochondrial protein import motor. Mol Cell Biol 25:7449-7458

Van der Laan M, Rissler M, Rehling P (2006) Mitochondrial preprotein translocases as dynamic molecular machines. FEMS Yeast Res 6:849-861

Van der Pol B, Kwok C, Pierre-Louis B, Rinaldi A, Salata RA, Chen PL, et al. (2008) *Trichomonas vaginalis* infection and human immunodeficiency virus acquisition in African women. J Infect Dis. 197(4):548–54.

van Grinsven KW, van Hellemond JJ, Tielens AG (2009) Acetate:succinate CoA-transferase in the anaerobic mitochondria of Fasciola hepatica. Mol Biochem Parasitol. 164(1):74-9.

Vanácová S, Rasoloson D, Rázga J, Hrdý I, Kulda J, Tachezy J. (2001) Iron-induced changes in pyruvate metabolism of *Tritrichomonas foetus* and involvement of iron in expression of hydrogenosomal proteins. Microbiology. 147(Pt 1):53-62.

Viscogliosi E, Gado-Viscogliosi P, Gerbod D, Dauchez M, Gratepanche S, Alix AJP, Dive D (1998) Cloning and expression of an iron-containing superoxide dismutase in the parasitic protist, *Trichomonas vaginalis*. FEMS Microbiol Lett 161:115–123

Wagner G, Levin R. (1978) Oxygen tension of the vaginal surface during sexual stimulation in the human. Fertil Steril. 1:50-3.

Watt L, Jennison RF. (1960) Clinical evaluation of metronidazole. A new systemic trichomonacide. Br Med J.2(5203):902-5.

Wickner W, Schekman R (2005) Protein translocation across biological membranes. Science 310:1452-1456

Wiedemann N, Truscott KN, Pfannschmidt S, Guiard B, Meisinger C, Pfanner N (2004) Biogenesis of the protein import channel Tom40 of the mitochondrial outer membrane: intermembrane space components are involved in an early stage of the assembly pathway. J Biol Chem 279:18188-18194

Williams K, Lowe PN, Leadlay PF (1987) Purification and characterization of pyruvate: ferredoxin oxidoreductase from the anaerobic protozoon *Trichomonas vaginalis*. Biochem J 246:529–536.

Wolfe MT, Heo J, Garavelli JS, Ludden PW. (2002) Hydroxylamine reductase activity of the hybrid cluster protein from Escherichia coli. J Bacteriol. 184(21):5898-902.

Wood BA, Monro AM. (1975) Pharmacokinetics of tinidazole and metronidazole in women after single large oral doses. Br J Vener Dis 51:51–3.

Wood ZA, Schroder E, Harris JR, Poole LB (2003) Structure, mechanism and regulation of peroxiredoxins. Trends Biochem Sci 28:32–40.

Workowski KA, Bolan GA; (2015) Centers for Disease Control and Prevention. Sexually transmitted diseases treatment guidelines, 2015. MMWR Recomm Rep. 5;64(RR-03):1-137.

Zuo X, Lockwood BC, Coombs GH . (1995) Uptake of amino acids by the parasitic, flagellated protist *Trichomonas vaginalis.* Microbiology. 141 (Pt 10):2637-42.

Yang D, Oyaizu Y, Oyaizu H, Olsen GJ, Woese CR. 1985. Mitochondrial origins. Proc Natl Acad Sci U.S A. 1985; 82:4443–7

Yarlett N, Hann AC, Lloyd D & Williams A. (1981). Hydrogenosomes in the rumen protozoon *Dasytricha ruminantium*. Biochem. J. 200, 365-372

Yarlett N, Lindmark DG, Goldberg B, Moharrami MA, Bacchi CJ. (1994). Subcellular localization of the enzymes of the arginine dihydrolase pathway in *Trichomonas vaginalis* and *Tritrichomonas foetus*. J Eukaryot Microbiol. 41(6):554-9.

Yarlett N, Martinez MP, Moharrami MA, Tachezy J (1996) The contribution of the arginine dihydrolase pathway to energy metabolism by *Trichomonas vaginalis*. Mol Biochem Parasitol 78:117–125

Yarlett N, Orpin CG, Munn EA, Yarlett NC, Greenwood CA.(1986a). Hydrogenosomes in the rumen fungus *Neocallimastix patriciarum*. Biochem J. 236(3):729-39.

Yarlett N, Rowlands CC, Evans JC, Yarlett NC, Lloyd D. (1987) Nitroimidazole and oxygen derived radicals detected by electron spin resonance in hydrogenosomal and cytosolic fractions from *Trichomonas vaginalis*. Mol Biochem Parasitol.3:255-61.

Yarlett N, Yarlett NC, Lloyd D.(1986b) Metronidazole-resistant clinical isolates of *Trichomonas vaginalis* have lowered oxygen affinities. Mol Biochem Parasitol. 2:111-6.

Yarunin, A., Panse, VG.,Petfalski, E.,Dez, C., Tollervey, D.,Hurt, EC.(2005). Functional link between ribosome formation and biogenesis of iron-sulfur proteins. EMBO J.; 24:580-588.

Zimorski V, Ku C, Martin WF, Gould SB (2014). Endosymbiotic theory for organelle origins. Curr Opin Microbiol. 2014 Dec; 22C:38-48. doi: 10.1016/j.mib.2014.09.008. Epub 2014 Oct 10. Review.

Zwart, Goosen, Van Schijnde, Broers, Stumm and Vogels.(1988) Cytochemical Localization of Hydrogenase Activity in the Anaerobic Protozoa *Trichomonas vaginalis, Plagiopyla nasuta* and *Trimyema compressum.* Microbiology. *134 no. 8 2165-2170*